DISSERTATION

VIRUS CLEARANCE DURING MICROFILTRATION

Submitted by

Saengchai Akeprathumchai

Department of Chemical Engineering

In partial fulfillment of the degree requirements

For the Degree of Doctor of Philosophy

Colorado State University

Fort Collins, Colorado

Fall 2003

COLORADO STATE UNIVERSITY

August 26, 2003

WE HEARBY RECOMMEND THAT THE DISSERTATION PREPARED UNDER OUR SUPERVISION BY SAENGCHAI AKEPRATHUMCHAI ENTITLED "VIRUS CLEARANCE DURING MICROFILTRATION" BE ACCEPTED AS FULFILLING IN PART REQUIREMENTS FOR THE DEGREE OF DOCTOR OF PHILOSOPHY.

Committee on Graduate Work

Co-advisor

Advisor

Department Head

ABSTRACT OF THESIS:

VIRUS CLEARANCE DURING MICROFILTRATION

Biotechnology and biopharmaceutical industries use mammalian derived raw materials such as growth medium and genetically engineered vectors to produce recombinant proteins of prophylactic and therapeutic character. The demand of these compounds is increasing tremendously. The use of mammalian derived raw materials enhances the possibility of virus contamination in the final product. The Food and Drug administration (FDA) mandates that manufacturers demonstrate levels of virus removal in excess of calculated levels of contamination in the purification train. Consequently, there is a great need to validate virus clearance in existing unit operations.

Microfiltration is usually used to remove cells, cell debris and small particulates from biomass suspensions. The filtrate flux is often relatively low since biomass suspensions are particularly difficult to filter due to their highly fouling nature and the fact that the cake formed is also highly compressible. Limited clearance of virus is expected during microfiltration since they are much smaller than the microfiltration membrane pores. Here, a method to improve filtrate flux and obtain virus clearance during microfiltration is proposed.

In this project, a feed suspension containing CHO-DG44 cells and A-MLV pseudotypes is pretreated with cationic polyacrylamides prior to microfiltration. By flocculation, the average particle size is increased leading to filtrate flux enhancement.

Further, while flocculation of biomass takes place, the capture of A-MLV pseudotypes into the floc network occurs. Therefore, significant removal of A-MLV from feed suspension may be attained during microfiltration.

Cationic polyacrylamides with molecular weight of $4-8\times10^6$ and 40 % charge density were successfully used to flocculate CHO cell suspension. However, the combination of molecular weight and charge density may play a significant role on the level of virus clearance. The average particle size of the flocculated suspension is increased from 18 to ~120 μm. As a result, a considerable improvement of filtrate flux of flocculated CHO cell suspension is accomplished compared to that of unflocculated suspensions. Further, removal of A-MLV pseudotypes as high as 5 log titer reductions may be achieved by flocculating the suspension containing CHO cells and A-MLV prior to microfiltration.

Saengchai Akeprathumchai
Chemical Engineering Department
Colorado State University
Fort Collins, CO 80523
Fall, 2003

ACKNOWLEDGEMENTS

I would like to thank my advisor, Dr. Ranil Wickramasinghe, for his guidance, advice and support throughout my study. I would also like to express my sincere appreciation to my co-advisor, Dr. Jonathan Carlson, for allowing me to work in his laboratory and for the countless hours of his valuable time he spent discussing and explaining things I have not understood. His guidance and advice is always appreciated. In addition, I thank my committee members, Dr. James Liden and Dr. Bryan Batt, for their support and availabilities to discussion.

My thanks also go to Andrew Peterson and the members of the Carlson lab for helping me with all my experiments and making my time in the lab more compfortable and enjoyable. Special thank goes to Dr. Janice Phillips whose support, advice and words of encouragemenr are of highly valuable and will always forever be appreciative.

"It is with passion, courage of conviction and strong sense of self that we take
our next steps into the world remembering that first impressions are
not always correct. You must always have faith in
people and, most importantly, you must
always have faith in yourself."

TABLE OF CONTENTS

LIST OF FIGURES

LIST OF TABLES

CHAPTER 1

INTRODUCTION

1.1 General Introduction

Presently, the demand for recombinant proteins, which have therapeutic, prophylactic and/or diagnostic application, such as insulin and monoclonal antibodies is increasing tremendously. However, the production of these proteins is strictly regulated by the Food and Drug Administration (FDA) due to the high risk of contamination of the products by biologically active components such as viruses. Since the biopharmaceutical and biotechnology industries use genetically engineered vectors, cell lines, and mammalian derived media as raw materials and the fact that some cell lines can produce virus particles either spontaneously or by chemical induction. There is possibility of virus contamination in the final product.

In addition, the FDA mandates that the manufacturers of these therapeutic proteins intended for human use demonstrate virus clearance in their purification processes. The FDA has also specified model viruses together with the acceptable methods of virus clearance to be used in the validation of the purification trains. Specific unit operations, accepted by FDA for removal and/or inactivation of viruses, are inactivation of viruses by heating, solvent and detergents, filtrations and alteration of pH.

Removal of these viruses is much more difficult since viruses are of colloidal size, 40-200 nm. Therefore, typical solid-liquid separation processes, i.e., precipitation and extraction, are of little use. Further, other methods to remove viruses from suspension are chromatography and virus filtration. Chromatography techniques targeted for virus clearance are time-consuming and tend to result in low product yields. Virus filtration utilizes the membranes with pore size smaller than the viruses. Often poor virus rejection and loss of protein product through the membrane pores is observed. Additionally, the purification steps used to remove contaminated viruses from the suspension tend to be located toward the end of the purification train where the concentration of the desired products is high. Therefore, yield loss is almost inevitable.

Cell suspensions from the biotechnology and biopharmaceutical industries almost always contains small particles of colloidal size resulting from dead cell lysis. Separation of cells, cell debris and other small aggregates from suspensions is typically accomplished by crossflow (tangential flow) microfiltration. However, the efficiency of microfiltration is often rather low due to the presence of these small particulates. Microfiltration is frequently used for bioreactor harvesting. Further, it has been shown that pretreatment of feed suspension by flocculation may be used to increase the permeate flux (Wickramasinghe et al. (2002), Kim et al. (2001)). Further, since viruses tend to be negatively charged, addition of cationic flocculants should lead to capture of virus particles in the biomass leading to virus clearance in the permeate.

Suspensions containing CHO cells and A-MLV pseudotypes are flocculated with cationic polyacrylamide, as a result, the particle size distribution of the suspension is altered. Subsequently, microfiltration is performed. Additionally, it is believed that the

cationic flocculants used to induce particle aggregation will have a minimum effect on the product yield because at this point the product concentration is still low. Furthermore, this procedure introduces only a minor deviation from the current industrial practice, which will not greatly increase the marginal cost of the whole purification processes.

In this project, removal of A-MLV pseudotypes, an FDA model virus, is studied by flocculation of a suspension containing CHO cells and A-MLV pseudotypes prior to microfiltration. The theoretical background of flocculation and microfiltration including cell lines and A-MLV characteristics is given in Chapter 2; experimental procedure and cell culture techniques are described in detail in Chapter 3. The experimental results for flocculation and microfiltration are illustrated in Chapter 4. Chapter 5 provides a discussion of the experimental results obtained in this study.

1.2 Objectives

Objectives of this study are the following

1. To gain more insight into the interaction between the particles being flocculated and the polymers
2. To develop the mathematical model to predict the average particle size of the flocculated suspension as a function of the operating parameters such as initial particle size, time, shear rate (velocity gradient), polymer dosages, and particle concentrations
3. To predict the virus clearance in the permeate based on the mathematical expression and operating conditions

CHAPTER 2

GENERAL BACKGROUND

This chapter describes the theoretical background and previous work related to flocculation and microfiltration. The system used here consisting of Murine Leukemia viruses (MLV) and Chinese hamster ovary (CHO) cells is also described. Microfiltration is discussed first including a concise review of virus removal by flocculation and microfiltration. Subsequently, the flocculation process is reviewed in some detail including some relevant topics. Finally, characteristics of CHO cells and MLV are also described.

2.1 Microfiltration

In the downstream processing of pharmaceutical and biotechnology industries, microfiltration is usually the first unit operation that is used in the purification train to separate solids such as cells, cell debris and other insoluble materials from growth media, which usually contains desired products. However, it is well known that biological feeds are notoriously difficult to filter either because they are highly non-Newtonian or because the cake formed is highly compressible and highly fouling (Belter et al. (1988)). As the filtration process proceeds, the cake deforms into an insoluble mat leading to lower permeate flux at high transmembrane pressure (TMP). In addition, the

cell viability of the feed suspension may play an important role in determining the filterability of the suspension.

Microfiltration is a pressure-driven process. It is generally used to remove small particulates in the range of 0.1 – 10 μm (Cheryan (1986), Davis, (1992)) from suspension. There are two configurations (Figure 2-1) usually used in the filtration processes, dead-end and crossflow (tangential flow) microfiltration. For dead-end microfiltration (Figure 2-1a), the feed flows perpendicularly to the porous membrane surface leading to rapid accumulation of the particulate matter on the membrane surface. The thickness of cake on the membrane surface grows with time. Eventually, filtration has to be stopped and the membrane has to be cleaned. For crossflow microfiltration (Figure 2-1b), the feed solution flows tangentially to the membrane surface, which results in shear force that can sweep away the deposited particulates on the membrane surface leading to lower membrane fouling.

The advantages (Brose et al. (1996)) of crossflow microfiltration over dead-end microfiltration are less membrane fouling, lower pore blocking and less cake build-up including smaller concentration polarization layer. In addition, for crossflow microfiltration, continuous operation requires less complicated equipment. For filtration processes, high permeate flux is always desirable, however, as filtration proceeds permeate flux declines due to concentration polarization and fouling of the microporous membrane.

In order to maximize the permeate flux and the capacity of the membrane module, a number of different approaches have been persued. These methods could be classified into three main categories, which are chemical, hydrodynamic and physical

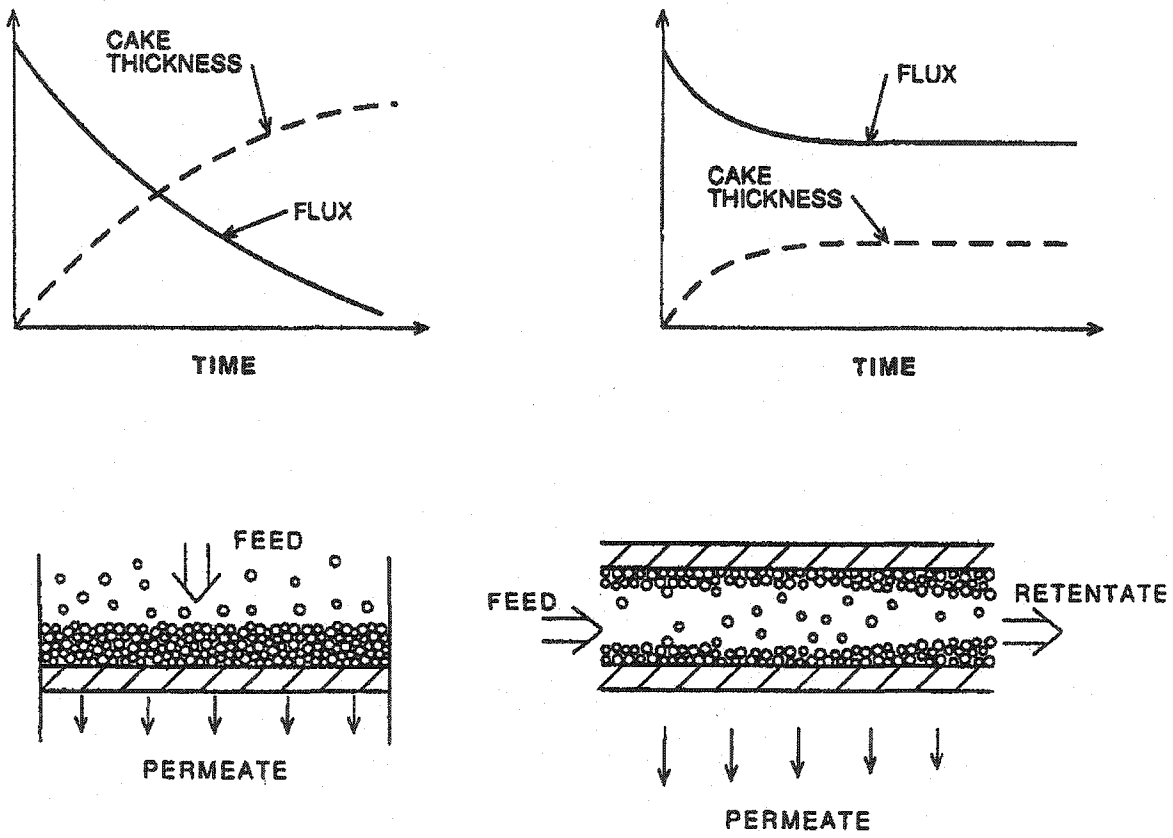

(a) Dead-end Microfiltration (b) Crossflow Microfiltration

Figure 2-1 Schematic of Dead-End and Crossflow Microfiltration

(Oftshun (1989)). Chemical methods involve modification of the surface chemistry of the membrane in order to increase the repulsion between the membrane and the particulate matter. This repulsion results in reduced deposition and fouling of the membrane. Hydrodynamic methods involve modifying the design of the module to induce turbulent flow. While chemical and hydrodynamic methods focus on changes of the membrane and the module design, respectively, physical methods involve pretreatment of the feed solution by altering the particle size distribution. This can be achieved by introducing flocculating agents such as polyelectrolytes and metal salts.

2.1.1. Microfiltration Theory

In general, the permeate flux across the membrane is driven by the pressure gradient or TMP. As filtration proceeds, the solid is retained by the membrane and then accumulates on the membrane surface resulting in an enormous reduction of the filtrate flux. While the liquid is allowed to pass through the membrane, the solid is retained and sometimes is compressed into an insoluble mat (cake) on the membrane surface. Performance of filtration systems could be aggravated by two prominent phenomena, which are concentration polarization and fouling. While fouling is considered to be an irreversible process, concentration polarization is described as a reversible phenomenon. Fouling is attributed to the deposition and/or adsorption of macrosolutes onto the membrane surface and/or into the membrane pores leading to changes in the membrane behavior. Concentration polarization, on the other hand, is characterized by the increase of the local concentration of the retained solutes on the membrane surface leading to an additional resistance to flow on the membrane surface.

When the sieving mechanism is dominant, the filtrate flux is directly proportional to the pressure gradient across the membrane module and inversely proportional to the viscosity and the resistance of both the membrane and the solids accumulated on the membrane surface (Davis (1992)), which is also known as Darcy's law.

$$J = \frac{\Delta P}{\mu(R_m + R_s)} \tag{2-1}$$

where ΔP is the transmembrane pressure, μ is the viscosity of the suspending medium and R_m and R_s are the membrane resistance and cake resistance, respectively. In microfiltration, particles move toward the membrane surface due primarily to the convective transport of the bulk solution. At the same time, particles in close proximity to the membrane surface can move away from the membrane surface into the bulk solution by several mechanisms such as Brownian movement (Weisner and Chellam (1992)) and shear induced diffusion (Eckstein et al. (1977), Zydney and Colton (1986)). Inertial lift forces (Green and Belfort (1980), Altena and Belfort (1984), Altena et al. (1985), which are also know as tubular pinch effect or lateral migration also play a role. With the formation of the cake layer in front of the membrane surface, there exists a concentration gradient between the bulk solution and the membrane surface. At steady state, it is established that the convective transport of the particles to the membrane surface is balanced by the back diffusion of the particles to the bulk solution; therefore, it could be mathematically expressed as

$$-D\frac{dC}{dy} = JC \tag{2-2}$$

where D is diffusion coefficient, y is the coordinate normal to the membrane surface, C is particle concentration and J is the solvent flux across the membrane. The first term in

(2-2) represents the rate of back diffusion of particles away from the membrane surface while the second term on the right denotes the rate of convective transport of particle towards the membrane surface. Integration of (2-2), subjecting the boundary conditions $C = C_w$ at $y = 0$ (the cake surface) and $C = C_b$ at $y = \delta$, results in the well-known "film theory" that is also known as the "concentration polarization model" (Porter (1972))

$$J = k \ln\left(\frac{C_w}{C_b}\right) \tag{2-3}$$

where C_w is the concentration of solid accumulated on the membrane surface, C_b is the concentration in the bulk solution and k ($= D/\delta$) is the mass transfer coefficient which could be determined by means of Lévêque approximation (Lévêque (1928)). According to Lévêque solution, for the developing laminar flow, mass transfer coefficient can be estimated by

$$\frac{kd}{D} = 1.86\,\mathrm{Re}^{1/3}\,Sc^{1/3}\left(\frac{d}{L}\right)^{1/3} \tag{2-4}$$

while for fully developed turbulent flow, the Dittus-Boelter correlation of mass transfer coefficient is given as

$$\frac{kd}{D} = 0.023\,\mathrm{Re}^{4/5}\,Sc^{1/3} \tag{2-5}$$

where Sc and Re are the Reynolds' number and Schmidt number, respectively.

2.1.2. Empirical Model

In filtration processes, the main objective is to obtain as high a permeate flux as possible. Initially, the permeate flux reaches a quasi-steady state value after which a slow long-term decline has been observed. However, it is typical that the permeate flux

declines with time as filtration process proceeds. A number of theoretical models have been developed in order to predict the quasi-steady state permeate flux during crossflow microfiltration. Typically, these models relate the permeate flux to variables such as wall shear rate, average particle diameter, length of hollow fibers and particle concentrations (Belfort et al. (1994)). In crossflow microfiltration, there is an initial short period of rapid flux decline followed by an extended period of quasi-steady state operation (Belfort et al. (1994)). In the region of quasi-steady state operation, short-term flux declines due to cake build-up; however, there is still a slow long-term flux decline due to membrane fouling.

The convective transport of particles towards the membrane is balanced by the back migration of particles due to mechanisms such as Brownian movement (Wiesner and Chellam (1992)), shear induced diffusion (Eckstein et al. (1977)) and tubular pinch effect or lateral migration (Green and Belfort (1980), Altena and Belfort (1984), Altena et al. (1985). The pseudo-steady state flux decline may be predicted by the relationship of the form

$$J = K(\dot{\gamma}_w)^a (d)^b \qquad (2\text{-}6)$$

where a and b are arbitrary constants, $\dot{\gamma}_w$ is wall shear rate and d is the average particle diameter while K is constant depending on viscosity of feed, length of the fiber and particle concentration.

The long term permeate flux decline due to the membrane fouling may empirically be predicted by (Kuo and Cheryan (1983), Russotti et al. (1995), Defrise and Gekas (1988))

$$J = J_2 t^{-c} \qquad (2\text{-}7)$$

where J and J_2 are the permeate flux at any time and at 2 minutes, respectively. t is the filtration time and c is the fouling index. It is speculated that this behavior of flux decline is due to the compression of the cell layer formed on the membrane surface (Kroner and Kula (1984)). There are a number of other mathematical expressions that attempt to predict the permeate flux during microfiltration (Belfort et al. (1994), Zydney and Colton (1986)), which have been developed in order to take particular back transport effect into account.

2.1.2.1. Generalized Pore Blocking Model

Hermia (1982) was the first to propose the intermediate pore blocking model for dead end microfiltration. This model was subsequently generalized for crossflow microfiltration (Field et al. (1995)), which reads

$$\frac{dJ}{dt} J^{n-2} = k'(J - J^*) \qquad (2\text{-}8)$$

where J and J^* are volumetric flux and critical flux, respectively, while n and k' are constants depending on fouling mechanism. For the case of intermediate pore blocking model, n takes on the value of unity whereas, for complete pore blocking and cake filtration, n is equal to 2 and 0, respectively (Field et al. (1995)).

2.1.2.2. Brownian Diffusion Model

Originally, based on analogous developments for ultrafiltration, it was believed that, for microfiltration, back transport of particles away from the membrane is due

solely to Brownian diffusion. In this model, it is implicitly assumed that with the presence of a stagnant film on the membrane surface, the rate of convective transport of particle towards the membrane is balanced by the rate of back diffusion of particles to the bulk solution. In case of laminar flow at steady state, it has been shown that the limiting flux is of the form (Defrise and Gekas (1988))

$$J = 0.807\left(\frac{D_B^2\dot{\gamma}_w}{L}\right)^{1/3}\ln\left(\frac{C_w}{C_b}\right) \tag{2-9}$$

where D_B, $\dot{\gamma}_w$ and L are the particle diffusivity, wall shear rate and membrane length, respectively. For Brownian diffusion, the particle diffusivity could be calculated from Stoke-Einstein correlation, which reads

$$D_B = \frac{kT}{6\pi\mu r_p} \tag{2-10}$$

On the other hand, for turbulent flow regime, it is found that the limiting flux could be expressed as (Defrise and Gekas (1988))

$$J = \left[0.023\cdot(u^{0.8}\cdot D^{0.67}\cdot d_h^{-0.2}\cdot\dot{\gamma}_w^{-0.47}\right]\ln\left(\frac{C_w}{C_b}\right) \tag{2-11}$$

Trettin and Doshi (1980) have as well proposed the mathematical model accounting for Brownian diffusion as the only back-transport mechanism. They found, by neglecting the influence of particle concentration on both viscosity and diffusion coefficient, that the averaged limiting flux are, for concentrated suspensions,

$$J = 0.81\left(\frac{\dot{\gamma}_w D^2}{\mu L}\right)^{1/3}\ln\left(\frac{C_w}{C_b}\right) \tag{2-12}$$

and, for dilute suspensions,

$$J = 1.31\left(\frac{\dot{\gamma}_w D^2}{\mu L}\right)^{1/3} \ln\left(\frac{C_w}{C_b}\right) \qquad (2\text{-}13)$$

where $\dot{\gamma}_w$ is the wall shear rate, μ is the permeate viscosity, L is the filter length, C_w is the concentration at the membrane surface, C_b is the concentration in the bulk solution and D is the Brownian diffusion coefficient for dilute suspensions of spheres which may be calculated from the Stoke-Einstein correlation.

Recently, Huisman and Trägårdh (1999) have numerically solved the convective-diffusion equation governing concentration polarization by assuming that particles are transported towards the membrane surface by convection and transported away by either Brownian diffusion, shear-induced diffusion or the combined effects. They found theoretically that the model gives comparatively good agreement to the experimental results. They have further shown that the turbulent diffusion contributes only marginally to particle transport within the concentration polarization layer.

2.1.2.3. Shear Induced Diffusion Model

Due to the fact that some experimental results could not be sufficiently explained by the existing models due to the phenomenon known as "flux paradox", Zydney and Colton (1986) proposed that the discrepancy of the experimental results to that of the concentration polarization model is due principally to an augmentation of the diffusivity motion of large particles in the shear flow of a concentrated suspensions (Zydney and Colton (1982)). Therefore, they further proposed that the concentration polarization model could be applied to microfiltration providing the Brownian diffusivity was

replaced by the shear-induced diffusivity first measured by Eckstein et al. (1977). This so called "shear induced hydrodynamic diffusivity" of the particles occurs because the individual particles undergo random displacement from the streamlines in shear flow. As they interact with other particles by contact, there is a net motion away from the cake. Zydney and Colton (1986) found the expressions for the local flux

$$J = 0.052\left(\frac{a^4}{x}\right)^{1/3}\dot{\gamma}_w \ln\left(\frac{C_w}{C_b}\right) \tag{2-14}$$

and the length averaged flux

$$J = 0.078\left(\frac{a^4}{L}\right)^{1/3}\dot{\gamma}_w \ln\left(\frac{C_w}{C_b}\right) \tag{2-15}$$

The authors also found good agreement of the model prediction to that of the experimental results with various particulate suspensions such as bovine blood and whole blood, platelets, bacteria, clay and latex spheres.

2.1.2.4. Lateral Migration Model

From a theoretical analysis of the lateral migration phenomenon for infinitely dilute suspensions, Ho and Leal (1974) and Vasseur and Cox (1976) derived the lift velocity of the particles in the presence of the boundary layer by explicitly combining the inertial effect into their analyses and found that the lift velocity is of the form

$$U_L = \frac{\dot{\gamma}_w^2 a^3}{\nu} f(y/h) \tag{2-16}$$

where the position dependence, $f(y/h)$, is maximum at the wall with a value of 0.095 (Vasseur and Cox (1976)) or between 0.26 and 0.42 (Ho and Leal (1974)). Madsen (1977) proposed that the lift velocity and the filtration velocity estimated from the concentration polarization theory are additive, therefore, the permeate flux could be expressed as

$$J = U_L + k \ln\left(\frac{C_w}{C_b}\right) \tag{2-17}$$

The above equation is known as the "Lift theory". Altena and Belfort (1984) have shown theoretically that the prediction from lift theory gave fairly good agreement to the experimental results only in the limit of infinitely dilute suspension. Subsequently Green and Belfort (1980) mentioned that in Madsen's model the radial migration velocity should rather be evaluated at $(d_t/2 - \delta_c)$ than at $(d_t/2)$ as done by Madsen.

2.1.2.5. Cake Filtration Model

The cake filtration theory, which explicitly considers the build-up of an immobile cake on the membrane surface to be the major mechanism that governs the permeate flux, was proposed by Green and Belfort (1980).

$$J = \frac{\Delta P}{R_c} \tag{2-18}$$

where ΔP is the transmembrane pressure drop across the membrane module and R_c is the cake resistance which could be estimated by using the Kozany-Carman relation (Carman (1939))

$$R_c = \frac{5\mu(1-\varepsilon)^2 \delta_c}{\varepsilon^3}\left(\frac{S_p}{V_p}\right)^2 \qquad (2\text{-}19)$$

where ε is the void fraction in the cake, δ_c is the cake layer thickness, μ is the fluid viscosity and (S_p/V_p) is the particle surface to volume ratio.

2.1.2.6. Combined Effect Model

Recently, due to the fact that in microfiltration of colloids and fine particulates the effects of surface charge interaction could not be ignored, McDonogh et al. (1989) have modified the film theory model to include electrostatic force into their model. They found that the permeate flux could be approximated by

$$J = k \ln\left(\frac{C_w}{C_b}\right) + k\int_0^{\delta} \frac{P_{elect}\, A}{kT}\partial x \qquad (2\text{-}20)$$

In the above equation, the electrostatic interaction force between charged particles is incorporated by utilizing the fact that the repulsive force per unit area between two planar double layers is equal to the increase in osmotic pressure which occurs during the accumulation of ions between the planes (Langmuir (1938)). Therefore, the electrokinetic pressure (P_{elect}) between charged colloids could be expressed, after some mathematical manipulation (McDonogh et al. (1989)), as

$$P_{dl} = 2n^o kT\left[\left(-\frac{z_i e\Psi}{kT}\right) - 1\right] \qquad (2\text{-}21)$$

where k, A and x are the mass transfer coefficient, the projected area of particle and distance from the wall, respectively, while P_{elect}, P_{dl}, Ψ and n^o are electrokinetic

pressure, double layer pressure, double layer potential and number of ions, respectively. With this model, the authors found that good agreement could be established between experimental results and the model predictions. However, the model fails when a suspension of low particle concentration is under investigation.

Yoon et al. (1999) have theoretically studied the effects of charged particle interaction on the deposition of multidipersed system. In their model, both van der Waals attractive force and repulsive electrostatic double layer force were taken into account as back transport mechanisms, namely, interaction enhanced migration. The authors made use of the theoretical model (Bacchin et al. (1995, 1996)) which described the deposition of colloidal particles onto the membrane surface accounting for surface interaction.

$$J = \frac{D_B}{\delta} \ln\left(\frac{V_B}{\delta}\right) \tag{2-22}$$

with

$$V_B = \int_0^{\infty} (e^{\frac{V_T}{kT}} - 1) dh \tag{2-23}$$

and the thickness of the boundary layer, δ, is obtained from Lévêque solution

$$\frac{d_h}{\delta} = 1.62 \left[\mathrm{Re} \cdot Sc \cdot \left(\frac{d_h}{L}\right) \right]^{1/3} \tag{2-24}$$

From their model, the authors found that the simulated flux decline agreed well with the experimental results and subsequently concluded that for non-flocculating suspension the major flux controlling parameter is the cake resistance rather than pore blocking mechanism.

Table 2-1 summarizes the models discussed here. Recently, more models have been proposed to predict the permeate flux dufing microfiltration. The concept of surface renewal of the membrane is proposed by Koltuniewicz (1992). Furthermore, with the development of the "Direct Observation through the membrane, DOTM", Li et al. (1998) have found experimentally that there exists the critical permeate flux at which, below this critical flux, particle deposition is negligible, and above this critical flux, particle layers started to form on the membrane surface. However, there is no universal mathematical model that can predict the permeate flux behavior for all feed streams due to the complex dynamics of the process. Due to the fact that each mathematical model used to predict the permeate flux is formulated for the particular system under investigation, each model should be applied with caution. In addition, extensive review on crossflow microfiltration and mathematical model to predict permeate flux is given elsewhere (Belfort et al. (1994) , Zydney and Colton (1986)). Further, a comprehensive review of the mathematical models for membrane filtration of colloids and fine particulates is given by Bowen and and Jenner (1995).

2.1.3. Virus Removal by Microfiltration and Flocculation

Given the large number of products such as monoclonal antibodies and recombinant DNA derived proteins that are intended for human use, virus contamination in the final products is an important issue owing to the fact that mammalian derived medium components and genetically engineered mammalian hosts are utilized. Additionally, the FDA mandates that the manufacturers of these DNA derived products demonstrate virus clearance in excess of the calculated level of virus contamination

Table 2-1 Summary of mathematical model to predict filtrate flux

Name	Mathematical Expression	Back-Transport Mechanism	Reference
Generalized pore blocking	$\frac{dJ}{dt}J^{n-2} = k'\left(J - J^*\right)$	-	Field et al. (1995)
Cake filtration	$J = \frac{\Delta P}{R_c}$	-	Green and Belfort (1980)
Brownian diffusion	$J = 0.807\left(\frac{D_B^2\dot{\gamma}_w}{L}\right)^{1/3}\ln\left(\frac{C_w}{C_b}\right)$ for laminar flow $J = 0.023\left(u^{0.8}\cdot D^{0.67}\cdot d_h^{-0.2}\cdot\gamma_w^{-0.47}\right)\ln\left(\frac{C_w}{C_b}\right)$ for turbulent flow	Brownian diffusion	Defrise and Gekas (1988)
Shear induced diffusion	$J = 0.052\left(\frac{a^4}{x}\right)^{1/3}\dot{\gamma}_w\ln\left(\frac{C_w}{C_b}\right)$ local flux $J = 0.078\left(\frac{a^4}{L}\right)^{1/3}\dot{\gamma}_w\ln\left(\frac{C_w}{C_b}\right)$ length average flux	Augmented Brownian diffusion	Zydney and Colton (1986)
Inertial lift	$J = U_L + k\ln\left(\frac{C_w}{C_b}\right)$	Lateral migration	Madsen (1977)
Modified film theory	$J = k\ln\left(\frac{C_w}{C_b}\right) + k\int_0^{\delta}\frac{P_{elect}A}{kT}\partial x$	Electrostatic force	McDonogh et al. (1989)
Surface interaction	$J = \frac{D_B}{\delta}\ln\left(\frac{V_B}{\delta}\right)$ $V_B = \int_0^{\infty}\left(e^{-\frac{V_T}{kT}} - 1\right)dh$	van der Waals and electrostatic force	Yoon et al. (1996)

during the purification process. Further, the FDA specifies model viruses to be used in validation studies (FDA (1993, 1997)). However, other than the FDA model viruses (Table 2-2), a number of bacteriophages and viruses, i.e., MS2, $Q\beta$, T4, poliovirus, hepatitis A and reovirus, are used simply because of the resemblance of these viruses to those of the model viruses, for example, MS2 is used as the model viruses due to its resemblance to polioviruses in size, shape and type of nucleic acid (Chaudhuri and Engelbrecht (1970)). In general, filtration and flocculation (coagulation) are usually used to remove viruses from suspension simply because of their colloidal nature.

2.1.3.1.Virus Removal by Microfiltration

Theoretically, virus particles may be removed from feed solution by the mechanism of size exclusion filtration (DiLeo et al. (1993), Urase et al. (1994)), which simply implies that the smaller the virus particles to be removed from the suspension, the membrane with even smaller pore size has to be utilized. A number of studies have shown that viruses can be removed from the suspension by ultrafiltration (Urase et al. (1994)) and microfiltration (Belkowski (1992), van Voorthuizen et al. (2001), Jacangelo et al. (1995), Herath et al. (1999)) including nanofiltration (Otaki et al. (1998), Abe et al. (2000), Omar and Kempf (2002)). However, in spite of sieving mechanism, it is more likely that other mechanisms such as interaction between viruses and membrane or self-aggregation of viruses may play a significant role. Therefore, hydrophilic membranes with small pore distribution are of special interest. For instance, Aranha-Creado et al. (1998) found that membrane filtration with hydrophilic polyvinylidene fluoride porous membrane, Ultipor® VP grade 50, could be effectively used to remove xenotropic

Table 2-2 FDA model viruses commonly used in viral clearance evaluation study

Virus	Family	Envelope	Genome	Size (nm)
Adenovirus type 5[1]	Adeno	No	DNA	70 – 90
Amphotropic Murine Leukemia Virus [1-3]	Retro	Yes	RNA	80 – 130
Bovine Parainfluenza Virus [1-3]	Paramyxo	Yes	RNA	150 – 300
Bovine Parvovirus[1]	Parvo	No	DNA	18 – 26
Bovine Viral Diarrhea Virus [1-3]	Flavi	Yes	RNA	60 – 70
Cytomegalovirus[1]	Herpes	Yes	DNA	180 – 200
Duck Hepatitis B Virus[1]	Hepadna	Yes	DNA	~ 40
Encephalomyocarditis Virus [1-3]	Picorna	No	RNA	28 – 30
Hepatitis A Virus[1-2]	Picorna	No	RNA	28 – 30
Human Immunodeficiency Virus[1]	Retro	Yes	RNA	80 – 130
Herpes Simplex Virus[1-2]	Herpes	Yes	DNA	150 – 200
Infectious Bovine Rhinotracheitis Virus[1]	Herpes	Yeas	DNA	150 – 200
Influenza A Virus[1,3]	Orthomyxo	Yes	RNA	80 – 120
Poliovirus[1-3]	Picorna	No	RNA	28 – 30
Porcine Parvovirus[1-3]	Parvo	No	DNA	18 – 26
Pseudorabies Virus[1-3]	Herpes	Yes	DNA	150 – 200
Reovirus type 3[1-4]	Reo	No	RNA	60 – 80
Simian Virus 40[1-3]	Papova	No	DNA	~ 45
Transmissible Gastroenteritis Virus[1]	Corona	Yes	RNA	80 – 160
Vesicular Stomatitis Virus[1]	Rhabdo	Yes	RNA	75 – 180
Xenotropic Murine Leukemia Virus[1-3]	Retro	Yes	RNA	80 – 130

[1] Viromed Biosafety Laboratories (1999); [2] Aranha and Forbes (2001); [3] ICH (2001); [4] FDA (1997)

murine leukemia virus (X-MLV) from suspension. They found that up to 7-log titer reduction could be achieved.

For ultrafiltration membranes with a molecular weight cut-off of 100,000 Daltons, it has been demonstrated that 99.9% of poliovirus, sindbis virus and vesicular stomatitis virus can be removed from suspensions (Bechtel et al. (1988)). In a microfiltration study to remove MS2 phage, it has been illustrated that pH has no effect on the degree of MS2 removal even though the pH of the suspension was varied from three to ten (McGahey and Olivieri (1993)). It has also been shown that with polypropylene membranes, microfiltration could be used to completely remove virus contaminants from feed solution. Belkowski (1992) has shown that microfiltration with 0.04 μm filters could be used to remove both E- and X-MLV from the suspension with the removal of up to more than 7 log titer reduction of virus could be accomplished.

The removal of poliovirus from tap water by microfiltration with 0.22 μm membrane was shown to be approximately 54% (Hou et al. (1980)). However, the level of removal was increased to 99% when an electropositive membrane was utilized and decreased to 35% when the electronegative membrane was utilized. Moreover, a Millipore cellulose nitrate membrane with 0.22 μm pore size was reported to be able to retain poliovirus up to 95 - 100% (Kostenbader and Cliver (1983)).

Urase et al. (1994) have demonstrated that membrane module configuration was not a major factor affecting virus retention. They found that pore size distribution is the most important parameter to be considered when membrane filtration is to be used to remove viruses from suspension. Furthermore, they conducted experiments on coliphage Qβ removal by membrane filtration processes and found that with new

membranes virus adsorption to both membrane and surface deposits is probable (Urase et al. (1993)). However, even though virus is negatively charged at neutral pH, virus adsorption to the membrane surface is not critical if the membrane possesses no strongly positive charge (Urase et al. (1994)). They further found that as filtration proceeds the resistance of the membrane as well as the rejection of viruses increases. Further, they inferred that deposits on the membrane surface may play a significant role in virus rejection by the membrane.

2.1.3.2. Virus Removal by Flocculation

It is well known that mammalian cells are negatively charged due to sialic acid residues present on the cell surface glycoprotein (Aunins and Wang (1989), Greig and Jones (1976)) in aqueous-based medium. Additionally, cell surface charges may originate from membrane phospholipids and glycolipids (Alberts et al. (1983)). A number of studies have shown that either chemical flocculants (coagulants) such as metal salts or (cationic) polymeric polyelectrolytes could be used to induce aggregation of mammalian cells in suspension. Baran (1988), who carried out flocculation of cellular suspensions by cationic polymers, has postulated that the key mechanism of cellular flocculation is surface charge neutralization. The author further suggested that the effectiveness of polyelectrolytes could be estimated from either their molecular weight or their molecular parameters in solution depending on both charge density and rigidity of the polymer chains. Baran (1988) subsequently concluded that good flocculants for cellular suspensions are the flexible cationic polyelectrolytes.

Hughes et al. (1990) found that there are differences between flocculating washed cells and suspended cells in complex medium. Washed cells can easily be flocculated by cationic polymers while suspended cells are quite difficult to flocculate because of the interference of the organic compounds in the growth medium (Johnson et al. (1967), Hughes et al. (1990)). In addition, bacteria and yeast, i.e., *Escherichia coli* and *Saccharomyces cereviseae*, have been used extensively in a number of flocculation studies. It has been shown that bacteria and yeast cells are successfully flocculated by cationic polymers. It is not surprising that yeast cells can be easily flocculated due to the fact that yeast cells have zeta potential in the range of – 30 to 10 mV at a pH of 6.5 and 3.0, respectively, in distilled water (Thonart et al. (1982)). Due to the fact that envelope (capsids) of virus particles derived from the cytoplasmic membrane of the host cells which usually possesses negative charges at neutral pH in aqueous suspension (Bitton (1975)), virus particles are also negatively charged in aqueous solution at neutral pH. Consequently, it is possible to induce flocculation of virus suspension by cationic polyelectrolytes.

Conventionally, the removal of viruses from suspension has been carried out by flocculation by chemical reagents in conjunction with gravitational settling (or sedimentation). Regularly, $FeCl_3$, $Fe_2(SO_4)_3$ and $Al_2(SO_4)_3 \cdot 18H_2O$ were used as primary flocculants in surface and ground water treatment processes. For water treatment plants, enteroviruses are of primary concern since these enteric viruses were found to be able to survive for a long period of time. For instance, it has been found that polioviruses (Gilcrease and Kelly (1955), Poynter (1968)) and hepatitis viruses (Neefe and Stokes (1945)) could survive and retain infectivity after exposure to surface water

for 91 and 70 days, respectively. There are a number of studies on virus removal from suspension for the past half century. These studies used both metal salts and polymers either as primary flocculants or flocculant aids to remove viruses from dilute suspension by flocculation (or coagulation) (Amirhor and Engelbrecht (1975), Thorup et al. (1970), York and Drewry (1974)). Metal salts especially $Al_2(SO_4)_3 \cdot 18H_2O$ and $FeCl_3$ were found to be effective in removing viruses from dilute suspension, however, high dosages were imperative to achieve high flocculation efficiency (Chaudhuri and Engelbrecht (1970)). Further, flocs formed by metal salts are of high volume that cause disposal problems (Yang (1996)). Therefore, due to the economic constrains alternative flocculants were investigated.

Polyelectrolytes have gained considerable attention due to their effectiveness in cellular flocculation. However, the findings are inconsistent. Cationic, anionic and nonionic polyelectrolytes are utilized to remove viruses from many processes including potable water, surface water (Chaudhuri and Engelbrecht (1970)) and wastewater treatment plants (Thorup et al. (1970), York and Drewry (1974)). While some investigators found that polyelectrolytes have no effect on virus removal (York and Drewry (1974)), a number of studies have demonstrated that polyelectrolytes are highly effective. Cationic polymers were found to be superior to both anionic and nonionic polymers in removing viruses from dilute suspension (Nasser et al. (1995), Johnson et al. (1967)). Malek et al. (1981) found that as much as 98% removal of bacteriophage MS2 could be achieved in the presence of turbidity. They further proposed that the effectiveness of virus removal by polyelectrolyte flocculation was due primarily to the entrapment of virus particles in the aggregates.

Chaudhuri and Engelbrecht (1970) have shown that up to 99.9% removal of both bacteriophage T4 and MS2 could be achieved by aluminium sulfate (alum) coagulation. They further found that organic matter such as albumin could interfere with virus removal (Amirhor and Engelbrecht (1975), Manwaring et al. (1971)). Thorup et al. (1970) who studied the removal of T2 phage and poliovirus type 1 by ferric chloride and ferric sulfate coagulation found that 93 – 96 % of T2 phage removal could be expected; 85% removal of polioviruses was observed at high salt concentration. York and Drewry (1974) found that while one cationic polyelectrolyte, Cat Floc (Calgon), was highly effective for virus removal, another, Drewfloc 21 (Dow Chemical) was ineffective. However, no information on the polymer characteristics was provided, therefore, no comparison of the properties of the polymers could be made.

Nonetheless, it is noteworthy to keep in mind that polymer properties such as charge density, molecular weight and type of ionogenic (ionizable) group are highly significant when choosing polymeric flocculants. Additionally, it has also been found that cationic polyelectrolytes are highly toxic to mammalian cells, and viruses can be recovered by eluting the sludge with appropriate eluant (Manwaring et al. (1971)). Johnson et al. (1967) carried out flocculation of both tobacco mosaic viruses (TMV) and polioviruses in 0.17 M NaCl at 7.0 pH suspensions and found that 52% of adsorbed viruses could be recovered by eluting the aggregates with 1 M NaCl. The author also found that 99.9 – 99.99 % of the polioviruses could be removed from suspension, and that 100 % of TMV were found to be completely adsorbed by the polymers. Viruses were found by some investigators to be inactivated by cationic polymers as well (Chaudhuri and Engelbrecht (1970), Thorup et al. (1970)).

As the pH of the viral suspension was increased, a decrease in the degree of removal of MS2 phage was observed (Amirhor and Engelbrecht (1975), Manwaring et al. (1971)). This may be due to the fact that changes of the ionic environment affect the thickness of the electrical double layer on the virus particles as well as on the polymer chains; these factors lead to a lower degree of floc formation. On the other hand, the degree of removal of phage T4 was shown to be increased as the pH of the suspension was decreased (Chaudhuri and Engelbrecht (1970)). Aggregation kinetics of both polioviruses and reoviruses is qualitatively in agreement with the Smoluchowski theory of flocculation (Floyd and Sharp (1978)).

2.2 Flocculation

In a number of areas, such as mining, water and wastewater treatment, and biotechnology and pharmaceutical production, removal of particles (typically 0.1 – 10 μm) from suspensions and/or solutions is required. These small particles are often thermodynamically and chemically stable in suspension. Therefore it is more difficult to separate them from suspension. In order to remove these colloidal particles, particles in suspension are destabilized. Consequently, these particles tend to aggregate into larger size particles. There are a number of ways to alter the stability of suspensions such as changes of temperature and addition of chemicals, i.e., metal salts and organic/inorganic polymers.

Furthermore, in order to quantitatively understand the flocculation process, several topics are important. To begin with, when charged particles are present in the suspension, there exists the electrical double layer around the particle surfaces. This

electrical double layer, which gives rise to the potential at the particle surfaces, dictates ranges of interaction between particles. There are several models (Gouy-Chapman (Gouy (1910, 1917), Chapman (1913)) and Stern (1924)) that have been proposed to schematically explain this phenomenon. Moreover, the stability of charged particles in suspension could be at the least qualitatively approximated by the DLVO theory (Derjaguin and Landau (1941), Verwey and Overbeek (1948)). These topics are discussed in some detail below.

2.2.1. Definition

Flocculation is the process that takes advantage of the shifted stability by addition of polyelectrolytes, such as water-soluble polymers, and complex metal salts to induce aggregation of small particulates in suspension. Sometimes, flocculation is used to describe aggregation of particles that is reversible while, for coagulation, the aggregation is irreversible (Eidsath (1989)). Furthermore, in some cases, coagulation is referred to as a process in which aggregation of the particles is induced by addition of metal salts such alum ($Al_2(SO_4)_3$) and ferric chloride ($FeCl_3$) whereas flocculation is referred to the aggregation induced by polymeric flocculants (Vincent (1974)). However, there is no definitive indication to distinguish between the two processes. Therefore, the term "flocculation" will be used throughout this thesis.

2.2.2. Flocculation Theory

When charged particles are present in aqueous solution they may be either thermodynamically or chemically stable, which renders the difficulties in separating

them from suspension. The particle size distribution may be altered by inducing aggregation of these fine particles by adding metal salts such as alum, ferric chloride and polymer flocculants. For polymer flocculation, it has been successfully shown that cationic polyelectrolytes could be effectively used to induce aggregation of negatively charged cellular suspensions (Kim et al. (2001), Aunins and Wang (1989), Baran (1988), Hughes et al. (1990)).

The charged particles in suspension were destabilized by charge neutralization. Subsequently, collisions between these destabilized particles are induced by agitation of the suspension. The higher the frequency of collision the higher the flocculation rate. However, there are a number of important parameters that may play a significant role in flocculation processes such as shear rate, concentration of particles and polymers in the suspension, stirring speed and time including size distribution of the particles to be flocculated.

For flocculation induced by both polymer and metal salt flocculants, at low flocculant dosages the percentage of surface coverage of the particles by polymer is small. At this point, efficacy of flocculation is not sufficiently high. As the amount of added flocculants increases the efficiency of flocculation also increases up to the optimum dose, where the ratio of added flocculants is equivalent to the available particle surfaces and the flocculation efficiency is the highest. Beyond this optimum point, an excess amount of flocculants will deteriorate the flocculation efficiency due to the phenomenon know as "charge reversal" or "restabilization". In other words, adsorption of excess flocculant leads to a reverse of the charge on the particles and consequently restabilization of the particles.

2.2.3. Flocculation Mechanism

As mentioned earlier, flocculation is the process in which small particulates are induced to form aggregates. The essential steps (Gregory (1983)) in flocculation of suspended particles are destabilization of the particles and collision of these destabilized particles to form larger aggregates. Destabilization is the result of adsorption of ions and/or polyelectrolytes from the bulk solution onto the particle surfaces. With the presence of flocculating agents such as aluminum salts and polymeric flocculants, destabilization is achieved by means of charge neutralization of complex metal salts and polymeric flocculants by adsorbing onto the particle surfaces.

There are two mechanisms (Figure 2-2) responsible for the destabilization of particles, charge patch effect (Figure 2-2a) and polymer bridging (Figure 2-2b). The "electrostatic charge patch effect" model was independently proposed by both Gregory (1973), who studied the flocculation of polystyrene latex particles by cationic polymers, and Kasper (1971), who studied flocculation of charged particles by oppositely charged polyelectrolytes in aqueous solution. The polymer bridging was first proposed by Ruehrwein and Ward (1952) to explain the aggregation phenomenon of clay particles by polymers. The assumption, according to Gregory, for the electrostatic charge patch effect is based on the immobility of the charges on the latex particle surfaces while the assumption for bridging flocculation is that each polymer chain can bind to more than one particle and therefore "bridge" them together to form larger aggregates. The origin of the charge patch mechanism is the uneven distribution of charges on the particle surface leading to an additional attractive force due to the interaction energy, which is of an electrostatic nature, between two different particles (Gregory (1973)). Gregory

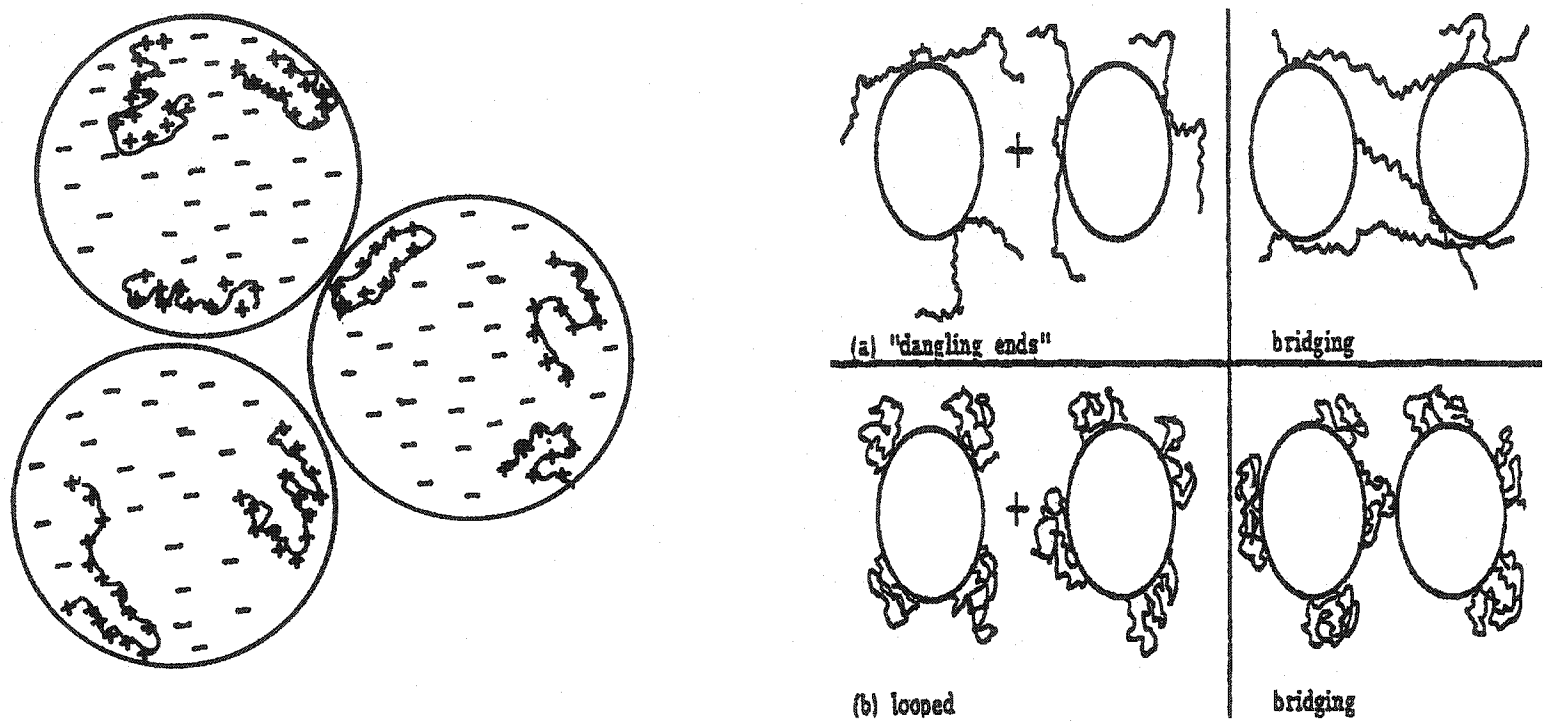

(a) Electrostatic patch model

(b) Polymer bridging

Figure 2-2 Flocculation mechanisms for negatively charged particles and cationic polyelectrolytes: (a) Electrostatic patch model and (b) Polymer bridging

(1973) has also stated that in order for the electrostatic charge patch effect to play an important role the polymeric flocculants should be of relatively low molecular weight, which is approximately 50,000 or smaller. The higher the molecular weight of the polymers the lower the efficiency of the polymeric flocculants to induce flocculation by electrostatic charge effect.

For polymer bridging to dominate, polymeric flocculants must possess a chain length that is sufficiently long to bridge two different particles together. The chain length of the polymer is generally assumed to be at least $2\kappa^{-1}$, which is twice the thickness of the double layer around the colloidal particles (Pelssers et al. (1989)). Furthermore, once a polymer attaches to a given particle, the polymer chain should ideally extend into the bulk solution as "loops" and "tails" (Figure 2-2b). These "loops" and "tails", which are dangling into the suspension from the particle surface, bind to other particles that came into contact via fluid motion or diffusion. It has been demonstrated that with polymers of high molecular weight bridging flocculation is favorable (Gill and Herrington (1987a)). However, molecular conformation of polymers is significantly governed by the ionic strength of the suspension. At low ionic strength, polymers with high molecular weight and high charge density tend to have an extended conformation due to the repulsion between the neighboring ionogenic (ionizable) groups while at high ionic strength the converse is true. Therefore, for bridging flocculation to take effect, a low ionic environment is advantageous.

On the other hand, in order for electrostatic patch effect to dominate the polymeric flocculants should be non-uniformly adsorbed onto the particle surfaces in a rather flat configuration, which is the case for a high charge density polymer. This

would result in particles whose surfaces having both negatively and positively charged patches (Figure 2-2a). Aggregation of the particles in this system takes place when the patch bearing positive charge of one particle collides to the portion bearing negative charge of another particle. However, whether polymer bridging or electrostatic patch effect is the dominant effect in polymeric flocculation may depend on the conditions of the system under study.

2.2.4. Flocculation Kinetics

It is not easy to predict the rate of flocculation for any particular system. However, in general, flocculation kinetics may be classified into 4 categories, which are perikinetic, orthokinetic (laminar), turbulent and differential settling. Perikinetic flocculation results from particle collision due to the Brownian motion of the particles. The random motion of the particles, which is caused by their thermal energy, leads to collisions between particles. Floc formation due to perikinetic is slow for a dilute system. The initial rate of decline of the total particle concentration may be estimated by the following relationship

$$-\frac{dn}{dt} = \left(\frac{4k_B T}{3\mu}\right) \cdot n_T^2 \qquad (2\text{-}25)$$

where $k_F = (4k_B T/3\mu)$ is known as the flocculation rate constant whose value is approximately 6.13×10^{-18} m^3s^{-1} for aqueous solution at 25 °C. The above equation may easily be integrated and rearranged to

$$n_k = n_0 \cdot \frac{(t/t_F)^{k-1}}{(1+(t/t_F))^{k+1}} \qquad (2\text{-}26)$$

The above equation is the general Smoluchowski equation to estimate the number of particles present in the suspension while the expression to estimate the collision rate is given as

$$J_{ij} = \frac{2k_B T}{3\mu} \cdot \frac{(a_i + a_j)^2}{a_i a_j} \cdot n_i n_j \tag{2-27}$$

Orthokinetic flocculation is the result of fluid motion by agitation. Floc size and strength is dependent on the fluid velocity gradient, which governs the collision rate of the particles. In orthokinetic flocculation, the particle number concentration decreases exponentially with time. The collision rate of the particles due to orthokinetic is defined as

$$J_{ij} = \frac{4}{3} \cdot (a_i + a_j)^3 \cdot G n_i n_j \tag{2-28}$$

Further, the rate of decline of the total particle concentration could be obtained from

$$-\frac{dn}{dt} = \frac{16}{3} \cdot n^2 G a^3 \tag{2-29}$$

Since in turbulent flocculation there exists an ensemble of eddies in which a single velocity gradient may not be used to describe the behavior of the system. A number of correlations to determine the collision frequency have been proposed by several investigators (Staffman and Turner (1956), Delichatsios and Probstein (1975)). The concise review of expression regarding to turbulent flocculation is provided by Han et al. (2003). The collision rate of particle due to turbulent flocculation is (Amirtharajah and Trussler (1986))

$$J_{ij} = \frac{(a_i + a_j)^3}{6} n_i n_j \left(\frac{\varepsilon}{\nu}\right)^{1/2} \tag{2-30}$$

For differential settling, different particle size will settle at different rates due to the effect of the gravitational field, which results in the collision of the particles and therefore flocculation. This effect is directly proportional to the differences of the densities of the particles and that of the medium. Differential settling will be more important when the particles are fairly large and dense. The collision rate of particles due to differential settling is given as

$$J_{ij} = \frac{2\pi g}{9\mu} \cdot (\rho_s - \rho)(a_i + a_j)^3 (a_i - a_j) \qquad (2\text{-}31)$$

Comparison of the apparent effect of some of these mechanisms is provided in Figure 2-3. Perikinetic collisions are predominant only when the size of the second particle is around 0.1 μm or less. For large particles, orthokinetic collisions are important and become dominant at about 1 μm. Differential settling becomes dominant when the second particles have the size of about 5 μm.

2.2.5. Electrical Double Layer

When particles are present in aqueous solution, surface charges on the particles may arise due to three mechanisms (i) ionization of surface groups, e.g., ionization of surface carboxyl and amino groups on biological particles, (ii) isomorphous substitution in lattices of solids, e.g., replacement of Si^{V} by Al^{III} in clay and (iii) specific ion adsorption of ionic surfactant at oil-water interface or preferential adsorption of Ag^{+} over I^{-} onto AgI solids. Each mechanism has characteristic properties, which causes the surface to have either constant charge or constant potential (Kasper (1971)). Due to surface charges on the particles, there exists an electrical double layer around them,

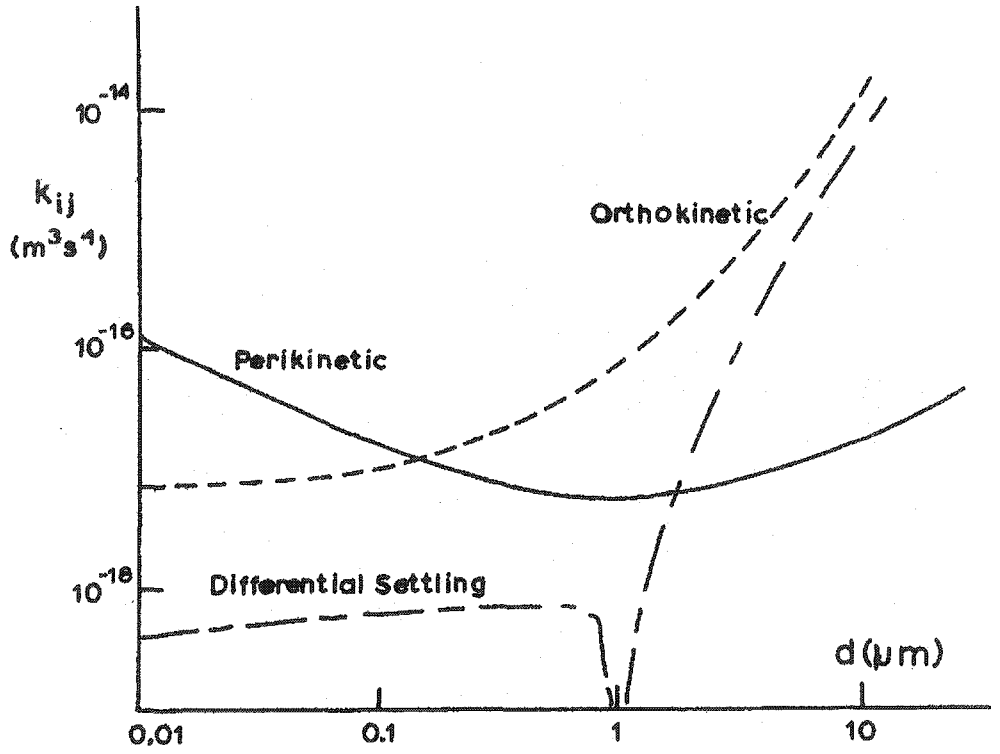

Figure 2-3 Calculated collision rate constants for a particle of 1 mm diameter and a second particle of diameter *d*. The shear rate is taken as 50 s^{-1}, and the specific gravity of the particles is 2

which may prevent particles possessing charges of the same sign to approach each other (Gregory (1983)) as a result of repulsive forces. This so called "electrical double layer" originates from the non-uniformed distribution of both co-ions and counter-ions around charged particles. With the presence of the electrical double layer, the potential of interaction on the particle surface cannot be determined directly. There are a number of theoretical models, which have been proposed to explain the phenomenon of electrical double layer and the distribution of potential around the particle surface.

2.2.5.1. Stern Model

Stern model (Stern (1924) of the electrical double layer is adopted here due to the fact that Stern model may readily be applied to more pragmatic systems. However, there are difficulties in using the Stern model since physical properties such as the viscosity and the dielectric constant of the solution in the double layer must be determined.

In the Stern model (Figure 2-4), it is assumed that the counterions are strongly adsorbed onto the surface of the particles. Therefore, the surface potential of the particles will be determined at some distance, δ, from the true particle surface. This distance is called Stern layer. The potential is called Stern potential, ψ_δ. However, this potential cannot be measured or calculated by classical electrokinetic methods. In addition to the "Stern layer", co-ions will form an ion cloud around Stern's layer. This layer is designated as a "diffuse layer". The true particle surface potential is assumed to be equal to the potential at the shear plane, namely zeta potential, ζ. According to Smoluchowski theory (Smoluchowski (1916)), zeta potential may be calculated from either Helmholtz-Smoluchowski or Hückel equation (Hunter (1981)).

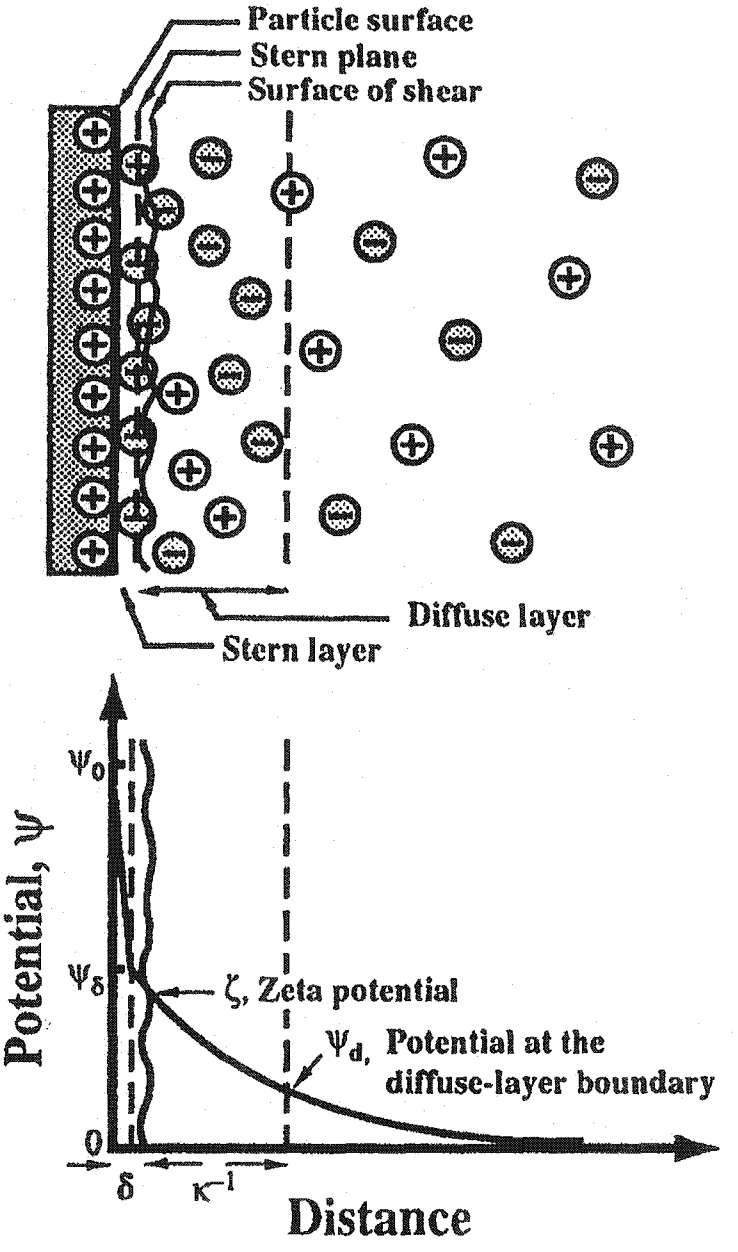

Figure 2-4 Schematic illustration of the variation of potential with distance from a charged wall in the presence of a Stern layer

The Hückel equation (2-32) may be applied when $\kappa R < 0.1$ whereas the Helmholtz-Smoluchowski equation (2-33) could be used when $\kappa R > 100$ where κ is the Debye-Hückel length and R is the radius of the particle. These equations are of the form

$$u = \frac{2\varepsilon\zeta}{3\eta} \tag{2-32}$$

$$u = \frac{\varepsilon\zeta}{\eta} \tag{2-33}$$

where u, η and ε are electrophoretic mobility, kinematic viscosity of the medium and dielectric constant, which is defined as the products of the dielectric constant of free space (ε_o) and that of the medium (ε_r), respectively.

2.2.5.2. Debye-Hückel Parameter

From Stern's model of the electrical double layer around the particles, the thickness of the double layer (κ^{-1}) may be calculated from the inverse of the Debye-Hückel length, κ, which is given as (Hiemenz and Rajagopalan (1997))

$$\kappa^2 = \left(\frac{e^2}{\varepsilon k_B T}\right) \cdot \sum_i z_i^2 n_{i\infty} \tag{2-34}$$

Due to the fact that $n_{i\infty} = 1000 M_i N_A$, where M_i and N_A are molar concentration and Avogadro's number, respectively, (2-34) may take the alternative form of

$$\kappa^2 = \frac{1000 e^2 N_A}{\varepsilon\ k_B T} \cdot \sum z_i^2 M_i \tag{2-35}$$

which involves the calculation of ionic strength, I, (Yang et al. (1997))

$$I = \frac{1}{2} \cdot \sum z_i^2 M_i \tag{2-36}$$

Therefore, by combining (2-35) and (2-36), the Debye-Hückel parameter may be approximated by (Greig and Jones (1976))

$$\kappa = \left[\frac{2000 e^2 N_A I}{\varepsilon k_B T} \right]^{1/2} \tag{2-37}$$

The Stern layer around particles in aqueous solution is in the range of 0.3 – 0.5 nm from the particle surface, which corresponds to the diameter of the hydrated ions. In general, the thickness of double layer around the particles is in the range of 1 μm in pure water and less than 1 nm in concentrated salt solutions (Gregory (1989)).

2.2.5.3. Zeta Potential

It is desirable to know the true potential at the particle surfaces. However, with the presence of the double layer around the particles, the true surface potential is difficult to determine experimentally. Therefore, an indirect approach must be used. Electrokinetics could be used to measure the motilities, which are defined as the ratio of particle velocity to the electric field strength, of the particles under the influence of electric field. Subsequently, the zeta potential could be easily obtained from the Smoluchowski theory by either the Helmholtz-Smoluchowski or Hückel equations.

On the other hand, zeta potential may be analytically determined. This is due to the fact that the variation of potential with distance from a charged surface of arbitrary shape can be described by the Poisson equation, and the ion concentration may be expressed in terms of the potential by means of a Boltzmann factor. By this method, the equation to be solved is the Poisson-Boltzmann equation, which reads

$$\nabla^2 \psi = -\left(\frac{e}{\varepsilon} \right) \cdot \sum_i z_i n_{i\infty} \exp\left(-\frac{z_i e \psi}{k_B T} \right) \tag{2-38}$$

where ∇^2 is Laplace operator, which can be transformed into spherical coordinates (Bird et al. (1960)) as:

$$\nabla^2 = \frac{1}{r^2}\frac{\partial}{\partial r}\left(r^2\frac{\partial}{\partial r}\right)+\frac{1}{r^2\sin\theta}\frac{\partial}{\partial\theta}\left(\sin\theta\frac{\partial}{\partial\theta}\right)+\frac{1}{r^2\sin^2\theta}\left(\frac{\partial^2}{\partial\phi^2}\right) \qquad (2\text{-}39)$$

According to Debye-Hückel approximation, the potential distribution around spherical particles is

$$\psi = \psi_0\left(\frac{R_s}{r}\right)\exp\left(-\kappa\left(r-R_s\right)\right) \qquad (2\text{-}40)$$

where R_s is the radius of the spherical particles and r is the distance at any point in the double layer from the center of the particles. The above expression satisfies the following boundary conditions

1. $\psi \to \psi_o$ as $r \to R_s$
2. $\psi \to 0$ as $r \to \infty$

2.2.6. The DLVO Theory

The interaction potential between charged particles in suspension may be quantitatively determined by using the DLVO theory that was independently developed by Derjaguin and Landau (1941) and Verwey and Overbeek (1948). This theory forms the basic understanding of colloid stability. According to the DLVO theory, there are primarily two important forces that are taken into account in calculating the interaction potential between charged particles, the London-van der Waals force and the electrical double layer force. While the London-van der Waals is attractive in nature, the electrical double layer is repulsive. A typical interaction potential curve is shown in Figure 2-5.

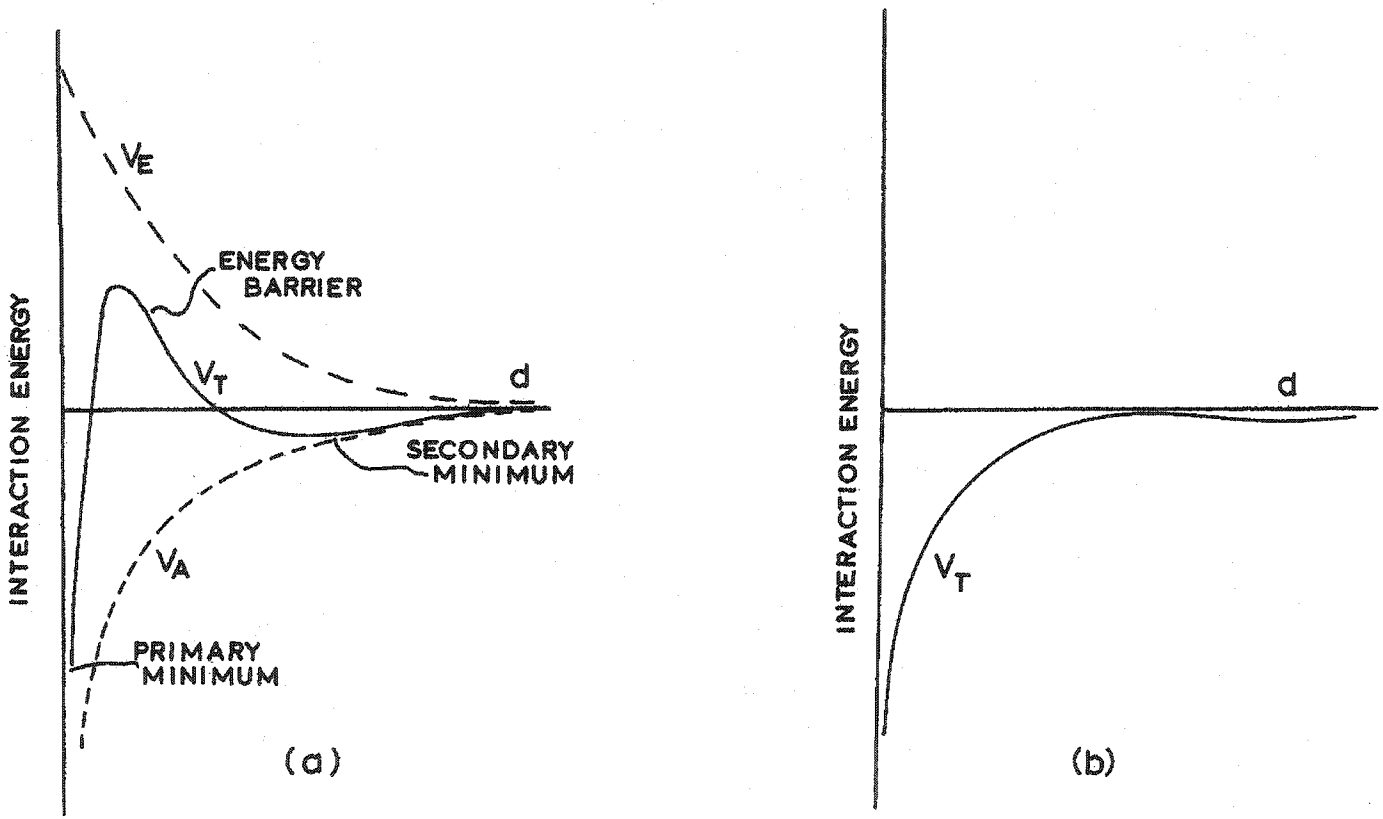

Figure 2-5 Potential curve: (a) Interaction potential diagram for the interaction of colloid particles. The van der Waals attraction, V_A, electrical repulsion, V_E, and the total energy, V_T, are shown as a function of the particle separation, d. (b) The total interaction potential, V_T, when the particles are at the onset of rapid flocculation.

As can be seen, at the onset of rapid flocculation (Figure 2-5b) the total interaction potential is negative when the attractive force outweighs the repulsive force leading to aggregation of particles in the system.

2.2.6.1. London-van der Waals Attractive Force

The London-van der Waals forces originate from the intermolecular forces of every molecule in the particle. It was proposed by Hamaker (1937) that these intermolecular forces, which are attractive in nature, complied with the pairwise additivity rule, which implies that the interaction between two particles may be estimated by summing up all intermolecular forces of every molecule in one particle with those of all of the molecules in the others. The interaction potential between two interacting spheres of unequal sizes is given as (Russel et al. (1989))

$$V_A = -\frac{A}{6}\left[\frac{2a_i a_j}{r^2-(a_i-a_j)^2}+\frac{2a_i a_j}{r^2-(a_i-a_j)^2}+\ln\frac{r^2-(a_i-a_j)^2}{r^2-(a_i-a_j)^2}\right] \qquad (2\text{-}41)$$

According to Lifshitz theory (Lifshitz (1956)), all screening effects due to the presence of electrolytes and retardation effects are included in the Hamaker constant (Eidsath (1989)). However, it is difficult to find an accurate Hamaker constant for either biological or non-biological system since the experimentally determined values of Hamaker constants are scarcely reported in literature except for silica (Vosel et al. (1999)) and mica surfaces (Tabor and Winterton (1969), Dahlgren et al. (1994)). In any case, according to Gregory (1989), Hamaker constants for all aqueous dispersions are in

the range of $0.3-10\times10^{-20}$ J. For dense mineral particles, the values of Hamaker constants are in the upper limit of this range whereas biological materials have the values of Hamaker constant towards the lower limit.

2.2.6.2. Repulsive Electrical Double Layer

In an aqueous solution of charged particles, an electrical double layer gives rise to repulsive forces or the electrical double layer forces, which are believed to be responsible for suspension stabilization, between particles with charges of the same signs. Therefore, the magnitude of these repulsive forces may be indirectly used as an indication of the range of interactions between particles in suspension. At some distance where attractive force outweighs repulsive force, flocculation will take place, otherwise, the particles remain in the suspension. The electrical double layer forces between two spherical particles of unequal size may be quantitatively estimated by (Gregory, (1975)).

$$V_R = \frac{4\pi a_i a_j \varepsilon}{(a_i + a_j)} \psi_i \psi_j \cdot \exp(-\kappa h) \qquad (2\text{-}42)$$

where a and ψ are radius and surface potential (zeta potential) of particle i and j, respectively, while κ and h are the Debye-Hückel parameter and separation distance, respectively.

There are a number of experimental observations that are not accurately described by the DLVO theory. It was subsequently found that there are a number of forces, i.e., hydration, Born repulsive forces, steric (Leong and Boger (1991), Leong et

al. (1993b)), depletion (Prestidge and Tadros (1988), Leong (1996)) and hydrophobic interactions (Leong et al. (1993a, 1996), Leong (1994,1997)), that play an important role in determining the range of interaction of charged particles.

2.2.7. Important Parameters

The rate and efficiency of flocculation are important from a practical perspective. If the flocculated suspension has to be further processed, size and strength of the formed flocs are also important. In order to achieve high flocculation rates, flocculation efficacies and strong flocs, several parameters such as velocity gradient, flocculation time, pH and ionic strength and concentrations of particles and flocculants have to be taken into consideration.

2.2.7.1. Velocity Gradient

To ensure effective flocculation, efficient collisions between particles and flocculant molecules must occur. This may be achieved by agitation of the suspension. Therefore, turbulent conditions, which ensure rapid mixing, must be attained since the velocity gradient is responsible for particle collision, and consequently, floc formation. Further, strength and size of flocs are also affected by the velocity gradient. Even though the velocity gradient induces particles collision, an excess velocity gradient could lead to fragmentation of large flocs. Therefore, it is likely that there exists an optimum value of the velocity gradient at which the maximum floc size and strength may be accomplished.

Camp and Stein (1943) were the first to simplify the Smoluchowski theory by introducing the concept of velocity gradient, G, which is usually defined as the following relationship (Cleasby (1984))

$$G = \left(\frac{\varepsilon}{\nu}\right)^{1/2} \tag{2-43}$$

where ε and ν are power dissipation per unit mass and kinematic viscosity, respectively. For flocculation processes, Camp and Stein (1943) derived a correlation between the total number of particle contacts and the velocity gradient. Further, they suggested that the flocculation rate is directly proportional to the velocity gradient and, therefore, the power input (dissipation) during mixing. Generally, velocity gradient is widely used as a design parameter in the design of rapid mixing and flocculation facilities (Cleasby (1984)). For water treatement, the traditional design values of the velocity gradient for rapid mixing and flocculation are 700-1,000 s^{-1} for 20-40 seconds and 10 -100 s^{-1} for 1,200-3,600 seconds, respectively (Amirtharajah and Trussler (1986)). While Smoluchowski theory was developed for the laminar flow region, the modified Smoluchowski theory, developed by Camp and Stein, was for the turbulent flow regime.

However, it is still questionable whether the velocity gradient is an appropriate parameter in turbulent flocculation. Cleasby (1984) proposed that the velocity gradient is an appropriate parameter when the particles to be flocculated are smaller than the Komogorov's microscale, η, which is defined as (Amirtharajah and Trussler (1986))

$$\eta = \left(\frac{\nu^3}{\varepsilon}\right)^{1/4} \tag{2-44}$$

Cleasby (1984) has further suggested that when the particles to be flocculated are larger than the Komogorov's microscale, the appropriate parameter for turbulent flocculation is

$(\varepsilon)^{2/3}$. In addition, the maximum floc size, d_{max}, may be correlated to the velocity gradient (Smith and Kitchener (1978), Parker et al. (1972), Tambo and Hozumi (1979), Mühle (1933)) by:

$$d_{max} = C \cdot G^{-n} \tag{2-45}$$

In order to estimate the power dissipation into the system, there are a number of correlations that could be used depending on the geometry of the system of interest. The energy dissipation for a stirred vessel may be estimated by (Spicer and Pratsinis (1996), Spicer et al. (1996))

$$\varepsilon = \left(\frac{N_P N^3 D^5}{V} \right) \tag{2-46}$$

where N_p is the impeller power number, N is the impeller rotational speed, V is the stirred tank volume and D is the impeller diameter. For Rushton impeller type, N_p is equal to 5 (Oldshue and Trussell (1991), Holland and Chapman (1966), Shaw (1994)). It is necessary to bear in mind that the impeller Reynolds number has to be larger than 1,000 in order to use the relatively constant N_p.

For a spinner flask equipped with 4-blade impeller, Aunins et al. (1989) have shown that the power dissipation into the system could be expressed as

$$N_p = \frac{P_o g_c}{N^3 D_i^5 \rho} \tag{2-47}$$

where P_o, N_p and N are power dissipation, impeller power number and impeller rotational speed, respectively, whereas D_i, ρ and g_c are impeller diameter, fluid density and gravitational constant, respectively. However, if the impeller Reynolds' number is

not sufficiently large, Aunins et al. (1989) found that the impeller power number, N_p, could be correlated to the impeller Reynolds' number as, for small impeller,

$$N_p = 52 \cdot \mathrm{Re}_i^{-0.45} \tag{2-48}$$

or for large impeller and $\mathrm{Re}_i > 2 \times 10^4$

$$N_p = 22 \cdot \mathrm{Re}_i^{-0.42} \tag{2-49}$$

While the impeller Reynolds' number is given as

$$\mathrm{Re}_i = \frac{D_i^2 N \rho}{\mu} \tag{2-50}$$

Alternatively, Nagata (1975) has demonstrated that the impeller power number for stirred vessels could be correlated to the impeller Reynolds' number (Appendix J). From relationship proposed by Nagata, it may be realized that both laminar and turbulent effects contribute to the power dissipation.

2.2.7.2. Flocculation Time

The floc strength and size are determined by the velocity gradient. However, the duration of exposure of the formed flocs to a velocity gradient is also important. Even though the velocity gradient induces collision between particles, it could also have an adverse effect if flocs were overexposed. For agitated systems, the frequency of exposure of flocs to the high shear impeller zone can be qualitatively estimated from the circulation time, t_c (Oldshue (1984))

$$t_c = \frac{V}{N_q N D^3} \tag{2-51}$$

where N_q is the dimensionless impeller capacity, which is equal to 0.9 for Rushton impeller type. Moreover, it has also been shown that the retention time is a function of impeller diameter and stirring speed (Uhl and Gray (1966)).

Additionally, the effect of flocculation time is almost always expressed as a combination of agitation time, t, and velocity gradient, G. This combination is designated as "Camp number", Gt, which is dimensionless. It has been demonstrated that there exists a range of Camp number over which the maximum floc size could be obtained, however, beyond the critical camp number, significant floc break-up will take place (Young et al. (2000)).

2.2.7.3. pH and Ionic Strength

Due to the fact that both particles and polymeric flocculants bear ionogenic groups on their surfaces when these particles are present in an aqueous solution the degree of ionization of these groups is strongly dependent on the pH of the suspending medium. This is particularly pronounced for amphoteric molecules that can readily exhibit either negative or positive charge depending on the pH of the solution. It is advantageous, therefore, when using cationic polyelectrolytes, to flocculate cells in a pH range where the colloidal particles are negatively charged.

Another important parameter that plays a critical role in flocculation is the ionic strength of the suspension. In general, ionic strength of the solution is dependent upon the salt content of the suspension. It is convenient to divide ions into two categories, potential determining and indifferent ions. Potential determining ions are important since these ions can adsorb onto the particle surface and alter the potential of the

particles, while the latter do not affect the potential of the system. Typically, the ionic strength is the parameter that determines the thickness of the double layer or the range of the double layer interaction around the particles (Figure 2-6a). It is evident from Figure 2-6 that the higher the ionic strength the thinner the thickness of the double layer and the lower the surface potential (Greig and Jones (1976)). Moreover, not only the concentration of electrolytes (ionic strength) but also the types of electrolytes (Figure 2-6b), e.g., 1:1, 2:2 and 3:3, have an effect on the thickness of the double layer.

For virus flocculation, it has been suggested that there should be an optimum ionic strength, which gives the optimum polymer chain contraction that allows the tightest binding of the polymer molecules to the virus particles (Thorup et al. (1970)). Further, it has also been shown that the binding of polymer and viruses becomes looser when the ionic strength of the suspension is not at optimum. It was found that, for a given dose of polymer (divinylbenzene-crosslinked styrene/maleic anhydride copolymer) to remove tobacco mosaic virus, the degree of removal increased as the ionic strength of the suspension increased (Johnson et al. (1967)). In order to choose the combination of pH and ionic strength, several parameters such as the polymer type and cell type have to be taken into consideration. However, it is difficult to quantitatively determine the role of pH and ionic strength due to the fact that the effects of both pH and ionic strength are complex and interrelated.

2.2.7.4. Particle and Flocculant Concentration

A high particle number density will result in a higher collision rate between particles and, consequently, according to Smoluchowski theory a higher rate of

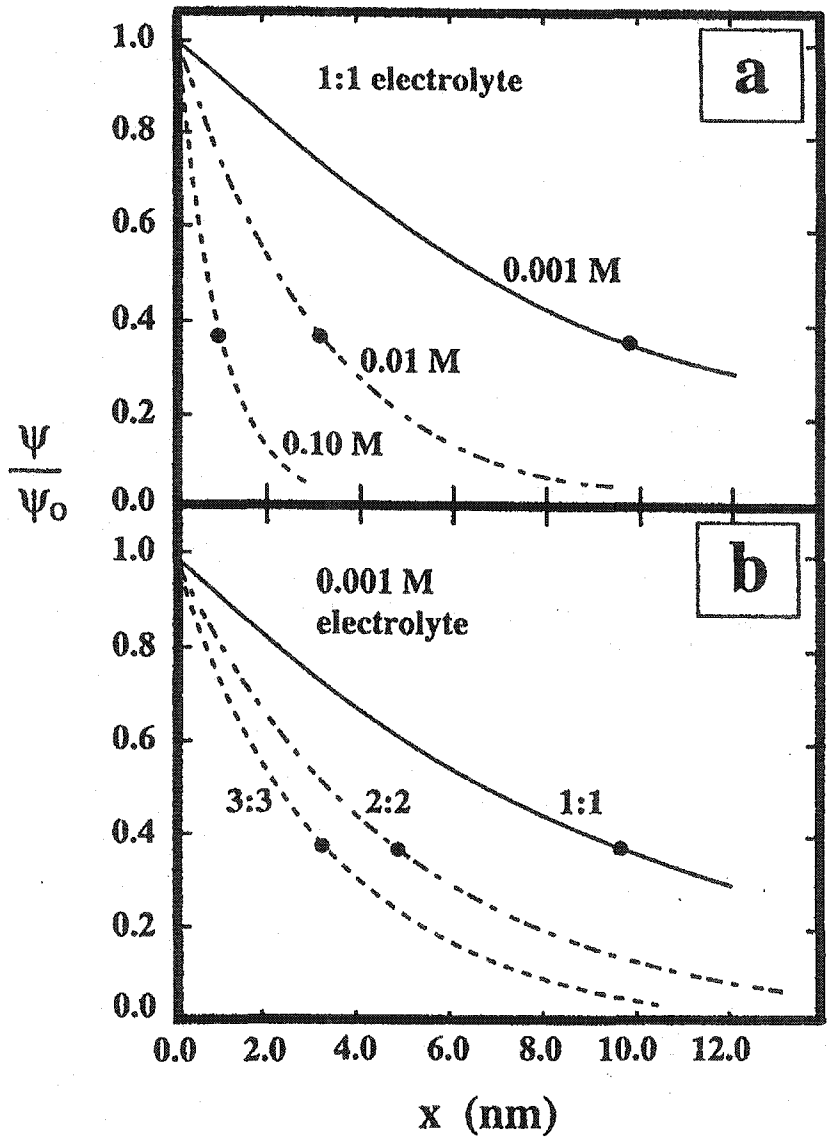

Figure 2-6 Fraction of double layer potential versus distance from a surface according to the Debye-Hückel approximation, (a) curve drawn for 1:1 electrolyte at three concentrations, (b) curves drawn for 0.001 M symmetrical electrolytes of three different valence types

flocculation. It is not surprising that a number of studies found that the higher the particle concentration the higher the collision efficiency and therefore the faster the flocculation rate of the particles (Higashitani et al. (1983), De Boer et al. (1989)). De Boer et al. (1989) and Higashitani et al. (1983) found that the coagulation rate of polystyrene particles destabilized by KCl in turbulent flow depended on the particle concentration to the power of 2 and 1.49, respectively.

Moreover, the concentration of polymeric flocculants is also important. It has been shown that an optimum dose of polymeric flocculants exists for flocculation of cellular suspension (Kim et al. (2001), and Drewry (1974)). For example, in our preliminary study with yeast (Kim et al. (2001)), it was found experimentally that the optimum dose of polymeric flocculant is a direct function of the number density (concentration) of yeast cells present in a given suspension. At this so called "optimum dose", it is believed that all the polymeric flocculants were used up to induce floc formation while, at the same time, almost all of the particles in suspension were included in the aggregates. At doses larger than the optimum dose, restabilization (charge reversal) is likely to take place whereas below the optimum dose inefficient (poor) flocculation may be expected.

2.2.7.5. Polymeric Flocculation

Even though collision of particles leads to particle aggregation, in reality, not all collisions result in flocculation of particles. La Mer and Healy (1964) proposed the concept of collision efficiency (E) as

$$E = \theta(1-\theta) \tag{2-52}$$

where θ is the fractional coverage of particle surface by adsorbed polymers. However, it was subsequently shown that the formulation proposed by La Mer and Healy (1964) is statistically incorrect whereas the correct formulation, after taking into account the statistics of collision between bare and coated particles, reads

$$E = 2\theta(1-\theta) \tag{2-53}$$

According to La Mer and Healy (1964), the fraction of surface coverage by adsorbed polymers that yields the highest capture efficiency is approximately 0.5. Other forms of collision, for instance, the collision efficiency of bridging flocculation, are given by Dickinson and Eriksson (1991).

In polymeric flocculation, the dynamics of the flocculation process may be described by three important characteristic times, the time for polymer adsorption (t_a), time for adsorbed polymer rearrangement (t_r) and time for particle collision (t_f). The time for polymer in suspension to adsorb onto the particle is

$$t_a = -\frac{\ln(1-f)}{k_{12}} N_0 \tag{2-54}$$

while the time for the total number of particles to reduce to half of the initial number concentration, for monodisperse suspension, reads

$$t_f = \frac{1}{k_{11}} N_0 \tag{2-55}$$

where N_o and f are the initial particle concentration and the fraction of polymer required to form stable flocs, respectively. If the polymer-particle and particle-particle encounters are diffusion controlled, the rate constants, k_{11} and k_{12}, are given by the Smoluchowski expression for perikinetic flocculation

$$k_{ij} = \left(\frac{2kT}{3\eta}\right) \cdot \frac{(a_i + a_j)^2}{a_i a_j} \qquad (2\text{-}56)$$

In the above equation, it is implicitly assumed that each polymer molecule may be represented as an effective hard sphere. For flocculation in shear suspensions, the expression for the rate constant may be replaced by the Smoluchowski expression for orthokinetic flocculation

$$k_{ij} = \frac{4G}{3} \cdot (a_i + a_j)^3 \qquad (2\text{-}57)$$

The relative values of t_a and t_f have been estimated by Gregory (1988) for typical polymeric flocculation conditions. For an initial number concentration of particles of 10^9 cm^{-3}, a shear rate of 50 s^{-1}, fraction coverage of 90% and particle diameter of 1 and 100 nm, t_a for perikinetic and orthokintic are 62 and 26 seconds, respectively. Further, Gregory (1988) has shown that under the same condition, t_f for both perikinetic and orthokinetic are 163 and 3.8 seconds, respectively.

For bridging flocculation, high molecular weight polymers with long chains are required. When polymer chains bind to particles there are some segments of the polymer chains that protrude into the suspension, which may "bridge" to other particles to form large flocs. However, upon binding to the surface, polymer molecule (chain) may take the form of "loops", "trains" and "tails" (Figure 2-7). Therefore, it is also believed that for the polymers to be highly effective in inducing "bridging" the polymer molecules should form "loops" and "tails" on the particle surface after binding (Figure 2-7). Further, the length of these so called "loops" and "tails" must be sufficiently long, at least $2\kappa^{-1}$, where κ^{-1} is the thickness of the double layer around the particle, in order

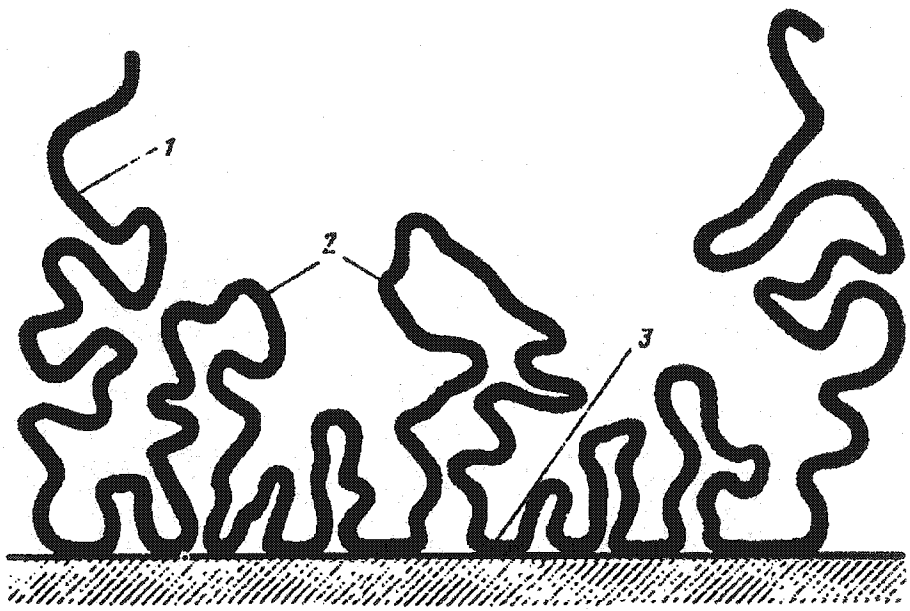

Figure 2-7 Distribution between "trains" (3), "loops" (2) and "tails" (1) in adsorbed polymer layers

to bridge two particles (Kitchener (1972)). For the electrostatic patch effect, it is proposed experimentally by Leong (1999) that each patch of the polyelectrolyte on the particle surface is composed of only one adsorbed molecule. Further, the author proposed that the patch area could be estimated from the radius of gyration of polymer in suspension. Consequently, if the patch area is known, the patch charged densities could be determined.

Polymers with high charge density when presents in a low ionic strength environment tend to stretch out (Gregory (1977), Michaels (1954)), therefore, resulting in longer chain length. These polymers were found to bind strongly to oppositely charged particles and have a rather flat configuration. It is well known that nonionic and low charge density polymers possess random coiled configurations in low ionic strength environment. Therefore, it is still questionable as to what types of polymers should be used to induce bridging flocculation. It has been shown that high molecular weight polymers, especially cationic polyacrylamides, induce flocculation of negatively charged particles mainly by bridging (Gill and Herrington (1987a)). It has also been demonstrated that the percentage of positive charge densities on the polymer molecules is not as important as the chain length of the polymer in determining the efficacy of flocculation by polymer bridging (Gill and Herrington (1987b)).

2.3 Colloid Titration

Colloid titration technique (Terayama (1952)) is based on the metachromatic shift in the absorption spectrum of the basic dye, toluidine blue O, which is capable of forming a purple complex when bound to anionic groups. Primarily, the method of

colloid titration is used to determine charge density of polyelectrolytes (Thethi et al. (1997), Horn and Heuck (1983)). However, this method can also be used to determine the concentration of polyelectrolytes in suspension (Hutter et al. (1991), Wang and Shuster (1975)) as well as the negative surface charge content of cells (Ando and Tsuzuki (1984), van Damme et al. (1992, 1994)).

2.3.1. Cationic Polyacrylamide Concentration

Since, due to ionic interactions, polymeric flocculants adsorb onto the surface of cells to neutralize surface charges of CHO cells, which are usually negative at neutral pH, therefore, the level of cationic polyacrylamide uptake or the adsorption isotherm is of significant interest. There are a number of techniques that may used to determine the concentration of cationic polyacrylamides in suspension; these include turbidimetric (Dubin and Davis (1990), Mattison et al. (1995)) and Distillation-Nesslerization (Thompson and Morrison (1951)). However, these techniques are either time-consuming or too complicated to be performed routinely. For example, even though the turbidimetric method is applicable over a wide range of pH, this technique is sensitive to the concentration of added salt (buffer).

By using colloid titration, the concentration of cationic polyelectrolytes in suspension may be quantified by direct titration with standard polyanion and an appropriate indicator. Potassium polyvinyl sulfate (PVSK) and Glycolchitosan (Gch) (Ueno and Kina (1985)) are used as a standard polyanion and a standard polycation, respectively, while toluidine blue O, which is cationic blue colored dye, is used as indicator. Due to the fact that toluidine blue does not interact with the cationic

polyelectrolytes, the color of the solution is bluish when the suspension contains only cationic polyelectrolyte.

As the titration proceeds, the color of the solution remains unchanged until the endpoint is reached when the color of the solution changes sharply to bluish purple due to the interaction between toluidine blue and anionic groups (Wang and Shuster (1975)). For anionic polyelectrolytes, direct titration with standard polycation (Gch) is not possible due to the lack of a suitable indicator (Ueno and Kina (1985)). Therefore, the anionic polyelectrolyte sample has to be primarily reacted with excess standard polycation and, subsequently, the unreacted standard polycation is back-titrated with standard polyanion using toluidine blue as an indicator.

2.3.2. Negative Surface Charge Content

Typically, surface charges of biological materials especially mammalian cells and viruses are generally determined by measuring electrophoretic mobilities of cells and virus particles under the influence of the electric field, i.e., microelectrophoresis (Penrod et al. (1995)) and electrophresis (Seaman (1975)), and then make use of mathematical expressions to relate these mobilities to zeta potential. Generally, fairly good agreement between electrophoretic mobility techniques and chemical analysis is achieved, e.g., red blood cells (Seaman et al. (1977), Janot et al. (1990), Vargas et al. (1989)). However, the charge density of endothelial cells, which is determined by electrophoretic techniques, was found to be much smaller than the chemically determined amount of sialic acids alone and the charge density remains unchanged even though the cells were treated with neuraminidase (Vargas et al. (1990)). Subsequently, it

was concluded that sialic acid weakly contributes to the surface charges determined by electrophoresis whereas the principal contributor to surface charges of the endothelial cells is glycoaminoglycans (Vargas et al. (1989, 1990)).

For surface charge determinations by colloid titration, toluidine blue is primarily reacted with anionic groups on the cell surface yielding purple-colored complexes. Subsequently, the cationic polyelectrolyte (Cat-Floc) is added leading to the displacement of toluidine blue from the anionic group and, at the same time, free anionic group (AC) then reacted with Cat-Floc. The reaction mixture turns from bluish purple to light blue and the volume of Cat-Floc is recorded (PC_1). Then twice the recorded amount of Cat-Floc (PC_2) is added to the suspension to saturate all the anionic groups on the cell surface. An excess amount of Cat-Floc is back-titrated by standard polyanion, dextran sulfate (DS). The negative surface charge can simply be calculated as

$$AC = PC_1 + PC_2 - DS \qquad (2\text{-}58)$$

where AC is the total free anionic charge on the cell surface, PC_1 and PC_2 are the total charge of Cat-Floc added at the first and the second time, respectively, and DS is the total charge of dextran sulfate. It was established that the charge concentration for Cat-Floc is 5.48 μeq/mg whereas the charge concentration for dextran sulfate is 5.74 μeq/mg, which is independent of molecular weight in the range of $8\times10^3 - 5\times10^5$ (van Damme et al. (1992)).

2.4 Murine Luekemia Virus

Viruses are obligate intracellular parasites (Flint et al. (2000)) meaning they can replicate only in the host cells. The virions can stay dormant outside host cells for a long

period of time and can resume all of the intracellular activities once again after entering host cells. Virus particles contain either RNA or DNA, which can be either single or double stranded, inside the protein capsid or envelope.

2.4.1. Structure and Classification

Murine Leukemia Virus (MLV), belonging to the genus of Mammalian C Type retroviruses, is a member of the *Retrovidae* family. Retroviruses consist of a large number of infectious agents (Murphy et al. (1995)). While some retrovirus infections can be deadly causing diseases such as AIDS, neurological disease and a variety of malignancies, on the other end, infection by retroviruses may cause no adverse effect. In the latter case, the retroviral genome can become established as a part of the host DNA and can pass through as an "endogenous virus" from generation to generation (Coffin (1992). These viruses are sometimes called "oncoviruses" since they may cause malignant tumors upon infection.

Retroviruses may be classified, according to virion structure and mode of replication into five groups, as particles of type A, B, C, D and lentivirus (Coffin (1992)). A-type particles are not true virions but are strictly intracellular structures composed of nucleocapsids. They are believed to represent the "retrotransposons" which are the elements that strongly resemble retroviruses in genome organization and mechanism of replication but lack *env* genes and do not have an extracellular phase in their life cycle. B type particles, for example, the mature virion of mouse mammary tumor virus, are assembled via budding of A particles into an immature form resembling A particles with an envelope. While C particles are true virions with a centrally located

form whose surface projection is visible but less prominent, D particles resemble B particles in assembly, maturation and morphology but have a less prominent surface projection and a cylindrical core.

The C type particles which are the true virions can be further classified into five groups according to the membrane tropism (Hunters (1997, Rein (1982), Rein and Schultz (1984), Sommerfelt and Weiss (1990)) and interference pattern, which are ecotropic, xenotropic, amphotropic, polytropic (or pantropic) and 10A1. Ecotropic MLV (E-MLV) was the first to be isolated. It can efficiently infect only its natural hosts, which are mice. Xenotropic MLV (X-MLV), in contrast to E-MLV, cannot productively infect cells of its natural host but can easily infect cells of the nonrodent species. The polytropic MLV differ from E-MLV and X-MLV in their host range and interference pattern (Hartley et al. (1977), Fischinger et al. (1975), Rein (1982)). This group of MLV can infect both rodent and nonrodent hosts, however, their ability to infect nonrodent species is more restricted than that of the X-MLV. The polytropic MLV are sometimes called mink focus-forming MLV due to their abilities to induce foci on mink lung cells (Hartley et al. (1977)).

Amphotropic MLV (A-MLV) can infect both rodent and nonrodent species; nevertheless, they differ from other MLV in their antigenic and interference properties (Rein (1982)). It has been demonstrated by tryptic mapping and restriction enzyme analysis that there is little variation among A-MLV isolates. 10A1 is a recombinant derivative between A-MLV and MX27, a prototype of the endogenous sequences involved in the creation of MCFs (mink cell focus forming viruses) that are capable of infecting hamster and rats cells (Rasheed et al. (1982). Receptors for 10A1 are Pit1

(Ram1 or Glvr2) and Pit2 (Glvr) which are classified as sodium-dependent inorganic phosphate transporter (Sommerfelt (1990), Kavanaugh et al. (1994), Miller and Miller (1994)). The amino acid sequences of 10A1 are found to be closle related to that of both the A-MLV and MCF (Ott et al. (1990).

The MLV virions (Figure 2-8) are spherical, enveloped and approximately 80 – 130 nm in diameter (Murphy et al. (1995)). They also have glycoprotein surface projection (or "knob-like" structure) of about 8 nm in length and 60 – 80 °A in diameter (Nermut et al. (1972)). These "knobs" were found to be loosely attached to the virion surface and could be partially removed by proteolytic enzyme treatment (Murphy et al. (1995)). The virions are sensitive to heat, detergent and organic solvents such as formaldehyde, however, they are relatively resistant to UV light and pH treatment (McClure et al. (1990)). The genome of MLV consists of a dimer of linear, positive sense, single stranded RNA. The RNA monomers (8.3 kb) are held together by hydrogen bonding. The buoyant density of retrovirus particles in sucrose is approximately 1.16 – 1.18 gram per cm^3.

2.4.2. Entry and Receptors

In order for an effective infection to take place, interaction between virus and host cell surface receptors (binding) is imperative. Entry of retroviruses is believed to take place by the mediation of virion envelope glycoprotein and receptors on host cell surface. After entering host cells, cDNA is transcribed by reverse transcriptase (RT) using 3′-OH of a tRNA as a primer and, at the same time, the RNA template is destroyed by the RNase H activity. However, the process of intracellular uncoating of

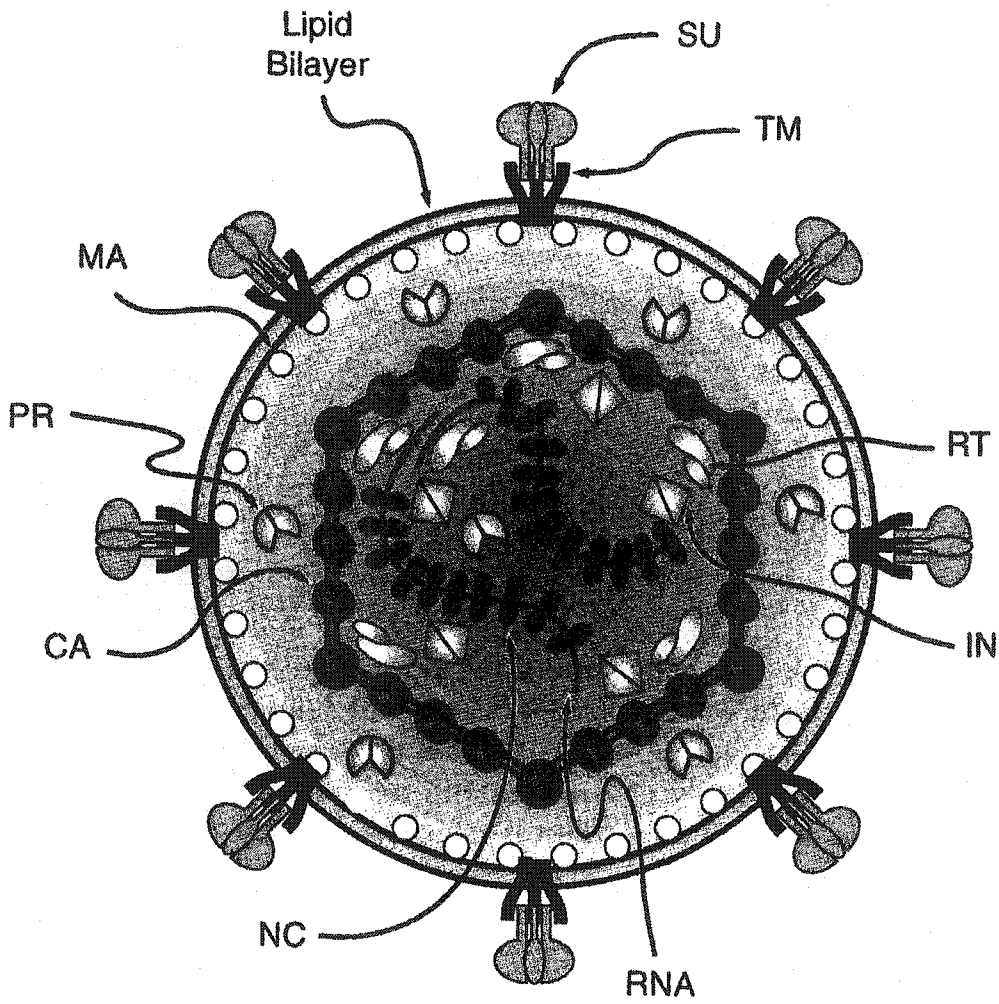

Figure 2-8 Schematic cross section through a retroviral particle. The viral envelope is formed by a cell-derived lipid bilayer into which proteins encoded by the *env* region of the viral genome are inserted. These consist of the transmembrane (TM) and the surface (SU) components linked together by disulfide bonds. Internal nonglycosylated structural proteins are encoded by the gag region of the viral genome. They are the matrix (MA) protein, capsid (CA) protein, and nucleocapsid (NC) protein. The suggested icosahedral structure of the retroviral capsid is not definitely established. Major products of the *pol*-encoding region are reverse trancriptase (RT) and integrase (IN). The protease (PR) is derived from the *pro* gene between *gag* and *pol*.

the viral particles is not yet understood. Finally, the double stranded DNA (dsDNA) is obtained. These DNA become integrated, by a mechanism involving the viral integrase (IN) protein, into the chromosomal DNA of the host to form a provirus. The viral RNA is transcribed by the cellular RNA polymerase II. The capsid assemblies occur either as intracytoplasmic (A type) particles or at the plasma membrane (C type) and are released from the host cells by a process of budding.

Envelope proteins of retroviruses are synthesized as glycosylated polyprotein precursors, PrENV or Pr85env (Van Zaane et al. (1976)), which are not generally detected on the (host) cell surface and thought to be confined to the endoplasmic reticulum (Pinter et al. (1984), Bilello et al. (1982). This polyprotein is then cleaved by an unknown cellular protease (Klenk and Garten (1994)) to give two separate protein units, a surface unit (SU), N-terminal, and transmembrane protein (TM), C-terminal, which are designated as gp70 and pE15 (Leis et al. (1988)), respectively. The association of gp70 and pE15 is by a labile disulfide bond, which can be stabilized by thiol blocking agents (Pinter et al. (1978)). The association of these two subunits forms the surface projection or the "knob-like" structures on the surface of retrovirus particles and functions as receptors for retroviruses. Virus binding is also believed to trigger a conformational change in the SU domain, resulting in an exposure of a hydrophobic peptide (fusion domain) in the TM region, which subsequently catalyzes fusion between the viral envelope and the cellular membrane. It is also believed that the viral glycoprotein interacts with the receptor twice, first on the initial binding and then following the conformational change of the envelope glycoprotein (Sommerfelt (1999)). The conformational change that results in the exposure of the fusion domain of the TM

unit is pH-independent for a number of murine leukemia viruses, however, this reaction is pH-dependent in case of E-MLV (McClure et al. (1990)).

The surface unit (SU) is speculated to compose of a homooligomer of two, four, or six glycoprotein monomers (Pinter and Fleissner (1979), Takemoto et al. (1978)). There are two hypervariable regions within the SU domain, which are variable region A (VRA) and variable region B (VRB) (Battini et al. (1992)). It is believed that there are three cysteine loops, of which two are located in the VRA. Size and composition of the amino acids within the cysteine loops vary among different retrovirus isolates. The VRA region is believed to be a key determinant of the host ranges of the MLV (Battini et al. (1992), Morgan et al. (1993)) while, by analyzing the amphotropic, xenotropic and polytropic chimeras, the VRB region has been shown to be important in stabilizing the viral specific structure (Battini et al. (1992)).

The TM domain is shown to be a trimeric consisting of three amino acid sequence motifs that are highly conserved among the C and D type retroviruses. Crystal structure of Moloney murine leukemia virus (MoMLV) transmembrane (TM) unit was studied and found to resembled those of HA of influenza (Fass et al. (1996). In addition, the crystal structure of the receptor-binding domain of the MLV has also been elucidated at 2 ^{o}A (Fass et al. (1997). However, the definitive structure of the MLV glycoprotein is not yet available.

2.4.3. Amphotropic Murine Leukemia Virus

There are two commonly studied isolates, which are 1504A and 4070A. While the 1504A isolates can effectively infect Chinese hamster cells, the 4070A isolates are

incapable of infecting Chinese hamster cell line (Cloyd et al. (1985)). Amphotropic murine leukemia virus strain 4070A was first isolated from wild mice (*Mus Musculus)* trapped at Lake Casitas in California (Hartley and Rowe (1976)). This particular strain was found to be unable to cause the cytopathic effects (CPE), in this case "syncytium" formation, growth inhibition and plaque formation on XC cells (Klement et al. (1969).

Amphotropic Murine Leukemia Virus (A-MLV) enters host cells by a pH-independent membrane fusion mechanism (McClure et al. (1990), Wilson et al. (1992)). Receptors for A-MLV are designated as Ram1 (Sommerfelt (1999), Miller et al. (1994), Vanzeijl et al. (1994)) or, alternatively, Pit2 (Miller et al. (1994), Wilson et al. (1994)), which is a sodium-dependent inorganic phosphate transporter whereas receptor for E-MLV was found to be a basic amino acid transporter (Wang et al. (1991), Kim et al. (1991)). These receptors were found to be located on the chromosome 8 for both human (Garcia et al. (1991), Sommerfelt (1999)) and mice (Gazdar et al. (1977)).

For A-MLV, it was initially believed that the first 208 amino acids of SU region are sufficient for recognizing the host cell surface receptors. Subsequently, it was demonstrated that the first 120 amino acids of the SU domain are sufficient to function as virus binding sites (Battini et al. (1992)). However, it was demonstrated that the first 72 amino acids of the SU domain of the 4070A strain are not required for A-MLV receptor interaction (Peredo et al. (1996)). Further, it was hypothesized that most parts of both VRA and VRB, which are composed of hydrophilic residues, are exposed to the outer surface (Han et al. (1998)). Nevertheless, structural characterization of the SU domain of A-MLV has not yet been elucidated even though the amino acid sequences of the SU domain have been characterized (Han et al. (1998)).

2.5 Chinese Hamster Ovary Cells

Chinese hamster ovary (CHO) cells have been widely used in biotechnology and biopharmaceutical industries to manufacture recombinant proteins with therapeutic application (Collen et al. (1984), Patzer et al. (1986), Smith et al. (1987), Hubbard et al. (1992)). There are a number of features that make CHO cells attractive for biotechnology and biopharmaceutical manufacturing processes. CHO cells can be easily adapted to grow in suspension at high density and, furthermore, complex proteins produced by CHO cells undergo more appropriate posttranslational modification than in both prokaryotic and eukaryotic cells such as yeast and insect cells. Additionally, CHO cells are non-permissive for the replication of many human pathogenic viruses. The average doubling time of CHO cells is approximately 12.4 hrs (Puck et al. (1964), Lee et al. (1997)). The average diameter of CHO cells is found to be approximately 18 – 20 μm.

It also has been demonstrated that CHO cells could begin to spontaneously produce retrovirus-like particles after hundreds of "virus-free" generations *in vitro* (Lieber et al. (1973)). Furthermore, chemically induced normal CHO cells can start to produce retrovirus-like particles as well. Treatment of CHO cells with either dibutyryl cyclic adenosyl monophosphate (dbc AMP) or testosterone induced the appearance of C-type retrovirus-like particles (Tihon and Green (1973), Tihon and Hellman (1976)). Generally, two types of these particles, which are intracytoplasmic type A and budding type C particles, are usually observed (Lieber et al. (1973), Anderson et al. (1990, 1991), Lie et al. (1994)). However, these retrovirus-like particles are found to be defective (Anderson et al. (1991)). In addition, it is estimated that 0.04 % of the mouse genome is

composed of provirus of retrovirus sequences (Callahan and Todaro (1978)). Whether hamster cell lines can produce infectious retrovirus particles has not been shown.

It has also been shown that CHO cells are resistant to all major classes of murine leukemia viruses (MLV) (Teich (1984), Miller and Miller (1992, 1993), Eglitis et al. (1993)) by secretion of protein inhibitor. It was subsequently demonstrated that the proteinaceous factor secreted by CHO cells is composed of two protein factors that can prevent retrovirus infection. These two factors whose molecular weights are 20 – 45 kDa and 45 – 70 kDa can prevent both A-MLV and GALV (Gibbon-Ape Leukemia Virus) infection, respectively (Miller and Miller (1993). In addition, the inhibitor was found not to be an interferon or an intact *env* protein but a proteinaceous factor secreted by CHO cells, which acts in *trans* to prevent retrovirus infection. However, CHO cells are susceptible to A-MLV infection after treating with tunicamycin, a glycosylation inhibitor (Miller and Miller (1992)). Tunicamycin prevents an N-linked glycosylation of proteins on the CHO cell surface. It has been postulated that the receptors on wild type CHO cells are nonfunctional, however, after treating with tunicamycin, the protein factor cannot block the receptors on CHO cell surfaces, as a result, rendering CHO cells susceptible to infection by murine leukemia viruses including A-MLV.

It has been demonstrated that CHO cells in suspension culture may form aggregates under suboptimum growth conditions. It was also found that clusters were formed around the dead cells leading to the conclusion that deoxyribonucleic acid (DNA) released from the dead cells mediated the cell-cell adhesion (Renner et al. (1993)). However, aggregation resulting from DNA mediation may be prevented by addition of DNase I to the growth medium.

2.6 Human Embryonic Kidney 293 Cells

Even though both rat and hamster cells have been successfully transformed by Adenovirus type 5 (Ad-5) which is a human adenovirus, transformation of human cells is not as efficient. This is due to the fact that in human cells infection by adenoviruses generally leads to cell lysis with the production of a large number of infectious virions. However, transformation of human cells maybe induce by exposing the cells to sheared or fragmented DNA of adenoviruses (Graham et al. (1974), Graham and van der Eb (1973)) since sheared fragments of human adenovirus DNA are incapable of causing lytic infection of the cells. The 293 or HEK 293 cell line, which is of epithelial origin (Chan et al. (1997)), was established by exposing the original (parental) human embryonic kidney (HEK) to sheared or fragmented Ad-5 DNA (Graham et al. (1977)). The 293 cell line was established after more than 100 passages of the subculture. Further, oncogenicity of the human transformed (HEK 293 or 293) cells in nude mice is much lower than that of the transformed rat cells.

The 293 cells tend to grow in islands or clumps and continued dividing after reaching confluency. Further, 293 cells are found to exhibit large (dense) ovoid bodies in the region of the nuclear membrane when stained by phenanthrenequinone which appears to react specifically with arginine residues (Russell et al. (1971)). Due to the fact that the 293 cells can be superinfected by Ad-5 and other human adenoviruses leading to a more practical application of the 293 cells the monolayer of 293 cells, for instance, may be employed as a substrate for the plaque assay for adeno serotypes 1, 2, 5, 7 and 12 which are incapable of forming plaques on other human cell lines (Graham et al. (1977)). Recently, it has been illustrated that infection of hantaviruses induced

cytophatic effect (CPE) in HEK 293 cells (Markotic et al. (2003)) even though it is generally known that hantavirus infection causes little to no cytopahtology (Meyer and Schmaljohn (2000)).

Currently, HEK 293 cells may also be used as packaging cell lines to produce pseudotypes of retroviruses (Miller and Buttimore (1986)). The HEK 293 cells are transformed by stably integrating the viral structural genes, *gag*, *pol* and *env*, of viruses of interest into the genome of the HEK 293 cells (Mann et al. (1983), Miller and Buttimore (1986)). The structural genes, which are necessary for particle formation and replication, were separately introduced by using bleomycin and puromycin resistant genes. To produce infectious and replication incompetent viruses, viral vectors containing packaging signal (Ψ^+), transcription and processing elements and selection marker, must be transfected into the packaging cell lines. By separately introducing and integrating of the viral structural genes, the possibility of infectious and replication competent particles is minimized (Miller and Chen (1996), Morgenstern and Land (1990)).

2.7 NIH/3T3 Cells

The original 3T3 cell line was first established by Todaro and Green in 1963 (Todaro and Green (1963)). These original 3T3 cells were established from Swiss mice. The cells are fibroblast in character. The NIH/3T3, continuous cell line of highly contact inhibited cells, was established from the NIH Swiss mouse cultures in the same manner as the original random bred 3T3 and the inbred BALB/c 3T3 cells (Jainchill et al. (1969)). Iwamoto et al. (1985) have reported that there are two NIH/3T3 cell lines of

different origins, which are N and B types, circulating in the world. The N-type NIH/3T3 cells, were derived from the NIH Swiss mice whereas one of the sublines of the original 3T3 cells, also designated as NIH/3T3 cells, exhibited B tropism (B-type) (Todaro and Huebner (1972)). The DNA from both the B-type and N-type NIH/3T3 cells exhibit similar patterns when digested with Eco R1 and hybridized with the PR1 probe (Kominami et al. (1983)) or the MLV probe (Berns et al. (1980)).

Since the NIH/3T3 cells are permissive to infection of the four major classes of murine leukemia viruses (MLVs), which are ecotropic, pantropic, xenotropic and amphotropic, NIH/3T3 cells are generally used to propagate retroviruses (Clontech (2001)). Further, the NIH/3T3 cells have been used to isolate and assay the transforming genes (oncogenes) (Bishop (1984)). Even though the 3T3 cells are relatively insensitive to focus formation by murine sarcoma viruses, the NIH/3T3 cells are highly sensitive to sarcoma focus formation and murine leukemia virus growth (Jainchill et al. (1969)).

For this project, interaction potential of the flocculation system containing CHO cells, A-MLV and cationic polyacrylamide will be established by using the DLVO theory. Even though a number of studies have demonstrated that several forces play a significant role, only the London-van der Waals attractive force and the repulsive electrical double layer force will be considered. Further, a mathematical model to predict average particle size of flocculated suspension will be formulated by utilizing the dimensional analysis technique. Several important operating parameters such as velocity gradient, time, and Komogorov's microscale will be taken into consideration.

CHAPTER 3

MATERIALS AND METHODS

This chapter describes the experimental methods used in this project including some of the detailed information regarding the components relevant to the each experiment. Firstly, a brief description of cell line characterization and cell culture techniques including plasmid characterization is given. Then, a description of A- MLV pseudotypes used for the entire study is given together with the protocol to produce these pseudotype viruses. Finally, the experimental procedure for flocculation and microfiltration is described.

3.1 Cell Culture

3.1.1. NIH/3T3 Cell

The NIH/3T3 cells are a continuous cell line of highly contact inhibited cells. They were established from the NIH Swiss mouse cultures in the same manner as the original random bred 3T3 and the inbred BALB/c 3T3 cells. This particular cell line (ATCC # 1658) was used as indicator cells to quantify the A-MLV pseudotypes by the $TCID_{50}$ assay. These cells were maintained in Dulbecco's Modified Eagle's Medium (ATCC # 30-2002) supplemented with 4 mM L - glutamine, which was adjusted to

contain 1.5 g/L sodium bicarbonate, 4.5 g/L glucose, and 10 % fetal calf serum (FCS), and incubated at 37 °C and 5 % CO_2.

Medium was removed by aspiration and cells were then rinsed once with 2 mL of phosphate buffer saline (PBS) solution in order to subculture the cells. Subsequently, cells were trypsinized with 1.5 mL of 0.25 % trypsin-EDTA (Sigma) for 10 -15 minutes (or until cells detached) at room temperature or at 37 °C. The fresh medium containing FCS was added to inactivate trypsin and mixed by pipetting to disperse the cells. For a 60-mm plate, the inoculum containing approximately 100 cells was dispensed into a new 60-mm plate containing 5 mL of fresh medium. The cells were subjected to subculturing every three or four days.

The frozen stock of the NIH/3T3 cells was prepared using a culture of approximately 80 % confluency (log growth phase). The medium was discarded and the cells were washed once with 2 mL of PBS. Then the cells were trypsinized by 1.5 mL of 0.25 % trypsin-EDTA and allowed to stand at room temperature (or at 37 °C) for 10-15 minutes. After the cells detached, 5 mL of fresh medium containing FCS was added and then transferred to the 15-mL centrifuge tube. The suspension was centrifuged at 2,000 rpm for 5 minutes. The supernatant was discarded, and then1 mL of cell freezing medium (Sigma) was added, aspirated and transferred to the 1.5 mL prelabeled cryovials. The cryovials were then put into the Styrofoam box and kept at –70 °C overnight. The frozen cryovials were eventually transferred into liquid nitrogen. After two or more weeks, the viability of the frozen stock was tested and found to be over 96 – 98 % viable.

3.1.2. Human Embryonic Kidney Cells

The Human Embryonic Kidney (HEK-293) cell line was used as the packaging cell line to produce Amphotropic Murine Leukemia Virus (A-MLV) pseudotypes. The doubling time of this particular cell line is approximately 24 – 36 hrs. It is recommended that if adherence is poor, the HEK-293 cell line should be plated on collagen-coated plates to promote adherence after thawing. Subsequently these cells may be cultured on non-collagen coated plates after recovery.

To start the HEK-293 culture, the frozen vial containing cells was rapidly thawed in 37 ^{o}C water bath. Then, 1 mL of complete medium (Dulbecco's Modified Eagle's Medium, see Appendix A for media formula) was added and the contents were pipetted up and down several times to disperse the cells. The contents were subsequently transferred to a 15 mL tube and two additional 5 mL of complete medium were added and mixed by pipetting. The total volume of the suspension should be 12 mL. Subsequently, the cell suspension was centrifuged at 125 g for 10 minutes. The supernatant was discarded and 5 mL of fresh medium was then added and mixed by aspiration. HEK-293 cells were plated at approximately 1×10^{5} cells per 60-mm plate. At first, the cells from the frozen stock were grown using the collagen-coated plate since HEK-293 cells were not efficiently attached to the non-collagen coated plates. This was done to ensure the viability of the frozen HEK-293 cells. In the second passage, the HEK-293 cells were easily grown on non-collagen coated plate, however, at the same time, the cells detached easily from the non-collagen coated plates.

To maintain the HEK-293 cells, once they reached approximately 80 – 90 % confluency, the growth medium was removed and the cells were washed once with 2 mL

of PBS. After removal of PBS, these cells were trypsinized with 1.5 mL of 0.25 % trypsin-EDTA and allowed to stand at room temperature (or incubated at 37 °C) for 5 minutes or until the cells detached. Subsequently, 5 mL of complete medium was added and aspirated several times to disperse the cells. Approximately, 1 $\times 10^5$ cells were plated into a 60-mm culture dish and were maintained at 37 °C and 5 % CO_2. These cell lines were subjected to subculturing of every three days.

The frozen stock of the HEK-293 cells was prepared according to the protocol for NIH/3T3 cells. The frozen cells were stored in liquid nitrogen for future experiments. The viability of the frozen cells was tested after two or more weeks and found to be approximately 98 – 99 %.

3.1.3. Chinese Hamster Ovary Cells

CHO-DG44 cells were obtained from Dr. Kompala (University of Colorado, Boulder, CO). CHO-DG44 cells (James et al. (2000)) are derived from the CHO-DUK cells (Urlaub et al. (1986)). In these cell line genomes, the dihydrofolate reductase (dhfr) genes have been deleted, therefore, these cell lines are designated as "$dhfr^-$" mutants. Due to this fact, CHO-DG44 lines cannot be grown in a medium containing methotrexate (MTX). In some cases, $dhfr^-$ can be used as the selection marker. The $dhfr^-$ mutant that lacks the enzyme dihydrofolate reductase cannot synthesize tetrahydrofolate and therefore can grow only in medium supplemented with thymidine, glycine, and purines. The $dhfr^-$ mutants can be inhibited by MTX, a folate analog.

To start the culture of the CHO-DG44 cells, the frozen cryovial was rapidly thawed in a 37 °C water bath. Once the contents were liquefied, 1 mL of fresh medium

(α-Minimum Essential Medium, α-MEM) containing 10 % FCS was added, aspirated and transferred to a 15 mL centrifuge tube. Subsequently, another 9 ml of fresh medium was added and the suspension was aspirated several times by pipetting. Then the contents were centrifuged at 800 rpm for 5 minutes. The supernatant was discarded and 5 mL of fresh medium was added and mixed by aspiration. Approximately 0.5 mL of cell suspension was dispensed into 60-mm plate containing 5 mL of fresh medium and incubated at 37 °C and 5 % CO_2. To subculture and establish the frozen stock of the CHO-DG44, the same procedures as those used for NIH/3T3 cells given above were followed.

To start the suspension culture of CHO-DG44 cells, the attachment dependant CHO-DG44 cells were expanded by using T-75 flasks. The growth medium was again removed by aspiration, and the cells were then washed once with 2 mL of PBS. To disperse the cells, 1.5 mL of 0.25 % trypsin-EDTA was added and the flasks were incubated at 37 °C for 5-10 minutes (or until the cells detached). Subsequently, fresh medium containing FCS was added to inactivate trypsin. The suspension was aspirated several times to disperse the cells and then transferred to a 15 mL centrifuge tube and centrifuged at 800 rpm for 5 minutes. The supernatant was discarded and approximately 10 mL of the serum free medium, IS CHO (Irvine Scientific, Santa Ana, CA), supplemented with 0.0816 g/L of hypoxanthine (Sigma), 1.168 g/L of L-glutamine (Sigma), and 0.0233 g/L of thymidine (Sigma) was added. After aspiration 100 μL of cell suspension was stained by 100 μL of trypan blue dye (Juliano and Bannelier (1975), Seigel et al. (2000), Appendix B) and a cell count was performed using a hemacytometer (Appendix B). A cell density of $2-3\times10^5$ cells per mL was used to start a new

suspension culture.

The number of flasks needed was based upon the assumption of 2×10^5 cells per cm^2 for each T-75 flask (Batt (2001)). The cell suspension was transferred to the Celstir Flask (Wheaton) and maintained at 37 °C and 5 % CO_2 incubation. The agitation rate was approximately 70 rpm (James et al. (2000)) using Biostir4 Magnetic Stirrer (Wheaton). The cell density of the suspension culture was estimated on the second day using trypan blue dye and hemacytometer. The highest cell density, which can be achieved in the Celstir Flasks, is in the range of $1.1-1.5\times10^6$ cells per mL. The average particle size distribution of CHO cells was found to be approximately 20 μm.

The frozen stock of CHO-DG44 cells was prepared using the attachment dependent form of the cells. The protocol for preparing CHO-DG44 cell frozen stock was the same as that of NIH/3T3 cells. Further, the viability of the frozen stock of CHO-DG44 cells was found to be 97-98 % after two or more weeks.

3.2 Amphotropic Murine Leukemia Virus Pseudotype

In order to produce the pseudotype of Murine Leukemia Virus, the "Amphopack-293", which is simply a packaging cell line for murine leukemia virus, was purchased from Clontech (Palo Alto, CA). For the "Amphopack-293", Human Embryonic Kidney (HEK-293) cells were used as the packaging cell line due to the fact that the structural genes, i.e., *gag*, *pol* and *env*, necessary for virus production are stably integrated into the cell genomes (Figure 3-1). However, the packaging signal, which is important in the process of viral assembly into complete virions, is not present in this cell line genome. Therefore, there is no virus production from this cell line alone. Further, virus particles

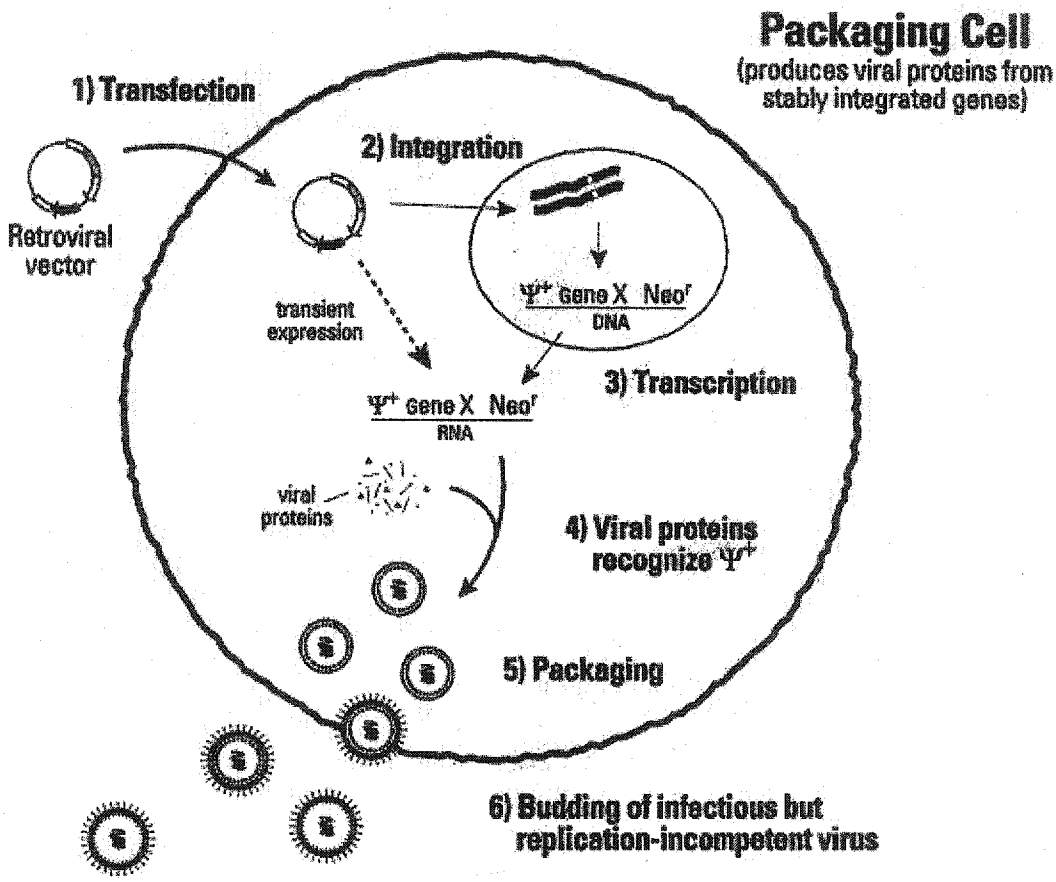

Figure 3-1 A-MLV pseudotype production system

obtained from this system bear the 4070A envelope, which expresses the amphotropic tropism. Therefore, viruses used in this project will be designated as "amphotropic murine leukemia virus" (A-MLV). These viruses can infect a broad range of mammals. In addition, the receptors for this particular MLV strain are Ram1 (Sommerfelt (1999), Miller et al. (1994), Vanzeijl et al. (1994)) or Pit2 (Miller et al. (1994), Wilson et al. (1994)).

To produce the A-MLV pseudotype, the pLEGFP-C1 plasmid (Figure 3-2, Clontech, Palo Alto, CA) was transfected into the HEK-293 cells since this plasmid contains the packaging signal (Ψ^+) genes. With all of the components necessary for virus assembly, the titers of A-MLV pseudotypes, which are infectious but replication-incompetent, can be harvested from the growth medium of the packaging cell line, HEK-293. The techniques recommended by the FDA for detecting the presence of retroviruses are transmission electron microscopy (TEM), reverse transcriptase (RT) assay and cell culture infectivity assay (FDA (1993)). Therefore, the tissue culture infectious dose 50 ($TCID_{50}$), an infectivity assay (Fisher and Yates (1963), was chosen to quantify the A-MLV in this study. However, it is well known that retroviruses, in general, do not cause the morphological changes, which is known as cytopathic effect or CPE, in the host cells. In order for the $TCID_{50}$ assay to be effective for the A-MLV, the pLEGFP-C1 plasmid is chosen since it contains the enhanced green fluorescence protein (EGFP) which will facilitate the quantification of the number of virus particles present in the suspension by the $TCID_{50}$ assay. In the process of viral assembly, the RNA segment containing EGFP and the packaging signal, Ψ^+, is packaged into the virus particles. As a result, the presence of A-MLV infection in the target cells, NIH/3T3, is indicated by

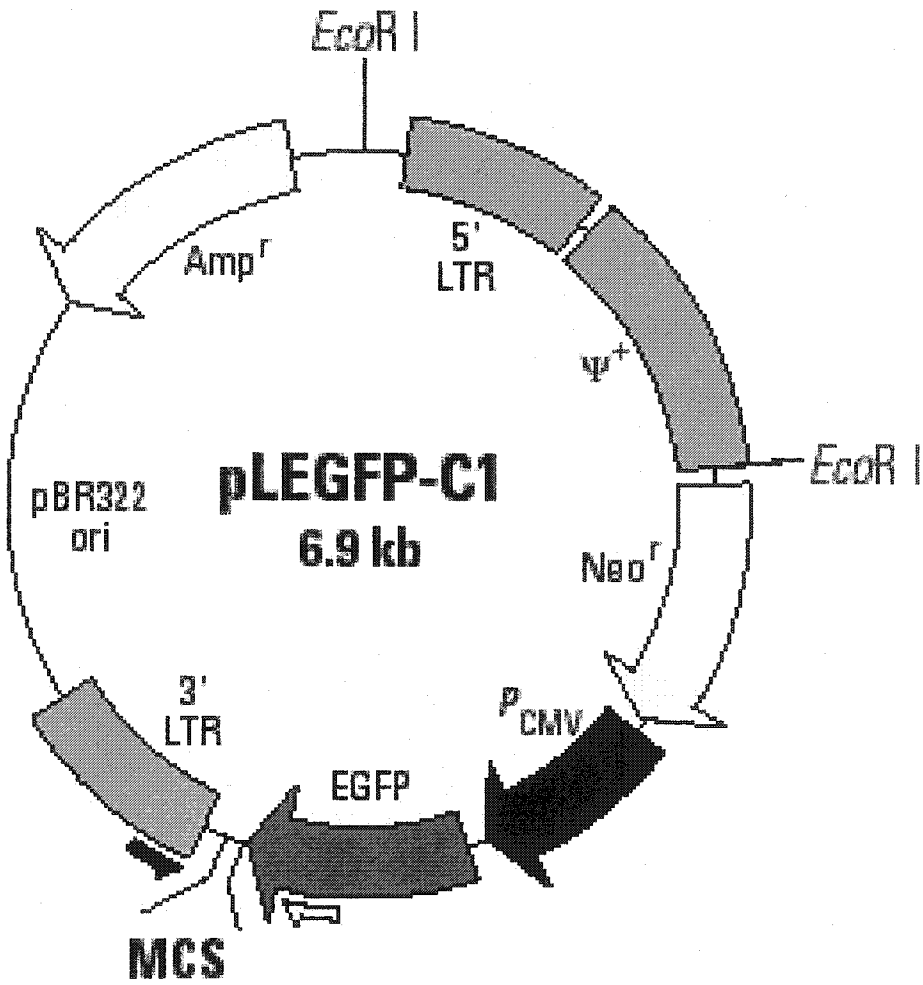

Figure 3-2 pLEGFP-C1 plasmid

the expression of EGFP which can be visualized under UV light.

3.2.1. pLEGFP-C1 Plasmid

The pLEGFP-C1 (Figure 3-2) plasmid contains three very important regions, which are enhanced green fluorescent protein (EGFP), packaging signal (Ψ^+) and neomycin resistant (Neo^r) genes. The molecular weight of the pLEGFP-C1 is approximately 6.9 kb. EGFP, which gives a brighter fluorescence than the original GFP due to higher expression in mammalian cells, is a red-shifted variant of the wild-type GFP of the jellyfish *Aequorea Victoria*. The excitation maximum and the emission maximum for EGFP are 488 and 507 nm, respectively. The retroviral elements (the 3′ and 5′ long terminal repeat, LTR) in pLEGFP-C1 are derived from the Molony murine leukemia virus (MoMLV). The promoter to drive the expression of the EGFP gene is from Cytomegalovirus (CMV), which is the strong promoter in the mammalian cell systems. The neomycin resistant gene is used as the selection marker for the A-MLV pseutdotype production system. Therefore, G418, which is the analog of neomycin, is used in the selection of the stable transformants. Further information regarding pLEGFP-C1 plasmid is given in Appendix C.

3.2.2. Transfection Methods

Owing to the fact that the quantity of the purchased pLEGFP-C1 plasmid is small, amplification and purification (Appendix C) is therefore necessary. While the plasmid amplification involved transformation of DH5α, which is the strain of *Escherichia coli* treated with $CaCl_2$, the purification of the plasmid from DH5α was

accomplished by using QIAgen DNA purification kit. However, the kill curve must be established (Appendix E) before transfection of HEK-293 cells can be carried out. There are two important steps in constructing the kill curve, which are the optimum drug (antibiotic) concentration and the optimum cell density. The optimum antibiotic concentration is determined first and then followed by the optimum cell density. The construction of a kill curve is necessary since the optimum cell density is used to plate the transfected cells after transfection to select either stable or transient transformants at the optimum antibiotic concentration. However, it is the intention of this project to establish the stable clones that are capable of continuously producing the A-MLV pseudotypes.

Prior to transfection, HEK-293 cells were plated at 5×10^5 cells per 60 mm plate overnight to yield approximately 40 – 60 % confluency on the day of transfection. It is recommended that the confluency of the cells should not be greater than 60 % in order to accomplish high transfection efficiency. Transfection (Appendix D) is carried out using the Effectene Transfection Kit. The Effectene transfection Kit is a liposome-based transfection reagent. This procedure causes less stress and is less toxic to the cells. Only 1 and 2 μg of the pLEGFP-C1 plasmid were used to transfect the HEK-293 cells. Transfection reagents were incubated with HEK-293 cells for approximately 18 hrs at 37 °C and 5 % CO_2. The transfection efficiency was observed by using an inverted microscope equipped with UV light. The successfully transfected cells expressed a bright green fluorescence under the UV light. After 18 hrs of incubation, the growth medium containing transfection reagent was aspirated and replaced with 5 mL of fresh medium. Approximately 24 hrs later, the transfected cells were subcultured at 5×10^5

cells per 60-mm plate and medium containing G418 at a concentration of 250 μg/mL was introduced 48 hrs post-transfection. Under the influence of G418, massive cell death took place approximately on the fifth day; however, these cells were kept under G418 for 14-16 days until the visible healthy single colonies of the transformants could be selected.

Approximately, 30 - 40 clones were selected and individually transferred to new plates. After the transformant colonies were selected, the G418 was withdrawn from the growth medium. Subsequently, the determination of viral titer was carried out (Appendix F). Indicator cells, NIH/3T3, were plated at a density of $0.2-0.5\times10^5$ cells per well of the 12 well-plate. Due to the fact that both A-MLV virions and NIH/3T3 cells are negatively charged, polybrene (Sigma), a polycation, was added to the growth medium at a final concentration of 8 μg/mL to reduce the repulsive force between A-MLV pseudotype virions and indicator cells and to accelerate binding of virus particle to the host cells. Expression of the EGFP was checked on the fourth and fifth days after infection under an inverted fluorescent microscope. The colonies that gave high viral titers were selected to continuously produce the A-MLV pseudotype for the whole project.

3.3 Cationic Polyacrylamide

In this project, water-soluble cationic polyacrylamides were chosen as the flocculating agents since these cationic polyelectrolytes were found to give the best flocculation efficiency according to the preliminary results with yeast (Kim et al. (2001)). All of the cationic polyacrylamides, Figure 3-3c, used in the entire project are

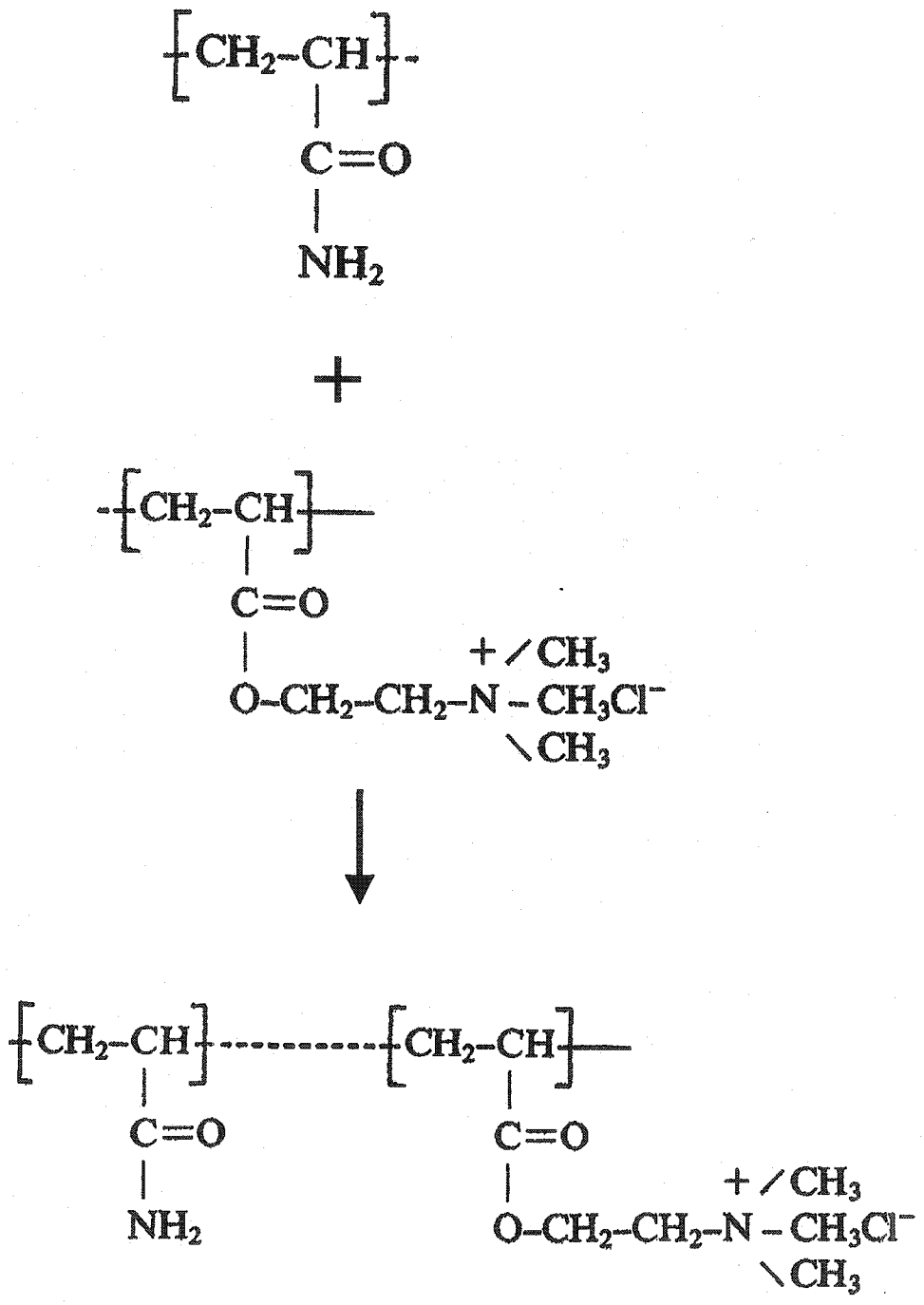

Figure 3-3 Cationic polyacrylamide: (a) acrylamide monomer, (b) acryloxyethyltrimethyl - ammonium chloride and (c) copolymer of acrylamide and acryloxyethyltrimethyl - ammonium chloride

the copolymer of acrylamide (Figure 3-3a) and acryloxyethyltrimethyl ammonium chloride (Figure 3-3b) and were obtained from Chemtall Inc. (Riceboro, GA). The cationic properties of the copolymers are the result of the quaternary amine nitrogen on the acryloxyethyltrimethyl - ammonium chloride units. All cationic polyacrylamides are linear chains with a variety of charge densities and molecular weights (Table 3-1). The charge densities of the cationic polyacrylamide vary from 5 to 80 % while molecular weights are in the range of $2-8\times10^{6}$. Polymers of high molecular weight and of linear structure are chosen in this study since a number of the previous studies (Gill and Herrington (1986a, b)) have shown that linear cationic polymers with high molecular mass were highly effective in inducing particle flocculation by bridging. Polymer solutions were prepared by diluting the original polymer with double distilled water (ddH_2O). All of the solutions were kept in the dark to prevent degradation by visible light, which can in turn reduce the efficacy of the polymer in flocculation processes.

3.4 Flocculation Methods

Due to the fact that flocculation is a dynamic process there are several factors, such as velocity gradient, flocculation time as well as polymer concentrations and particle (cell) densities that play important roles in determining the characteristics of the resulting flocs. Therefore, it is necessary to optimize these parameters for each system of interest. The optimum polymer dose and the optimum stirring speed and time were determined. The optimum polymer concentration is used as an estimate of the optimum amount of polymer necessary to induce flocculation for a given particle density while the optimum stirring speed and time will reveal the effects of the velocity gradient and the

Table 3-1 Cationic polyacrylamide characteristics

Polymer	Molecular Weight ($\times 10^6$)	Concentration (wt %)	Charge Density (%)
EM 1540 CT	5 – 8	30	5
EM 1540 L	4 – 6	36	5
EM 240 CT	5 – 8	41	20
EM 240 L	4 – 6	49	20
EM 240 LH	2 – 3	39	20
EM 440 CT	5 – 8	44	40
EM 441 L	4 – 6	44	40
EM 440 LH	2 – 3	44	40
EM 840 CT	5 – 8	43	80
EM 840 L	4 – 6	46	80

flocculation time on floc size and strength.

3.4.1. Determination of Optimum Flocculant Dose

A predetermined amount of CHO cell suspension of known cell density was added to the 50 mL centrifuge tube. Next, polymer solution was added to the cell suspension to achieve the desired final polymer concentration in the suspension. The final volume was then brought up to the total of 50 mL. Subsequently, the suspension was rigorously shaken by hand for 1 minute to induce collisions and thus flocculation. The flocculated suspension was centrifuged at 11,000 rpm for 2 minutes. The absorbance (Ab) of the supernatant was measured at 330 nm. This wavelength was chosen by simply scanning the absorbance of both flocculated and unflocculated CHO cell suspensions over the wavelength of 200 to 800 nm. The wavelength that yielded the biggest differences between the absorbance of the flocculated and unflocculated CHO cell suspension was chosen. The polymer concentrations tested in these experiments were in the range of 0 to 400 ppm (parts per million). The relationship between the polymer concentration and the Ab at 330 was then plotted. The polymer concentration, which gave the lowest Ab, was designated as the optimum polymer dose for the corresponding CHO cell density.

3.4.2. Determination of Stirring Speed and Time

Having determined the optimum polymer concentration, the optimum stirring speed and time were measured. It is important to keep in mind that the optimum stirring speed and time are necessary for the flocculation processes since the shear rate and the

flocculation time are the most important parameters that determine the strength and size of the resulting flocs. Therefore, it is essential to find the optimum combination of the stirring speed and time for the system of interest.

Approximately 110 mL of CHO cell suspension were transferred to the Celstir flask (125 mL with sidearm, Wheaton) and stirred at the desired speed. The designated amount of polymer solution of known concentration was then added to achieve the optimum polymer concentration (optimum dose). The total volume of the mixture was 120 mL. The suspension was then stirred at the designated speed for a specified period of time. At various intervals for each combination of stirring speed and time, a small sample of suspension (approximately 15 mL) was taken. Subsequently, 4 mL of the sample was centrifuged at 11,000 rpm for 2 minutes and the absorbance of the supernatant at 330 nm was measured while the remaining sample was used to determine the particle size distribution of the flocculated suspension by a Coulter (Miami, FL) LS 230 laser diffraction particle sizer. Then, the relationship between the Ab at 330 nm and the stirring speed was plotted. The combination of the stirring speed and time that yielded the lowest Ab was taken as the optimum. The stirring speeds used were in the range of 0 – 500 rpm while the stirring times were 1, 3, 5 and 10 minutes. Further, flocculated suspensions for microfiltration experiments were prepared by using the optimum polymer dose and stirring speed and time found in previous step.

3.5 Colloid Titration

Colloid titration is typically used to determine the charge density of polyelectrolyes. However, this technique may also be used to determine the

concentration of polyelectrolytes in suspension (Hutter et al. (1991)) as well as the negative charge of the cells (Ando and Tsuzuki (1984), van Damme et al. (1994)).

3.5.1. Polyacrylamide Concentration

Prior to determining the concentration of cationic polyacrylamide in solution, a standard curve must be constructed. A series of 125 mL Erlenmeyer flasks containing a known amount of cationic polyacrylamide (0 – 10 mg) was prepared and subsequently 30 μL of 0.10 % (wt) of toluidine blue O (Sigma), Figure 3-4c, was added to each flask. In the presence of a cationic polyacrylamide, the solution should yield a bluish color. The samples were titrated with standard potassium polyvinyl sulfate (PVSK) (Figure 3-4a), anionic polyelectrolyte, until the color of the samples turns from light blue to bluish purple (Figure 3-4c). The amount of PVSK is recorded. A blank is also titrated by using ddH_2O. The calibration curve is plotted as grams of cationic polyacrylamide against mL of standard PVSK used.

Trace amount of polyacrylamide was quantified by colloid titration technique. A series of 125 mL of Erlenmeyer flasks containing 40 mL of CHO cells at the density of 0.50 wt% (1×10^6) cells/mL was prepared. Then a specified amount of polymers was added to each flask to achieve desired final polymer concentration. Suspensions were stirred at 180 rpm for 3 minutes and then centrifuged at 11,000 rpm for 4 minutes. Subsequently, 10 mL of supernatant was transferred to new 125 mL Erlenmeyer flasks containing 40 mL of deionized water and 20 μL of 0.10 wt% toluidine blue O was added. The color of the mixture is bluish. Subsequently, the sample was titrated with potassium polyvinylsulfate (PVSK). The endpoint was reached when the color of

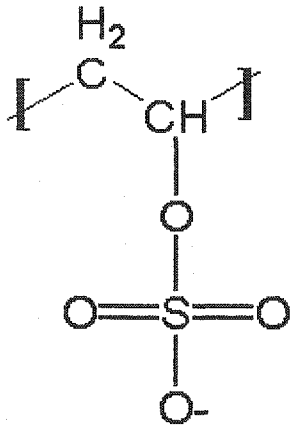

(a) Potassium polyvinyl sulfate

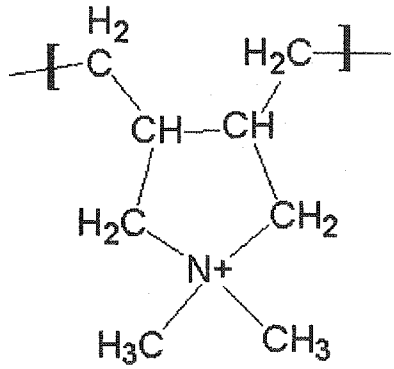

(b) Cat-Floc

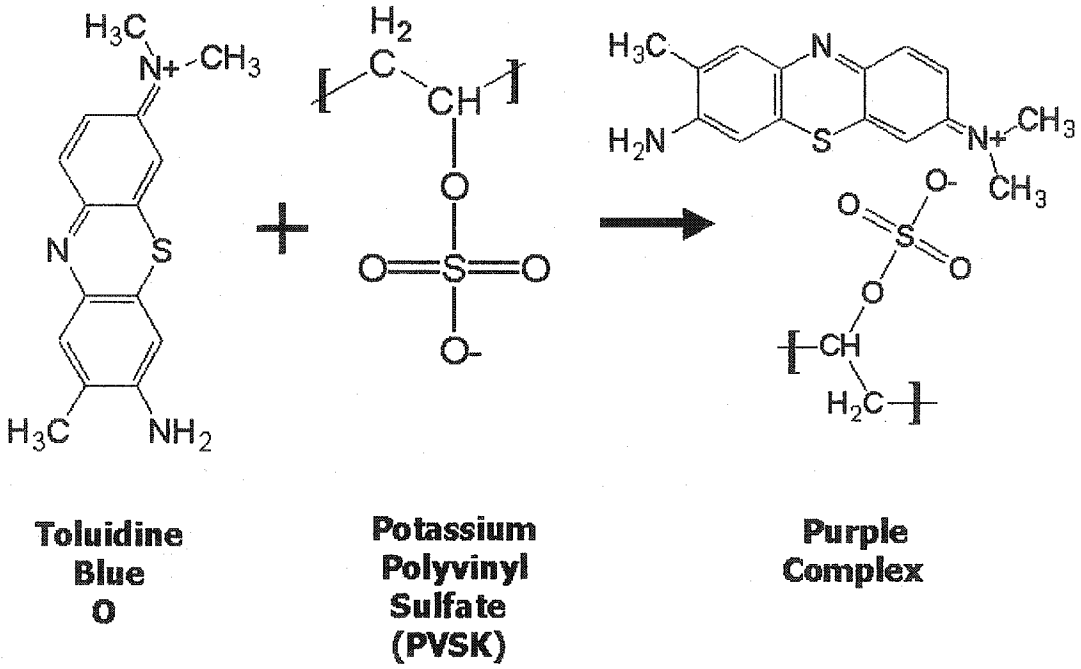

(c) Colloid Titration Reaction

Figure 3-4 Colloid titration reagents and reaction

the mixture turned reddish blue. The volume of PVSK was recorded and the amount of polyacrylamides present in the sample was calculated using the relationship found when constructing the standard curve.

3.5.2. Negative Surface Charge Content of CHO-DG44 Cell

Due to the fact that a high cell density is needed when colloid titration is to be used to determine the negative charge content of mammalian cells (van Damme et al. (1994)), e.g., $2-4\times10^{6}$ cells/mL for endothelial cells and $2-4\times10^{9}$ cells/mL for erythrocyte ghosts, the suspension of CHO cells in serum free medium was centrifuged at 2,500 rpm for 5 minutes and the cell density was determined by a hemacytometer. Subsequently, an aliquot (0.5 mL) of cell suspension in 0.25 M sucrose at $2-4\times10^{6}$ cells/mL was placed in a polystyrene microconical cup (2 mL) to which toluidine blue was added (20 μL of 0.1 % w/v) and titrated. The amount of standard polycation, Figure 3-3b, (Cat-Floc 0.002 – 0.2 % w/v) needed to obtain a visual transition from purple to blue was recorded. Excess of Cat-Floc equal to twice that amount recorded was then added and back-tirated with standard polyanion (Dextran Sulfate, 0.001 – 0.1 % w/v) until a purple endpoint was reached.

3.6 Control Experiments

Minimum control experiments are required since the flocculated suspension, which includes polymers, CHO cells, and viruses, is subjected to the shear stress during microfiltration and temperature of the suspension is far from the optimum growth conditions of both cells and viruses. Further, A-MLV, which are enveloped viruses,

could be inactivated due to the loss of the envelope glycoprotein under shear conditions. Control experiments are designed to eliminate these external factors that might lead to false results.

For all the control experiments, the total volume of suspension, either PBS solution or growth medium, was approximately 500 mL. The concentration of the A-MLV pseudotypes and the CHO cell density was approximately 5×10^5 infectious units/mL and 5×10^5 cells/mL, respectively.

3.6.1. A-MLV Alone

A-MLV pseudotypes in PBS solution were allowed to stand at room temperature for 3 hrs to investigate whether the A-MLV is inactivated by the suspension conditions. Subsequently, the infectivity of the remaining viruses in suspension was determined using the $TCID_{50}$ assay. Further, the effect of temperature on A-MLV survival was also investigated. Three T-25 flasks to which 20 mL of medium containing A-MLV were stored at three different temperatures of 4, 25 and 37 °C. Every 24 hrs, small samples from each of the flask were taken for A-MLV titration by the $TCID_{50}$ assay for viable A-MLV in suspension.

3.6.2. A-MLV and Microfiltration

A-MLV pseudotypes suspended in PBS solution were run through a microfiltration module for at least 3 hrs to assess whether the shear stress applied during microfiltration is capable of inactivating A-MLV. There was no sample taken during

microfiltration. However, after microfiltration, the $TCID_{50}$ assay was conducted to assess the effects of microfiltration on A-MLV viability.

3.6.3. A-MLV and Cationic Polymer without Microfiltration

A number of studies have demonstrated that cationic polymers are capable of inactivating viruses (Chaudhuri and Engelbrecht (1970), Thorup et al. (1970)). Consequently, flocculation of A-MLV by cationic polymers was conducted to investigate the effects of the interaction between A-MLV and the cationic polymer. A-MLV pseudotypes in PBS solution were flocculated with small amount of cationic polymer at the optimum conditions. The flocculated suspension was allowed to stand at room temperature for 3 hrs. Then a small sample of suspension was withdrawn to determine the A-MLV concentration by the $TCID_{50}$ assay.

3.6.4. A-MLV and Cationic Polymer with Microfiltration

The same suspension as that in 3.6.3 was prepared and subsequently the flocculated suspension was run through the membrane module for 3 hrs at 4,500 s^{-1} shear rate in total recycle mode. A small sample of the retentate was withdrawn and saved for virus infectivity by the $TCID_{50}$ assay to investigate whether the combined effects of cationic polymer and microfiltration conditions affected A-MLV survival.

3.6.5. A-MLV and CHO Cells

Even though several studies have demonstrated that A-MLV is not capable of infecting CHO cells (Teich (1984), Miller and Miller (1992, 1993), Eglitis et al. (1993)),

it was desired to investigate whether the A-MLV pseudotypes produced in this study were capable of infecting the CHO-DG44 cells.

CHO-DG44 cells were plated in a 6 well plate at a concentration of $2-5\times10^4$ cells per well over night prior to A-MLV pseudotype inoculation. Five tubes of ten fold serially diluted of A-MLV ($10^{-1}-10^{-5}$ dilution) were prepared by adding 0.9 mL of (CHO) fresh medium containing polybrene at a final concentration of 8 μg/mL and 0.1 mL of virus containing (filtered) growth medium from the packaging cell line into 1.5 mL centrifuge tube. Consequently, a total of 1 mL of A-MLV dilution was inoculated onto the cells. The CHO-DG44 cells were the incubated at 37°C and 5% CO_2 for at least 48 hrs and, subsequently, expression of EGFP was determined under an inverted microscope equipped with UV light. In this experiment, CHO-DG44 cells that were not inoculated with A-MLV pseudotype were used as a negative control.

3.6.6. A-MLV and CHO Cells with Microfiltration

A suspension of CHO-DG 44 cells was inoculated with 60 mL of the virus containing HEK growth medium at a concentration of 5×10^5 infectious units/mL of the A-MLV pseudotypes. The final concentration of A-MLV was 1×10^5 infectious units/mL. The total volume of the suspension was approximately 300 mL. Then, a microfiltration experiment was performed by using the above suspension as feed. Suspension was run through the system that is the same as that of Figure 3-5 without a membrane module. The suspension was allowed to run through the system for 3 hours at room temperature in the laminar flow hood. Samples were collected only at the

beginning and the end of experiment. The titers of A-MLV in suspension were determined by $TCID_{50}$ assay.

3.7 Microfiltration

Crossflow (tangential flow) microfiltration was carried out using hollow fiber membrane modules (A/G Tech, Needham, MA). The modules contain two fibers whose pore size is approximately 0.1 μm. The membranes are made from polysulfone while the cartridge is made of polycarbonate. The module is 30 cm long and 1.0 mm in diameter (nominal lumen inner diameter (ID)). The active membrane area is approximately 16 cm^2. The experimental setup used is shown as in Figure 3-5. For new membrane modules, the module was run with deionized water for 10 – 20 minutes to remove preservatives (Sheldon et al. (1991)) from the membrane surface. Subsequently, the pure water flux was measured as a function of transmembrane pressure. Microfiltration experiments were conducted under sterile conditions as the permeate had to be assayed for viral infectivity. To achieve this, the microfiltration setup including the membrane module was autoclaved at 225 °F for 35 minutes and left to dry over night prior to the microfiltration experiment.

In order to conduct microfiltration of CHO cell suspensions, the flocculated CHO cell suspension was placed in the feed tank, Celstir 1000 mL, and agitated at 70 rpm (James et al. (2000)) to prevent flocs from sedimenting. A peristaltic pump was then used to draw feed suspension to the membrane module. Retentate was returned to the feed tank via the retentate line while the permeate was collected in a graduate cylinder. Every five minutes during the first 10 minutes and, from then onwards, every ten

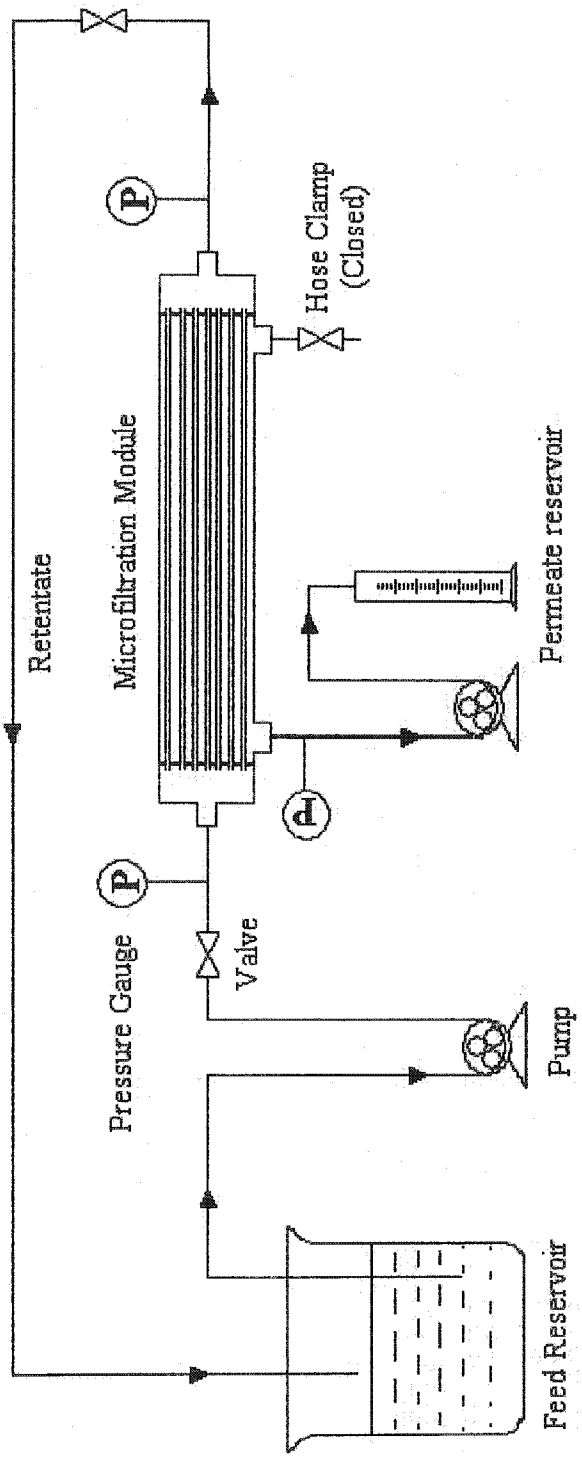

Figure 3-5 Experimental setup

minutes, the volume of the permeate was recorded and a small sample of the permeate was withdrawn for the A-MLV infectivity assay. Microfiltration was stopped when the permeate flux was approximately constant. Each microfiltration experiment was carried out at a fixed transmembrane pressure (TMP). The TMP used was in the range of 0 – 5 psi. Since the permeate was always at atmospheric pressure, the TMP was estimated by averaging the retentate and the feed pressures. Wall shear rates in the range of 2500 and 6000 s^{-1} were investigated. From Hagen-Poiseuille equation, the shear rate at the membrane surface may be derived (Bird et al. (1960)

$$\dot{\gamma}_w = \frac{4Q}{\pi R^3 N} \qquad (3\text{-}1)$$

where $\dot{\gamma}_w$, R, Q and N are wall shear rate, fiber diameter, flow rate and the number of fibers, respectively.

Each microfiltration experiment was performed in two modes; total recycle and concentration mode. For the total recycle mode, the permeate was periodically returned to the feed tank after a small volume of sample (5 mL) was taken to quantify the amount of A-MLV by the $TCID_{50}$ assay. For the concentration mode, the permeate was not returned to the feed reservoir. However, a small sample (5 mL) was also taken for the $TCID_{50}$ assay.

At the end of microfiltration, the pure water flux of the module was determined both before and after preliminary cleaning of the membrane module was carried out with approximately 1 - 2 L of ddH_2O. The system was then cleaned with 0.1 M NaOH at 50 °C for 1 hour. The TMP used during cleaning was the same as that used during the microfiltration experiment. At the end of cleaning process, at least 4 - 5 L of deionized water was run through the module to remove residual NaOH and the pure water flux was

again determined. The pH was also measured to ensure all residual NaOH had been removed. When not in use, the membrane was maintained by submerging in the 0.01 M NaOH solution to prevent drying and bacterial growth.

CHAPTER 4

RESULTS

This chapter presents the experimental results obtained in this study. In order to select the appropriate cationic polyacrylamides, the optimization results (optimum dose and stirring speed and time) for flocculation conditions are described. In addition, adsorption isotherms for cationic polyacrylamides are also given. Then, the results of the control experiments are presented. Finally, results for microfiltration and virus removal of flocculated suspensions containing CHO cells and A-MLV are provided.

4.1 Flocculation

4.1.1. Optimum Flocculation Conditions

In this study ten of the commercially available cationic polyacrylamides (Table 3-1) with molecular weights in the range of $2-8\times10^6$ and charge densities from $5-80$ % were tested for their capabilities to induce flocculation of suspensions containing both CHO cells and A-MLV virions. The CHO cell concentrations tested were 5×10^5, 1×10^6 and 2×10^6 cells per mL, which corresponds to 0.25, 0.50 and 1.0 wt%, respectively.

4.1.1.1. Wavelength

The optimum polymer dose is initially defined as the concentration of cationic polyacrylamides that minimizes the absorbance of the supernatant of the flocculated suspension whereas the optimum stirring speed and time is defined as the combination of the agitation intensity and time that yields the lowest supernatant absorbance. The wavelength to be used in measuring the absorbance of the supernatant is determined by means of wavelength scan over the range of 200 – 800 nm. The samples used were supernatants of both flocculated and unflocculated CHO cell suspension while fresh CHO cell medium is used as blank. The supernatants were obtained by simply centrifuging both cell suspensions at 11,000 rpm for 2 minutes.

The suitable wavelength is defined as the wavelength that results in the biggest difference in absorbance between the supernatant of the flocculated CHO cell suspension and the unflocculated CHO cell suspension. This experiment was carried out by using both the UV and visible lamps. It can be seen from Figure 4-1 that the wavelength at 330 nm gave the biggest difference between the absorbance of the unflocculated suspension and that of the flocculated suspension. Therefore, the wavelength of 330 nm was chosen and used for the whole project.

4.1.1.2. Optimum Flocculant Dose

Cationic polyacrylamide concentrations in the range of 0 – 400 ppm were tested. It was assumed in preparing polymer stock solutions that the original concentrations of cationic polyacrylamides obtained from the manufacturer are 1,000,000 ppm. It is apparent for all CHO cell densities that optimum doses required to induce flocculation of

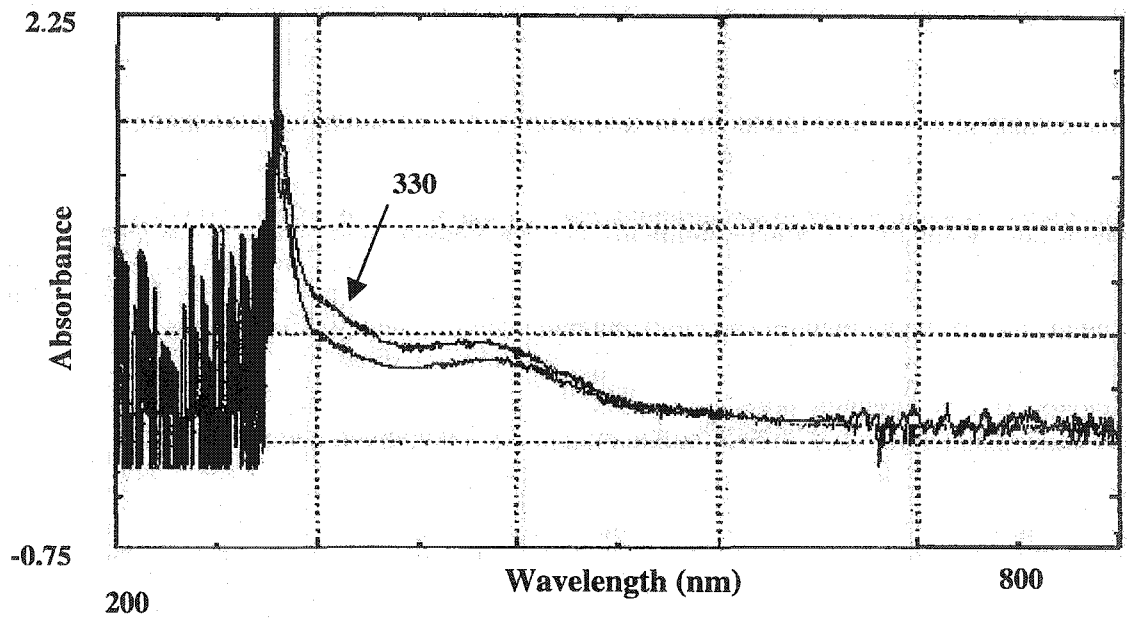

Figure 4-1 Wavelength scan of the supernatants of both flocculated and unflocculated CHO cell suspensions. The wavelength is in the range of 200 – 800 nm. The biggest difference between the absorbance of the supernatants of flocculated and unflocculated CHO cell suspension occurs at a wavelength of 330 nm. The polymer used to flocculate the CHO cell suspension is EM441L (charge density and molecular weight are, respectively, 40% and $4-6\times10^{6}$).

CHO cell suspension increase as molecular weight of the polymer flocculants decreases. It was also found that the optimum dose necessary to induce flocculation of CHO cell suspension increases as CHO cell densities increase. For example, optimum dose of EM441L for CHO cell density of 1.0×10^6 cells/mL is approximately double (Table 4-1) the optimum dose for CHO cell density of 5.0×10^5 cells per mL.

For cationic polyacrylamides with 5 % charge density (Figures 4-2a and 4-2b), EM1540 series, it can be seen that, for both CHO cell densities, EM1540L whose molecular weight is $4-6\times10^6$ gave lower absorbance than that by EM1540CT (MW = $5-8\times10^6$) even though at low cell density the EM1540CT yielded smaller optimum dose. The optimum dose of EM1540CT for 0.25 and 0.50 wt% CHO cell densities are 30 and 60 ppm, respectively, whereas the optimum dose of EM1540L for the two respective CHO cell densities are 60 and 100 ppm.

Figures 4-3a and b illustrate the optimum polymer doses for 20% charge density cationic polyacrylamides (EM240 series) for CHO cell densities of 0.25 and 0.50 wt%, respectively. It can be seen from Figure 4-3a that EM240L was as effective in minimizing the absorbance of the supernatant of the flocculated suspension as EM240CT while EM240LH was the least effective. In addition, the optimum polymer doses of EM240CT, EM240L and EM240LH for 0.25 wt% cell density are 25, 35 and 45 ppm, respectively, while the corresponding optimum doses for 0.50 wt% CHO cell density (Figure 4-3b) are 50, 60 and 70 ppm, respectively. Further, it can be seen that EM240L is the most effective in minimizing absorbance of the flocculated CHO cell suspensions while the effectiveness of EM240CT and EM240LH are comparable.

Table 4-1 Optimum Polymer Dose

Polymer	Molecular Weight ($\times 10^{-6}$)	Cell Concentration (wt %)			Optimum Polymer Dose (ppm)
		0.25	0.50	1.00	
EM 1540 CT	5 – 8	30	60	-	
EM 1540 L	4 – 6	60	100	-	
EM 240 CT	5 – 8	25	50	-	
EM 240 L	4 – 6	35	60	-	
EM 240 LH	2 – 3	40	70	-	
EM 440 CT	5 – 8	30	60	120	
EM 441 L	4 – 6	35	70	150	
EM 440 LH	2 – 3	40	80	-	
EM 840 CT	5 – 8	35	6 0	-	
EM 840L	4 – 6	30	65	-	

Note: In accordance to adsorption isotherm experiment, optimum doses may be expressed in terms of mg/m^2 rather than "ppm" by utilizing the weight concentration of each polymers specified by the manufacturer and CHO cell surface area at each cell density. In the calculation of surface area, CHO cell diameter is taken to be 18 μm. In case of EM440CT, for instance, the optimum ratio of milligram of EM440CT to CHO cell surface is 20.98 mg/m^2 for all CHO cell number density.

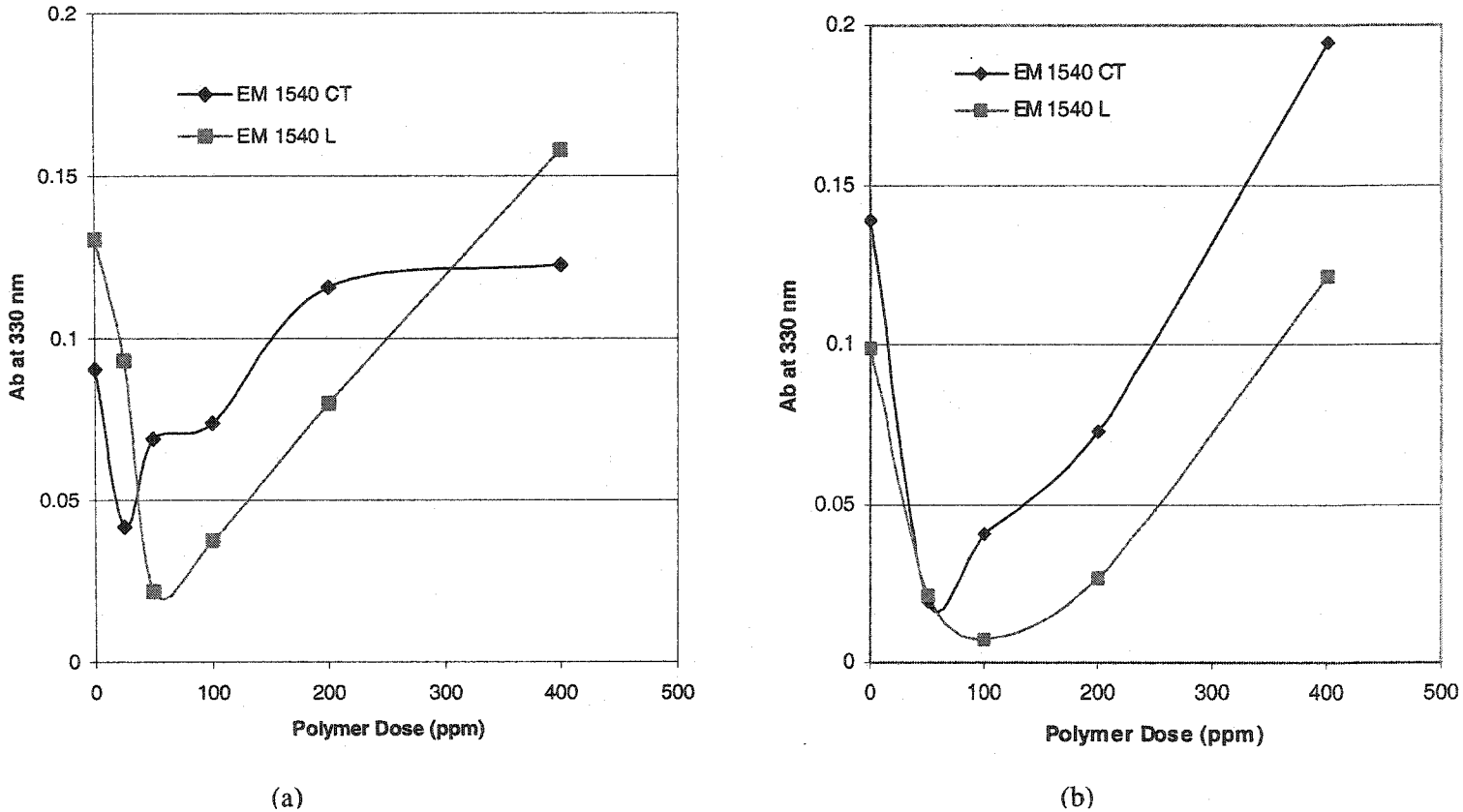

Figure 4-2 Optimum dose for cationic polyacrylamide with 5 % charge density (a) 0.25 and (b) 0.50 wt% CHO cell concentration

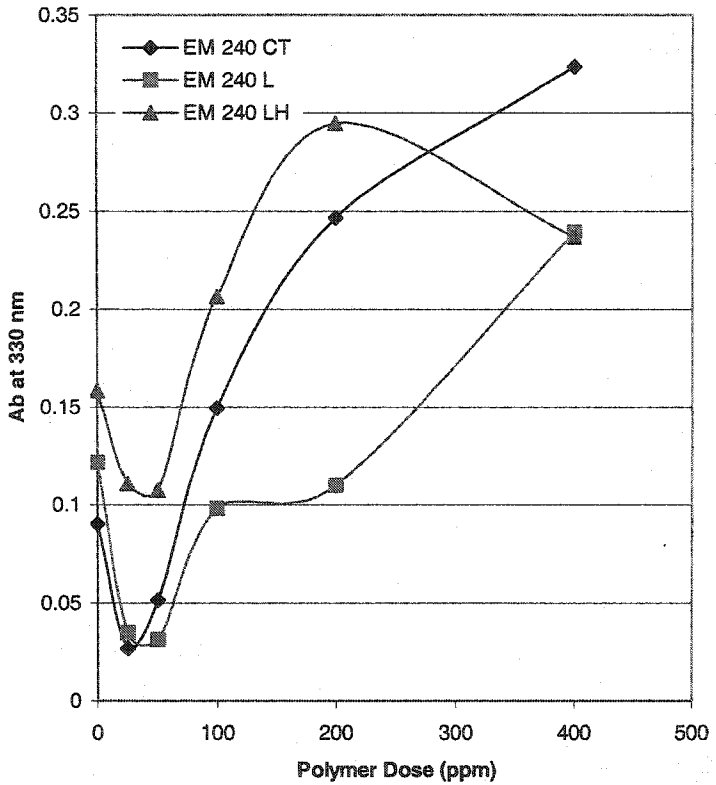

(a)

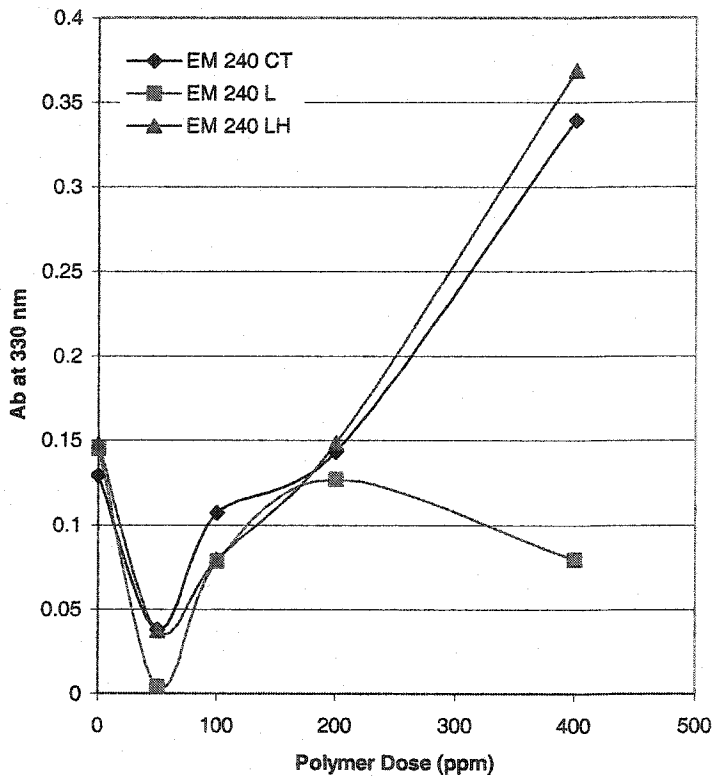

(b)

Figure 4-3 Optimum dose for cationic polyacrylamide with 20 % charge density (a) 0.25 and (b) 0.50 wt% CHO cell concentration

For cationic polyacrylamides with 40 % charge density (EM440 series), it can be seen from Figure 4-4 that cationic polyacrylamide with the lowest molecular weight (EM440LH, MW = $2-3\times10^6$) was the least effective in inducing flocculation of CHO cell suspensions. Further, it is apparent that EM440CT was as effective as EM441L in flocculating CHO cell suspensions. At 0.25 wt% (Figure 4-4a) cell density, the optimum doses for EM440CT, EM441L and EM440LH are 30, 35 and 40 ppm, respectively, while the optimum doses for EM440CT, EM441L and EM440LH for 0.50 wt% (Figure 4-4b) CHO cell density are 60, 70, and 80 ppm, respectively.

Results for cationic polyacrylamides with 80% charge density are shown in Figure 4-5. It can be seen from Figure 4-5a that at 0.25 wt% cell density EM840L is more effective in inducing flocculation of the CHO cell suspension while, at a higher CHO cell density (0.50 wt%, Figure 4-5b), both EM840CT and EM840L are effective in flocculating CHO cell suspensions. The optimum doses of EM840CT and EM840L for 0.25 and 0.50 wt% CHO cell densities are 35 and 60 ppm and 30 and 65 ppm, respectively.

Table 4 – 1 summarizes the results for the optimum dose experiment. It was found experimentally that at constant CHO cell density the EM1540 series required higher dose to induce flocculation than did other series tested. Further, the optimum doses for the EM240 and EM440 series were comparable while the EM840 series required the lowest dose of any of the other series tested. Therefore, due to the high optimum dose necessary to induce flocculation of CHO cell suspension at the same cell density, the EM 1540 series were eliminated even though the absorbance at 330 nm was of the same order of magnitude as other series.

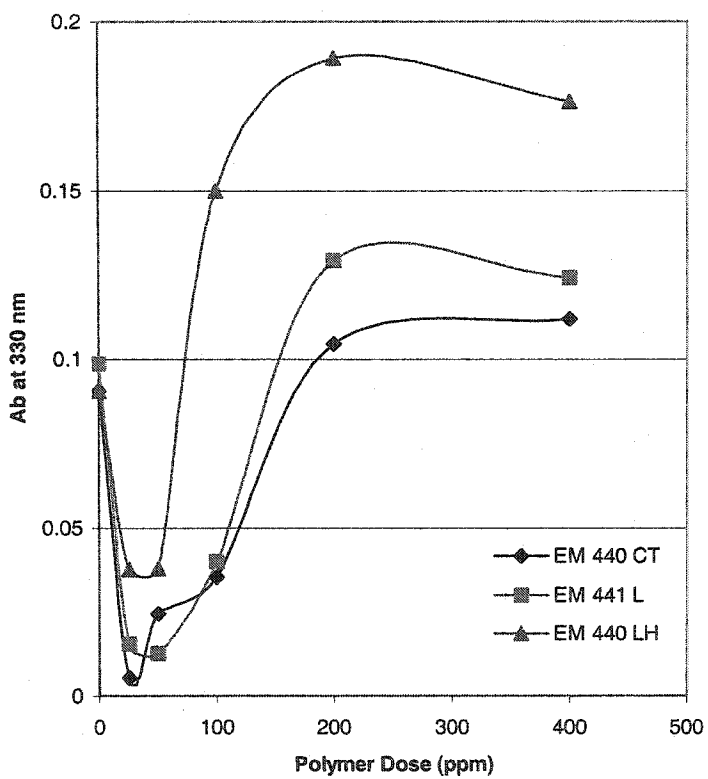

(a)

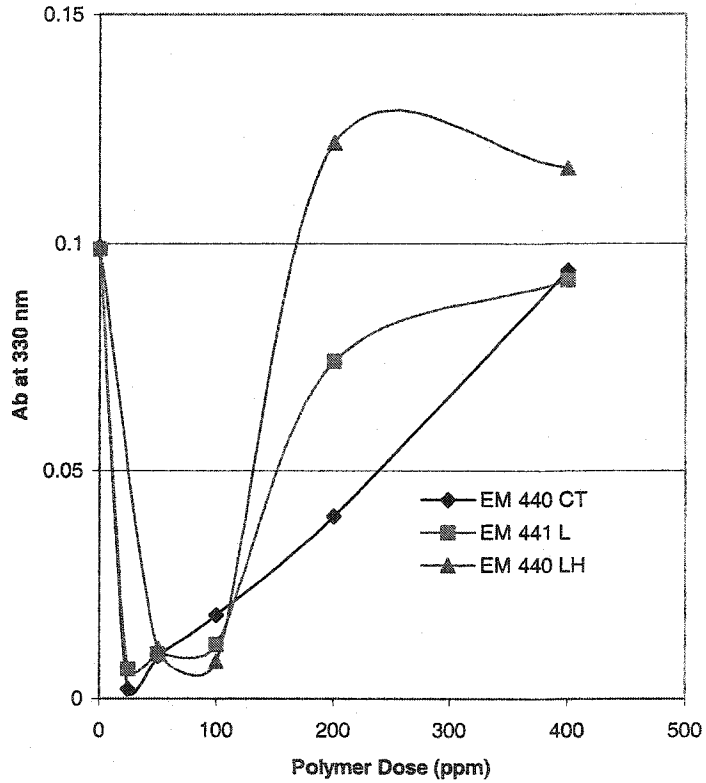

(b)

Figure 4-4 Optimum dose for cationic polyacrylamide with 40 % charge density (a) 0.25 and (b) 0.50 wt% CHO cell concentration

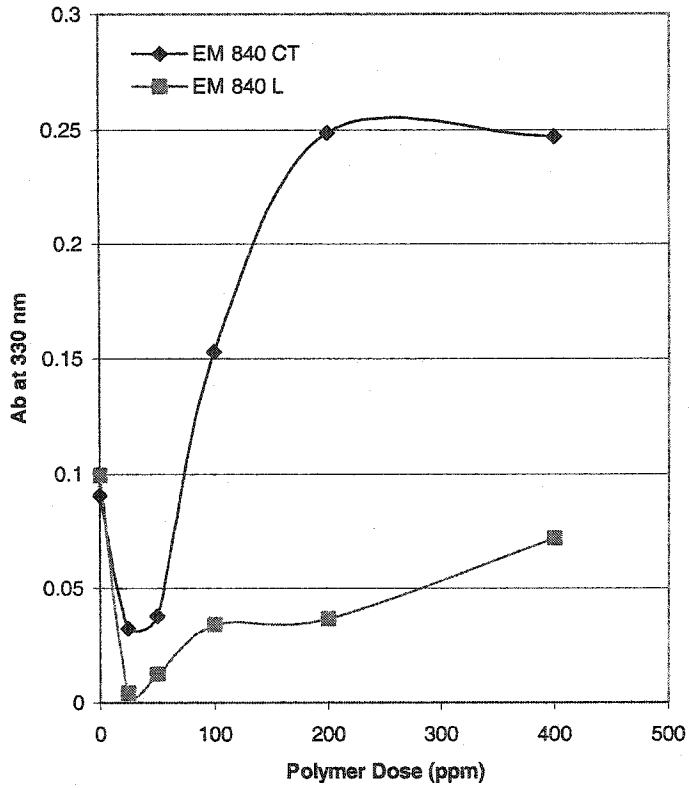

(a)

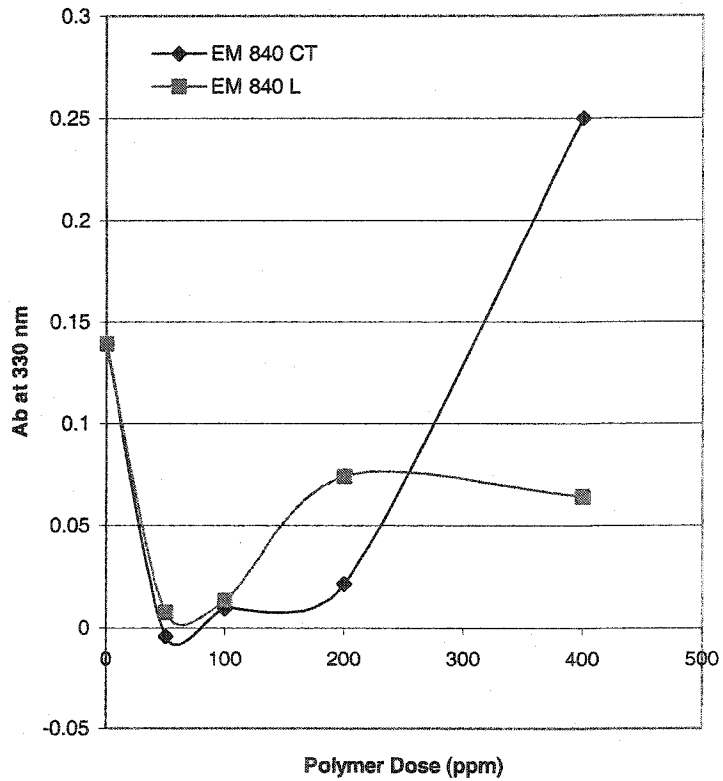

(b)

Figure 4-5 Optimum dose for cationic polyacrylamide with 80 % charge density (a) 0.25 and (b) 0.50 wt% CHO cell concentration

4.1.1.3. Optimum Stirring Speed and Time

Due to the fact that the average particle size in the flocculated suspensions is governed by the shear stress and the duration of shear stress, the optimum stirring speed and time were determined for each cationic polyacrylamide. The stirring speeds tested were 100, 300 and 500 rpm while the stirring times were 1, 3, 5 and 10 minutes. Since flocculation was carried out for 0.25 and 0.50 wt% CHO cell densities, optimum stirring speed and time was performed for all polymers tested at the optimum doses found previously. Only results for 0.50 wt% CHO cell concentration are given here. For other CHO cell concentrations, results may be found in Appendix K.

Results for the stirring speed and time at 0.50 wt% CHO cell density for EM440CT, EM441L and EM440LH are provided in Figure 4-6. It can be seen from Figure 4-6a that for all stirring times of 1, 3, 5 and 10 minutes the agitation speed of approximately 180 rpm gives the lowest absorbance. Further, it is evident that stirring time of 3 minutes minimized the absorbance of the supernatant of the flocculated suspension. For EM441L (Figure 4-6b), it is also apparent from that the minimum absorbance is found at 3 minutes and 130 rpm. For the cationic polyacrylamide of low molecular weight, EM440LH, the stirring speed of 200 rpm and agitation time 1 minute was found to yield the lowest absorbance (Figure 4-6c).

It is apparent that for different cationic polyacrylamides with different cationicity and molecular weight the combination of stirring speed and time that yields the lowest absorbance is different. However, from particle size distribution experiments (below), it was found that only EM440CT and EM441L are effective in flocculating CHO cell suspension. Therefore, the stirring speed and time, 180 rpm and 3 minutes, respectively,

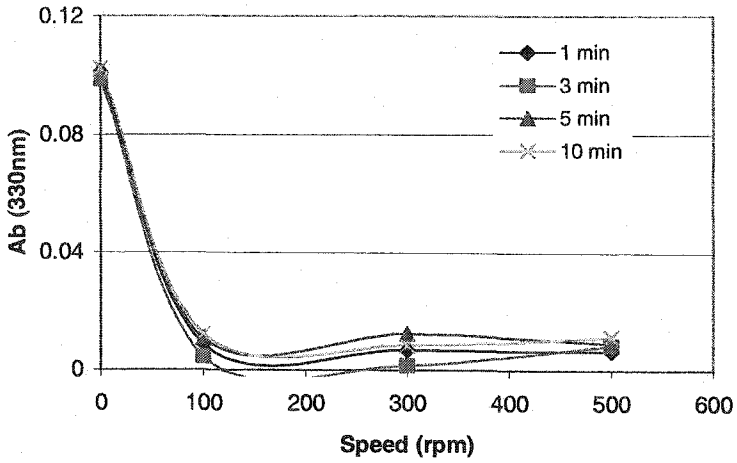

(a)

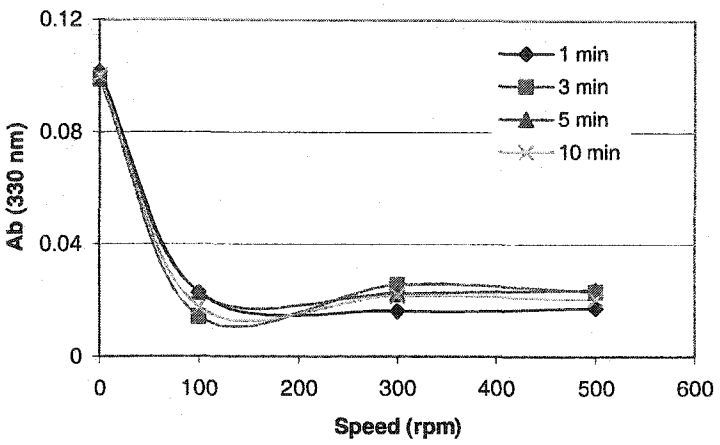

(b)

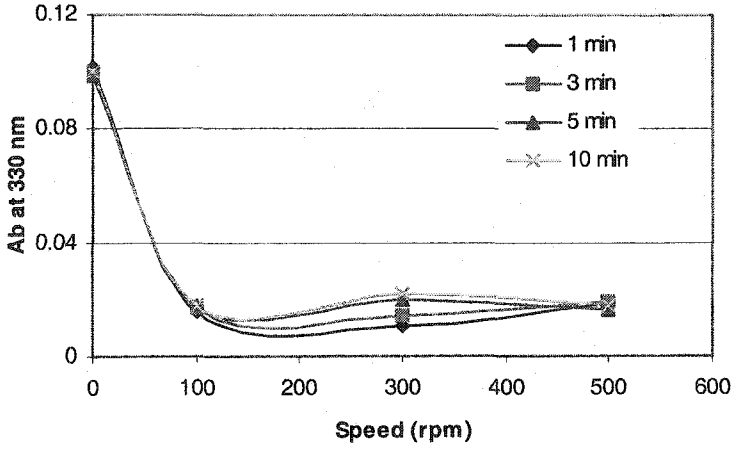

(c)

Figure 4-6 Optimum stirring speed and time for cationic polyacrylamides with 40 % charge density for 0.50 wt% CHO cell concentration: (a) EM 440CT, (b) EM 441L and (c) EM 440LH

of EM440CT will be used to induce flocculation in future experiments. Further, the optimum stirring speed and time is redefined as a combination of the stirring speed and time at which the average particle size of flocculated particles reaches steady state.

4.1.2. Particle Size Distribution

As can be seen from the results from the optimum stirring speed and time experiments, it appears that almost all of the cationic polyacrylamides used were capable of minimizing the absorbance of the supernatant of flocculated CHO cell suspensions to approximately the same degree regardless of stirring speed and time. Furthermore, during the optimum stirring speed and time experiments, it was found that both EM840CT and EM840L did not disperse well after addition to CHO cell suspensions. The flocs formed stuck to the paddle of the stirred vessel rather than being homogenously suspended in the suspending medium. Consequently, particle size distributions of the flocculated CHO cells for EM840CT and EM840L were omitted. The particle size distribution was determined for EM240 (EM240CT, EM240L and EM240LH) and EM440 (EM440CT, EM441L and EM440LH) series.

The particle size distribution for each polymer was determined for both CHO cell concentrations of 0.25 and 0.50 wt% at stirring speeds of 100, 300 and 500 rpm and stirring times of 1, 3, 5, 10 and 50 minutes. At each designated time, a small sample of 10 mL was withdrawn and particle size distribution was determined as soon as possible. In general, as anticipated, the average particle size grows with time at constant stirring speed as flocculation proceeds. However, at longer agitation time, the average particle size becomes smaller due to the fact that the agglomeration rate and the break-up rate of

the formed flocs are kinetically balanced. It can be further seen that the average particle size reached a steady state value which depended upon the polymeric flocculants used. Results for particle size distribution of CHO cells flocculated by EM 440CT are given below while results for particle size distribution of other cationic polyacrylamides are provided in Appendix J.

For EM440CT (charge density and molecular weight are 40% and $5-8\times10^{6}$) particle size distribution of 0.50 wt% CHO cell density at 100, 300 and 500 rpm are illustrated in Figure 4-7. At 100 rpm stirring speed (Figure 4-7a), it can be seen that for a stirring time of 1 minute the majority of the particle size increases from approximately 18 – 20 μm to 120 μm. However, at the same time, a number of smaller particles still exist in the suspension. As the flocculation time was increased to 3 minutes, the particle size further grew in size and became larger than that at 1 minute. Simultaneously, the number of smaller particles (8 – 50 μm) was reduced while a small portion of larger particles (800 – 1000 μm) was observed. After approximately 5 minutes of agitation, the average particle size shifts slightly back to a smaller value of ~ 115 μm while the number of the particle in the size range of 8 – 50 and 800 – 1000 μm is significantly reduced. It should be noted that particles (cell debris) of 0.5 – 8 μm in size exist in the suspension at every stage of the experiment. After 10 minutes of agitation, the average particle size remains the same as that at 5 minutes, however, it is apparent that the number of small particles is significantly increased. For the stirring time of more than 50 minutes, it can be seen that the number of small particles decreases as the average particle size of the suspension is approximately the same (115 μm). It is noteworthy to recognize that even though the average particle size of the suspension remains nearly

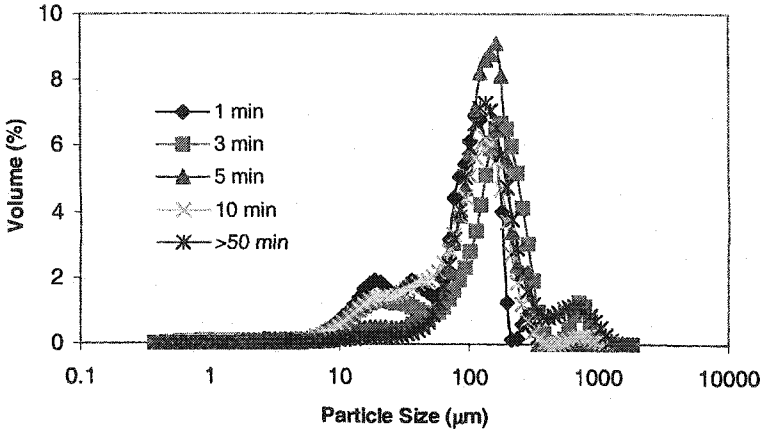

(a)

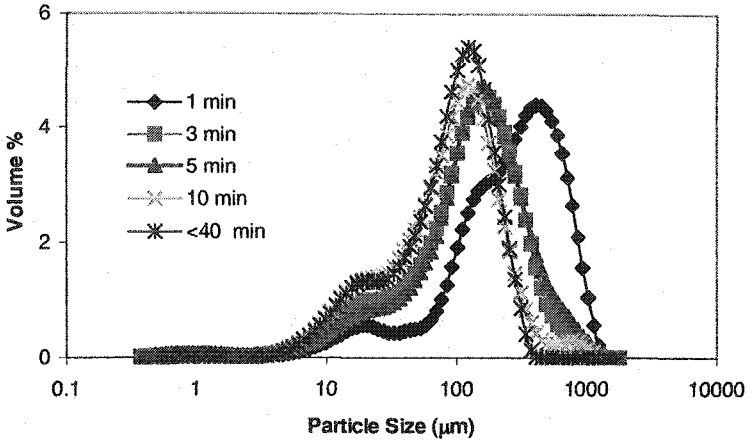

(b)

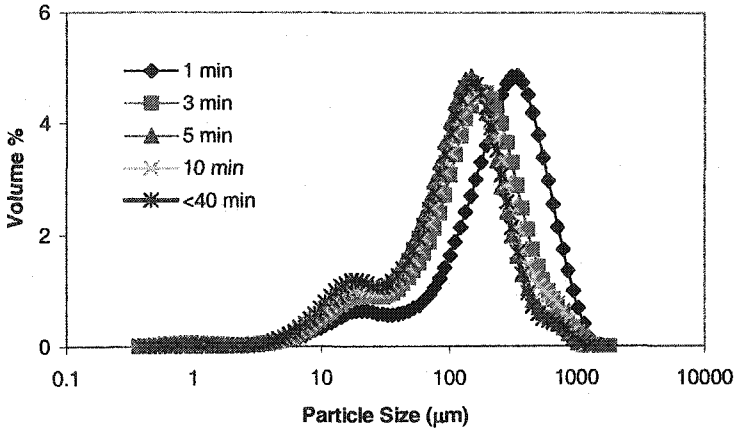

(c)

Figure 4-7 Particle size distribution of flocculated CHO cells at cell concentration of 0.50 wt% with cationic polyacrylamide with 40 % charge density: (a) 100, (b) 300 and (c) 500 rpm stirring speed

constant at the asymptotic size of 115 μm, the percentages of the existing size are not constant which may be due to the dynamic characteristics of the system.

Figure 4-7b shows the particle size distribution at a stirring speed of 300 rpm. It is evident that EM440CT is effective in flocculating of the CHO cell suspension. After stirring for 1 minute, the average particle size increases from 18 μm to 500 μm. However, the average particle size decreases as the flocculation process progresses. For stirring times of 3 and 5 minutes, the shape of the particle size distribution is almost identical with an average particle size of nearly 200 μm. Further, as the flocculation time increases to 10 minutes the average particle size shows a slight decrease in size to approximately 160 μm. However, the presence of smaller particles increases while larger particles seem to decrease. At a stirring time of more than 40 minutes, the shape of the particle size distribution takes the same form and average size as that at 10 minutes, however, the volume percentage of the average particle size at 160 μm increases and the presence of large particles (flocs) decreases.

The particle size distribution for EM440CT at 500 rpm stirring speed is shown in Figure 4-7c. It is apparent that the average particle size at 1 minute is smaller than that at 1 minute of 300 rpm. As the agitation time increases to 3 minutes, the average particle size decreases from approximately 320 to 180 μm while the presence of small particles increases slightly. When the stirring time was increased to 5 minutes, the average particle size becomes even smaller than that at 3 minutes. However, when the agitation time was increased to 10 minutes, the average particle size grew somewhat larger than that at 5 minutes. For stirring times more than 50 minutes, the average particle size yet again decreases slightly to approximately 130 μm.

For a CHO cell density of 0.25 wt%, the particle size distributions for 100, 300 and 500 rpm are shown in the Figure 4-8. It can be seen for a stirring speed of 100 rpm (Figure 4-8a) that for 1 minute agitation the average particle size shifted from that of unflocculated CHO cells to the size of approximately 150 μm. However, there is a significant portion of single particles present in the suspension. As the flocculation time was increased to 3 minutes, the average particle size becomes slightly smaller with a decrease in the percentages of single particles. Further, after 5 minutes stirring, the average particle size is approximately the same as that at 3 minutes, however, the percentages of such sizes is somewhat increased. For 10 and more than 50 minutes flocculation time, the average particle sizes for both times are almost identical to that at 3 and 5 minutes. Nevertheless, the percentages of the average size increase as flocculation time increases while the portions of single CHO cells decrease.

For 300 rpm stirring speed, Figure 4-8b, the shape of the particle size distribution for 1 minute agitation time shows the same trend as that at 100 rpm at the same stirring time. Further, the average particle size is found to be 150 μm with a large portion of single CHO cells present in suspension. It can be further seen that as the particles undergo longer flocculation times (3 and 5 minutes), the average particle size becomes slightly smaller while the presence of single CHO cells decreases. The average particle size for 10 minute stirring time is found to be 140 μm. It should be noted that as the flocculation time increases from 1 to 10 minutes, the volume percentages of the particle of such size increase as well. For a flocculation time of more than 50 minutes, the average particle size is approximately 130 μm with the portion of single CHO cells that is almost identical to that at 5 and 10 minutes. As can be seen from Figure 4-8c that at

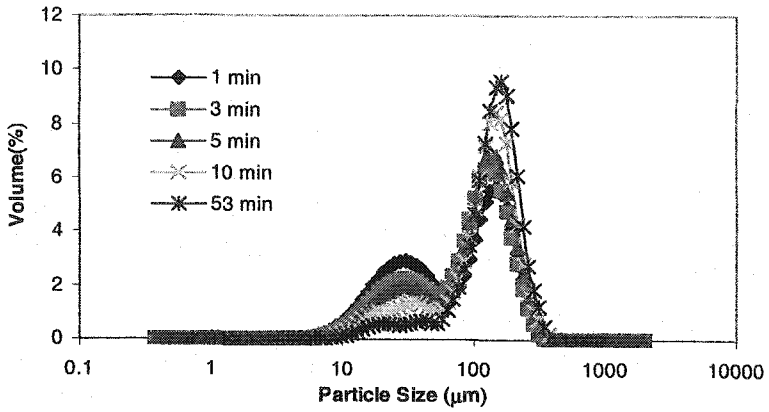

(a)

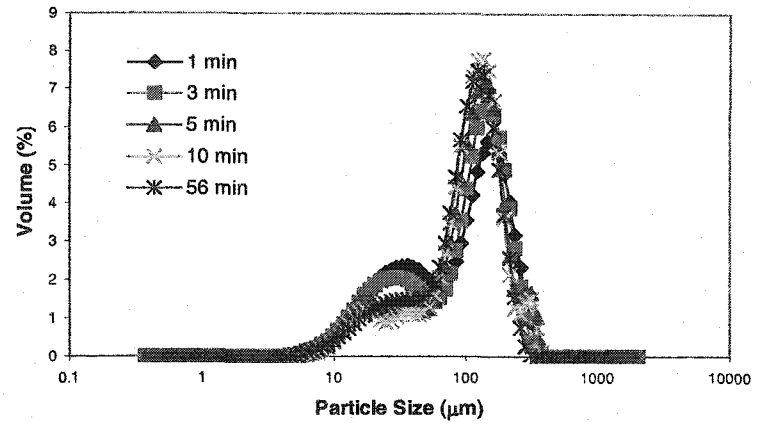

(b)

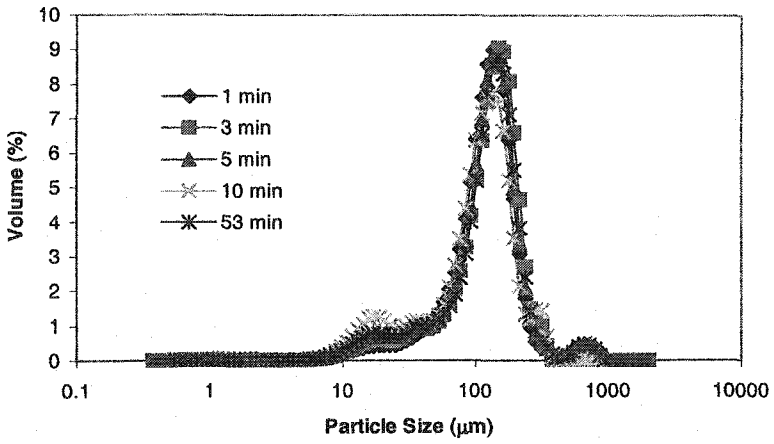

(c)

Figure 4-8 Particle size distribution of flocculated CHO cells at cell concentration of 0.25 wt% with cationic polyacrylamide with 40 % charge density: (a) 100, (b) 300 and (c) 500 rpm stirring speed

500 rpm agitation speed the average particle size reaches the asymptotic value of approximately 105 μm regardless of the agitation time. Additionally, the shapes of the particle size distribution at all agitation times are nearly identical except for that at 10 minutes flocculation.

In general, at low stirring speed (100 rpm), the shape of the particle size distribution shifted to the right (larger particles) while at the same time there exists a large portion of single CHO cells in the flocculated suspension. As flocculation time increases the particle size distributions shifted slightly back to the left toward the original average size of single CHO cells and eventually the average size of particles reaches an asymptotic (steady state) value. For a moderate stirring speed of 300 rpm, the average particle size of the flocculated suspension at an early stage becomes definitely smaller than that at 100 rpm stirring speed at the same flocculation time. Further, the average particle size attains the steady state size faster than that at the stirring speed of 100 rpm. As for the highest agitation speed of 500 rpm, the average particle size at 1 minute flocculation time is found to be the smallest in comparison to those at 100 and 300 rpm at the same time. In the same fashion, the average particle size decreases as the flocculation time increases. Moreover, particles that have been subjected to a high agitation speed (velocity gradient) are found to attain the steady state size the fastest.

For cationic polyacrylamides with 20% charge densities (EM240CT, EM240L and EM240LH), the foregoing explanation holds only for the first minute of flocculation. As the flocculation time increases the formed flocs are broken down to approximately the same size as that of single CHO cells. The particle size distributions of EM240CT, EM240L and EM 240LH may be found in Appendix J.

From results of particle size distribution, stirring speed and time and optimum dose, it is clearly that out of 10 cationic polyacrylamides tested only EM440CT and EM441L can be successfully used to induce flocculation of CHO cells suspensions. Further, the optimum doses of both EM440CT and EM441L are 30 and 35 ppm for 0.25 wt% and 60 and 70 ppm for 0.50 wt%, respectively. However, since EM440CT results in the lowest dose required to induce flocculation of suspension for both CHO cell densities, the rest of flocculation experiments in this study were therefore carried out solely with EM440CT. It is also obvious that the optimum dose doubles as cell densities increase implying that the ratio of particle surface area to polymer is constant for flocculation of CHO cells by EM440CT.

4.2 Particle Size Modelling

The law of conservation of dimensions may be applied to group variables and parameters in a system into sets of dimensionless numbers. The original variables may then be replaced by the corresponding dimensionless groups. These dimensionless groups are particularly useful in that they are independent of size or scale of the system. However, it is important to realize that the process of dimensionless analysis only replaces the original set of the original variables with a smaller set of dimensionless variables.

In an agitated system, it is reasonable to assume that the average particle sizes are dependent upon several important parameters such as the impeller diameter (D_i), kinematic viscosity of the suspending fluid (ν), velocity gradient (G). Consequently, the dependency of the average particle sizes may be written mathematically as

$$f(\rho, G, D_i, \nu, t, d) = 0 \tag{4-1}$$

There are a number of ways of determining the relevant dimensionless groups (Darby (2001)). One of the best-known methods is the Buckingham Π theorem that states $\Pi = q - u$ where Π is the number of dimensionless variables, q is the number of dimensional variables and u is the number of fundamental dimensions. A fundamental dimension is one that cannot be expressed in terms of any other dimensions such as time, length and mass. Consequently, a set of three arbitrarily chosen variables, ρ, G, and D_i, maybe used as fixed variables in the process of dimensional analysis. As a result, an empirical model is

$$\frac{d}{D_i} = K\left(\frac{D_i^2 G}{\nu}\right)^a \left(\frac{1}{Gt}\right)^b \tag{4-2}$$

It should be noted that the first and second terms on the right hand side in (4-2) are, respectively, the so called "impeller Reynolds' Number" and the inverse "Camp Number". However, it is generally suggested that, in order to take the concentration of the primary particles into account, the Camp number may be slightly modified by simply multiplying the volume fraction (ϕ) of the particles in suspension (Bernhardt and Schell (1993)). Therefore, Eq. (4-2) may be written as

$$\frac{d}{D_i} = K\left(\frac{D_i^2 G}{\nu}\right)^a \left(\frac{1}{G\phi t}\right)^b \tag{4-3}$$

Figure 4-9 shows the fitted experimental data to the developed model. It is evident that average particle sizes can be divided into two groups, which are effective and non-effective flocculants. The average particle sizes of CHO cells flocculated by EM441L were used to determine each exponent of the model. It was found that the

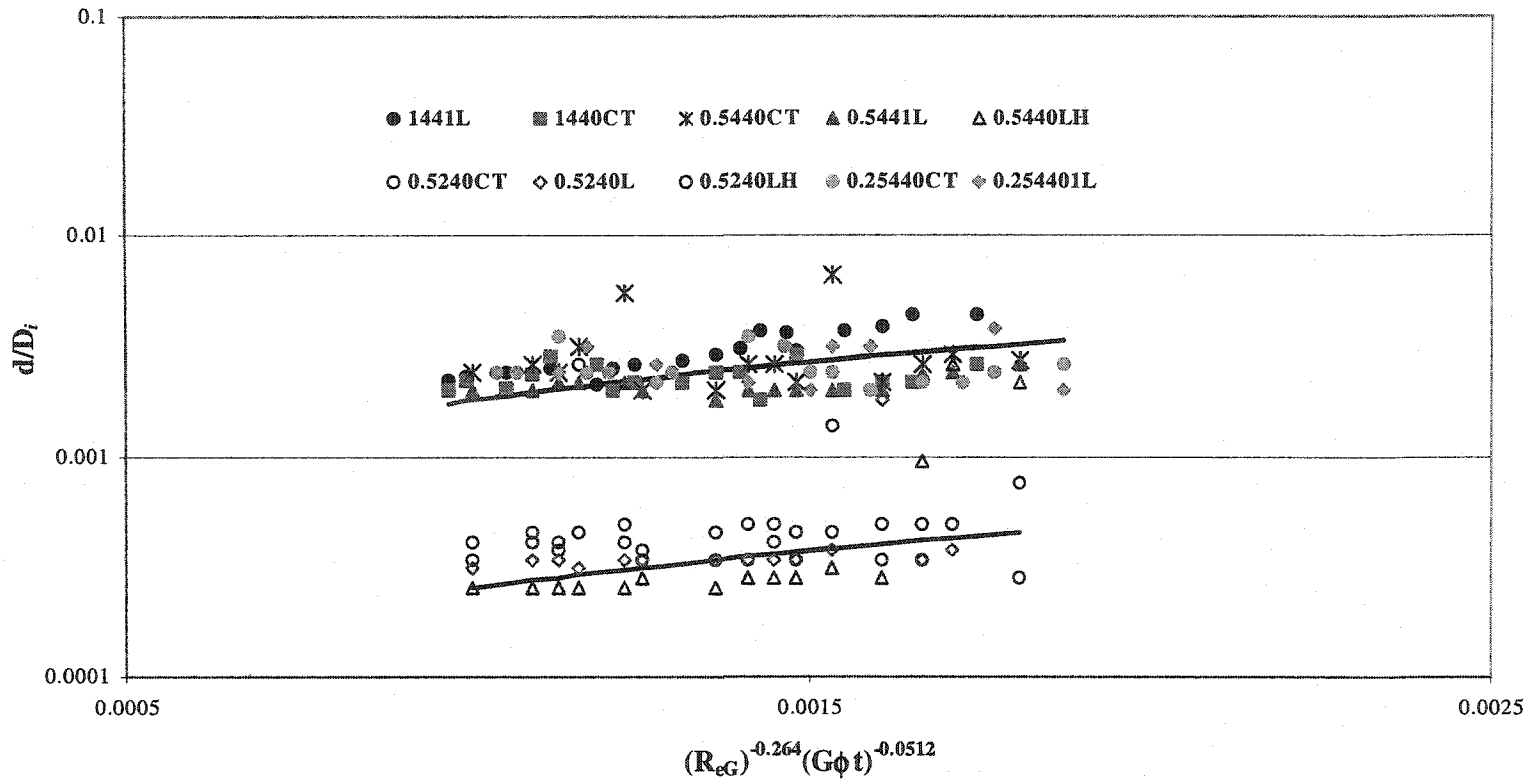

Figure 4-9 Modeling of average particle size after flocculation with cationic polyacrylamides. The concentrations of CHO cells are 0.25, 0.50 and 1.00 wt% whereas charge densities of cationic polyacrylamides are 20 and 40 %. Stirring speed used in flocculation are 100, 300 and 500 rpm while flocculation times are 1, 3, 5 and 10 minutes. There are two separate groups of particle sizes, which are for effective (top) and non-effective flocculants (bottom). The solid lines are empirically predicted average particle sizes.

values for both a and b are – 0.264 and – 0.0512, respectively. The constant K is used as fitted parameter. As a result, it was therefore found that average particle sizes for effective flocculants may be predicted by

$$\frac{d}{D_i} = 1.8R_{eG}^{-0.264}(G\phi t)^{-0.0512} \tag{4-4}$$

and for non-effective flocculants

$$\frac{d}{D_i} = 0.25R_{eG}^{-0.264}(G\phi t)^{-0.0512} \tag{4-5}$$

It can be seen from Figure 4-9 that the correlation is quantitatively in good agreement with the experimental data. At low velocity gradients, the model slightly over predicts the average particle size, while at high velocity gradient the model tends to under predict the average particle size.

4.3 Interaction Potential

The stability of colloidal particles in suspension may be estimated by the DLVO theory. Accordingly, an interaction potential between particles in suspension may be determined by assuming that the attractive van der Waals and the repulsive electrical double layer forces are additive. In this section, both attractive van der Waals force and repulsive electrostatic double layer force are determined for each suspension. Stabilities of CHO cells, A-MLV and CHO-A-MLV suspension are therefore semi-quantitatively determined for each suspension using the DLVO theory.

4.3.1. Debye-Hückel Parameter

An electrical double layer develops when charged colloidal particles present in suspension gives rise to the repulsive force between particles with charge of the same sign. This repulsive force consequently prevents particles from coming into close contact. The thickness of the double layer (κ^{-1}) can be quantitatively determined from the inverse Debye-Hückel parameter (κ). However, to calculate the Debye-Hückel parameter, the ionic strength of the suspension of interest is necessary due to the fact that the higher the ionic strength the larger the Debye-Hückel parameter and subsequently the thinner the thickness of the double layer.

The reported osmolality of IS-CHO medium is approximately 270 mOsm/L (Irvine Scientific, Santa Ana, CA), which is almost identical to that of the α-MEM (the medium for attachment dependant CHO cells), of 280 mOsm/L (Life technologies, Grand Island, NY). Accordingly, it is assumed here that the ionic strength of the IS-CHO medium is the same as that of α-MEM. Therefore, the ionic strength of α-MEM was estimated from the available inorganic salts in the medium using (2-36). In the calculation of the ionic strength for the α-MEM, it is further assumed that there is no interaction between the constituent salts. In addition, it is assumed that all the parameters used in the calculation of the Debye-Hückel parameter are those of water at 25 °C. It was found, as a result, that the ionic strength of α-MEM is 0.315 M. Subsequently, the Debye-Hückel parameter (κ) is calculated from (2-37) and, consequently, it was found that κ is approximately $1.3\times10^{9}\ m^{-1}$ which corresponds to the thickness of the double (κ^{-1}) of 0.77 nm.

4.3.2. Interaction Potential between CHO Cells in Suspension

For the calculation of an attractive van der Waals force, the Hamaker constant of the system is assumed to have the value of 1×10^{-21} J for both CHO cells and A-MLV. It is further assumed that the retardation effect is accounted for by the Hamaker constant. The van der Waals attractive force is calculated using (2-41).

In order to determine the repulsive electrical double layer force between particles in suspension, potentials at the surface of the particles are required. Therefore, the values of zeta potential of CHO cells and A-MLV virions reported in literature are used in all calculations. Due to the scarcity of zeta potential of CHO cells in literature, the zeta potential of the Chinese hamster fibroblast cells, -22 mV (Greig and Jones (1976)), was used. The repulsive electrical double layer force is determined using (2-42) with all the parameters assumed to be those of water at 25 °C.

The interaction between CHO cells in suspension is shown in Figure 4-10. It is evident that CHO cells in suspension whose ionic strength is 0.315 M are kinetically stable due to the fact that the energy barrier is of the order of 2,000 kT where k is the Boltzmann constant (1.38×10^{-23} JK^{-1}) and T is absolute temperature. At this level, it is apparent that aggregation of CHO cells is not likely to take place due to the fact it is not probable for single CHO cell to gain sufficient thermal energy to overcome the energy barrier and consequently aggregate into the primary minima. Even though it has been reported that nucleic acids released from dead cells may cause CHO cells to aggregate in suspension (Renner et al. (1993)), it is experimentally observed that CHO-DG44 cells stay mostly as a singlet and doublet with a very small portion of aggregates.

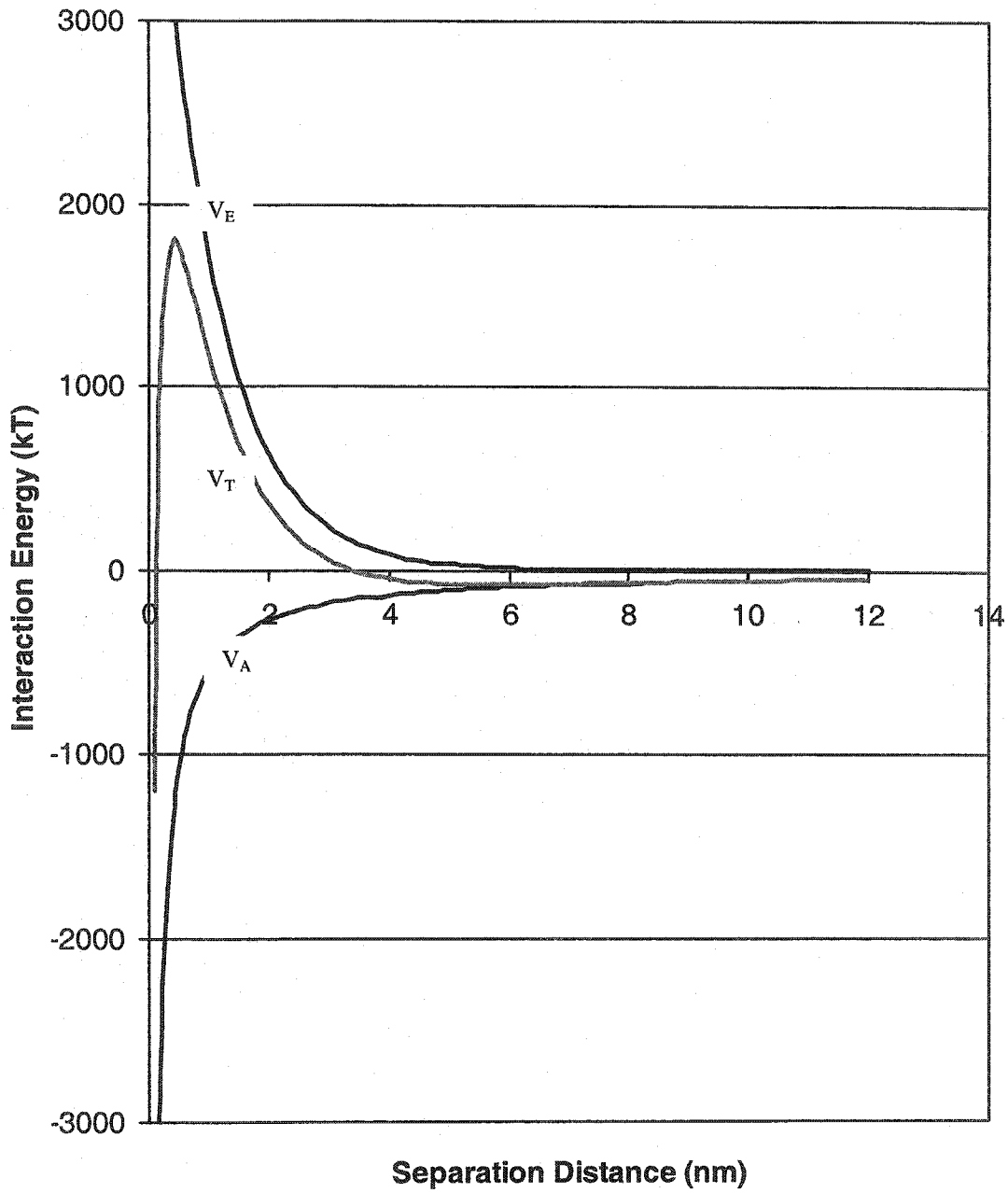

Figure 4-10 Interaction potential for CHO cells in suspension. In the calculation, Hamaker constant and Debye-Hückel parameter (κ) are 1×10^{-21} J and 0.77 nm, respectively, while the surface potential of CHO cells is – 22 mV.

4.3.3. Interaction Potential between A-MLV Particles in Suspension

The electrophoretic mobility of mouse mammary tumor virus (MMTV) (Sarkar et al. (1973)) in 0.01 M NaCl is -6.9×10^{-5} $cm^2V^{-1}s^{-1}$, which corresponds to the zeta potential value of – 15.11 mV. In prior calculations, (2-32) was used while other parameters are those of water at 25 °C

The interaction potential between A-MLV particles in suspension is given in Figure 4-11. It can be seen from Figure 4-11 that the energy barrier between each A-MLV virion in suspension is approximately 6 kT. It was reported that colloidal suspensions with an energy barrier of the order 1 – 2 kT may naturally form aggregates (Gregory (1989)) due to the fact that particles in suspension may gain thermal energy of a magnitude that is higher than the energy barrier thus overcoming the energy barrier and then flocculating into the primary minima. It is evident that A-MLV in suspension is also thermodynamically stable. Therefore, it is not likely for A-MLV to form self-aggregates in suspension.

4.3.4. Interaction Potential between CHO Cell and A-MLV in Suspension

Figure 4-12 shows the potentials of interaction between CHO cells and A-MLV particles in suspension for different ionic strengths and surface potentials of CHO cells and A-MLV. It can be seen from Figure 4-12 that at 0.315 M ionic strength ($\kappa = 1$) CHO cells and A-MLV particles are not likely to form self-aggregates in suspension due to the fact that the energy barrier between CHO cells and A-MLV is approximately 10 kT. The energy of interaction is reduced to zero at approximately 3 nm which may be referred to as the distance of closest approach. For the purpose of comparison the

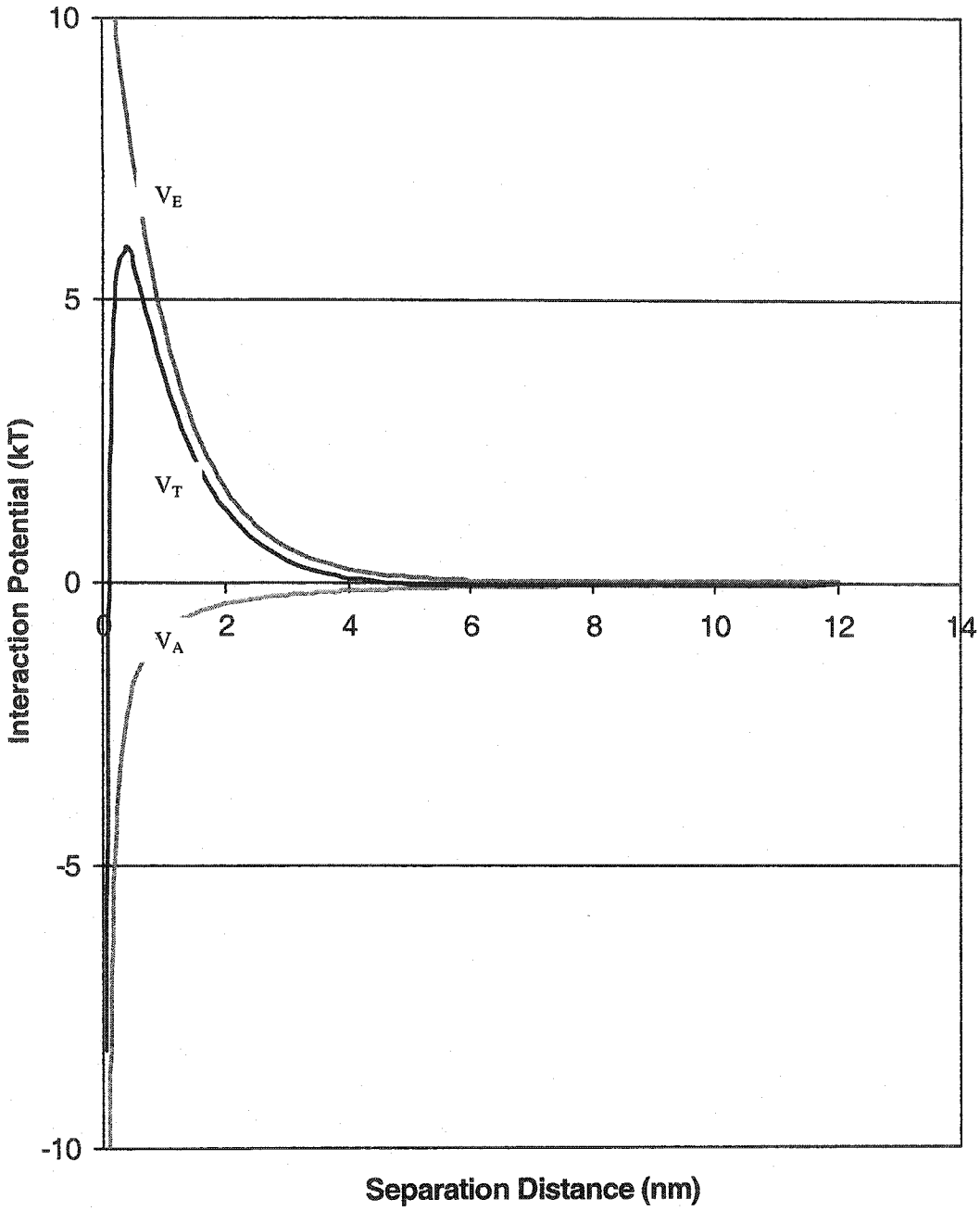

Figure 4-11 Interaction potential for A-MLV in suspension. Hamaker constant and the inverse Debye-Hückel parameter (κ^{-1}) are 1×10^{-21} J and 0.77 nm, respectively, while the surface potential of A-MLV virions is taken to be –15.11 m

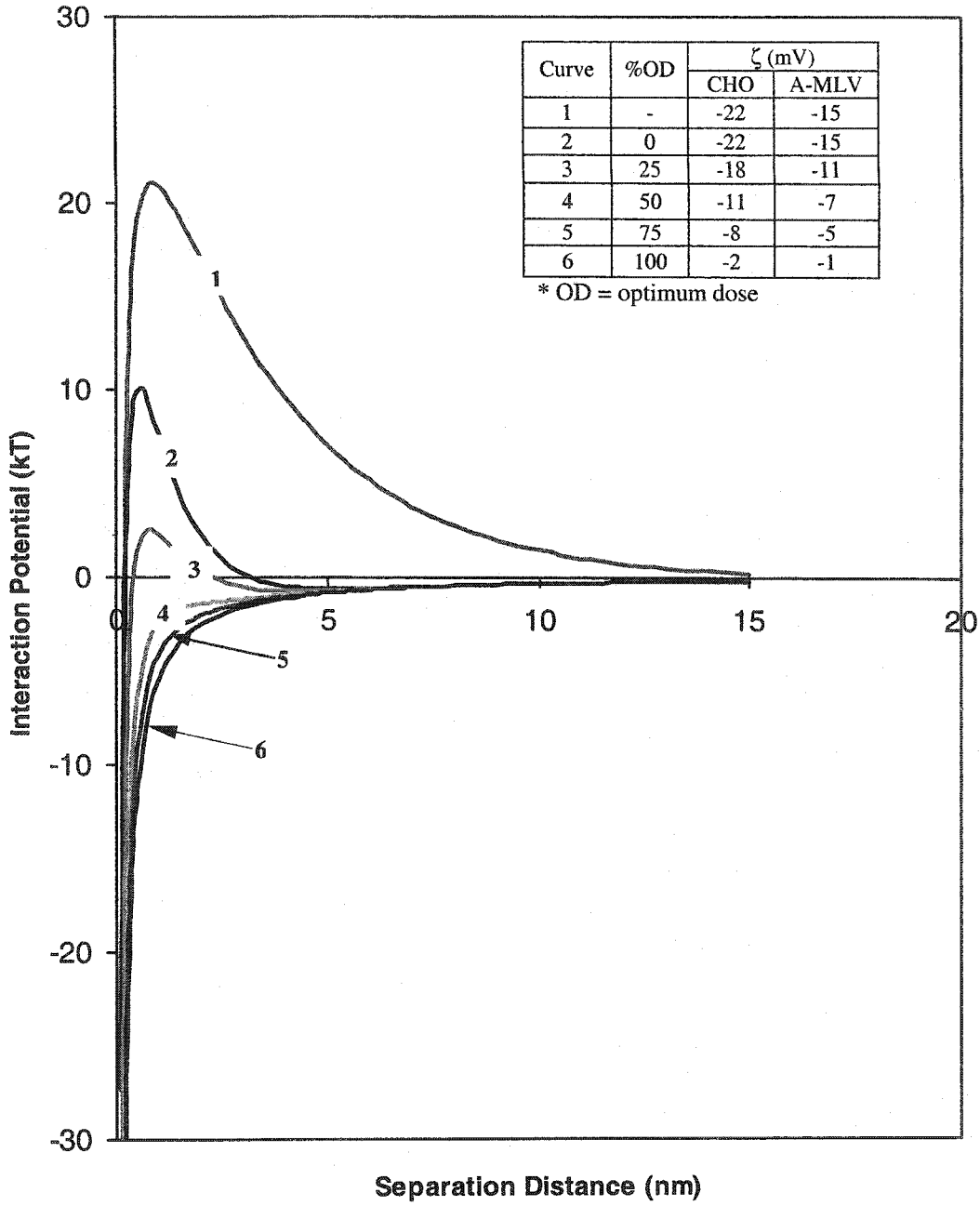

Figure 4-12 Interaction potential curve for CHO cells and A-MLV virions in suspension. Lines 1 ($\kappa = 0.3$) and 2 ($\kappa = 1$) show interaction potential between CHO cells and A-MLV virions in the absence of cationic polyacryamide. Lines 3, 4, 5 and 6 simulate the interaction potential between CHO cells and A-MLV virions after flocculation with cationic polyacrylamides at various percentates of optimum dose.

interaction energy curve at low ionic strength ($\kappa = 0.3$) is also provided. It can be clearly seen that at low ionic strength the energy of interaction rises to value of 22 kT. Further, the distance at which the energy of interaction is reduced to zero is greater than 15 nm. Therefore, it is reasonable to conclude that at low ionic strength ($\kappa = 0.3$) CHO cells and A-MLV particles are unable to come into close contact to allow flocculation to occur while at high ionic strength ($\kappa = 1$) close approach between CHO cells and A-MLV virions may be expected. This is due to the fact that at high ionic strength the thickness of double layer around the particles is reduced by the screening effect of counter-ions in suspension.

As cationic polyacrylamide is added to the suspension containing CHO cells and A-MLV, the zeta potential of both CHO cells and A-MLV should be continuously reduced due to charge neutralization. Figrue 4-12 shows interaction potential curves for flocculated suspension containing CHO cells and A-MLV at various percentages of optimum dose. As can be seen from Figure (4-12), when small amounts of cationic polymers (0.25 %OD) are added, energy barriers of the system are reduced to approximately 3 kT. As can be seen from Figure 4-12 the energy barrier of the system vanishes after the amounts of cationic polymers to achieve 50% of optimum dose are added. It is evident that when surface potentials of both CHO cells and A-MLV are reduced due to the adsorption of cationic polymers, the energy barriers also significantly decrease. This fact indicates agglomeration of primary particles (CHO cells and A-MLV virions) took place. Additionally, at high ionic strength, the total potential of interaction between CHO cells and A-MLV particles is attractive and, moreover, no energy barrier is present.

From Figures 4-10, 11 and 12, it is theoretically found that DLVO theory predicts aggregation of CHO cells and A-MLV virions into larger aggregates in the presence of cationic polyacrylamides while in the absence of cationic polymers DLVO theory indicates that flocculation is unlikely. Further, at high ionic strength the distance of closest approach is much smaller than that at low ionic strength due to the screening effect of counter-ions that adsorbed onto the surfaces of the primary particles.

4.4 Adsortion Isotherm

In order to induce flocculation of CHO cell suspensions, cationic polyacrylamides were used as flocculating agents. According to the theoretical mechanisms involved in flocculation in the presence of polyelectrolytes, the surface coverage of particles by polymeric flocculants is of significant interest. If the flocculant dose is too small, poor flocculation results due to the fact that few polymeric chains adsorb onto single particles. On the contrary, excess polymeric flocculant results in charge reversal and then restabilization of the suspension, which leads also to poor flocculation.

In this project, adsorption of cationic polyacrylamides was investigated by means of colloid titration. From particle size experiments, only EM440CT and EM441L are effective in flocculating CHO cell suspensions. Therefore, adsorption studies of these two polymers and EM440LH were conducted. Standard curves for the colloid titration of EM440CT, EM441L and EM440LH are provided in Figure 4-13. For 0.50 wt% CHO cell, it is worthy to keep in mind that optimum doses for EM440CT, EM441L and EM440LH are, respectively, 60, 70 and 80 ppm. It can be seen from Figure 4-14a that at

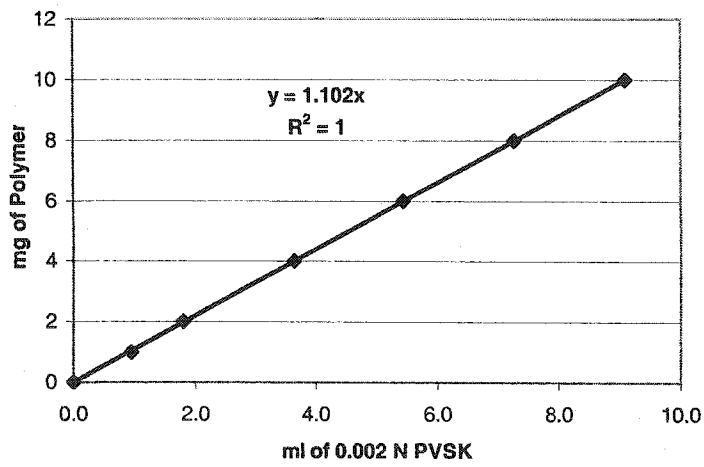

(a)

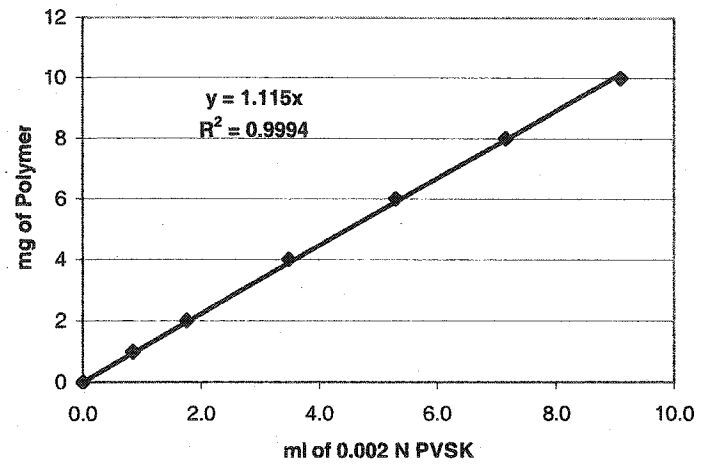

(b)

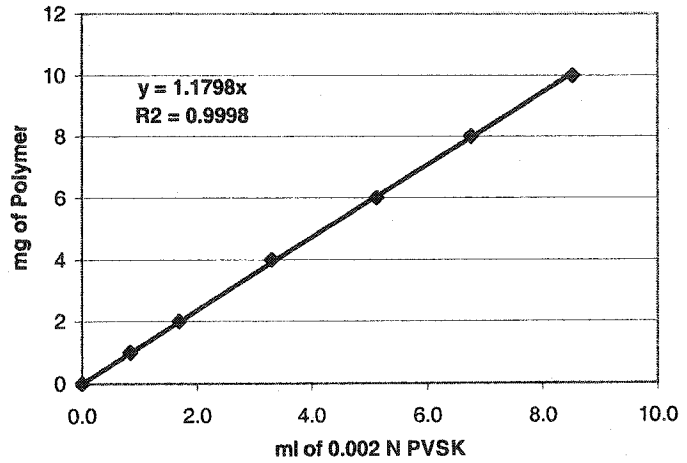

(c)

Figure 4-13 Standard curves for colloid titration: (a) EM440CT, (b) EM441L and (c) E440LH

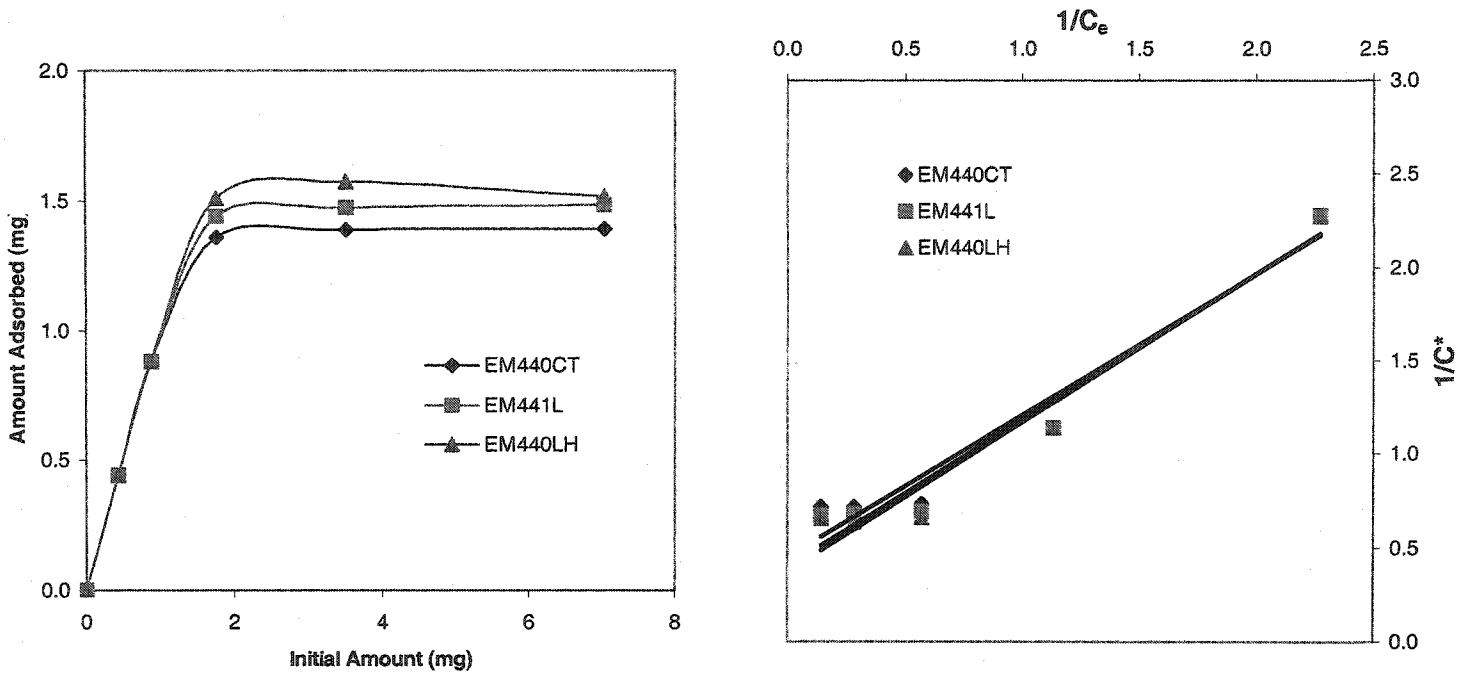

Figure 4-14 Adsorption isotherm of cationic polyacrylamides with 40 % charge density: (a) Lagmuir isotherm and (b) inverse Langmuir isotherm. The optimum dose of of EM440CT, EM441L and EM440LH are 60, 70 and 80, respectively, which correspond to 0.98, 1.15 and 1.31 mg, respectively.

low polymer doses all of the polymers were adsorbed onto cell surfaces. As the polymer doses increase the amount of polymer adsorbed also increases, however, to some limiting values at which adsorption reaches saturation. For all the cationic polyacrylamides tested, at below optimum doses, the adsorbed amount increases linearly with the amount of polymers added while farther beyond optimum dose adsorption reaches equilibrium. Further, it can be clearly seen that the optimum doses lie within the transition regions indicating that particle surface coverage of the primary particles are not at saturation, and therefore, presumably at optimum.

According to the Langmuir isotherm, it is assumed that the polymeric molecules act as rigid sphere particles and each molecule has a fixed volume. As time proceeds, equilibrium is established between adsorption and desorption processes. Therefore, it can be shown that the Langmuir isotherm takes the form (Gill and Herrington (1987b))

$$\frac{1}{C^*} = \frac{1}{KC_eC_m} + \frac{1}{C_m} \qquad (4\text{-}6)$$

where C_e is the initial amount of polymer (mg), C^* is the amount of polymer adsorbed (mg/m^2), C_m is the amount of polymer adsorbed at saturation (mg/m^2) and K is the Langmuir constant. The plot of $\frac{1}{C^*}$ vs. $\frac{1}{C_e}$ yields a straight line whose slope and intercept are the Langmuir equilibrium constant and the maximum concentration of adsorbed molecules, respectively.

From Figure 4-14b it can be shown that the adsorption of cationic polyacrylamides with 40% charge density also follows the behavior of the Langmuir isotherm. By extrapolation, it was found that for EM440CT, EM441L and EM440LH the maximum concentration of adsorbed polyacrylamides (Figure 4-14b) are 2.22, 2.48

and 2.86 mg, respectively. At a concentration of 0.50 wt% of CHO cells, the calculated surface area is approximately 0.0503 m^2 per 120 mL, therefore, the saturation concentration of polymer adsorbed for EM440CT, EM441L and EM440LH are 44.09, 49.23 and 53.31 mg/m^2, respectively. From Table 4-1, the calculated optimum dose for EM440CT, EM441L and EM440LH is 20.98, 24.48 and 27.97 mg/m^2, respectively. It is evident that at optimum doses for EM440CT, EM441L and EM440LH surface coverage of CHO cells is approximately 50 % of that at saturation for all the cationic polyacrylamides tested. This finding is in good agreement with the previous findings of La Mer and Healy (1964)), who found theoretically that the surface coverage of 0.5 would yield the most efficient flocculation process.

4.5 Amphotropic Murine Leukemia Virus Pseudotype

Due to the fact that the A-MLV wild types are infectious and highly difficult to handle, the pseudotypes of A-MLV, which are infectious, but replication incompetent were used in this study. To produce A-MLV pseudotypes, transfection of HEK-293 cells with PLEGFP-C1 plasmid having a packaging signal necessary for viral particle assemble and EGFP as a marker was carried out. With EGFP expression by indicator cells, the concentration of A-MLV pseudotype was determined by the $TCID_{50}$ assay.

4.5.1. HEK-293 Cell Transfection

Transfection of HEK-293 cells (packaging cell line) with PLEGFP-C1 plasmid was carried out with Effectene transfection kit, which is a liposome based transfection method. Transfection efficiency was determined approximately 24 hrs post-transfection

by observing an expression of EGFP under ultraviolet light. The transfection efficiency was found to be approximately 70 – 80% (Figure 4-15). Transfected cells were then subjected to subculturing and antibiotic (G418) selection for high titer A-MLV pseudotype producing colonies.

4.5.2. Amphotropic Murine Leukemia Virus Titer

After G418 selection, a single colony was selected and transferred to a new 12 well-plate containing 2 mL of fresh medium per well. Approximately 36 colonies were selected. These colonies were allowed to amplify and subsequently the concentrations of A-MLV pseudotypes produced by each colony were determined. NIH/3T3 cells were used as indicator cells for these A-MLV pseudotypes. The viral titer is defined as the product of the number of NIH/3T3 cells that expressed EGFP divided by the highest dilution that demonstrates the expression of EGFP after 3 - 4 days post infection.

A preliminary screening of the A-MLV production revealed that out of 36 colonies primarily selected, only 3 colonies were found to produce higher enough titers of the A-MLV pseudotypes. Therefore, the viral titers of these three colonies were determined. Viruses in the growth medium were harvested after 2 – 3 days after subculturing (Clontech (2002)). In order to determine the viral titer, indicator cells were plated overnight at a density 2×10^5 cells per well of the 12 well-plate. (a high density of indicator cells was used to ensure that there were enough cells for the viruses to infect). Subsequently, the medium containing A-MLV pseudotype was serially diluted to the range of $10^0 - 10^{-6}$ and 100 μL of each dilution was used to infect the NIH/3T3 cells, which were pretreated with 8 - 10 μg/mL of polybrene for at least 15 minutes prior to

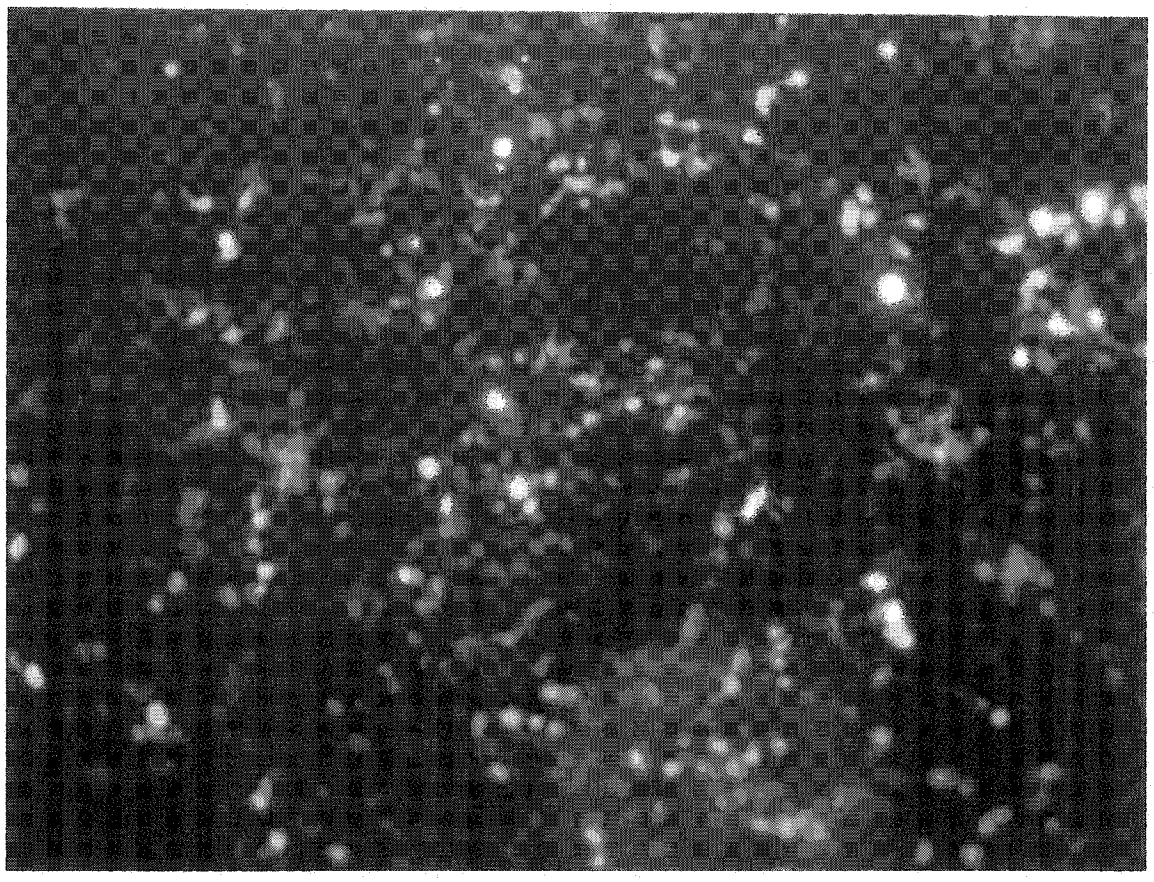

Figure 4-15 Transfection efficiency of HEK-293 cells transfected with pLEGFP-C1 plasmid. The transfection efficiency is evaluated 24 hrs post transfection by observing expression of EGFP of the transfected HEK-293 cells under a fluorescence microscope. It is found that the transfection efficiency is approximately 70 – 80 %.

infection. After 3-4 days post infection, expression of EGFP by the infected NIH/3T3 cells was observed.

Several attempts to determine the viral titer at high indicator cell densities were attempted without success. Consequently, the plating density of indicator cells was lowered. Further, infection was carried out at the time of plating (Carlson (2002)). The density of NIH/3T3 cells used was lowered to $0.2-0.5\times10^5$ cells per well of the 12 well-plate. To avoid overgrowth of NIH/3T3 cells and to reduce the volume of the target cells at plating, polybrene was added the cell suspension to the final concentration of 10 μg/mL. Subsequently, 100 μL of NIH/3T3 cells were transferred to each well of the 12 well-plate and 100 μL of virus dilution was then added and mixed by aspiration. Subsequently, 2.0 mL of fresh medium was added to each well and the assay plate was incubated at 37°C and 5% CO_2.

On day 3, expression of EGFP was observed under the inverted microscope equipped with an ultraviolet light. Expression of EGFP was much easier to discern even though the target cells were sligthly overgrown. At this plating cell density, the highest titer of the A-MLV pseudotype was approximately 5×10^5 infectious units/mL. This colony was chosen to produce the A-MLV pseudotypes for the whole project.

4.6 Control Experiments

Prior to flocculation and microfiltration experiments, control experiments were designed and conducted in order to eliminate the effects of external factors such as shear stress, temperature, contact time and toxicity of the cationic polyacrylamide that may

interfere with the analyses of the experimental results. Results for each control experiment are provided below.

4.6.1. A-MLV Alone

In order to investigate the effect of temperature on A-MLV deactivation, three T-25 flasks contained approximately 20 mL of medium with A-MLV pseudotypes were incubated at three different temperatures of 4, 25 and 37 °C for 15 days. Samples were taken at specified times and the infectivity of the samples was determined. The results of the effect of temperature on A-MLV are given in Figure 4-16. It is evident that temperature had almost no effect on A-MLV survival except at 37°C. However, at 37 °C the titers of A-MLV started to continuously decrease after 2 days of incubation while the titers of A-MLV at both 4 and 25 °C remained constant. Due to the fact during each freeze-thaw cycle the reduction of one to two orders of magnitude of A-MLV titers may be expected the medium containing A-MLV was maintained at 4 °C instead of freezing for all subsequent experiments. However, the virus was not stored for more than 10 days even though it was found experimentally that the reduction of A-MLV titer maintained at 4 °C for 15 days is negligible.

Since all the flocculation and microfiltration experiments were conducted at room temperature (25 °C) for three hours, it may be concluded that during the flocculation and microfiltration experiments the reduction of A-MLV titer due to temperature is negligible.

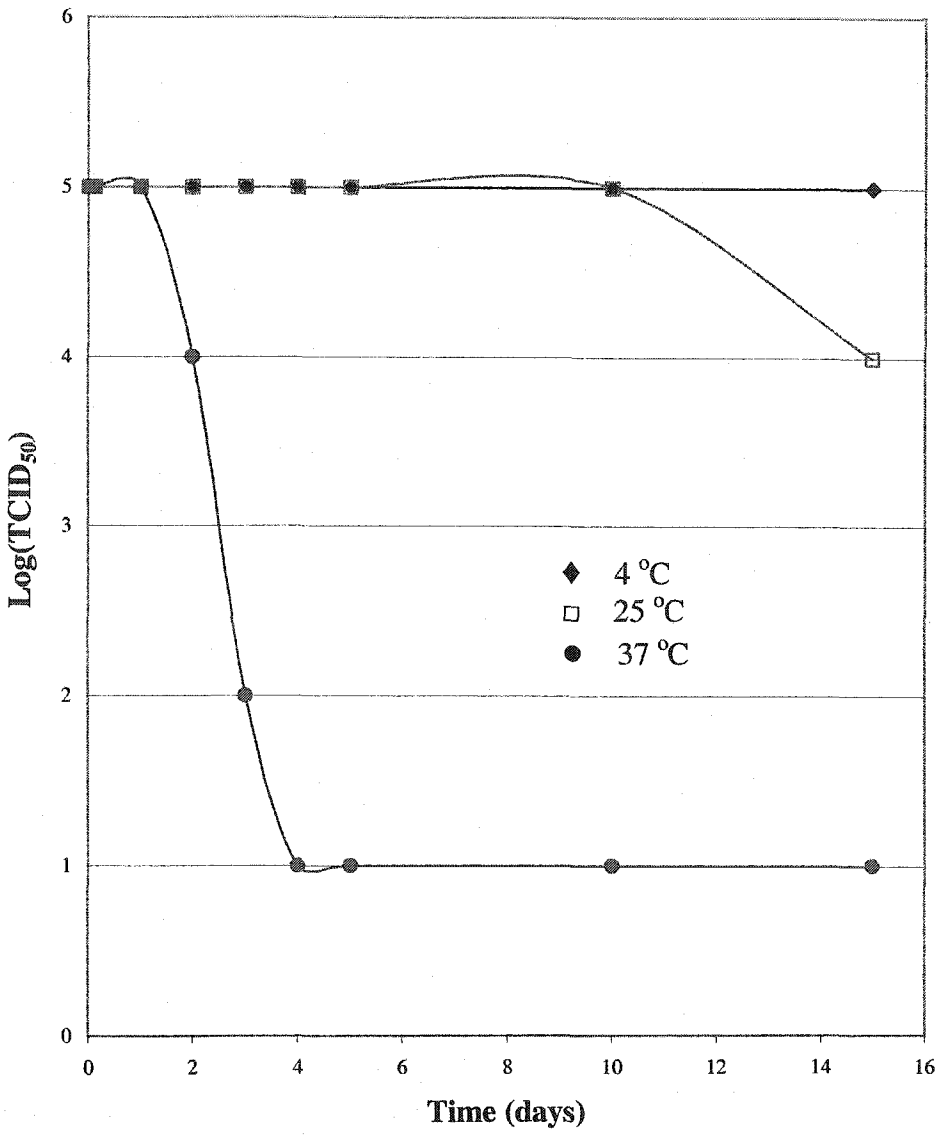

Figure 4-16 Effect of Temperature and time on A-MLV survival. The medium containing A-MLV is stored at three different temperatures, 4, 25 and 37 °C. A small sample of 0.5 mL was taken at a specified time and the $TCID_{50}$ assay was carried out immediately. The initial concentration of A-MLV is 5×10^5 infectious units/mL.

4.6.2. A-MLV and Microfiltration

The effect of shear stress on A-MLV deactivation during flocculation and microfiltration was investigated by running the suspension of A-MLV in PBS solution through a microfiltration module for three hours while small samples were taken every hour to determine the A-MLV titers remaining in suspension. It was found that the titers of A-MLV in the feed suspension remained constant (as determined by $TCID_{50}$ assay) during the course of experiment. It appeared that the shear stress during microfiltration does not deactivate A-MLV.

4.6.3. A-MLV and Cationic Polymer without Microfiltration

The toxicity of the cationic polyacrylamides on A-MLV survival was investigated by introducing a small amount of EM441L into the PBS solution containing A-MLV. A small sample was taken every hour for three hours. Then A-MLV titers were determined by $TCID_{50}$ assay. The titers of A-MLV remained constant throughout the course of experiment. Therefore, it is likely that cationic polyacrylamide has no effect on A-MLV deactivation.

However, it was found experimentally during $TCID_{50}$ assay that cationic polyacrylamide is toxic to NIH/3T3 (indicator) cells. When carrying out $TCID_{50}$, the sample was serially diluted with serum containing medium in the range of $10^0 - 10^{-6}$. Then 100 μL of each dilution was used to infect indicator cells. At the dilution of 10^0 after 24 hrs post-infection, substantial amounts of indicator cells started to die and after 48 hrs post-infection almost of indicator cells die out. Therefore, it is evident that cationic polyacrylamide is toxic to NIH/3T3 cells.

4.6.4. A-MLV and Cationic Polymer with Microfiltration

The combined effect of shear stress and cationic polyacrylamide on A-MLV deactivation was investigated by inducing flocculation of A-MLV in PBS solution and then conducting microfiltration. Microfiltraion was run in total recycle. A small sample of the retentate was taken every hour for the $TCID_{50}$ infectivity assay. There was no reduction of A-MLV titers during the course of experiment. However, as was the case in 4.6.3, the cationic polyacrylamides were found to be toxic to NIH/3T3 cells. It may be, therefore, concluded that A-MLV is not deactivated by shear stress and cationic polyacrylamide experienced by A-MLV during flocculation and microfiltration experiments.

4.6.5. A-MLV and CHO Cells

Even though a number of studies have demonstrated that CHO cells are not susceptible to A-MLV infection (Teich (1984), Miller and Miller (1992, 1993), Eglitis et al. (1993)), it was decided to investigate whether the A-MLV pseudotypes produced in this project are, in fact, incapable of infecting the CHO-DG44 cells. During the attempt to induce infection of CHO cells by A-MLV, polybrene at a concentration of 10 μg/mL, which was primarily used to reduce the repulsive forces between cells and virus virions subsequently expedite infection, was toxic to the CHO-DG44 cells. Even a polybrene concentration of 4 μg/mL was toxic to CHO-DG44 cells. Consequently, the experiment was conducted in the absence of polybrene. At day 4 post-infection, out of three replicates there were 2 – 3 small colonies that expressed EGFP with each of the colony

contains 5 – 6 cells. Therefore, it is evident that CHO-DG44 cells are highly resistant to the A-MLV infection, which is consistent with the findings reported in the literature.

4.6.6. A-MLV and CHO Cells and Microfiltration

This experiment was designed to investigate the effect of CHO cells on possible A-MLV removal. After flocculation, microfiltration was conducted in total recycle and the retentate sample was withdrawn at the beginning and the end of microfiltration experiment. It was found from the $TCID_{50}$ assay that the titers of A-MLV in the sample taken at the end of experiment were the same as that of the sample taken at the beginning of the experiment. It is therefore evident that A-MLV was not deactivated by the presence of both shear stress and CHO cells even though the period of exposure was three hours. Further, due to the fact that the A-MLV titers remained constant from the beginning to the end of the experiment, adsorption of A-MLV onto CHO cell surface is, therefore, unlikely to take place.

In summary, during the period of three hours for which microfiltration shear stress was applied, temperature alteration and duration of exposure to such temperature have no effect on A-MLV viability. Further, cationic polyacrylamides used as flocculants have no effect in deactivating A-MLV. It was also experimentally found that CHO-DG44 cells were highly resistant to A-MLV infection. From 4.3.4, it is evident that A-MLV and CHO cells are not likely to naturally form aggregates in suspension due to either hydrophobic or electrostatic interaction. Therefore, the removal of A-MLV from suspension should be the result of flocculation induced prior to microfiltration of the suspension containing CHO cells and A-MLV. Even though cationic

polyacrylamide was found not to be toxic to A-MLV, there was an indication that mammalian cells are highly sensitive to these polyelectrolytes.

4.7 Microfiltration

In this project, removal of A-MLV from CHO cell suspensions was investigated. However, the efficiency of virus removal should be significantly enhanced if a suspension containing both CHO cells and A-MLV were flocculated prior to microfiltration. Therefore, microfiltration of suspensions containing CHO cells and A-MLV virions, which were flocculated with cationic polyacrylamide at previously established optimum conditions, was carried out.

4.7.1. Pure Water Flux

New membrane modules were always run with deionized water for at least 30 minutes to remove wetting agents on the membrane surface. Subsequently, the pure water flux of the membrane module was determined as a function of transmembrane pressure (TMP). It can be seen from Figure 4-17a that the pure water flux linearly increased as the TMP increased within the range tested, 1 - 5 psi, as expected.

4.7.2. Microfiltration of Unflocculated CHO Cell Suspension

This experiment was intended to study the effect of CHO cells on membrane fouling without flocculation. The normalized flux of the unflocculated CHO cell suspension at a cell density of 1.0×10^6 cells/mL and a wall shear rate of 4,500 s^{-1} is given in Figure 4-17b. The highest attainable flux is the pure water flux which is

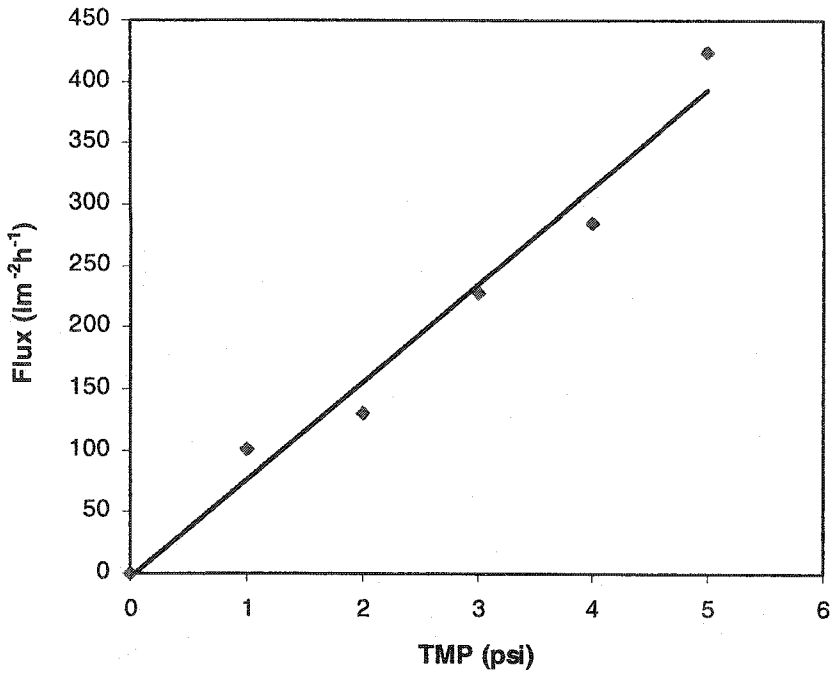

(a)

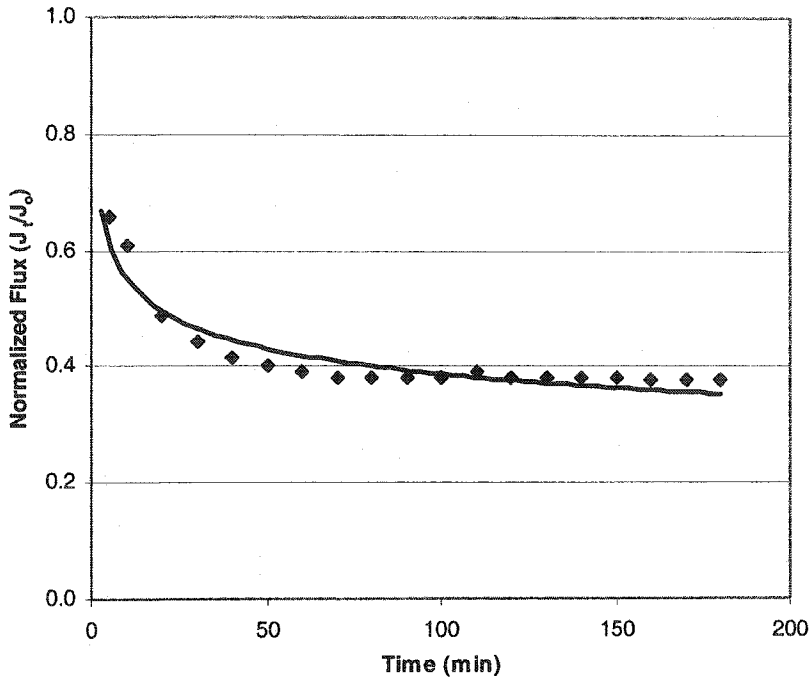

(b)

Figure 4-17 Microfiltration: (a) Pure water flux of new membrane as a function of transmembrane pressure (TMP) and (b) Normalized flux of unflocculated CHO cells suspension at CHO cell density of 1×10^6 cells/mL and shear rate of 4,500 s^{-1} with the fouling index of –0.2557.

assumed to be the initial flux. The normalized flux at 1 minute after microfiltration is reduced to approximately 76 % of the pure water flux. Subsequently, as microfiltration proceeds, the permeate flux declines rapidly and then reaches an asymptotic value. At later stages of microfiltration the permeate flux was reduced to approximately 17.5 % of the initial water flux.

Further, in our previous studies with yeast (Kim et al (2001)), the permeate flux may be successfully modeled by (2-7). Therefore, all of the microfiltration results are fitted to the aforementioned model. Further, the fouling index (c) indicates how rapidly fouling of the membrane takes place. The higher the fouling index the faster the membrane fouls. It can also be seen from Figure 4-17b that the fouling index of the unflocculated CHO cell suspension is – 0.2577 indicating that at the same CHO cell density the unflocculated suspension fouled the membrane much faster than the flocculated suspension (below).

4.7.3. Microfiltration of Flocculated CHO Cell and A-MLV Suspension

Removal of A-MLV from CHO cell suspensions was studied by spiking A-MLV pseudotypes at a titer of 1×10^5 infectious units/mL to suspensions of CHO cells at various cell densities of 0.25, 0.50 and 1.0 wt%. Subsequently, the suspensions were flocculated with EM440CT at optimum flocculation conditions established earlier. Microfiltration was then performed at two different shear rates of 4,500 and 6,000 s^{-1}.

The permeate flux usually reaches steady state after 50 – 60 minutes of microfiltration. However, each microlfiltration experiment was carried out for 3 hrs. Further, for each experiment, two modes of microfiltration were performed which are (i)

total recycle for the first 90 minutes and (ii) concentration mode after 100 minutes of microfiltration. Since the degree of membrane fouling progressively increased, the initial water flux continuously decreased with the number of uses. Therefore, for the purpose of comparison, the permeate flux is presented as the normalized permeate flux (J_t/J_o) for all the microfiltration experiments where J_o and J_t are the permeate flux at $t = 0$ and at any time t, respectively.

Figure 4-18 shows the normalized flux for microfiltration of flocculated suspensions containing CHO cells at the density of 0.25 wt% for the shear rates of 4,500 and 6,000 s^{-1}. It can be clearly seen from Figure 4-18 that at the early stage of microfiltration the normalized flux for both shear rates is approximately 70 % of the initial flux. The permeate flux at 6,000 s^{-1} shear rate is slightly higher than that at 4,500 s^{-1} shear rate. As the filtration time increases the permeate flux declines rather rapidly and then a slow long term flux decline takes place. At approximately 40 minutes after the commence of microfiltration the permeate flux at 6,000 s^{-1} declines more rapidly to level that is lower than that at 4,500 s^{-1}. Further, the fouling indices (Table 4-2) for the shear rates of 4,500 and 6,000 s^{-1} are – 0.1171 and – 0.1552, respectively.

For a CHO cell density of 0.50 wt%, normalized fluxes for the microfiltration performed at 4,500 and 6,000 s^{-1} are provided in Figure 4-19. For both shear rates of 4,500 and 6,000 s^{-1} shear rate the normalized permeate fluxes are 77 and 74 % of the initial water flux, respectively. Further, the permeate fluxes in both cases decline rapidly during the first 50 minutes of microfiltration. For both shear rates after the first 50 minutes of operation, steady state was reached with the final normalized flux of 26 and 29 % of the initial water flux. It can be seen from Table 4-2 that the fouling rates indices

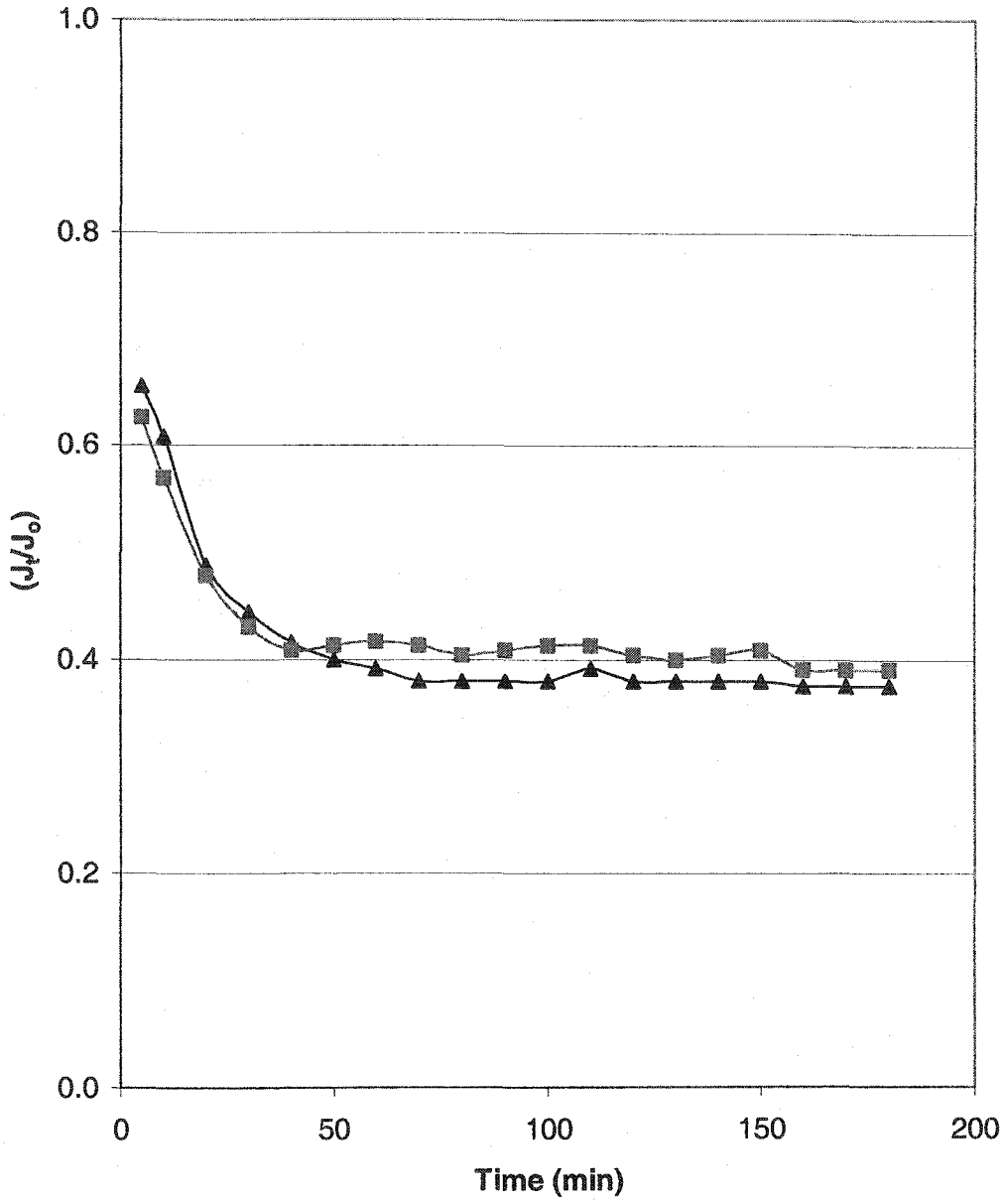

Figure 4-18 Variation of normalized permeate flux (J_t/J_o) of flocculated suspension containing CHO cells at the density of 0.25 wt% and A-MLV at the titers of 1×10^5 infectious units/mL. Shear rates used are: (■) 4,500 and (▲) 6,000 s^{-1}

Table 4-2 Fitted parameters of microfiltration of flocculated suspension data to empirical model ((2-7))

CHO Cell Density (wt%)	Shear Rate (s^{-1})	J_o (Lmh)	J_{180} (Lmh)	Fouling Index (c)
0.25	4 500	60.14	33.64	- 0.1171
	6 000	74.15	35.63	- 0.1552
0.50	4 500	67.48	24.75	- 0.2006
	6 000	94.42	29.25	- 0.2491
1.0	4 500	65.75	15.94	- 0.2929
	6 000	116.85	22.84	- 0.3314

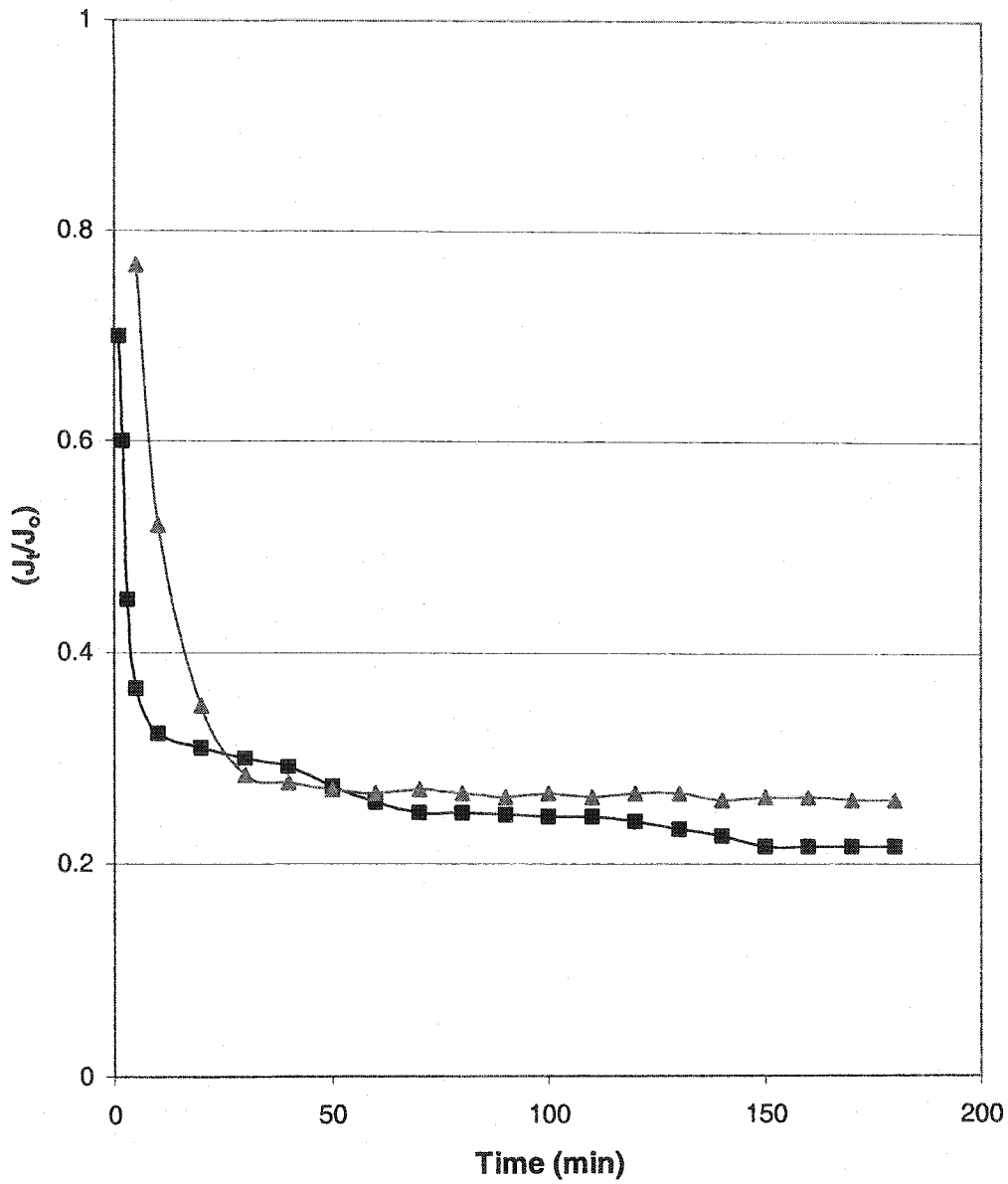

Figure 4-19 Variation of normalized permeate flux (J_t/J_o) of flocculated suspension containing CHO cells at the density of 0.50 wt% and A-MLV at the titers of 1×10^5 infectious units/mL. Shear rates used are: (■) 4,500 and (▲) 6,000 s^{-1}

are – 0.2006 and – 0.2491 for the shear rates of 4,500 and 6,000 s^{-1}, respectively.

Figure 4-20 illustrates normalized fluxes for the shear rates of 4,500 and 6,000 s^{-1} at CHO cell concentration of 1.0 wt%. As can be seen from Figure 4-20 the normalized fluxes are 74 and 78 % for shear rates of 4,500 and 6,000 s^{-1}, respectively. The permeate flux reached steady state at approximately 50 minutes after microfiltration started. Microfiltration at 6,000 s^{-1} shear rate results in higher permeate flux than that of 4,500 s^{-1} shear rate. Further, the fouling indices (Table 4-2) for the shear rates of 4,500 and 6,000 s^{-1} are – 0.2929 and – 0.3314, respectively. Therefore, fouling of the membrane at the higher shear rate takes place much faster than that of at lower shear.

In summary, microfiltration of flocculated suspensions yields higher overall permeate fluxes than that of unflocculated suspensions. For instance, at 1×10^6 cells/mL (0.50 wt%) CHO cell density, the quasi steady state permeate flux of both flocculated and unflocculated CHO cell suspensions were 26 and 17.5 % of the initial pure water flux, respectively. Permeate fluxes for microfiltration performed at high shear rate are generally higher than those performed at low shear. Further, fouling of the membrane takes place much faster with microfiltration performed at high shear rate even though an initial biomass density is similar.

4.7.4. Virus Removal

During microfiltration of flocculated suspensions with different CHO cell densities and A-MLV concentration of 1×10^5 infectious units/mL, small samples were withdrawn at the designated times, 10 minute interval, until the permeate flux reached steady state at which point where microfiltration was terminated. Subsequently, $TCID_{50}$

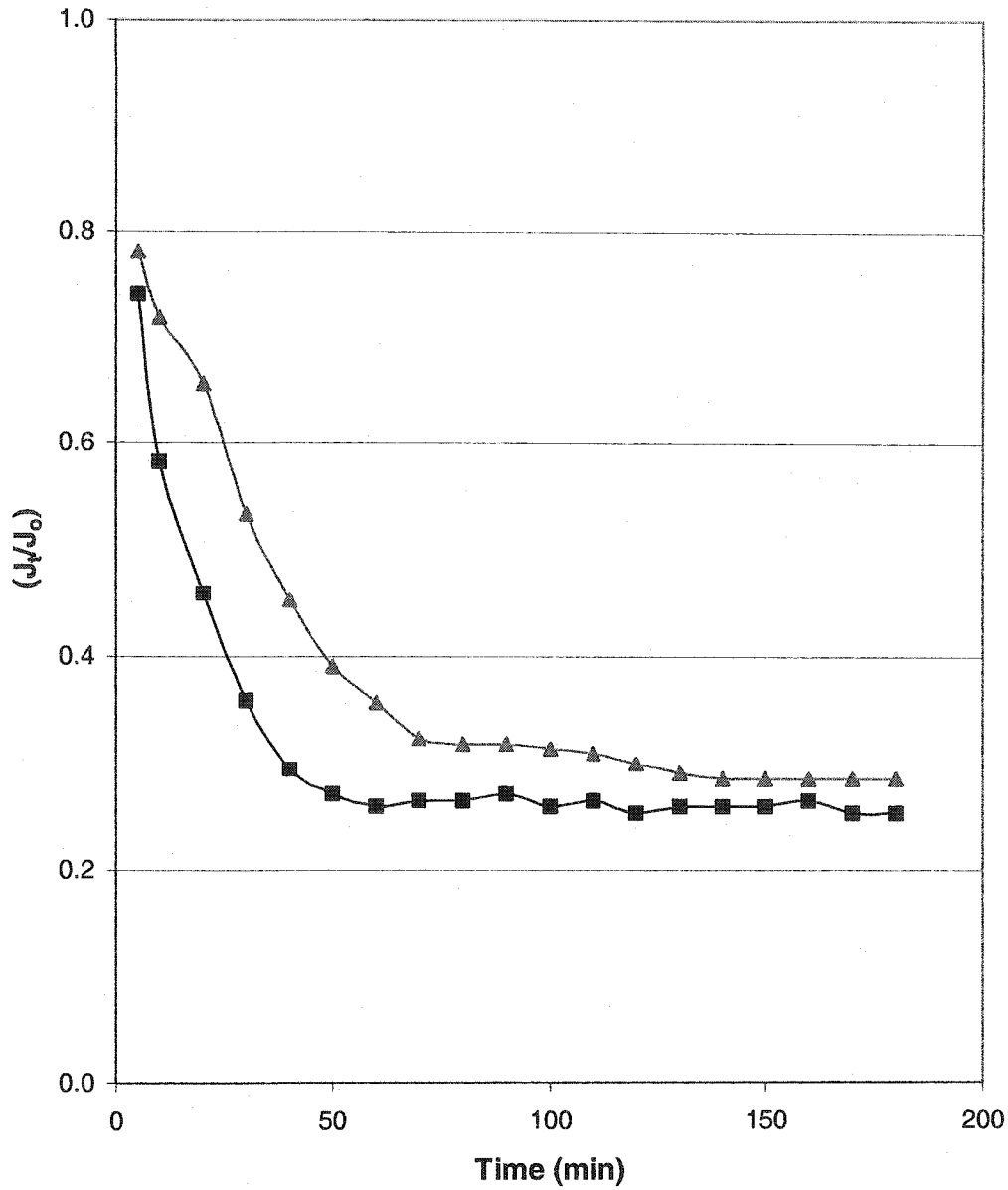

Figure 4-20 Variation of normalized permeate flux (J_t/J_o) of flocculated suspension containing CHO cells at the density of 1.00 wt% and A-MLV at the titers of 1×10^5 infectious units/mL. Shear rates used are: (■) 4,500 and (▲) 6,000 s^{-1}

assay was performed on every sample to determine the titers of A-MLV in the permeate samples. The sample was first serially diluted into the range of $10^0 - 10^{-7}$. Then 100 μL of each dilution was used to infect NIH/3T3 cells in 96 well-plate. The 96 well-plate was then incubated at 37 °C and 5 % CO_2. At day 3 post infection, expression of EGFP of infected NIH/3T3 cells was observed under a fluorescent microscope.

As mentioned earlier each microfiltration was performed at both total recycle and concentration modes at the same time. The samples from the first 90 minutes should yield information on whether free A-MLV virions were present in the flocculated suspension, which indicates the efficacy of flocculation between CHO cells and A-MLV in suspension. The samples from 100 minutes (concentration mode) onwards should represent the effect of volume changes on A-MLV retained by the membrane.

Of all the samples tested, no EGFP expression was observed within the detection limit of the $TCID_{50}$ assay. There are no A-MLV pseudotypes present in the permeate since it was experimentally found that A-MLV pseudotypes were not inactivated by the operating conditions. Therefore, it is reasonable to conclude that flocculation of CHO cells and A-MLV pseudotypes by cationic polyacrylamide with 40 % charge density can be used to accomplish up to 5 log titer reduction of A-MLV pseudotype from flocculated suspension containing CHO cells and A-MLV.

4.7.5. Concentration of Particles at the Membrane Surface

It has been demonstrated that the concentration of particles on the membrane surface may be estimated by utilizing the film theory model (2-3) (Porter (1972)).

However, by utilizing (2-3), it is implicitly assumed here that the principal mechanism responsible for membrane fouling is concentration polarization. The slope of the plot J vs $\ln(C_B)$ gives the mass transfer coefficient and the intercept is the product of mass transfer coefficient and gel concentration.

The plot of J vs $\ln(C_B)$ is provided in Figure 4-21. It is evident from Figure 4-21 that, by extrapolation, the gel concentrations are found to be 3.48 and 11.90 wt% for microfiltration conducting at the shear rates of 4,500 and 6,000 $^{-1}$, respectively. Accordingly, for the shear rate 4,500 s^{-1} the mass transfer coefficient is 12.768 lmh (or 3.55×10^{-4} cm/s) while the mass transfer coefficient of 9.226 lmh (or 2.56×10^{-4} cm/s) is obtained for the shear rate of 6,000 s^{-1}.

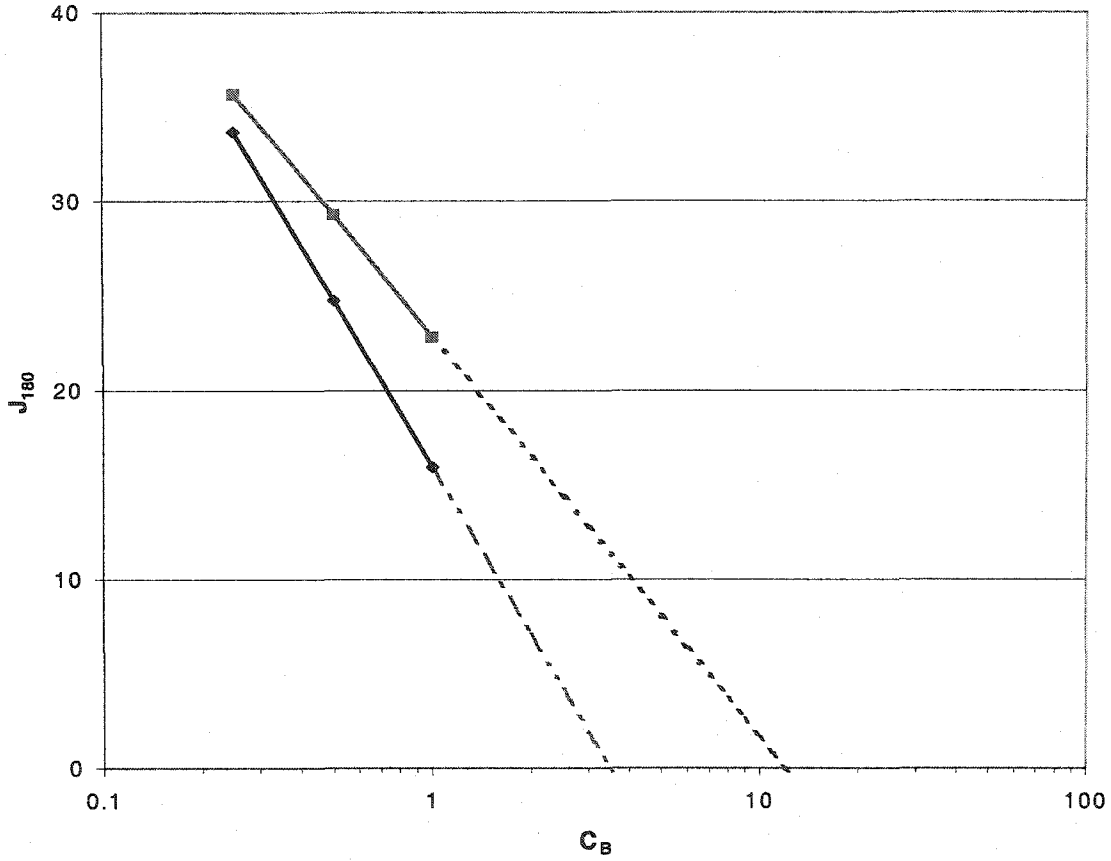

Figure 4-21 Prediction of concentration of flocculated particles at the membrane surface. Data used in constructing this plot are those in Table 1. It can be seen that for shear rate of 4,500 (▲) and 6,000 (■) s^{-1} the gel concentrations on the membrane surface are 3.48 and 11.90 wt%, respectively.

CHAPTER 5

DISCUSSION

This chapter discusses some of the experimental results found in this study. First, optimum flocculation conditions, particle size distribution and interaction potential are discussed. Then a discussion on the effect of shear rate and CHO cell density on microfiltration flux is provided. Finally, virus removal and modeling of flocculated particle size are discussed.

5.1 Optimum Flocculation Conditions

In this project, cationic polyacrylamides with molecular weight and charge densities ranging from $2-8\times10^6$ and $5-80$ %, respectively, were tested to determine their abilities to induce flocculation of CHO cell suspensions. Optimum dose and stirring speed and time were experimentally determined for all cationic polyacrylamides at each CHO cell density tested. Further, the optimum dose for EM440CT was found to be 20.98 mg/m^2 while the optimum stirring speed and time are 180 rpm and 3 minutes, respectively.

5.1.1. Optimum Flocculant Dose

It can be clearly seen from Figure 4-2 to 4-5 that at both high and low flocculant doses the absorbance of the supernatant is fairly large. Since at low polymer dose flocculation may have not been complete, due to the fact that the ratio of the number of polymer chains to particles is rather small, a larger absorbance is observed. On the other hand, when an excess amount of polymer is introduced to the CHO cell suspension, charge reversal and restabilization (Michaels (1954)) take place also leading as well to higher absorbance. It appears that at the optimum dose at which the absorbance is the lowest, the formation of aggregates of CHO cells, cell debris and small particulates is the most effective indicating that small particulates were significantly reduced.

It can be seen from Table 4-1 that as the CHO cell density increases the optimum flocculant dose also increases. Even though the optimum dose increases with CHO cell number density, the ratio of milligram polymer to the cell surface area is almost constant. For example, optimum doses of EM440CT for CHO cell densities of 0.25, 0.50 and 1.0 wt% are 30, 60 and 120 ppm, respectively, which corresponds to the ratio of milligrams of EM440CT to cell surface area of 21.0 mg/m^2 which indicates the ratio of the number of polymer chains to particles is at an optimum. The surface coverage of particles (CHO cells) at the optimum dose for all CHO cell densities tested should be of comparable value.

Further, it can be seen from adsorption experiments (Figure 4-13a) of EM440CT, EM441L and EM440LH that the optimum dose lies within the transition region before the saturation plateau is reached. Additionally, it is evident that the calculated saturation concentration of adsorbed EM440CT is 44.0 mg/m^2, which is slightly higher than twice

the optimum concentration found in the optimum dose experiment (21.0 mg/m^2). Consequently, at optimum doses the optimum particle surface coverage by adsorbed polymer is 0.48. This value of surface coverage is in very good agreement with that proposed theoretically by La Mer and Healy (1964). Therefore, it is concluded that in order to accomplish the highest flocculation efficiency, the surface coverage of CHO cells by EM440CT is approximately 50 %.

5.1.2. Optimum Stirring Speed and Time

Generally, for the flocculation of CHO cell suspensions, as stirring speed increases, the absorbance of the supernatant decreases, reaches a minimum and then continuously increasing due to substantial CHO cell lysis at high stirring speeds. It can be seen from Figure 4-6 that at low stirring speed the absorbance of the supernatant is large. This may be due to the fact that at low stirring speed, i.e., low G, flocculation of CHO cells in suspension may not have been complete. As a result, a high absorbance resulted due to the presence of small unflocculated particles. However, at high stirring speeds, the absorbance of the supernatant is not as high as expected even though lysis of CHO cell is very likely. It is probable that adsorption of the small cellular fragments that result from cell breakage to polymers that have adsorbed onto CHO cells may also occur. Owing to the fact that flocculation of biological solution is a dynamic and complex phenomenon the effect of stirring and time on flocculation of CHO cells by cationic polyacrylamide is subtle. Further, at each stirring speed, absorbance of the supernatant obtained at different flocculation times is sometimes indistinguishable.

For a stirred system, in order for rapid mixing to occur, turbulent mixing condition must be attained to achieve effective flocculation. It is well known that isotropic turbulence (local isotropy) ensures rapid mixing of suspensions (Amirtharajah and Mills (1982)). It is generally assumed for mixing systems that if the *Re* of the system is approximately 5×10^4, local isotropy exists (Shinnar and Church (1960)). The optimum stirring speed and time for EM440CT are 180 rpm and 3 minutes, respectively. It can be seen from Table 5-1 that the corresponding Reynolds' number (*Re*) and velocity gradient (*G*) are 1.51×10^4 and 3.86×10^3 s^{-1}, respectively, while Komogorov's microscale is found to be 15.2 μm. However, it is assumed here that local isotropy is attained even though *Re* of the system is slightly lower than 5×10^4. Therefore, rapid mixing of CHO cells, A-MLV pseudotypes and cationic polyacrylamides is accomplished and as a result, so is effective flocculation.

5.2 Particle Size Distribution

In general, all cationic polyacrylamides are capable of inducing flocculation of CHO cell suspension owing to the fact that when cationic polyacrylamide was first introduced to CHO cell suspension, large aggregates were observed visually. However, upon exposure of these aggregates to prolonged shear stresses, break down of the aggregates was observed. The charge density and molecular weight of cationic polyacrylamides play a significant role in the effectiveness of these polyacrylamides to induce flocculation of CHO cell suspensions.

For cationic polyacrylamides with low (5 %) and moderately low (20 %) charge density, neither high nor low molecular weight is effective at yielding good flocculation.

Table 5-1 Parameters used in flocculation of CHO cell suspensions

N		R_e	N_P	P_o	G (s^{-1})	η (μm)
rpm	rps					
0	0	0	0	0	0	0
100	1.67	7.57×10^3	0.934	4.59×10^4	1.60×10^3	23.7
200	3.33	1.51×10^4	0.684	2.69×10^5	3.86×10^3	15.2
300	5.00	2.27×10^4	0.570	7.56×10^5	6.48×10^3	11.7
500	8.33	3.79×10^4	0.453	2.78×10^6	1.24×10^4	8.48

Note: R_e is the Renold's number calculated using (2-50)
N_p is the power number calculated using (2-48)
P_o is the power input calculated using (2-47)
G is the velocity gradient calculated using (2-43)
η is the Komogorov's microscale calculated using (2-44)

This may be due to the fact that for cationic polyacrylamides with low charge density and high molecular weight the distances between each charge residue on the polymer backbone are fairly large, therefore, when these polymer chains form bridges between two or more particles the number of charges that bind onto each particle is small leading to weakly bound flocs. These weakly formed flocs may easily be disrupted by hydrodynamic forces exerted by agitation.

On the other hand, for cationic polyacrylamides with high charge density but low molecular weight, even though distances between each charge group are rather small, each molecule of these polymers is relatively short. Consequently, the capability for these polymers to bind to more than one particle is also small. Further, it has been shown that polymers of low molecular weight destabilize particles by charge neutralization (Gregory (1973)) rather than polymer bridging. Polyelectrolytes with low charge density tend to assume a coiled conformation in suspension and, as a result, shorten the chain length. Therefore, polymer bridging is unlikely to take place.

Some of cationic polyacrylamides with 40 % charge density could be successfully used to create of CHO cell suspensions in the presence of shear stresses. Charge density of these cationic polyacrylamides is 40 % while the molecular weights of EM440CT, EM441L and EM440LH are 5 – 8, 4 – 6 and 2 – 3 million, respectively (Table 3–1). Only EM440CT and EM441L were effective whereas EM440LH was not. Charges on EM440CT and EM441L are properly distributed in the same fashion as that of the charges on CHO cell surfaces leading to stronger flocs (Dickinson and Eriksson (1991), Eriksson et al. (1993)).

The flexibility of cationic polyacrylamide chains with 40% charge density should be higher than that of the polymers with 80% charge density. Therefore, when experiencing the same level of shear forces, polymer chains with lower charge densities should yield better flocculation efficiency, and, thus, larger average particle size and stronger flocs. Additionally, the radius of gyration of the polymer coil of hydrolyzed polyacrylamides with molecular weight in the range of 10^5 - 10^7 in 0.10 M NaCl is found to have the value ranging from 100 to 1000 nm (Anthony et al. (1975)). Since the thickness of double layer (κ^{-1}) in 0.315 M ionic strength was found to have the value of 0.77 nm, the radius of gyration of EM440CT whose molecular weight is $5-8\times10^6$ should be sufficiently large to readily accommodate effective flocculation of CHO cell suspension (by polymer bridging).

One may anticipate that cationic polyacrylamides with 80 % charge density should be the most effective flocculants. However, it was found that neither high nor low molecular weight of cationic polyacrylamides with 80 % charge density was effective. Even though the chain length of cationic polyacrylamides with high molecular weight may exceed the $2\kappa^{-1}$ distance (Kitchener (1972)), which should ensure good flocculant characteristics, the binding of highly charged polyelectrolytes led to morphological change in the animal cells. Katchalsky et al. (1959) and Katchalsky (1964) have shown that flocculation of red blood cells with polylysine led to the deformation of the cell membrane of red blood cells within the cluster of aggregated red blood cells. The deformation of CHO cells within the formed flocs may be expected and, as a result, floc strength may be greatly reduced. Further, when these flocs experience hydrodynamic forces exerted via agitation, floc breakage is inevitable.

Highly charged polyelectrolytes generally adopt a stretched conformation due to the repulsive forces between the neighboring charged groups (Gregory (1977), Michaels (1954)). However, these polymers are more likely to adopt flat configurations rather than loops and tails conformation upon adsorption (Gregory (1988)). As the chains of highly charged polyelectrolytes stretch out, the degree of rigidity of their chains is significantly increased. When these rigid chains are exposed hydrodynamic forces, the possibility of breakage of the carbon-carbon (C-C) bonds also increases since the external force that is sufficient to break a single C-C bond in the polymer chain is approximately 1- 10 nN (Levinthal and Davison (1961), Goldacre (1954)). For two equal sized particles of radius a, Goren (1971) found that the hydrodynamic force at short distance reads

$$F_{hydr} = 19.2\eta G a^2 \sin^2\theta \sin 2\varphi \qquad (5\text{-}1)$$

where G is the shear rate, η is the viscosity of the suspending medium, and θ and φ are polar angles describing the relative orientation of the spheres in shear flow.

van de Ven (1981), by utilizing the relation (5-1), has shown that, for aqueous suspension at room temperature at a velocity gradient of 1000 s^{-1} and particle diameter of 10 μm, the hydrodynamic force experienced by the particles is 1.92 nN which is of the same order that can disrupt the C-C bond in the polymer chain. Consequently, when highly charged polyelectrolytes are used to induce flocculation at high shear stress, the efficacy of flocculation is greatly reduced due to their configuration and the probability of C-C bond breakage.

Further, Mabire et al. (1984) studied flocculation of silica dispersion using cationic polyacrylamides of molecular weight 4×10^3 - 3×10^6 and charge density of 500

Cg^{-1} and found that their results were in good agreement with the "electrostatic patch" model (Gregory (1973), Kasper (1971)). However, it has been shown that, for flocculation of kaolin suspensions by high molecular weight cationic polymacrylamides, bridging flocculation is the predominant mechanism (Gill and Herrington (1987a, b, c), Heller (1966)). Therefore, it may be deduced that the predominant mechanism in flocculation of CHO cell suspension is polymer bridging since the molecular weight of both EM440CT and EM441L is in the range of $4-8\times10^{6}$ and their chain lengths should be larger than the $2\kappa^{-1}$ distance (1.54 nm).

In summary, it is obvious that both molecular weight and charge density of cationic polyacrylamides are the most important characteristics in selecting polymeric flocculants. Further, the particle size distribution of the flocculated suspension should be determined. Further, it is implicitly indicated that with high molecular weight flocculants, polymer bridging prevails in flocculation of CHO cell suspensions.

5.3 Interaction Potential

It has been demonstrated that CHO cells and A-MLV pseudotypes are unlikely to naturally form self-aggregates in suspension (Figures 4-10 and 4-11) since both CHO cells and A-MLV virions are negatively charged at neutral pH. For the suspension containing CHO cells and A-MLV, aggregation of CHO cells and A-MLV is also unlikely in the absence of polymeric flocculants due to a large energy barrier. However, when cationic polyacrylamides were introduced to suspensions, destabilization or charge neutralization took place via polymer adsorption leading to a reduction of particle surface potential (zeta potential). It is theoretically anticipated that at an optimum

polymer dose the zeta potential of the aggregates (particles) should be principally reduced to (near) zero (Yu and Somasundaran (1996), Ottewill and Rastogi (1960), Chen (1998)). However, the zeta potential of flocculated aggregates has been experimentally found to be nonzero depending upon the initial charges of the particles and polymeric flocculants (Somasundaran and Yu (1994)). Further, the zeta potential of negatively charged particles flocculated by high molecular weight cationic polyelectrolytes was found to be negative rather than zero (Brown et al. (1970), Gregory (1969), Kane et al. (1964)). In addition, flocculation kinetics of suspension by high molecular weight polyelectrolytes was found to be the fastest at nonzero rather than zero zeta potential (Dentel and Abu-Orf (1994), Nakamura et al. (1994)).

In this study, to simulate flocculation, zeta potentials of both CHO cell and A-MLV were reduced to half of the original values. As can be seen from Figure 4-12 at the original values of zeta potential (curve 1) the energy barrier between CHO cells and A-MLV is approximately 22 kT while after flocculation (curve 3), the energy barrier is greatly reduced to less than 2 kT which is of the same order as that of the average kinetic energy of particles undergoing Brownian diffusion (Gregory (1989)). It is evident that CHO cells and A-MLV virions would be able to come into close contact leading to successful flocculation after cationic polyacrylamides were introduced into suspension. If the zeta potential of both CHO cells and A-MLV virions is further reduced, which should be the case for a practical flocculation process the total interaction energy between CHO cells and A-MLV virions would be attractive. Therefore, successful flocculation is assured.

5.4 Microfiltration

At 0.25 wt% CHO cell density (Figure 4-18), the quasi-steady state permeate flux is the highest. This may be due to the fact that when the CHO cell density in the suspension is low the possibility of particles depositing onto the membrane surface is minimized. As a result, the likelihood of cake formation on the membrane surface is also significantly reduced, and a high permeate flux is obtained. At wall shear rate of 6,000 s^{-1}, the permeate flux is a little lower than at a shear rate of 4,500 s^{-1}. This unexpected result may be due to break up of the floc particles leads to a smaller average size at a higher wall shear rate. A similar result is observed for 0.50 wt% CHO cell suspensions (Figure 4-19).

Since flocs (aggregates) have been frequently known to have a fractal and self-similar structure, the effective density of the formed flocs may be related to fractal dimension (Gregory (1997)). Additionally, the lower the fractal dimension the more open is the aggregate structure. As the ratio of polymer chain to particle concentration increases, the fractal dimension of the aggregates increase (Stoll and Buffle (1998)). Therefore, it is more likely that at high CHO cell density the flocs formed may acquire a more close packed structure, which is much stronger than those formed at low cell density. Further, at high cell density, since the distance between these flocs is much smaller, re-flocculation of small flocs resulting from floc breakage may take place faster than that at low cell density.

In summary, it was found in this study that the permeate flux of flocculated suspensions is much higher than that of unflocculated suspension indicating flocculation can successfully be used to enhance filtrate flux of CHO cell suspensions. As can be

seen from Table 5-1 at a constant shear rate the fouling indices increase as CHO cell density increases indicating that fouling of the membrane takes place faster as the concentration of particles in suspension increases (Patel et al. (1987)).

5.4.1. Concentration of Particles at the Membrane Surface

It has been previously demonstrated that for ultrafiltration while concentration polarization is principally responsible for fouling of the membrane the gel concentration on the membrane surface remains constant as shear rate is increased (Porter (1972)). Further, the gel concentration for colloid suspensions (60 – 70 %) is higher than that of protein suspensions (25 – 45 %) since the structure of gel layer of colloidal suspensions would be expected to assume a close-packed structure (Porter (1972)).

As can be seen from Figure 4-21 the concentration of particles at the membrane surface increases as shear rate increases, which is not unexpected since the surface of the particles is not fully covered. Therefore, the possibility of polymer bridging or electrostatic patch interaction between deposited aggregates and aggregates brought into the vicinity of the membrane surface may take place. In our previous study with yeast using DOTM (Direct Observation Through the Membrane) technique, attachment of smaller flocs to the deposited aggregates on the membrane surface does take place (Wickramasinghe et al. (2003). As a result, these interactions (bonding) may outweigh the shear forces at which microfiltration is operated leading to an increase of particle deposition onto the membrane surface.

The gel concentration found in this study is very low compared to those reported in the literature. However, it should be realized that CHO cells, which are the primary

particles in floc structure, are susceptible to breakage due to strain from both polymeric flocculants (Katchalky et al. (1959)) and shear stress applied during microfiltration. Therefore, deformation of CHO cells in aggregates may be anticipated leading to a surge of the concentration of small particulates in an immediate vicinity of the membrane. As a result, membrane fouling is inevitable. Consequently, the gel layer, which is defined as the particle concentrations at zero flux, is smaller than those found in literature where hard spheres are used rather than deformable spheres.

5.5 A-MLV Pseudotype Removal

The A-MLV pseudotypes are not deactivated by the experimental conditions, i.e., shear rate, cationic polyacrylamide toxicity and temperature changes. Further, it was also found that the hollow fiber membranes tested are, to some extent, capable of retaining some A-MLV even though the average pore size of the membrane is of the same order as that of the size (0.1 μm) of A-MLV. However, there were no A-MLV particles found in the permeate (within the limit of detection of the $TCID_{50}$ assay) for a microfiltration experiment run in both total recycle and concentration modes. Microfiltration was operated in total recycle mode for the first 90 minutes. If free A-MLV virions are present in suspension at this stage, the possibility of A-MLV passing through the membrane should be significant since no deposits and gel layer has yet formed on the membrane surface. However, no A-MLV was found in the permeate during the first 90 minutes of microfiltration. Further, no A-MLV was found in the permeate when the concentration mode was adopted after 90 minutes due to the fact that concentration of A-MLV in the feed was increased.

Further, it has been illustrated that when polyelectrolytes are used to induce flocculation of unequal sized particles at high shear rate, heteroflocculation is more favorable than homoflocculation (van de Ven (1981)). Although the mechanism of flocculation of CHO cells and A-MLV is not known, it is more likely that A-MLV virions adsorbed onto the cationic polyacrylamide chains rather than CHO cell surfaces. Either hydrogen bonding or hydrophobic interaction are probable since both A-MLV and CHO cells are negatively charged.

Since polysulfone membranes are either negatively or neutrally charged, repulsion of A-MLV from the membrane surface is likely. The membrane is, to some extent, capable of rejecting A-MLV even though A-MLV virions and average pore size are of the same order. Urase et al. (1994) stated that adsorption of viruses to the membrane surface is unlikely to play an important role in reducing the titers of viruses in suspension even though the membrane used is opposite in sign to viruses. Therefore, it is unlikely that adsorption of A-MLV to the membrane surface would significantly affect A-MLV removal. However, it is likely that the deposited particles on the membrane surface may play a significant role in retaining A-MLV (Urase et al. (1993)) since it has been shown that fouling and concentration polarization (deposition of particles) takes place in the first few seconds or minutes of filtration.

In summary, complete removal (up to 5 log titer reductions) of A-MLV pseudotypes from CHO cell suspensions may be accomplished by flocculation prior to microfiltration. In the presence of polymeric flocculants and shear rate, heteroflocculation between CHO cells and A-MLV virions is favored. Significant removal of A-MLV from the suspension may be attributed to complete flocculation of

A-MLV and CHO cells by the cationic polyacrylamides, secondary resistance due to surface deposits and the nature, both physical and chemical, of the membrane.

5.6 Particle Size Modelling

Average particle size of flocculated CHO cell suspension may be predicted by $d/D_i = KR_{eG}^{a}(G\phi t)^{b}$ and are weakly dependent on the velocity gradient used to induce flocculation. The combined dependencies of average particle sizes on G were found to be – 0.315 rather than the widely reported value of – 1 (Parker et al. (1972)). This may be explained by the fact that since CHO cells (primary particles) are of the same size as that of the Komogorov's microscale, which is 15.2 μm in this study, collisions of CHO cells induced by velocity gradient are somewhat limited. It is generally believed that if particles to be flocculated are smaller than the Komogorov's microscale, collisions of particles are the results of the velocity gradient.

Further, a recent study on flocculation modeling has demonstrated that the velocity gradient is not as critically important as once believed (Han and Lawler (1992)). In flocculation between small and large particles the rectilinear model, which assumed that particles in suspension travel in straight line, is inferior to the curvilinear model (Han and Lawler (1992), Lawler (1993)). In the curvilinear model, the particle trajectory is modified from that in rectilinear model by taking into account the fact that small particles usually follow the fluid streamlines rather than to move in straight lines. Therefore, collisions due to the velocity gradient (orthokinetic) are much smaller than those predicted by rectilinear model (Han and Lawler (1992), Lawler (1993)). The

model developed in this study is qualitatively in good agreement with the curvilinear model.

CHAPTER 6

CONCLUSIONS

In this project, removal of amphotropic murine leukemia virus (A-MLV) pseudotypes from CHO cell suspensions was studied by flocculation and microfiltration. A-MLV pseudotypes produced in this study were found to be sufficiently robust to withstand the experimental conditions, i.e., shear stress, temperature alteration, used during both flocculation and microfiltration. Further, it was also found that CHO-DG44 cells are highly resistant to A-MLV pseudotype infection.

Cationic polyacrylamides (EM440CT and EM441L) with molecular weights of $4-8\times10^6$ and 40 % charge density can be successfully used to induce flocculation of CHO cell suspensions. However, EM440CT was chosen due to the low doses necessary to induce flocculation of CHO cell suspension. Optimum flocculant doses for these cationic polyacrylamides do exist at which the surface coverage of primary particles (CHO cells) is approximately 50 %. This is in a very good agreement with the previously reported values in the literature. In addition, the ratio of milligrams of cationic polyacrylamide to the surface area of CHO cells is constant at optimum doses irrespective of the CHO cell densities tested. Furthermore, the optimum stirring speed and time for flocculation are 180 rpm and 3 minutes, respectively.

According to DLVO theory, interaction potential curves for A-MLV, CHO cells and A-MLV – CHO cell suspension are established. The values of zeta potential for CHO cells and A-MLV are those reported in literature, which are – 22 and – 15.11 mV, respectively. It is unlikely that A-MLV and CHO cells will naturally form aggregates in suspension due to the presence of a high energy barrier between A-MLV and CHO cells in suspension. To simulate flocculation, the values of zeta potential of both CHO cells and A-MLV pseudotypes are arbitrarily chosen to be – 11 and – 7 mV, respectively, after destabilization. As a result, the energy barrier between CHO cells and A-MLV virions is reduced considerably indicating successful flocculation either between CHO cells and A-MLV or between themselves.

The average particle size of flocculated CHO cell suspension has been modeled mathematically and may be semi-quantitatively predicted by $d/D_i = KR_{eG}^{a}(G\phi t)^{b}$ with a and b are found to have the values of – 0.264 and – 0.0512. The values of K are found to be 1.8 and 0.25 for effective and non-effective flocculants, respectively. The model developed is found to give fairly good agreement with the experimental data.

The permeate flux decline, which is usually experienced during the microfiltration of biomass suspension, may be alleviated by pretreatment of the suspension by cationic flocculants prior to microfiltration. At the same shear rate the quasi-steady state, permeate flux of flocculated CHO cell suspensions is approximately 50 % higher than that of unflocculated suspensions. Further, the combination of flocculation and microfiltration can be effectively used to accomplish up to 5 log titer reductions of A-MLV pseudotypes from suspension. Moreover, according to film theory

the particle concentrations at the membrane surface are 3.48 and 11.89 wt% for 4,500 and 6,000 s^{-1} shear rate, respectively.

CHAPTER 7

RECOMMENDATION FOR FUTURE WORK

It has been shown that the zeta potential of flocculated aggregates of negatively charged particles by positively charged polymers is not necessarily zero. Therefore, in order to demonstrate successful flocculation of CHO cells by cationic polyacrylamides, the zeta potentials of CHO cells both before and after flocculation should be measured. This will enable the determination of the interaction potential curves.

While bridging flocculation is induced by cationic polymers with high molecular weight, charge patch flocculation is caused by low molecular weight cationic polymeric flocculants. The commercially manufactured flocculants tested here display a large range in mu\olecular weight. Therefore, cationic polyacrylamides with more defined characteristics such as molecular weight and charge density should be used to induce flocculation of CHO cells since molecular weight of cationic polymers determines to a great extent the mechanism of flocculation. Further, cationic polymers containing trace amount of fluorescent groups as ligands maybe used for visual verification of the mechanism of flocculation. If possible the chain length of the cationic polyacrylamides in suspension should be determined in order to further distinguish the flocculation mechanisms. In addition, the true (exact) ionic strength of the solution should also be directly determined enabling the thickness of the double layer to be estimated.

The mechanism of flocculation may be further verified if the morphology of flocculated suspension is monitored using microscope. Since CHO cell and A-MLV are negatively charged in a suspension of neutral pH, it is more likely that A-MLV adsorbed onto the cationic polymers cahins via electrostatic interaction rather than onto CHO cells through hydrophobic interaction. Further, it may also be possible to elucidate the flocculation mechanism of a flocculated suspension involving cationic polyacrylamides, CHO cells and A-MLV.

Sine permeate flux is directly proportional to the average size of the particles in suspension, the particle size distribution of the flocculated suspension should be monitored during the course of the microfiltration experiments. An inline particle sizer may be implemented to the experiment setup. With the inline particle sizer, an instantaneous average particle size of the flocculated suspension can be followed. There are several strategic points of interest: (1) suspension drawn directly from the feed reservoir prior to the peristaltic pump, (2) the point downstream of the peristaltic pump prior to the membrane module, and (3) the point downstream of the membrane module. The average particle size of the suspension after flocculation can be directly determined from (1) while the average particle size entering the microfiltration module can be monitored using (2). Therefore, the effect of the peristaltic pump on particle breakage can be estimated. Further, the magnitude of particle breakage from shear stress experienced while flowing through the membrane module can be examined using (3).

It is generally assumed that the kinetics of flocculation of particles in suspension is second order with respect to the particle number density. An effort to determine the numbers of particles in suspension should be made, if possible. However, the numbers

of particles in suspension is changing constantly since flocculation is a dynamic process. The particle counter may also be implemented in the system when flocculation is to be carried out. Further, it may also be advantageous to conduct flocculation under a microscope equipped with a video camera, since image analysis maybe use to estimate the number of particles. Results from the line particle sizer may allow accurate determination of the rates of fragmentation and flocculation. Further, these results may also be used to mathematically model the flocculation process.

NOMENCLATURE

a	=	particle diameter
a_i, a_j	=	particle radius
A	=	projected area of particle
c	=	fouling index
C	=	constant, concentration
C_b	=	solid concentration in bulk solution
C_w	=	solid concentration at the membrane surface
d	=	tube diameter (particle diameter)
d_{max}	=	maximum floc size
D	=	diffusion coefficient
D_B	=	Brownian diffusivity
e	=	electron charge
E	=	collision efficiency
f	=	fraction coverage
g	=	gravity
G	=	velocity gradient
H_o	=	separation distance
I	=	ionic strength
J	=	permeate flux
J_2	=	permeate flux at 2minutes
J_t	=	permeate flux at any time t
J^*	=	critical flux
k	=	mass transfer coefficient
k_B	=	Boltzmann's constant
k_{ij}	=	rate constant of flocculation

K, a, b, n	=	empirical constants
L	=	tube (membrane) length
lmh	=	liters per meter square per hour
M_i	=	molar concentration
N	=	impeller rotational speed
n	=	particle number density
n^o	=	number of ions
N_o	=	total (initial) number of particle
N_A	=	Avocado's number
N_p	=	impeller power number
N_q	=	impeller capacity (dimensionless)
n_T	=	total particle number density
P	=	transmembrane pressure
P_{elect}	=	electrokinetic pressure
P_o	=	power input
r	=	particle radius
R	=	particle radius
R_c	=	cake resistance
R_e	=	Reynolds's number
R_m	=	membrane resistance
r_p	=	particle radius
R_s	=	particle radius, cake resistance
S_c	=	Schmidt's number
S_p	=	particle surface area
t	=	(flocculation) time, filtration time
t_a	=	adsorption time
t_c	=	circulation time
t_f	=	flocculation time
t_F	=	flocculation time
t_r	=	polymer rearrangement time
T	=	absolute temperature

u	=	permeate velocity, electrophoretic mobility
U_L	=	lift velocity
V	=	tank volume
V_A	=	attractive van der Waals potential
V_B	=	total interaction potential
V_E	=	repulsive electrical double layer potential
V_p	=	particle volume
V_T	=	total interaction potential
x	=	normal coordinate
y	=	normal coordinate
z_i	=	valence electron
ζ	=	zeta potential
$\dot{\gamma}_w$	=	wall shear rate
η	=	dynamic viscosity, Komogorov's microscale
θ	=	fractional particle surface coverage, polar angle
φ	=	polar angle
μ	=	kinematic viscosity
κ	=	Debye-Hückel parameter (length)
κ^{-1}	=	thickness of the double layer
δ	=	thickness of cake layer
δ_c	=	cake thickness
ε	=	dielectric constant, particle volume fraction, power dissipation
ν	=	kinematic viscosity
ψ	=	double layer potential
ψ_o	=	potential at the particle surface

BIBLIOGRAPHY

Abe, H., Sugawara, H., Hirayama, J., Ihara, H., Kato, T., Ikeda, H. and Ikebuchi, K. (2000) *Removal of Parvovirus B19 from Hemoglobin Solution by Nanofiltration, Artif. Cell Blood Sub.*, 25(8): 375-383

Alberts, B., Bray, D., Lewis, J., Raff, M., Roberts, K. and Watson, J.D. (1983) *Molecular Biology of the Cell,* Garland, New York, p. 285

Altena, F.W. and Belfort, G. (1984) *Lateral Migration of Spherical Particles in Porous Flow Channels: Application to Membrane Filtration, Chem. Eng. Sci.,* 39(2): 343-355

Altena, F.W., Weigand, R.J. and Belfort, G. (1985) *Lateral Migration of Spherical Particles in Laminar Porous Tube Flows: Application to Membrane Filtration, Physicochem. Hydrodyn.,* 6(4): 393-413

Amirhor, P. and Engelbrecht, R.S. (1975) *Virus Removal by Polyelectrolyte-Aided Filtration, J. Am. Water Works Ass.*, 67(4): 187-192

Amirtharajah, A. and Mills, K.M. (1982) *Rapid-Mix Design for Mechanisms of Alum Coagulation, J. Am. Water Works Ass.*, 74(4): 210-216

Amirtharajah, A. and Trussler, S.L. (1986) *Destabilization of Particles by Turbulent Rapid Mixing, J. Environ, Eng.*, 112(6): 1085-1108

Anderson, K.P., Lie, Y.S., Low, M.A.L., Williams, S.R., Fennie, E.H., Nguyen, T.P. and Wurm, F.M. (1990) *Presence and Transcription of Intracisternal A Particle Related Sequences in CHO Cells, J. Virol.*, 64(5): 2021-2032

Anderson, K.P., Low, M.A.L., Lie, Y.S., Keller, G.A., Dinowitz, M. (1991) *Endogenous Origin of Defective Retrovirus-Like Particles from a Recombinant Chinese Hamster Ovary Cell Line, Virology,* 181(1): 305-311

Ando, Y. and Tsuzuki, T. (1984) *The Role of Surface Charge in Ionic Germination of Clostridium perfringens Spores, J. Gen. Microbiol.,* 130: 267-273

Anthony, A.J., King, P.H. and Randall, C.W. (1975) *Effects of Branching and Other Physical Properties of Anionic Polyacrylamides on Flocculation of Domestic Sewage, J. Appl. Polym. Sci.*, 19(1): 37-48

Aranha-Creado, H., Peterson, J. and Huang, P.Y. (1998) *Clearance of Murine Leukemia Virus from Monoclonal Antibody Solutions by a Hydrophilic PVDF Microporous Membrane Filter, Biologicals,* 26(2): 167-172

Aranha, H. and Forbes, S. (2001) *Viral Clearance Strategies for Biopharmaceutical Safety Part 3: A Multifaceted Approach to Process Validation, Bio. Pharm.,* 14(5): 42-54

Aunins, J.G. and Wang, D.I.C. (1989) *Induced Flocculation of Animal Cells in Suspension Culture, Biotechnol. Bioeng.,* 34(5): 629-638

Aunins, J.G., Woodson, B.A., Hale, T.K. and Wang, D.I.C. (1989) *Effects of Paddle Impeller Geometry on Power Input and Mass Transfer in Small-Scale Animal Cell Culture Vessels, Biotechnol. Bioeng.*, 34(9): 1127-1132

Bacchin, P., Aimar, P. and Sanchez, V. (1995) *Model for Colloidal Fouling of Membranes, AICHE J.,* 41(2): 368-376

Bacchin, P., Aimar, P. and Sanchez, V. (1996) *Influence of Surface Interaction on Transfer during Colloid Ultafiltration, J. Membrane Sci.,* 115(1): 49-63

Baran, A.A. (1988) *Flocculation of Cellular Suspensions by Polyelectrolytes, Colloid Surface,* 31: 259-264

Batt, B. (2001) Personal Communication

Battini, J.L., Heard, J.M. and Danos, O. (1992) *Receptor Choice Determinants in the Envelope Glycoproteins of Amphotropic, Xenotropic and Polytropic Murine Leukemia Viruses, J. Virol.*, 66(3): 1468-1475

Bechtel, M.K., Bagdasarian, A., Olson, W.P. and Estep, T.N. (1988) *Virus Removal or Inactivation in Hemoglobin Solutions by Ultrafiltration or Detergent/Solvent Treatment, Biomater. Artif. Cell.,* 16(1-3): 123-128

Belfort, G., Davis, R.H. and Zydney, A.L. (1994) *The Behavior of Suspensions and Macromolecular Solutions in Crossflow Microfiltration, J. Membrane Sci.,* 96(1-2): 1-58

Belkowski, L.S. (1992) *The Use of Microfiltration for the Removal of Viruses, Bioprocess Engineering Symposium-ASME*, 23: 79-83

Belter, P.A., Cussler, E.L. and Hu, W.S. (1988) *Bioseparations,* Wiley, New York, NY
Bernhardt, H. and Schell, H. (1993) *Effects of Energy Input during Orthokinetic Aggregation on the Filterability of Generated Flocs, Wat. Sci. Tech.*, 27(10): 35-65

Berns, A.J., Lai, M.H., Bosselman, R.A., McKennett, M.A., Bacheler, L.T., Fan, H., Maandag, E.C., van der Putten, H.V. and Verma, I.M.. (1980) *Molecular Cloning of Unintegrated and a Portion of Integrated Moloney Murine Leukemia Viral DNA in Bacteriophage Lambda, J. Virol.*, 36(1): 254-263

Bilello, J.A., Wivel, N.A. and Pitha, P.M. (1982) *Effect of Interferon on the Replication of Mink Cell Focus-Inducing Virus in Murine Cells: Synthesis, Processing, Assembly and Release of Viral Proteins, J. Virol.,* 43(1): 213-222

Bird, R.B., Stewart, W.E and Lightfoot, E.N. (1960) *Transport Phenomena*, John-Wiley & Sons, New York

Bishop, J.M. (1984) *Cellular Oncogenes and Retroviruses, Ann. Rev. Biochem.*, 53: 301-354

Bitton, G. (1975) *Adsorption of Viruses onto Surfaces in Soil and Water, Water Res.,* 9(5-6): 473-484

Bowen, W.R. and Jenner, F. (1995) *Theoretical Descriptions of Membrane Filtration of Colloids and Fine Particles: An Assessment and Review, Adv. Colloid Interface.,* 56: 141-200

Brose, D., Dosmar, M., Cates, S. and Hutchison, F. (1996) *Studies on the Scale-Up of Crossflow Filtration Devices, PDA J. Pharma. Sci. Tech.,* 50(4): 252-260

Brown, D., Livesey, P.J. and Tuckley, E.S.G. (1970) I.C.I. Internal Report, I.C.I. Corporate Laboratories, Runcorn, and I.C.I., Organics Division, Manchester, England

Callahan, R. and Todaro, G.J. (1978) *Four Major Endogenous Retrovirus Classes Each Genetically Transmitted in Various Species of Mus*, in "*Origins of Inbred Mice*" (H.C. Morse 3rd ed.), p. 689-713, Academic Press, New York

Camp, T.R. and Stein, P.C. (1943) *Velocity Gradient and Internal Work in Fluid Motion, J. Boston Soc. Civil. Eng.*, 30: 219-237

Carlson, J. O. (2002) Personal Communication

Carman, P. C. (1939) *Fundamental Principles of Industrial Filtration, Trans. Inst. Chem. Eng.,* 16: 168-188

Chan, C.W.Y., Song, Y., Ailenberg, M., Wheeler, M., Pang, S.F., Brown, G.M. and Silverman, M. (1997) *Studies of Melatonin Effects on Epithelia Using the Human Embryonic Kidney-293 (HEK-293) Cell Line, Endocrinology*, 138(11): 4732-4739

Chapman, D.L. (1913) *A Contribution to the Theory of Electrocapillarity, Phil. Mag.*, 25(6): 475-481

Chaudhuri, M. and Engelbrecht, R.S. (1970) *Removal of Viruses from Water by Chemical Coagulation and Flocculation, J. Am. Water Works Ass.*, 62(9): 563-567

Chen, W.J. (1998) *Effects of Surface Charge and Shear during Orthokinetic Flocculation on the Adsorption and Sedimentation of Kaolin Suspensions in Polyelectrolyte Solutions, Separ. Sci. Technol.*, 33(4): 569-590

Cheryan, M. (1986) *Ultrafiltration Handbook*. 1st Ed. Technomic Publishing Company Inc.

Cleasby, J.L. (1984) *Is Velocity Gradient a Valid Turbulent Flocculation Parameter? J. Environ. Eng.*, 110(5): 875-897

Clontech (2002) Personal Communication

Clontech (2001) *Retroviral Gene Transfer and Expression User Manual*

Cloyd, M.W., Thompson, M.M. and Hartley, J.W. (1985) *Host Range of Mink Cell Focus-Inducing Viruses, Virology,* 140(2): 239-248

Coffin, J.M. (1992) *Structure and Classification of Retroviruses,* p. 19-49. In Levy, J.A. (ed.) *The Retroviridae*, Vol. 1, Plenum Press, New York

Collen, D., Stassen, J.M., Marafino, B.J., Builder, S., Decock, F., Ogez, J., Tajiri, D., Pennica, D., Bennett, W.F., Salwa, J. and Hoyng, C.F. (1984) *Biological Properties of Human Tissue-Type Plasminogen-Activator Obtained by Expression of Recombinant DNA in Mammalian Cells, J. Pharmacol. Exp. Theor.,* 231(1): 146-152

Dahlgren, M.A.G., Claesson, P.M. and Audebert, R. (1994) *Highly Charged Cationic Polyeletrolytes on Mica: Influence of Polyelectrolyte Concentration on Surface Forces, J. Colloid Interf. Sci.,* 166(2): 343-349

Darby, R. (2001) *Chemical Engineering Fluid Mechanics*, 2nd Ed. Marcel Dekker, New York, NY

Davis, R.H. (1992) "*Microfiltration: Definitions" in "Membrane Handbook*" ed. Ho, W.S. and Sirkar, K., Van Nostrand Reinhold, New York, NY

De Boer, G.B.J., Hoedemakers, G.F.M. and Thoenes, D. (1989) *Coagulation in Turbulent Flow: Part I, Chem. Eng. Sci.*, 67(May): 301-307

Defrise, D. and Gekas, V. (1988) *Microfiltration Membranes and the Problem of Microbial Adhesion: A Literature Survey, Process Biochem.*, 23(4): 105-116

Dentel, S. and Abu-Orf, M. (1994) *Proc. Water Environ. Fed. Conf.*, 67th, Chicago, IL, Oct. 15-19, 1994, *Water Environment Federation*, Alexandria, VA, paper AC943805, pp. 541-552

Derjaguin, B.V. and Landau, L.D. (1941) *Theory of the Stability of Strongly Charged Lyophobic Sols and the Adhesion of Strongly Charged Particles in Solutions of Electrolytes, Acta Physicochimica. URSS*, 14: 633-662

Dickinson, E. and Eriksson, L. (1991) *Particle Flocculation by Adsorbing Polymers, Adv. Colloid Interface.*, 34: 1-29

Delichatsios, M. A. and Probstein, R.F. (1975) *Coagulation in Turbulent Flow: Theory and Experiment, J. Colloid Interface Sci.*, 51: 394-405

DiLeo, A.J., Vacante, D.A. and Deane, E.F. (1993) *Size Exclusion Removal of Model Mammalian Viruses Using a Unique Membrane System, II: Module Qualification and Process Simulation, Biologicals,* 21(3): 287-296

Dubin, P.L. and Davis, R.M. (1990) *Higher-Order Association in Polyelectrolyte Micelle Complexes, Langmuir,* 6(8): 1422-1427

Eckstein, E.C., Bailey, D.G. and Shapiro, A.H. (1977) *Self-Diffusion of Particles in Shear Flow of a Suspension, J. Fluid Mech.*, 79: 191-208

Eglitis, M.A., Eiden, M.V. and Wilson, C.A. (1993) *Gibbon Ape Leukemia Virus and the Amphotropic Murine Leukemia Virus 4070A Exhibit an Unusual Interference Pattern on E36 Chinese Hamster Cells, J. Virol.*, 67(9): 5472-5477

Eidsath, A.B. (1989) *Secondary Minimum Flocculation of Polymer Colloids, Ph.D. Dissertation*, Princeton University, Princeton, New Jersey

Eriksson, L., Alm, B. and Stenius, P. (1993) *Formation and Structure of Polystyrene Latex Aggregates Obtained by Flocculation with Cationic Polyelectrolytes. I. Adsorption and Optimum Flocculation Concentration, Colloid Surface A*, 70(1): 47-60

Fass, D., Davey, R.A., Hamson, C.A., Cunningham, J.M., Kim, P.S. and Berger, J.M. (1997) *Structure of a Murine Leukemia Virus Receptor-Binding Glycoprotein at 2 °A Resolution, Science*, 277(5332): 1662-1666

Fass, D., Kim, P.S. and Harrison, S.C. (1996) *Retrovirus Envelope Domain at 1.7 °A Resolution, Nat. Struct. Biol.*, 3(5): 465-469

Fisher, R.A. and Yates, F. (1963) In "*Statistical Table for Biological, Agricultural and Medical Research*" 6th Ed., pp. 8 and 66, Hafner, New York

Field, R.W., Wu, D., Howell, J.A. and Gupta, B.B. (1995) *Critical Flux Concept for Microfiltration Fouling, J. Membrane Sci.,* 100(3): 259-272

Fischinger, P.J., Nomura, S. and Bolognesi, D.P. (1975) *Novel Murine Oncornavirus with Dual Ecotropic and Xenotropic Properties, Proc. Natl. Sci. USA,* 72(12): 5150-5155

Flint, S.J., Enquist, L.W., Hrug, R.M., Racaniello, V.R. and Skalka, A.M. (2000) *Virology: Molecular Biology, Pathogenesis and Control,* ASM Press. Washington, D.C., 1st Ed.

Floyd, R. and Sharp, D.G. (1978) *Viral Aggregation: Quantitation and Kinetics of the Aggregation of Poliovirus and Reovirus, Appl. Environ. Mocrobiol.*, 35(6): 1079-1083

Food and Drug Administration (1993) *Points to Consider in the Characterization of Cell Lines Used to Produce Biologicals,* U.S. Department of Health and Human Services, Rockviller, MD, USA

Food and Drug Administration (1997), *Points to Consider in the Manufacture and Testing of Monoclonal Antibody Products for Human Use*, U.S. Department of Health and Human Services, Rockviller, MD, USA

Garcia, J.V., Jones, C. and Miller, A.D. (1991) *Localization of the Amphotropic Murine Leukemia Virus Receptor Gene to the Pericentromeric Region of Human Chromosome 8, J. Virol.*, 65(11): 6316-6319

Gazdar, A.F., Oie, H., Lalley, P., Moss, W.W., Minna, J.D. and Francke, U. (1977) *Identification of Mouse Chromosomes Required for Murine Leukemia Virus Replication, Cell,* 11(4): 949-956

Gilcrease, F.W. and Kelly, S.M. (1955) *Relation of Coliform-Organism Test to Enteric Virus Pollution, J. Am. Water Works Ass.*, 47(7): 683-694

Gill, R.I.S. and Herrington, T.M. (1987a) *The Effect of Surface Charge on the Flocculation of Kaolin Suspensions with Cationic Polyacrylamides of Varying Molar Mass but Similar Cationic Characters, Colloid Surface,* 25(2-4): 297-310

Gill, R.I.S. and Herrington, T.M. (1987b) *The Flocculation of Kaolin Suspensions with Cationic Polyacrylamides of Varying Molecular Mass but the Same cationic Character, Colloid Surface,* 22(1): 51-76

Gill, R.I.S. and Herrington, T.M. (1987c) *The Flocculation of Kaolin Suspensions using Polyethylemine and Cationic Polyacrylamides of the Same Molar Mass but Different Charge Density, Colloid Surface*, 28(1): 41-52

Goldacre, R.J. (1954) *Crystalline Bacterial Arrays and Specific Long Range Forces, Nature*, 174(4433): 732-734

Goren, S.L. (1971) *Hydrodynamic Forces on Touching Spheres along Line of Centers Exerted by a Shear Field, J. Colloid Interface Sci.*, 36(1): 94-96

Gouy, G. (1910) *Sur La Constitution De La Charge Electrique à la Surface D'un Electrolyte, J. de Physique Théorique et Appliquée,* (4) 9: 457-468

Gouy, G. (1917) *Ann. d. Phys.,* (9) 7: 129-184

Graham, F.L. and van der Eb, A.J. (1973) *Transformation of Rat Cells by DNA of Human Adenovirus 5, Virology*, 54(2): 536-539

Graham, F.L., Smiley, J., Russell, W.C. and Hairn, R. (1977) *Characteristics of a Human Cell Line Transformed by DNA from Human Adenovirus Type 5, J. Gen. Virol.*, 36: 59-72

Graham, F.L., van der Eb, A.J. and Heijneker, H.L. (1974) *Size and Location of the Transforming Region in Human Adenovirus Type 5 DNA, Nature*, 251 (5477): 687-691

Green, G. and Belfort, G. (1980) *Fouling of Ultrafiltration Membranes: Lateral Migration and the Particle Trajectory Model, Desalination,* 35: 129-147

Gregory, J. (1969) *Flocculation of Polystyrene Particles with Cationic Polyelectrolytes, Trans. Faraday Soc.*, 65(560P) 2260-2268

Gregory, J. (1973) *Rates of Flocculation of Latex Particles by Cationic Polymers, J. Colloid Interface Sci.,* 42(2): 448-456

Grogory, J. (1975) *Interaction of Unequal Double Layers at Constant Charge, J. Colloid Interface Sci.,* 51(1): 44-51

Gregory, J. (1977) "*Effects of Polymers on Colloid Stability*" In "*The Scientific Basis of Flocculation*" ed. Ives, K.J. NATO ASI series, Sijthoff and Noordhoff, Alphen ann den Rjin

Gregory, J. (1983) *Flocculation Test Methods, Effluent & Water Treatment J.*, 23(5): 199-205

Gregory, J. (1988) *Polymer Adsorption and Flocculation in Sheared Suspensions, Colloid Surface*, 31: 231-253

Gregory, J. (1989) *Fundamentals of Flocculation, Crit. Rev. Env. Contr.*, 19(3): 185-230

Gregory, J. (1997) *The Density of Particle Aggregates, Wat. Sci. Technol.*, 36(4): 1-13

Greig, R.G. and Jones, M.N. (1976) *The Possible Role of Steric Forces in Cellular Cohesion, J. Theor. Biol.*, 63(2): 405-419

Hamaker, H.C. (1937) *The London-van de Waals Attraction between Spherical Particles, Physica*, 4(10): 1058-1072

Han, B., Akeprathumchai, S., Qian, X. and Wickramasinghe, S.R. (2003) *Flocculation of Biological Cells: Comparisons between Experiment and Theory, AICHE J.*, 49(7): 16871701

Han, J.Y., Zhao, Y. Anderson, W.F. and Cannon, P.M. (1998) *Role of Variable Regions A and B in Receptor Binding Domain of Amphotropic Murine Leukemia Virus Envelope Protein, J. Virol.*, 72(11): 9101-9108

Han, M.Y. and Lawler, D.F. (1992) *The (Relative) Insignificant of G in Flocculation, J. Am. Water Works Ass.*, 84(10): 79-91

Hartley, J.W. and Rowe, W.P. (1976) *Naturally Occurring Murine Leukemia Viruses in Wild Mice: Characterization of a New "Amphotropic" Class, J. Virol.*, 19(1):19-25

Hartley, J.W., Wolford, N.K., Old, L.J. and Rowe, W.P. (1977) *New Class of Murine Leukemia Virus Associated with Development of Spontaneous Lymphomas, Proc. Natl. Acad. Sci. USA*, 74(2): 789-792

Heller, W. (1966) *Effects of Macromolecular Compounds in Disperse Systems, Pure Appl. Chem.*, 12: 249-273

Herath, G., Yamomoto, K. and Urase, T. (1999) *Removal of Viruses by Microfiltration Membranes at Different Solution Environments, Water Sci. Technol.*, 40(4-5): 331-338

Hermia, J. (1982) *Constant Pressure Blocking Filtration Laws: Application to Power Law Non-Newtonian Fluids, Trans. I. Chem. Eng.*, 60(3): 183-187

Hiemenz, P.C. and Rajagopalan, R. (1997) *Principles of Colloids and Surface Chemistry*, Marcel Dekker, Inc., New York

Higashitani, K., Yamauchi, K., Matsuno, Y. and Hosokawa, G. (1983) *Turbulent Coagulation of Particles Dispersed in a Viscous Fluid, Chem. Eng. Sci. Japan*, 16(4): 299-304

Ho, B. P. and Leal, L.G. (1974) *Inertial Migration of Rigid Spheres in Two Dimensional Unidirectional Flows, J. Fluid Mech.*, 65: 365-400

Holland, F.A. and Chapman, F.S. (1966) "*Liquid Mixing and Processing in Stirred Tanks*" p. 78. Reinhold, New York

Horn, D. and Heuck, C.C. (1983) *Charge Determination of Proteins with Polyelectrolyte Titration, J. Biol. Chem.*, 258(3): 1665-1670

Hou, K., Gerba, C.P., Goyal, S.M. and Zerda, K.S. (1980) *Capture of Latex Beads, Bacteria, Endotoxin and Viruses by Charge-Modified Filters, Appl. Environ. Microbiol.*, 40(5): 892-896

Hubbard, R.C., McElvaney, N.G., Birrer, P., Shak, S., Robinson, W.W., Jolley, C., Wu, M., Chernick, M.S. and Crystal, R.G. (1992) *A Preliminary Study of Aerosolized Recombinant Human Deoxyribonuclease-I in the Treatment of Cystic-Fibrosis, New Engl. J. Med.*, 326(12): 812-815

Hughes, J., Ramsden, D.K. and Symes, K.C. (1990) *The Flocculation of Bacteria using Cationic Synthetic Flocculants and Chitosan, Biotechnol. Tech.*, 4(1): 55-60

Huisman, I.H. and Trägårdh, C. (1999) *Particle Transport in Crossflow Microfiltration – I. Effects of Hydrodynamics and Diffusion, Chem. Eng. Sci.*, 54(2): 271-280

Hunter, R.J. (1981) *Zeta Potential in Colloid Science*, Academic Press

Hunter, E. (1997) *Viral Entry and Receptors*, p. 71-119. In Coffin, J.M., Hughes, S.H. and Varmus, H.E. (ed.) "*Retroviruses*", Cold Spring Harbor Laboratory Press, Cold Spring Harbor, New York

Hutter, J.M., Clarke, M.T., Just, E.K., Lichtin, J.L. and Sakr, A. (1991) *Colloid Titration: A Method to Quantify the Adsorption of Cationic Polymer by Bleached Hair, J. Soc. Cosmetic Chem.*, 42(2): 87-96

International Conference of Harmonisation (ICH) (2001) *Therapeutic Products Programme Guidance: Viral Safety Evaluation of Biotechnology Products Derived from Cell Lines of Human or Animal Origin.*

Iwamoto, A., Masuda, M. and Yoshikura, H. (1985) *Two NIH3T3 Cell Lines of Different Origins Circulating in the World, Jpn. J. Exp. Med.*, 55(3): 129-131

Jacangelo, J.G., Adham, S.S. and Laîné, J.M. (1995) *Mechanism of Cryptosporidium, Giardia and MS2 Virus Removal by MF and UF, J. Am. Water Works Ass.*, 87(9): 107-121

Jainchill, J.L., Aaronson, S.A. and Todaro, G.J. (1969) *Murine Sarcoma and Leukemia Viruses: Assay Using Clonal Lines of Contact-Inhibited Mouse Cells, J. Virol.*, 4(5): 549-553

James, R.I., Elton, J.P., Todd, P. and Kompala, D.S. (2000) *Engineering CHO Cells to Overexpress a Secreted Reporter Protein upon Induction from Mouse Mammary Tumor Virus Promoter, Biotech. Bioeng.*, 67(2): 134-140

Janot, C., Muller, S., Streiff, F., Donner, M. and Stoltz, J.F. (1990) *Application of Laser Doppler Electrophoresis to the Measurement of Blood Cell Surface Charge, Clin. HemoRheol.*, 10(1): 103-111

Johnson, J.H., Fields, J.E. and Darlington, W.A. (1967) *Removing of Viruses from Water by Polyelectrolytes, Nature*, 213(5077): 665-667

Juliano, R.L. and Bannelier, M.B. (1975) *Surface Polypeptides of Cultured Chinese Hamster Ovary Cells, Biochemistry-US,* 14(17): 3816-3825

Kane, J.C., Linford, H.B. and Lamer, V.K. (1964) *Filtration and Electrophoretic Mobility Studies of Flocculated Silica Suspensions, J. Am. Chem. Soc.*, 86 (17): 3450-3453

Kasper, D.R. (1971) *Theoretical and Experimental Investigations of the Flocculation of Charged Particles in Aqueous Solutions by Polyelectrolytes of Opposite Charge, Ph.D. Dissertation*, California Institute of Technology, California

Katchalsky, A., Danon, D., Nevo, A. and Devries, A. (1959) *Interactions of Basic Polyelectrolytes with the Red Blood Cells. II. Agglutination of Red Blood Cells by Polymeric Bases, Biochim Biophys Acta*, 33(1): 120-138

Katchalsky, A. (1964) *Polyelectrolytes and Their Biological Interactions, Biophys. J.*, 4(1SP): 9-41

Kavanaugh, M.P., Miller, D.G., Zhang, W., Law, W., Kozak, S.L., Kabat, D. and Miller, M.D. (1994) *Cell-Surface Receptors for Gibbon Ape Leukemia Virus and Amphotropic Murine Retrovirus are Inducible sodium-Dependent Phosphate symporters, Porc. Natl. Acad. Sci., USA*, 91: 7071-7075

Kim, J.S. Akeprathumchai, S. and Wickramasinghe, S.R. (2001) *Flocculation to Enhanced Microfiltration, J. Membrane Sci.*, 182(1-2): 161-172

Kim, J.W., Closs, E.I., Albritton, L.M. and Cunningham, J.M. (1991) *Transport of Cationic Amino Acids by the Mouse Ecotropic Retrovirus Receptor, Nature,* 352(6337): 725-728

Kitchener, J.A. (1972) *Principles of Action of Polymeric Flocculants, Br. Polym. J.*, 4: 217-229

Klement, V. Rowe, W.P., Hartley, J.W. and Pugh, W.E. (1969) *Mixed Culture Cytopathogenecity: A New Test for Growth of Murine Leukemia Viruses in Tissue Culture, Proc. Natl. Acad. Sci. USA,* 63(3): 753 –758

Klenk, H.D. and Garten, W. (1994) *"Activation Cleavage of Viral Spike Proteins by Host Protease"*, p. 241-280. In Wimmer, E. (ed.), *Cellular Receptors for Animal Viruses*. Cold Spring Harbor Laboratory Press, Cold Spring Harbor, New York.

Koltuniewicz, A. (1992) *Predicting Permeate Flux in Ultrafiltration on the Basis of Surface Renewal Concept, J. Membrane Sci.,* 68(1-2): 107-118

Kominami, R., Urano, Y., Mishima, M., Muramatsu, M., Moriwaki, K. and Yoshikura, H. (1983) *Novel Repetitive Sequence Families Showing Size and Frequency Polymorphism in the Genomes of Mice, J. Mol. Biol.*, 165(2): 209-228

Kostenbader, K.D. and Cliver, D.O. (1983) *Membrane Filter Evaluations using Poliovirus, J. Virol. Methods,* 7: 253-257

Kroner, K.H. and Kula, M.R. (1984) *Conference Sea Island-USA,* 29(1): 3

Kuo, K.P. and Cheryan, M. (1983) *Ultrafiltration of Acid Whey in a Spiral Wound Unit: Effect of Operating Parameters on Membrane Fouling, J. Food Sci.,* 48(4): 1113-1118

La Mer, V.K. and Healy, T.W. (1964) *Energetics of Flocculation and Redispersion by Polymers, J. Colloid Sci.,* 19(4): 323-332

Langmuir, I. (1938) *The Role of Attractive and Repulsive Forces in the Formation of Tactoids, Thixotropic Gels, Protein Crystals and Conservatives, J. Chem. Phys.,* 6: 873-896

Lawler, D.F. (1993) *Physical Aspects of Flocculation: From Microscale to Macroscale. Wat. Sci. Tech.*, 27(10): 165-180

Lee, J.H., Lee, J.W., Khang, G. and Lee, H.B. (1997) *Interaction of Cells on Chargeable Functional Group Gradient Surfaces, Biomaterials*, 18(4): 351-358

Leis, J., Baltimore, D., Bishop, J.M., Coffin, J., Fleissner, E., Goff, S.P., Oroszlan, S., Robinson, H., Skalka, A.M., Temin, H.M. and Vogt, V. (1988) *Standardized and Simplified Nomenclature for Proteins Common to all Retroviruses, J. Virol.*, 62(5): 1808-1809

Leong, Y.K. (1994) *Exploitation of Interparticle Forces in the Processing of Colloidal Ceramic Materials, Materials Design,* 15(3): 141-147

Leong, Y.K. (1996) *Depletion Interaction in Colloidal Suspensions: A Comparison between Theory and Experiment, Colloids Surfaces A,* 118(1-2): 107-114

Leong, Y.K. (1997) *Effects of Steric and Hydrophobic Forces on the Rheological Properties of ZrO_2 Suspensions, Colloid Polym. Sci.,* 275(9): 869-875

Leong, Y.K. (1999) *Interparticle Forces Arising from an Adsorbed Strong Polyelectrolyte in Colloidal Dispersions: Charged Patch Attraction, Colloid Polym. Sci.,* 277(4): 299-305

Leong, Y.K. and Boger, D.V. (1991) *Effects of Polycarboxylate on the pH and Magnitude of Maximum Yield Stress of m-ZrO_2 Suspensions, Ceram. Trans.,* 19: 83-90

Leong, Y.K., Boger, D.V., Scales, P.J. and Healy, T.W. (1996) *Interparticle Forces Arising from Adsorbed Surfactants in Colloidal Suspensions: An Additional Attractive Force, J. Colloid Interface Sci.,* 181(2): 605-612

Leong, Y.K., Boger, D.V., Scales, P.J., Healy, T.W. and Buscall, R. (1993a) *Control of the Rheology of Concentrated Aqueous Colloidal Systems by Steric and Hydrophobic Forces, J. Chem. Soc. Chem. Comm.,* 7: 639-641

Leong, Y.K., Scales, P.J., Healy, T.W., Boger, D.V. and Buscall, R. (1993b) *Rheological Evidence of Adsorbate-Mediated Short-Range Steric Forces in Concentrated Dispersions, J. Chem. Soc. Faraday Trans.,* 89(14): 2473-2478

Lévêque, M.A. (1928) *Les Lois De La Transmission De Chaleur Par Convection, Ann. Mines,* 13:201-362

Levinthal, D. and Davison, P.F. (1961) *Degradation of Deoxyribonucleic Acid under Hydrodynamic Shearing Forces, J. Mol. Biol.,* 3(5): 674-683

Li, H., Fane, A.G., Coster, H.G.L. and Vigneswaran, S. (1998) *Direct Observation of Particle Deposition of the Membrane Surface during Crossflow Microfiltration, J. Membrane Sci.,* 149(1): 83-97

Lie, Y.S., Penuel, E.M., Low, M.A.L., Nguyen, T.P., Mangahas, J.O. and Anderson, K.P. and Petropoulos, C.J. (1994) *Chinese Hamster Ovary Cells Contain Transcriptionally Active Full-Length Type-C Proviruses, J. Virol.,* 68(12): 7840-7849

Lieber, M.M., Benvenis, R.E., Livingston, D.M. and Todaro, G.J. (1973) *Mammalian Cells in Culture Frequently Release Type –C Viruses, Science,* 182(4107): 56-59

Lifshitz, E.M. (1956) *The Theory of Molecular Attractive Forces between Solids, Soviet Phys. JETP,* 2(1): 73-83

Mabire, F., Audebert, R. and Quivoron, C. (1984) *Flocculation Properties of Some Water-Soluble Cationic Copolymers Towards Silica Suspensions – A Semiquantitative Interpretation of the Role of Molecular Weight and Cationicity through a Patchwork Model, J. Colloid Interface Sci.*, 97(1): 120-136

Madsen, R.F. (1977) *Hyperfiltration and Ultrafiltration in Plate and Frame* Systems, Elsevier Sci. Pub. Co., New York

Malek, B., George, D.B. and Fillips, D.S. (1981) *Virus Removal by Coagulation and Flocculation, J. Am. Water Works Ass.,* 73(3): 164-168

Mann, R., Mulligan, R.C. and Baltimore, D. (1983) *Construction of a Retrovirus Packaging Mutant and Its Use to Produce Helper-Free Defective Retrovirus, Cell,* 33(1): 153-159

Manwaring, J.F., Chaudhuri, M. and Engelbrecht, R.S. (1971) *Removal of Viruses by Coagulation and Flocculation, J. Am. Water Works Ass.*, 63(5): 298-300

Markotic, A., Hensley, L., Geisbert, T., Spik, K. and Schmaljohn, C. S. (2003) *Hantaviruses Induce Cytophatic Effects and Apoptosis in Continuous Human Embryonic Kidney Cells, J. Gen. Virol.*, 84: 2197-2202

Mattison, K.W., Brittian, I.J. and Dubin, P.L. (1995) *Protein Electrolyte Phase Boundaries, Biotechnol. Progr.,* 11(6): 632-637

McClure, M.O., Sommerfelt, M.A., Marsh, M. and Weiss, R.A. (1990) *The pH Independence of Mammalian Retrovirus Infection. J. Gen. Virol.*, 71: 767-773

McDonogh, R.M., Fane, A.G. and Fell, C.J.D. (1989) *Charge Effects in the Crossflow Filtration of Colloids and Particulates, J. Membrane Sci.,* 43(1): 69-85

Meyer, B.J. and Schmaljohn, C.S. (2000) *Persistent Hantavirus Infections: Characteristics and Mechanisms, Trends Microbial.*, 8(2): 61-67

McGahey, C. and Olivieri, V.P. (1993) *Mechanism of Viral Capture by Microfiltration, Wat. Sci. Tech.*, 27(3-4): 307-310

Michaels, A.S. (1954) *Aggregation of Suspensions by Polyelectrolytes, Ind. Eng. Chem.*, 46(7): 1485-1490

Miller, A.D. and Buttimore, C. (1986) *Redesign of Retrovirus Packaging Cell-Lines to Avoid Recombination Leading to Helper Virus Production, Mol. Cell. Biol.*, 6 (8): 2895-2902

Miller, A.D. and Chen, F. (1996) *Retrovirus Packaging Cells Based on 10A1 Murine Leukemia Virus for Production of Vectors That Use Multiple Receptors for Cell Entry, J. Virol.*, 70(8): 5564-5571

Miller, D.G. and Miller, A.D. (1992) *Tunicamycin Treatment of CHO Cells Abrogates Multiple Blocks to Retrovirus Infection, One of Which is due to a Secreted Inhibitor, J. Virol.*, 66(1): 78-84

Miller, D.G. and Miller, A.D. (1993) *Inhibitors of Retrovirus Infection are Secreted by Several Hamster Cell Lines and are also Present in Hamster Sera, J. Virol.*, 67(9): 5346-5352

Miller, D.G., Edwards, R.H. and Miller, A.D. (1994) *Cloning of the Cellular Receptor for Amphotropic Murine Retroviruses Reveals Homology to That for Gibbon Ape Leukemia Virus, Proc. Natl. Acad. Sci. USA*, 91(1): 78-82

Morgan, R.A., Nussbaum, O., Muenchau, D.D., Shu, L.M., Couture, L. and Anderson, W.F. (1993) *Analysis of the Functional and Host Range-Determining Regions of the Murine Ecotropic and Amphotropic Retrovirus Envelope Proteins. J. Virol.*, 67(8): 4712-4721

Morgenstern, J.P. and Land, H. (1990) *Advanced Mammalian Gene Transfer: High Titer Retroviral Vectors with Multiple Drug Selection Markers and a Complementary Helper-Free Packaging Cell Line, Nucleic Acids Res.*, 18(12): 3587-3596

Mühle, K. (1933), in "*Coagulation and Flocculation*" (B. Dobiá, Ed.), p. 355. Dekker, New York

Murphy, F.A., Fauquet, C.M., Bishop, D.H.L., Ghabrial, S.A., Jarvis, A.W., Martello, G.P., Mayo, M.A. and Summers, M.D. (1995) *Virus Taxonomy, 6th Report of the International Committee on Taxonomy of Viruses*, Springer-Verlag Wien, New York

Nagata, S. (1975) *Mixing: Principles and Applications*, Wiley, New York, p. 24-32

Nakamura, Y., Kameyama, K.I., Igarashi, C., Tanaka, K., Kitamura, T. and Fujita, K. (1994) *Proc. Water Environ. Fed. Conf.*, 67th, Chicago, IL, Oct. 15-19, 1994, *Water Environment Federation*, Alexandria, VA, paper AC943804, pp. 533-540

Nasser, A., Weinberg, D., Dinoor, N., Fattal, B. and Adin, A. (1995) *Removal of Hepatitis A Virus (HAV), Poliovirus and MS2 Coliphage by Coagulation and High Rate Filtration, Water Sci. Tech.*, 31(5-6): 63-68

Neefe, J.R. and Stokes, J. (1945) *An Epidemic of Infectious Hepatitis Apparently due to a Waterborne Agent - Epidemiologic Observations and Transmission Experiments in Human Volunteers, JAMA - J. Am. Med. Ass.*, 128(15): 1063-1075

Nermut, M.V., Frank, H. and Schäfer, W. (1972) *Properties of Mouse Leukemia Viruses III. Electron Microscopic Appearance as Revealed after Conventional Preparation Techniques as well as Freeze-Drying and Freeze-Etching, Virology*, 49(2): 345-358

Oftshun, N.J. (1989) *Cross-Flow Membrane Filtration of Cell Suspension*, Ph.D. Dissertation, MIT, Cambridge, MA

Oldshue, J.Y. (1984) *Fluid Mixing Technology*, McGraw-Hill, New York

Oldshue, J.Y. and Trussell, R.R. (1991) in "*Mixing in Coagulation and Flocculation*", in Amirtharajah, A. and Clark, M. Eds., American Water Works Research Foundation, Denver

Omar, A. and Kempf, C. (2002) *Removal of Neutralized Model Parvoviruses and Enteroviruses in Human IgG Solutions by Nanofiltration, Transfusion*, 42(8): 1005-1010

Otaki, M., Yano, K. and Ohgaki, S. (1998) *Virus Removal in a Membrane Separation Process, Wat. Sci. Tech.*, 37(10): 107-116

Ott, D., Friedrich, R. and Rein, A. (1990) *Sequence Analysis of Amphotropic and 10A1 Murine Leukemia Viruses: Close Relationship to Mink Cell Focus-Inducing Viruses, J. Virol.*, 53: 100-106

Ottewill, R.H. and Rastogi, M.C. (1960) *The Stability of Hydrophobic Sols in the Presence of Surface Active Agents. II. The Stability of Silver Iodide Sols in the Presence of Cationic Surface Active Agents, Trans. Faraday Soc.*, 56(6): 866-866

Parker, D.S., Kaufman, W.J. and Jenkins, D. (1972) *Floc Breakup in Turbulent Flocculation Processes, J. Sanit. Eng. Div. ASCE.*, 98(NSA1): 79-99

Patel, P.N., Mehaia, M.A. and Cheryan, M. (1987) *Crossflow Membrane Filtration of Yeast Suspensions, J. Biotechnol.*, 5(1): 1-16

Patzer, E.J., Nakamura, G.R., Hershberg, R.D., Gregory, T.J., Crowley, C., Levinson, A.D. and Eichberg, J.W. (1986) *Cell Culture Derived Recombinant HBSAG is Highly Immunogenic and Protects Chimpanzees from Infection with Hepatitis-B Virus, Bio/Technology*, 4(7): 630-636

Pelssers, E. G.M., Stuart, M.A.C. and Fleer, G.J. (1989) *Kinetic Aspects of Polymer Bridging: Equilibrium Flocculation and Nonequilibrium Flocculation, Colloids Surfaces*, 38(1-3): 15-25

Penrod, S.L., Olson, T.M. and Grant, S.B. (1995) *Whole Particle Microelectrophoresis for Small Viruses, J. Colloid Interf. Sci.,* 173(2): 521-523

Peredo, C., O'Reilly, L., Gray, K. and Roth, M.J. (1996) *Characterization of Chimeras between the Ecotropic Moloney Murine Leukemia Virus and the Amphotropic 4070A Envelope Proteins, J. Virol.*, 70(5): 3142-3152

Pinter, A. and Fleissner, E. (1979) *Structural Studies of Retroviruses: Characterization of Oligomeric Complexes of Murine and Feline Leukemia Virus Envelope and Core Components Formed upon Cross-Linking, J. Virol.*, 30(1): 157-165

Pinter, A., Honnen, W.J. and Li, J.S. (1984) *Studies with Inhibitors of Oligosaccharide Processing Indicate a Functional Role for Complex Sugars in the Transport and Proteolysis of Friend Mink Cell Focus-Inducing Murine Leukemia Virus Envelope Proteins. Virology,* 136(1): 196-210

Pinter, A., Lieman-Hurwitz, J. and Fleissner, E. (1978) *The Nature of the Association between the Murine Leukemia Virus Envelope Proteins, Virology*, 91(2): 345-351

Porter, M.C. (1972) *Concentration Polarization with Membrane Ultrafiltration, Ind. Eng. Chem. Res. Dev.,* 11(3): 234-248

Poynter, S.F.B. (1968) *The Problem of Viruses in Water, Proc. Soc. Water Treat. Exam.,* 17: 187-204

Prestidge, C. and Tadros, Th. F. (1988) *Rheological Investigation of Depletion Flocculation of Concentrated Sterically Stabilized Polystyrene Latex Dispersions, Colloid Surface,* 31: 325-346

Puck, T.T., Sanders, P. and Petersen, D. (1964) *Life Cycle Analysis of Mammalian Cells 2: Cells from Chinese Hamster Ovary Grown in Suspension Culture, Biophys. J.*, 4(6): 441-450

Rasheed, S., Pal, B.K. and Gardner, M. (1982) *Characterization of a Highly Oncogenic Murine Leukemia Virus from Wild Mice, Int. J. Cancer*, 29: 345-350

Rein, A (1982) *Interference Grouping of Murine Leukemia Viruses: A Distinct Receptor for the MCF-Recombinant Viruses in Mouse Cells, Virology,* 120(1): 251-257

Rein, A and Schultz, A (1984) *Different Recombinant Murine Leukemia Viruses use Different Cell Surface Receptors, Virology,* 136(1): 144-152

Renner, W.A., Jordan, M., Eppenberger, H.M. and Leist, C. (1993) *Cell-Cell Adhesion and Aggregation: Influence on the Growth Behavior of CHO Cells, Biotechnol. Bioeng.,* 41(2) 188-193

Ruehrwein, R.A. and Ward, D.W. (1952) *Mechanism of Clay Aggregation by Polyelectrolytes, Soil Sci.*, 73(6): 485-492

Russel, W.B., Saville, D.A. and Schowalter, W.R. (1989) *Colloidal Dispersions*, Cambridge, Cambridge University Press

Russell, W.C., Brodaty, E. and Armstrong, J.A. (1971) *A Cytochemical Study of Basic Proteins in Adenovirus Infected Cells, J. Gen. Virol.*, 11: 87-93

Russotti, G., Osawa, A.E., Sitrin, R.D., Buckland, B.C., Adams, W.R. and Lee, S.S. (1995) *Pilot-Scale Harvest of Recombinant Yeast Employing Microfiltration: A Case Study, J. Biotechnol.*, 42(3): 235-246

Sarkar, N.H., Moore, D.H. and Charney, J. (1973) *The Effect of pH on the Morphology, Electrophoretic Mobility and Infectivity of the Mouse Mammary Tumor Virus, Cancer Res.*, 33(10): 2283-2290

Seaman, G.V.F. (1975) *Electrokinetic Behavior of Red Cells*, In, D.M. Surgenor (Ed.), *The Red Blood Cell*, Academic Press, New York

Seaman, G.V.F., Knox, R.J., Nordt, F.J. and Regan, D.H. (1977) *Red Cell Aging 1. Surface Charge Density and Sialic Acid Content of Density Fractionated Human Erythrocytes, Blood,* 50(6): 1001-1011

Seigel, G.M., Chiu, L. and Paxhia, A. (2000) *Inhibition of Neuroretinal Cell Death by Insulin-Like Growth Factor-1 and Its Analogs, Mol. Vis.*, 6(19): 157-163

Shaw, J.A. (1994) *Understand the Effects of Impeller Type, Diameter and Power on Mixing Time, Chem. Eng. Prog.*, 90(2): 45-48

Sheldon, J.M., Reed, I.M. and Hawes, C.R. (1991) *The Fine Structure of Ultrafiltration Membranes. II Protein Fouled Membranes, J. Membrane Sci.*, 62 (1): 87-102

Shinnar, R. and Church, J.M. (1960) *Statistical Theories of Turbulence in Predicting Particle Size in Agitated Dispersions, Ind. Eng. Chem.*, 52(3): 253-256

Smith, D.H., Byrn, R.A., Marsters, S.A., Gregory, T., Groopman, J.E. and Capon, D.J. (1987) *Blocking of HIV-1 Infectivity by a Soluble, Secreted Form of the CD4 Antigen, Science*, 238(4834): 1704-1707

Smith, D.K.W. and Kitchener, J.A. (1978) *Strength of Aggregates Formed in Flocculation, Chem. Eng. Sci.*, 33(12): 1631-1636

Smoluchowski, M. (1916) *Drei Vorträge über Diffusion, Brownsche Bewegung und Koagulation von Kolloidteilchen, Phys. Z.*, 17: 557-585.

Somasundaran, P. and Yu, X. (1994) *Flocculation Dispersion of Suspensions by Controlling Adsorption and Conformation of Polymers and Surfactants, Adv. Colloid Interface Sci.*, 53: 33-49

Sommerfelt, M.A. and Weiss, R.A. (1990) *Receptor Interference Groups of 20 Retroviruses Plating on Human Cells, Virology,* 176(1): 58-69

Sommerfelt, M.A. (1999) *Retrovirus Receptors, J. Gen. Virol.,* 80: 3049-3064

Spicer, P.T. and Pratsinis, S.E. (1996) *Coagulation and Fragmentation: Universal Steady-State Particle Size Distribution, AICHE J.*, 42(6): 1612-1620

Spicer, P.T., Keller, W. and Pratsinis, S.E. (1996) *The Effect of Impeller Type on Floc Size and Structure during Shear Induced Flocculation, J. Colloid Interface Sci.,* 184(1): 112-122

Staffman, P.G. and Turner, J. (1956) *On the Collisions of Drops in Turbulent Clouds, J. Fliud Mech.*, 1(16): 16-30

Stern, O. (1924) *Zur Theorie der Elektrolytischen Doppelschucht, Z. Elektrochem.*, 30: 508-516

Stoll, S. and Buffle, J. (1998) *Computer Simulation of Flocculation Processes: The Roles of Chain Conformation and Chain/Colloid Concentration Ratio in the Aggregate Structures, J. Colloid Interface Sci.,*205(2): 290-304

Tabor, D. and Winterton, R.H.S. (1969) *Direct Measurement of Normal and Retarded van der Waals Forces, Proc. R. Soc. London,* A312 (1511): 435-450

Takemoto, L.J., Fox, C.F., Jensen, F.C., Elder, J.H. and Lerner, R.A. (1978) *Nearest Neighbor Interactions of Major RNA Tumor Virus Glycoprotein on Murine Cell Surfaces, Proc. Natl. Acad. Sci. USA*, 75(8): 3644-3648

Tambo, N. and Hozumi, H. (1979) *Physical Characteristics of Flocs. 2. Strength of Floc, Water Res.*, 13(5): 421-427

Teich, N. (1984) *Taxonomy of Retroviruses*, p. 25-208. In R. Weiss, N. Teich, N., H. Varmus. and J. Coffin (ed.) *RNA Tumor Viruses*, Vol., 1. Cold Spring Harbor Laboratory, Cold Spring Harbor, New York

Terayama, H. (1952) *Method of Colloid Titration (A New Titration between Polymer Ions), J. Polym. Sci.,* 8(2): 243-253

Thethi, K., Jurasz, P., MacDonald, A.J., Befus, A.D., Man, S.F.P., and Duszyk, M. (1997) *Determination of Cell Surface Charge by Photometric Titration, J. Biochem. Biophys. Methods,* 34(2): 137-145

Thompson, J.F. and Morrison, G.R. (1951) *Determination of Organic Nitrogen: Control Variables in the Use of Nessler Reagent, Anal. Chem.,* 23(8): 1153-1157

Thonart, P., Custinne, M. and Paquot, M. (1982) *Zeta Potential of Yeast Cells: Application in Cell Immobilization, Enzyme Microb. Tech.,* 4(3): 191-194

Thorup, R.T., Nixon, F.P., Wentworth, D.F. and Sproul, O.J. (1970) *Virus Removal by Flocculation with Polyelectrolytes, J. Am. Water Works Ass.*, 62(1): 97-101

Tihon, C. and Green, M. (1973) *Cyclic AMP Amplified Replication of RNA Tumor Virus-like Particles in Chinese Hamster Ovary Cells, Nature-New Biol.*, 244(138): 227-231

Tihon, C. and Hellman, A. (1976) *Characterization of an Endogenous Chinese Hamster Virus, Fed. Proc.*, 35(7): 1612-1612

Todaro, G.J. and Green, H. (1963) *Quantitative Studies of the Growth of Mouse Embryonic Cells in Culture and Their Development into Established Lines, J. Cell Biol.*, 17(2): 299-313

Todaro, G.J. and Huebner, R. (1972) *The Viral Oncogene Hypothesis: New Evidence, Proc. Natl. Acad. Sci. USA*, 69(4): 1009-1015

Trettin, D.R. and Doshi, M.R. (1980) *Limiting Flux in Ultrafiltration of Macromolecular Solutions, Chem. Eng. Commun.*, 4 (4-5): 507-522

Ueno, K. and Kina, K. (1985) *Colloid Titration: A Rapid Method for the Determination of Charged Colloid, J. Chem. Educ.*, 62(7): 627-629

Uhl, V.W. and Gray, J.B. (1966) *Mixing Theory and Practice*, Academic Press, New York

Urase, T., Yamamoto, K. and Ohgaki, S. (1993) *Evaluation of Virus Removal in Membrane Separation Processes Using Coliphage Qβ, Wat. Sci. Tech.*, 28(7): 9-15

Urase, T., Yamamoto, K. and Ohgaki, S. (1994) *Effect of Pore size Distribution of Ultrafiltration Membranes on Virus Rejection in Crossflow Conditions, Wat. Sci. Tech.*, 30(9): 199-208

Urlaub, G., Mitchell, P.J., Kas, E., Chasin, L.A., and Funanage, V.L. (1986) *Effect of Gamma Rays at the Dihydrofolate Reductase Locus–Deletions and Inversions, Somat Cell Mol. Gen.*, 12(6): 555-566

van Damme, M.P.I., Blackwell, S.T., Murphy, W.H. and Preston, B.N. (1992) *The Measurement of Negative Charge Content in Cartilage using A Colloid Titration Technique, Anal. Biochem.,* 204(2): 250-257

van Damme, M.P.I., Tilias, J., Nemat, T.N. and Preston, B.N. (1994) *Determination of the Charge Content at the Surface of Cells Using A Colloid Titration Technique, Anal. Biochem.,* 223(1): 62-70

van de Ven, T.G.M. (1981) *Effects of Polymer Bridging on Selective Shear Flocculation, J. Colloid Interface Sci.,* 81(1): 290-291

Van Zaane, D., Dekker-Michielson, M.J.A. and Bloemers, H.P.J. (1976) *Virus-Specific Precursor Polypeptides in Cells Infected with Rauscher Leukemia Virus: Synthesis, Identification and Processing, Virology,* 75(1): 113-129

Vanzeijl, M.V., Johann, S.V., Closse, E., Cunningham, J., Eddy, R., Shows, T.B. and O'Hara, B. (1994) *A Human Amphotropic Retrovirus Receptor is a Second Member of the Gibbon Ape Leukemia Virus Receptor Family, Proc. Natl. Acad. Sci. USA,* 91 (3): 1168-1172

van Voorthuizen, E.M., Ashbolt, N.J. and Schäfer, A.I. (2001) *Role of Hydrophobic Interactions for Initial Enteric Virus Retention by MF Membranes, J. Membrane Sci.,* 194(1): 69-79

Vargas, F.F., Osorio, H.M., Ryan, U.S. and De Jesus, M. (1989) *Surface Charge of Endothelial Cells Estimated from Electrophoretic Mobility, Membr. Biochem.,* 8(4): 221-227

Vargas, F.F., Osorio, H.M., Basilio, C., De Jesus, M. and Ryan, U.S. (1990) *Enzymatic Lysis of Sulfated Glycoaminoglycans Reduces the Electrophoretic Mobility of Vascular Endothelial Cells, Membr. Biochem.,* 9(2): 83-89

Vasseur, P. and Cox, R.G. (1976) *The Lateral Migration of a Spherical Particle in Two-Dimensional Shear Flows, J. Fluid Mech.,* 78: 385-413

Verwey, E.J. W. and Overbeek, J.Th.G. (1948) *Theory of the Stability of Lyophobic Colloids,* Elservier, Amsterdam

Vincent, B. (1974) *The Effect of Adsorbed Polymers on Dispersion Stability, Adv. Colloid Interface Sci.,* 4: 193-277

Viromed Biosafety Laboratories (1999) *Biosafety Testing Services,* www.viromed.com

Vosel, S.V., Kalinin, D.V., Rudina, N.A. and Purtov, P.A. (1999) *Analysis of Aggregation Processes in Suspensions of Colloidal Silica Particles, Goel. Geofiz.,* 40(6): 926-929

Wang, H., Kavanaugh, M.P., North, R.A. and Kabat, D. (1991) *Cell Surface Receptor for Ecotropic Murine Retroviruses is a Basic Amino Acid Transporter, Nature,* 352(6337): 729-731

Wang, L.K. and Shuster, W.W. (1975) *Polyelectrolyte Determination at Low Concentration, Ind. Eng. Chem. Prod. Res. Dev.,* 14(4): 312-314

Wickramasinghe, S.R., Wu, Y.L. and Han,.B. (2002) *Enhanced Microfiltration of Yeast by Flocculation, Desalination,* 147(1-3): 25-30

Wickramasinghe, S.R., Han, B., Akeprathumchai, S., Chen, V., Neal, P. and Qian, X. (2003) *Improved Permeate Flux by Flocculation of Biological Feeds: Comparison between Theory and Experiment, J. Membr. Sci.,* (accepted)

Wiesner, M.R. and Chellam, S. (1992) *Mass Transport Considerations for Pressure-Driven Membrane Processes, J. Am. Water Works Ass.,* 84(1): 88-95

Wilson, C.A., Farrell, K.B. and Eiden, M.V. (1994) *Properties of a Unique Form of the Murine Amphotropic Leukemia Virus Receptor Expressed on Hamster Cells, J. Virol.,* 68(12): 7697-7703

Wilson, C.A., Marsh, J.W. and Eiden, M.V. (1992) *The Requirements for Viral Entry Differ from Those for Virally Induced Syncytium Formation in NIH 3T3/DTRAS Cells Exposed to Moloney Murine Leukemia Virus, J. Virol.,* 66(12): 7262-7269

Yang, M., Neubauer, C.M. and Jennings, H.M. (1997) *Interparticle Potential and Sedimentation Behavior of Cement Suspensions: Review and Results from Paste, Avd. Cem. Based Mater.,* 5(1): 1-7

Yang, X. (1996) *Effect of Mixing on the Kinetic of Polymer-aided Flocculation,* M.S. Thesis, University of Alberta, Canada

Yoon, S.H., Lee, C.H., Kim, K.J. and Fane, A.G. (1999) *Three Dimensional Simulation of the Deposition of Multi-Dispersed Charged Particles and Prediction of Resulting Flux during Crossflow Microfiltration, J. Membrane Sci.,* 161(1-2): 7-20

Young, S., Stanley, S.J. and Smith, D.W. (2000) *Effect of Mixing on the Kinetics of Polymer-Aided Flocculation, J. Water Serv. Res. Tech.,* 49(1): 1-8

York, D.W. and Drewry, W.A. (1974) *Virus Removal by Chemical Coagulation, J. Am. Water Works Ass.,* 66(12): 711-716

Yu, X. and Somasundaran, P. (1996) *Role of Polymer Conformation in Interparticle-Bridging Dominated Flocculation, J. Colloid Interface Sci.,* 177(2): 283-287

Zydney, A. L. and Colton, C.K. (1982) *Continuous Flow Membrane Plasmapheresis: Theoretical Models for Flux and Hemolysis Prediction, Trans. Am. Soc. Artif. Intern. Organs,* 28: 408-412

Zydney, A.L. and Colton, C.K. (1986) *A Concentration Polarization Model for the Filtrate Flux in Crossflow Microfiltration of Particulate Suspensions, Chem. Eng. Commun.,* 47(1-3): 1-21

APPENDICES

APPENDIX A

HEK–293 CELL GROWTH MEDIUM

HEK-293 cell, the Amphopack-293 packaging cell line which is designed for rapid production of high titer retroviruses, is a human embryonic kidney cell. The growth medium for HEK-293 Cells was prepared as follow:

1. 500 mL of Dulbecco's Modified Eagle's Medium (Sigma #D5671)
2. 50 mL of Fetal Bovine Albumin (Sigma #F2442)
3. 10 mL of 200 mM L-Glutamine (Sigma #G7513)
4. 5 mL of Penicillin/Streptomycin Solution (Sigma #P0781)
5. 5 mL of 100 mM Sodium pyruvate (Sigma #5280)

APPENDIX B

TRYPAN BLUE EXCLUSION ASSAY AND HEAMCYTOMETER

The viability of CHO cells in the suspension is assayed according to trypan blue dye assay (Juliano and Bannelier (1975), Seigel et al. (2000)). Due to the fact that dead cells when exposed to the trypan blue dye will allow the dye to penetrate into the cells because of the loss the semipermeability of the cell membrane. The live cells, on the contrary, will not take up the blue dye through their cell membranes. Therefore, under inverted microscope and with the presence of the trypan blue dye, live cells will be seen as the normal cells with clear cell content while the dead cells will appear blue for the whole cell. Consequently, this assay can be used to determine the viability of CHO cell in suspension.

Prior to each flocculation experiment, the viability and the cell density were determined by using a combination of the trypan blue dye assay and hemacytometer. Hemacytometer is essentially the cell counting chamber. The glass slide at which the sample after staining with trypan blue is loaded to has either 16 or 25 square grids. The protocol to determine the cell viability and density is given below

1. Approximately 0.5 mL of CHO cell suspension from spinner flask was withdrawn and transferred to 1.0 mL centrifuge tube
2. 100 μL of the sample was transferred to a new 1.5 mL centrifuge tube

3. 100 μL of trypan blue dye was added and mixed gently by pipetting
4. Sample was then loaded onto the 25 square grid hemacytometer
5. Under an inverted microscope, count the number of cells in 5 squares diagonally (a) or count the number of cells in the squares at the four corners and one in the center (b)

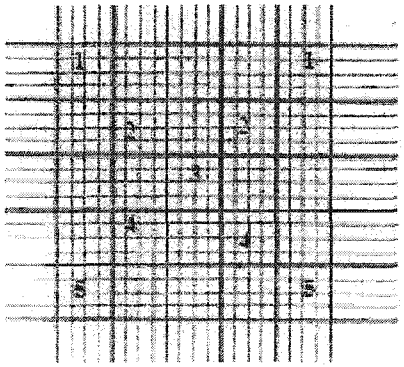

(a)

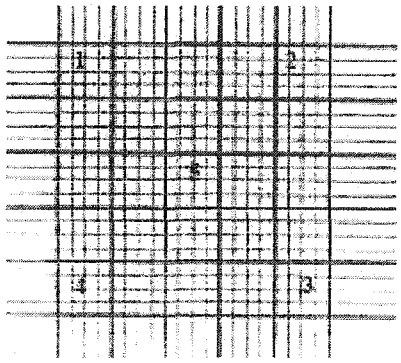

(b)

6. To calculate the total numbers of cells in the sample, the following relationship is used

$$C = 2 \times N \times 5 \times V \times 10^4 \qquad \text{(B-1)}$$

where

C	=	total numbers of cells per mL
N	=	number of cell count in 5 designated squares
5	=	factor to account for the 25 squares
V	=	dilution factor
10^4	=	conversion factor
2	=	dilution factor due to the trypan blue dye

For each sample, cell count by hemacytometer is performed twice, then the average value of the number of cells in suspension is taken as the cell concentration of that suspension. If cell suspension is too concentrated to count, dilution of the sample is necessary.

APPENDIX C

PLASMID CHARACTERIZATION, AMPLIFICATION AND PURIFICATION

This Appendix provides detailed information on pLEGFP-C1 used to produce A-MLV pseudotypes including the protocol for amplification and purification of the plasmid.

C.1.1. Plasmid Characterization

The plasmid used in the production of A-MLV pseudotypes is the pLEGFP-C1 plasmid. The pLEGFP-C1 is classified as a low copy number plasmid. Except for $DH5\alpha$ which is used in this project, the suitable host strains for plasmid amplification include $HB101$ and other general-purpose strains. Further, the selectable marker, which is the ampicillin resistance gene conferred the host cells to survive at the concentration of ampicillin up to 100 μg/mL. The detailed information concerning the amino acid sequences of the featured location on the pLEGFP-C1 is given as follows

1. 5′MoMLV LTR: 145 – 733
2. Ψ^+ (extended packaging signal): 803 – 1612
3. Neomycin resistant gene (Neo^r): 1656 – 2450
4. Immediate early CMV promoter (P_{CMV}): 2468 – 305

5. Enhanced green fluorescent protein (EGFP) gene: 3074 – 3790
6. Multiple cloning site: 3799 – 3868
7. 3′ MoMLV LTR: 3938 – 4531
8. pBR322 plasmid replication region: 5068
9. Ampicillin resistance gene ($\beta - lactamase$): 6687 – 5827
10. Sequencing primer locations
    10.1 EGFP-C sequencing primer: 3727 – 3748

    $5' - CATGGTCCTG CTGGAGTTCG TG - 3'$

    10.2 3′ Primer pLNCX Seq/PCR primer: 3960 – 3935

    $5' - ACCTACAGGT GGGGTCTTTC ATTCCC - 3'$

C.1.2. Plasmid Amplification

Due to the fact that the purchased plasmid is of small quantity, 500 ng/μL, amplification is recommended by the manufacturer. There are two principal steps in plasmid amplification which are the transformation of the plasmid into a suitable host, $DH5\alpha$, and the large scale production and purification of the plasmid. The transformation of the *E. Coli* $DH5\alpha$ is carried out first and, subsequently, the presence of the plasmid in the transformed $DH5\alpha$ is then determined. This step is also known as "Miniprep". After the presence of the plasmid in the transformants is confirmed, large-scale production is carried out and then the plasmid is purified and recovered by using the QIAgen plasmid purification Kit.

C.1.3. Transformation of *DH5α*

The bacterial host used is *DH5α* ,*E. Coli*. The amplification of the pLEGFP-C1 plasmid is possible in *E. Coli* because the pLEGFP-C1 contains the pBR322 origin of replication and *E. Coli Amp*^{r} gene for propagation and antibiotic selection of these bacteria. This particular strain of *E. Coli* was treated with $CaCl_2$ which in effect alters the cell membrane of the *DH5α* into the porous one. These pores are important in the transformation process due to the fact that they are the passages that allow the plasmid to get into the cells.

There are several methods of transformation such as liposome-mediated, phosphate-mediated and electroporation. Electroporation is chosen here because of its simplicity, high efficiency and availability of the equipment. The foreign DNA (plasmid) was admitted into the bacterial cells (host cells) via electrical shock. This method is sometimes capable of killing the host cells if a high voltage is used. The step-by-step procedure of electroporation is described below

1. Add 0.5 μL and 1.0 μL of pLEGFP plasmid into competent cells, DH5α
2. Mix gently by pipetting
3. Place 40 μL of the mixture on the side of the electroporation tube with pipette[2]
4. Tab the electroporation tube until sample reach the bottom
5. Tab flat to evenly distribute the mixture at the bottom of the tube

[2]Do not expel the last drop of the liquid because that will create bubbles which can cause a disruption during the electroporation process as evidence by "sparking"

6. Electroporation: insert the cuvette into the eletroporator with the preset conditions, which are 25 kV, 200 V and 25 μF. Two sides of the cuvette was wiped with Kimwipe to remove contaminants that may stuck to the tube surface [3]
7. After electroporation, aseptically add 250 μL of SOC media into the cuvette, mix and transfer the suspension to new test tube and incubate in the shaker for 1 h
8. Plate the cell suspension on TB + Amp (ampicilin) plate and incubate at 37 °C over night
9. By the next day, the DH5α culture that grew on the TB + Amp plate are transferred onto several new TB + Amp plates to isolate a single colony. The new plate is also incubated at 37°C overnight.

C.1.4. Miniprep

After the transformation and selection of the *DH5α*, the bacterial cells are propagated at a small volume first and then the presence of the plasmid is verified by performing gel electrophoresis. This step is called "Miniprep". This procedure involves plasmid extraction and purification. The protocol for the miniprep is as follows:

1. Individually transfer several single colonies to new test tubes containing 2.0 mL of LB + amp, using blue pipette tip (5.0 mL) and leave the pipette tip in the tubes
2. Shake overnight (or at least 6 h minimum) at 37 °C. After the bacteria grew the suspension turns turbid
3. Transfer 1 – 1.5 mL suspension to 1.7 mL centrifuge tube (ependoff)

[3] If the tube explodes, the high salt concentration in the sample is expected. Remember to hold the two buttons until the "peep" sound is heard from the machine or about 6 seconds

4. Spin down at full speed (14,000 rpm (Centrifuge 5415, Brinkman)) for 1 minute to collect the cells while the supernatant is discarded
5. Add 100 μL of STE (sodium chloride +Tris-buffer + EDTA) and resuspend the pellet by vortexing
6. Add 100 μL of phenol : chloroform, then vortex for 10 seconds
7. Spin at 14,000 rpm for 5 minutes
8. Transfer the top aqueous layer to a new 1.7 mL centrifuge tube
9. Add 25 μL (or one quarter) of CH_3COONH_4 (ammonium acetate) then mix
10. Add twice the volume of the whole mixture of 100 % EtOH (100 + 25 = 125μL) then the volume of EtOH added should be 250 μl (or $62.5 \times 2 = 125$ μL), then mix by vortexing, spin at 14,000 rpm for 5 minutes
11. Pour off the supernatant (no need of pipetting)
12. Add 250 μL of 70 % EtOH, pour off and add another 300 μL of 70 % EtOH
13. Spin at 14,000 rpm for 2 minutes
14. Pour off the supernatant, spin briefly and remove the remaining liquid by pipetting
15. Allow to air dry for 5 minutes (or by speed vacuum for 10 minutes)
16. Add a mixture of 25 μL + RNAse A, vortex, then left to sit at room temperature for 5 minutes to redissolve the nucleic acid
17. Gel Electrophoresis
    1. Prepare the gel by dissolving agarose powder in TAE buffer, Ethidium bromide is added to bind to agarose gel
    2. Pour into the gel cast with comb for sample addition

3. The sample is prepared on paraffin film to the final total volume of ~12 μL[4]
    1. 12 μL of bromophenol blue dye (ladder dye)
    2. 1 μL of pure (original) plasmid + 4 μL of dye + 7 μL of TAE buffer
    3. 8 μL of sample 1 + 4 μL of dye
    4. 8 μL of sample 2 + 4 μL of dye
    5. 8 μL of sample 3 + 4 μL of dye
4. Load sample from step 3 onto the agarose gel
5. Run at 100 V (rate: 1 cm / 4 minutes and 15 seconds)
6. Turn off the power when the ladder dye travel almost to the end of the gel
7. Take the gel to the reading machine
8. To take photo "click" print to get picture
9. Take out the gel, clean the machine by wiping with paper towel, EtOH, then paper towel again

For the minipreps' samples, due to the fact that PLEGFP-C1 plasmid did not have any foreign construct inserted, gel electrophoresis of the plasmids obtained from the minipreps is not necessary. However, gel electrophoresis was performed for these plasmids but without restriction enzyme treatment. It was found that the bands from the minipreps' plasmid and that from the original plasmids appeared at relatively the same

[4] Both of the original plasmid and the sample from the minipreps should have been cut with restriction enzyme. This way we can determine the molecular weight (MW) of the linear plasmid from the minipreps against both of the MW of the linear DNA from the ladder and that from the original plasmid having been cut with restriction enzyme. However, since there is no foreign construct being introduced into the plasmid, the samples were, therefore, not treated with restriction enzyme.

position. Therefore, it is concluded that the plasmids from miniprep are identical to the original plasmid, pLEGFP-C1.

C.1.5. Large Scale Production

After verifying that the plasmid obtained from the miniprep step is the original palsmid, large-scale production of the plasmid is conducted. Large-scale production of pLEGFP plasmid is then carried out. In the large-scale plasmid production, the plasmid is purified and recovered by QIAgen plasmid purification Kit. Subsequently, the presence of the plasmid is confirmed by gel electrophoresis.

1. From the liquid media containing transformed *E.Coli* from the minipreps step, inoculate 50 μL in to 100 mL of LB media containing 16 mg ampicilin
2. Grow the bacteria overnight (~ 12 - 16 hrs), the cell density can go up to 2×10^9 cells per mL
3. Harvest the bacterial cells by centrifugation at 6,000g (~ 6,000 rpm with Sorvall GSA or GS3) for 15 min at 4 °C. Then supernatant is discarded.
4. Resuspend the pellet with 4 mL of buffer P1, then thoroughly mix by vortexing or pipetting until no cell clumps are left to be seen
5. Add 4 mL of buffer P2, then mix gently but thoroughly by inverting 4 – 6 times, and incubate at room temperature for 5 min. (Vortexing is not recommended, as this will result in shearing the genomic DNA. The lysate should appear viscous. Lysis reaction should not be allowed to proceed for more than 5 minutes)

6. Add 4 mL of chilled buffer P3 to the lysate, and mix immediately but gently by inverting 4 – 6 times. (After adding buffer P3 a fluffy white precipitate containing genomic DNA, proteins, cell debris, and SDS becomes visible. The buffers must be mixed completely. If the mixture still appears viscous and brownish, more mixing is required to completely neutralize the solution.)
7. Transfer the lysate to the barrel of the QIAfilter Cartridge by pipetting. Incubate at room temperature for 10 minutes. Do not insert the plunger
8. Equilibrate a QIAGEN-tip 100 with 4 mL of QBT buffer and allow the column to empty by gravity flow. This step can be left unattended because the buffer will stop running when the meniscus reaches the upper frit in the column
9. Remove the cap from the QIAfilter outlet nozzle. Gently insert the plunger into the QIAfilter cartridge and filter the cell lysate into the previously equilibrated QIAGEN-tip. Approximately 10 mL of the lysate are generally recovered after filtration
10. Allow the cleared lysate to enter the resin by gravity flow
11. Wash the QIAGEN-tip with 2 × 10 mL of buffer QC. The first wash is to remove all the contaminant in the majority of plasmid preparations. The second wash is necessary when large culture volumes or bacterial strains producing large amounts of carbohydrates are used
12. Elute DNA with 5 mL of buffer QF. Collect the eluate with approximately 20 mL glass tube, do not used polycarbonate tube because it is not resistant to alcohol in the subsequent step

13. Precipitate DNA by adding 3.5 mL room temperature of isopropanol to the eluate DNA. Mix and centrifuge immediately at 12500 rpm for 30 minutes at 4 °C. Carefully decant the supernatant. Before putting the tube into the centrifuge, the tubes should be marked and placed tube into the centrifuge with the marker facing out of the rotor. That way we know the DNA pellet will stick to that area at the bottom
14. Add 400 μL of sterile ddH_2O and dissolve the DNA pellet. Then add ¼ V of ammonium acetate, mix and finally add double volume (~ 1 mL) of room temperature 100 % EtOH. Then centrifuge at 1,4000 rpm for 5 minutes. Carefully decant the supernatant into a clean beaker, this way the loss pellet may be easily recovered.
15. Wash the pellet with double volume (~1 mL) of room temperature of 70 % EtOH and mix but not too rigorously. Then centrifuge at 1400 rpm for 2 minutes with the back of the ependoff to the outside of the rotor.
16. Decant the supernatant, let the ependof stand upside down on a Kimwipe to get rid of the remaning EtOH
17. Speed vacuum dry for 30 seconds, then add 100 μL of sterile ddH_2O and dissolve the DNA pellet.
18. Aliquot the plasmid into small vial and freeze them down at –20 °C for future experiments.
19. The plasmid obtained from large-scale production is confirmed by the gel-electrophoresis (Figure C-1). Concentration of the resulting plasmid is then determined via UV absorbance. Since DNA adsorbs UV light at 260 nm while

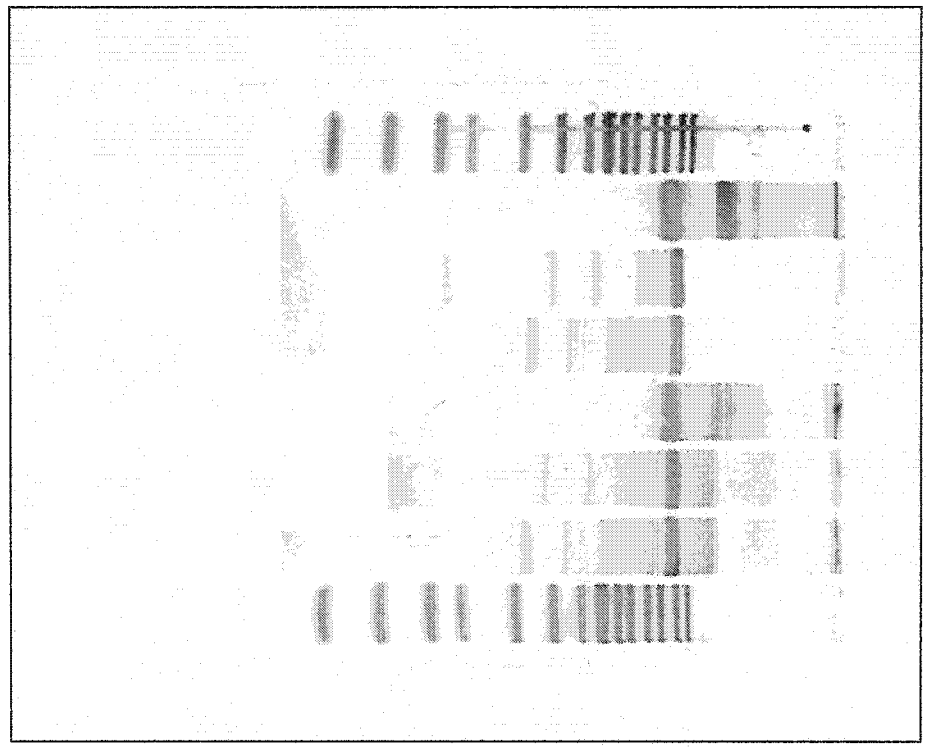

1. ladder
2. uncut pLEGFP-C1
3. pLEGFP-C1 + BamH I*
4. pLEGFP-C1 + Hind III**
5. uncut QIAgen prep
6. QIAgen prep + BamH I
7. QIAgen prep + Hind III
8. ladder

Figure C- 1 Gel Electrophoresis of QIAgen Prep Plasmid of Large Scale Production

* BamH I is an enzyme from Bacillus Amyloliquefaciens H
** Hind III is an enzyme from Haemophilus Influenzae Rd

protein adsorbs UV light at 280 nm, the ratio of the Ab at 260 and 280 nm is measured with the fact that the ratio Ab 260/280 nm of more than 1.8 is desirable. The higher the ratio of the Ab at 260/280 nm, the larger the plasmid yields. The plasmid yield obtained from the large-scale production is shown in Table C-1.

It can be seen from Figure C-1 that the plasmids obtained from the large scale production are the original plasmids since both plasmids after treating with restriction enzyme traveled at approximately the same rate, therefore, showed up at the same position. For the yield of pLEGFP plasmid obtained from the large-scale production, it can be seen from Table C-1 that the ratio of the absorbance 260 nm is 0.2319. After multiplying with conversion factor (50 μg/mL) and dilution factor, the obtained pLEGFP plasmid is approximately 580 μg/mL.

Table C- 1 Absorbance of the plasmid obtained from large-scale production after purified and recovered with QIAgen Kit

Absorbance (nm)		Ration of Abs		Protein (μg/mL)	Nucleic acid (μg/mL)
260	280	$\frac{260}{280}$	$\frac{280}{260}$		
0.2319	0.1389	1.6693	0.5990	8.0555	6.3149

APPENDIX D

TRANSFECTION METHOD

The Effectene transfection kit is based on a proprietary non-liposomal lipid, which is demonstrated to yield higher transfection efficiency than the classical liposome based transfection method. With Effectene transfection, the DNA is first condensed by interaction with the Enhancer in a defined buffer system. Then the Effectene reagent is added to the condensed DNA to produce condensed DNA-Effectene complexes. Subsequently, the Effectene – DNA complexes are mixed with growth medium and directly added to the cells.. This procedure may be used to transfect the mammalian cell even in the presence of serum.

Effectene Transfection Protocol

1. HEK-293 cells were plated at the 5×10^5 cells per 60-mm plate overnight in growth medium containing serum and antibiotics to reach about 40 – 60 % confluency. The cells were maintained at 37 °C and 5 % CO_2 incubator.
2. Dilute 2 μg of DNA dissolved in sterilized DI water, pH 7.4 (minimum DNA concentration should be 0.1 μg/mL) with the DNA-condensation buffer, Buffer EC, to a total volume of 150 μL. Add 8 μL of Enhancer and mix by vortexing for 1 second. However, it is important to always keep the ratio of DNA to Enhancer constant

3. Incubate at room temperature (20 - 25 °C) for 2-5 minutes and spin down the mixture for a few seconds to remove drops from the top of the tube.

   Note: it is not necessary to keep Effectene reagent on ice at all times because 10-15 minutes at room temperature will not alter its stability.

4. Add 25 μL of Effectene Transfection Reagent to the DNA-Enhancer mixture and mix by pipetting up and down 5 times or by vortexing for 10 seconds
5. Incubate the mixture for 5 – 10 minutes at room temperature to allow complex formation
6. While complex formation takes place, gently remove the growth medium from the plate by aspiration, and wash once with 2 mL of PBS. Add 4 mL of fresh medium (can contain serum and antibiotics) to the cells.
7. Add 1 mL of growth medium (can contain serum and antibiotics) to the reaction mixture, mix by pipetting up and down twice and then immediately add the transfection complexes drop-wise onto the cells in the 60-mm plate. Gently swirl the dish to ensure uniform distribution of the complexes.
8. Incubate cells with the complexes at 37 °C and 5 % CO_2 for 18 hrs to allow for gene expression. Removal of transfection complexes is not necessary; however, if toxicity is observed, remove the Effectene-DNA complexes after 18 hrs of addition, wash once with 2 mL of PBS, and add 5 mL of fresh medium containing serum and antibiotics.
9. Assay the cells for gene expression. For stable transfection, the HEK-293 cells were passed to the new 60-mm plate at the density of 5×10^5, which is obtained from the

kill curve construction step. Twenty-four hours later, the concentration of 250 μg/mL of G418 is introduced into the medium to select the stable transformants.

APPENDIX E

TITRATION OF ANTIBIOTIC STOCKS (KILL CURVE)

It is important to establish the kill curve before transfection of the cells can be carried out. There are two important steps in the kill curve construction, which are the optimum antibiotic concentration and the optimum plating cell density. The optimum antibiotic concentration is carried out first at the cell density of 2×10^5 cells per 60-mm plate. Then with the optimum antibiotic concentration, the optimum plating cell density can be estimated. The optimum antibiotic concentration and the optimum cell density found from the kill curve will be used to select the stable transformants following transfection. The protocols to determine the optimum antibiotic concentration and the optimum cell density are given below.

E.1 Optimum Antibiotic Concentration

The purpose of this experiment is to determine the lowest antibiotic concentration to be used in selection of the stable transformants after transfection. In this experiment, the cell density used is kept constant at 2×10^5 cells per 60-mm plate while the antibiotic concentration is varied incrementally. This procedure is described below.

1.1 Plate 2×10^5 cells in each of six of 60-mm plate containing 5 mL of fresh medium supplemented with various concentrations (0, 50, 100, 200, 400 and 800 μg/mL) of G418

1.2 Incubate the cells for 10 –14 days, replacing the selective medium every four days or more often if necessary

1.3 Examine the plates for viable cells every two days

To select the stable transformants, use the lowest concentration that begins to give massive cell death in ~ 5 days and kills all the cells within two weeks.

E.2 Optimum Plating Cell Density

The optimum plating cell density is important in the selection of the stable transformants since too high cell density will reach confluency before the selection by antibiotic can take effect. Therefore, it is essential to determine the optimum plating density before transfection and selection of the stable clones. From the optimum antibiotic concentration determination step, the antibiotic concentration is kept constant at 300 μg/mL while the cell density used to plate each of the 60-mm plate was varied. The cell density found in this step will be used to plate the transformed HEK-293 cells in the stable transformant selection step.

1.1 Plate cells at several different densities (5×10^6, 1×10^6, 5×10^5, 2×10^5, 1×10^5, and 5×10^4 cells) in each of six 60-mm tissue culture plate containing 5 mL of complete medium supplemented with 250 μg/mL of G418.

1.2 Incubate the cells for 10-14 days at 37 °C and 5 % CO_2, replacing selective medium every four days or more if necessary

1.3 Examine the dishes for viable cells every two days

For stable transformant selection, use a plating density that allows the cells to reach ~ 80 % confluency before massive cell death begins (at about 5 days). This is the cell density at which cells should be plated for selection of stable transformants.

APPENDIX F

DETERMINATION OF VIRAL TITER

Determination of viral titer is necessary for three important reasons which are (i) to confirm the viability of viruses, (ii) to estimate the multiplicity of infection (MOI), multiplicity of infection is the estimation of number of virus particles per infected target cell (NIH/3T3 cells), and (iii) to determine the maximum number of target cells to use in the infection (assay). By infecting the target cells, a rough but rapid estimation of successful infection can be approximated. The protocol to determine the viral titer is given below

1. Plate NIH/3T3 cells overnight in 6-well plate at the concentration of 1×10^5 cells per well with 2 mL fresh medium per well
2. Prepare 20 mL of complete medium and add 60 μL of 4 mg/mL polybrene
3. Collect virus containing medium from the packaging cell lines at 2-3 days after subculturing
4. Filter medium through a 0.45 μm cellulose acetate or polysulfonic filter. It is recommended that a nitrocellulose filter should not be used to filter the medium containing virus because nitrocellulose binds protein in the retroviral membrane and destroys the virus.
5. Prepare six 10-fold serial dilutions as follows:

1. Add 1.35 mL of medium (step 2) to six 1.5 mL microcentrifuge tubes
2. Add 150 μL of virus-containing medium (step 4) to the first tube and mix
3. Add 150 μL from tube 1 to tube 2. Continue dilutions

6. Infect NIH/3T3 cells by adding 1 mL of the diluted virus medium to each well
7. 48 hrs later, check for gene expression (EGFP) under the fluorescent light microscopy

The viral titer corresponds to the number of green cells present at the highest dilution, which contains colonies, multiplied by the dilution factor

APPENDIX G

METHOD OF INFECTING TARGET CELLS

In order to quantify the virus particles in suspension, the $TCID_{50}$ assay is used. Since the method of infecting target cells (NIH/3T3) is inefficient for this study, the method is slightly modified. Target cells are infected in suspended rather than attach-dependant form. The protocol for infecting suspended target cells is described below

1. NIH/3T3 cells were treated with 0.25 % trypsin-EDTA for 5 minutes (or until cells detach) at 37 °C
2. 4 mL of fresh medium was added to the suspension in step 1 and then mixed by aspiration
3. 3 mL of cell suspension was aseptically transferred to new 60-mm plate and polybrene was added to the final concentration of 8 μg/mL
4. 100 μL of medium containing suspended NIH/3T3 cells at the density of 1×10^5 cells/mL is transferred to each well of 6 well plate
5. 100 mL of medium containing A-MLV pseudotypes was added and mixed by aspiration
6. The volume was then brought to 2 mL with fresh medium
7. Cells were incubated at 37 °C and 5 % CO_2 for 2 days
8. Expression of EGFP is observed under inverted microscope equipped with UV lamps

APPENDIX H

TISSUE CULTURE INFECTIVE DOSE 50

The concentration of virus in suspension is usually determined by measuring its infectivity. There are two types of infectivity titration (assay), which are the quantal assay (or end-point assay) and the quantitative assay. While the quantal assay depends mainly on an all-or-none response of the host system, the quantitative assay relies primarily on the ability of single virus particle to form plague, pock or lesion on the host cells. The quantitative assay estimates the actual number of infectious virus particles in a given suspension. On the contrary, the quantal assay determines whether the suspension contains infectious particles by allowing them to replicate in a suitable host so that one or more infectious virus particles can be detected by amplification effect of the infection. To determine quantal infectivity titers, serial dilution of the original suspension is tested until the infectivity is diluted out. The result gives the dose (dilution) necessary to produce a defined response, which is usually based on a 50 % end-point. This end-point is estimated based on the presence or absence of a predetermined criterion such as death (lethal dose 50, LD_{50}) and infectivity (tissue culture infective dose 50, $TCID_{50}$, egg infective dose 50, EID_{50}). This method does not determine the exact number of virus particles in the suspension but only whether or not virus is present in a particular dilution.

In this project, $TCID_{50}$ which is the quantal assay is chosen to determine the number of infectious virus particles present in the permeate sample. $TCID_{50}$ yields rapid

and fairy accurate the number of infectious virus particles in the samples. However, it is generally known that murine leukemia virus (MLV) cause no or unclear cytopathic effects (CPE) in tissue culture after infection. As a result, quantification of these viruses is much more difficult. In order to circumvent this problem, the pLEGFP-C1 plasmid containing EGFP is used in the production A-MLV pseudotypes. The EGFP gene from the plasmid is packaged into the virus virions. Therefore, after susceptible host cells are infected, the expression of EGFP can be detected by using an inverted microscope equipped with fluorescent light. Consequently, the $TCID_{50}$ assay can be used to quantify the titers of A-MLV pseudotypes in the samples. Given below is the $TCID_{50}$ assay protocol.

1. Add 50 μL of cell suspension containing polybrene at the final concentration of 8 μg/mL at the cell density of 1×10^5 cells/mL to each well of 96 well plate
2. Prepare six 10 fold dilutions as follows
   2.1 Add 900 μL of fresh medium into six of 1.0 mL of centrifuge tubes
   2.2 Add 100 μL of medium containing A-MLV pseudotypes (permeate samples) to the first tube and mix by aspiration
   2.3 Transfer 100 μL of suspension from tube 1 to tube 2, continue dilution
3. Infect NIH/3T3 cells with 100 μL of the diluted virus medium to each well
4. Wrap the 96 well plate with paraffin film to prevent the loss of medium by evaporation and incubate at 37 °C and 5 % CO_2
5. Check for the expression of EGFP every two days

6. The $TCID_{50}$ can be calculated by utilizing either Karber or Reed – Muench method.

There are two formulas that can be used to calculate the 50 % endpoint, which are the Reed-Muench (R-M) and the Karber (K) methods. The latter is adopted to determine the $TCID_{50}$ of the samples. The formula for the Karber method is defined as:

$$\log_{10}(TCID_{50}) = X - d(P - 0.5) \qquad \text{(H-1)}$$

where

X = $\log_{10}$ of the highest concentration (lowest dilution)

d = $\log_{10}$ of the dilution factor

$$P = \frac{sum\ of\ \%\ green\ cells\ at\ each\ dilution}{100}$$

The $TCID_{50}$ is interpreted as the inoculation into cells (animals) of a given volume of the original virus suspension that causes 50 % infection of the tissue culture cells.

APPENDIX I

NAGATA'S POWER DISSIPATION CORRELATION

According to Nagata (1975), the power dissipation into stirred vessel may be estimated by the correlation between the impeller power number, N_p, and the impeller Reynolds' number, Re. From the correlation below (I-1), it may be supposed that there are two contributions that are responsible for the power dissipation in stirred vessels. The first term on the right hand of (I-1) may be assumed to represent the laminar shear power input whereas the second term may be considered to represent the turbulent dissipation.

$$N_p = \frac{A}{\mathrm{Re}} + B \cdot \left[\frac{10^3 + 1.2\mathrm{Re}^{0.66}}{10^3 + 3.2\mathrm{Re}^{0.66}} \right]^p \qquad \text{(I-1)}$$

with

$$A = 14 + \left(\frac{w}{D_T} \right) \cdot \left[670 \left(\frac{D_i}{D_T} - 0.6 \right)^2 + 185 \right] \qquad \text{(I-2)}$$

$$B = 10^C \qquad \text{(I-3)}$$

$$C = 1.3 - 4\left(\frac{w}{D_T} - 0.5 \right)^2 - 1.14\left(\frac{D_i}{D_T} \right) \qquad \text{(I-4)}$$

$$p = 1.1 + 4\left(\frac{w}{D_T} \right) - 2.5\left(\frac{D_i}{D_T} - 0.5 \right)^2 - 7\left(\frac{w}{D_T} \right)^4 \qquad \text{(I-5)}$$

and

$$\mathrm{Re} = \frac{D_i^2 N \rho}{\mu} \qquad \text{(I-6)}$$

APPENDIX J

PARTICLE SIZE DISTRIBUTION

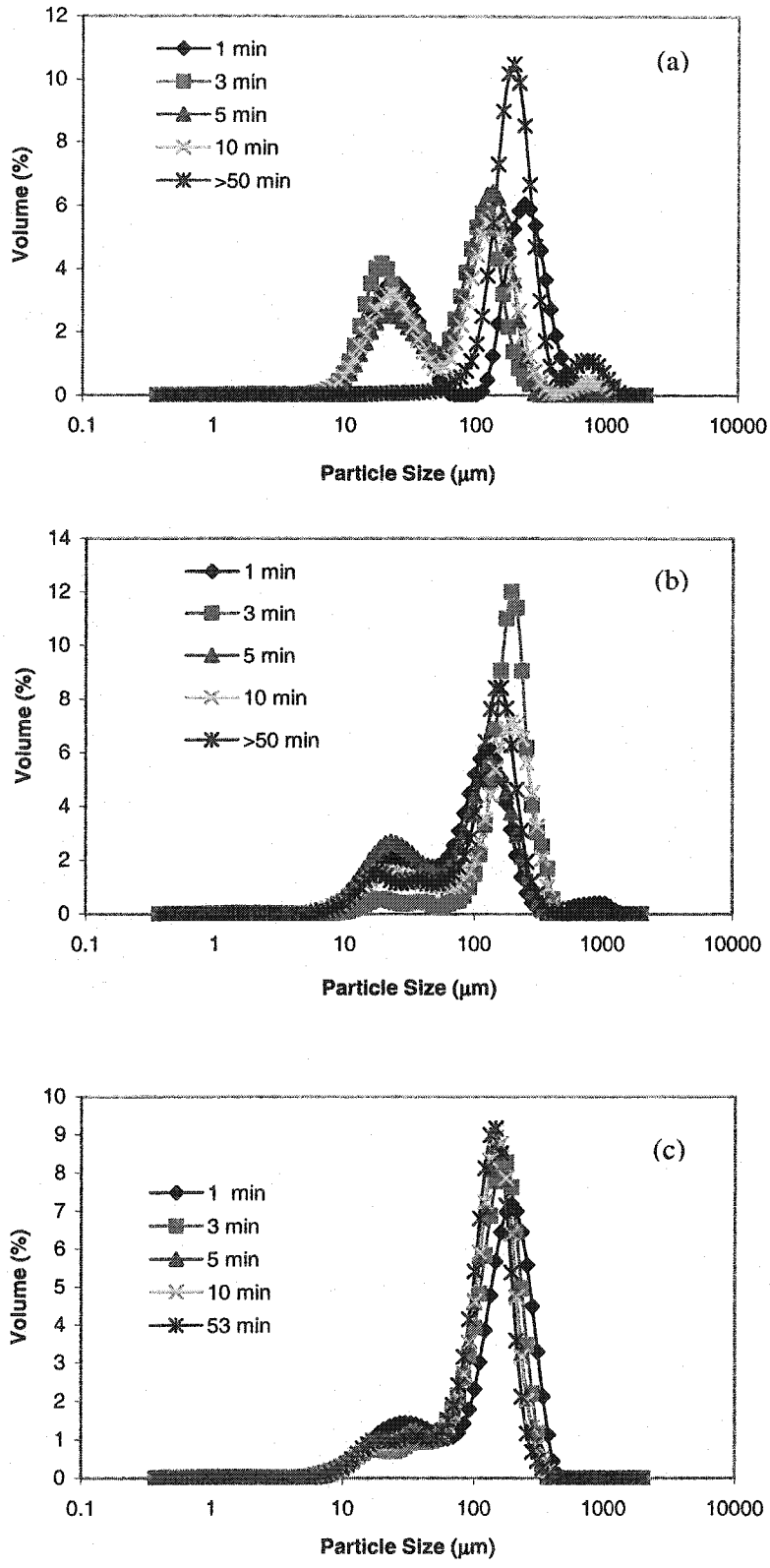

Figure J-1 Particle size distribution of flocculated CHO cells with EM441L at CHO cell density of 0.25 wt%: (a) 100, (b) 300 and (c) 500 rpm

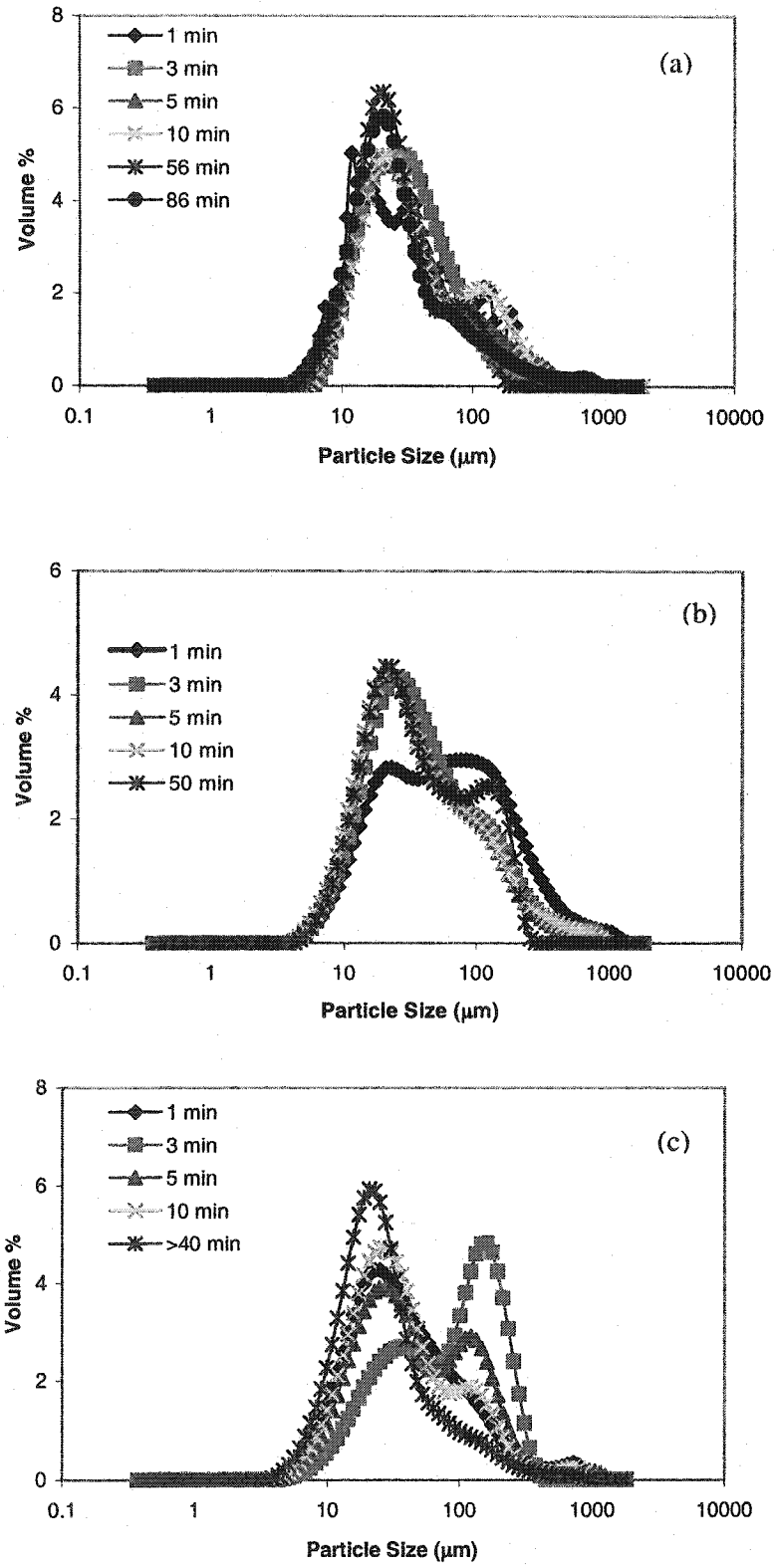

Figure J-2 Particle size distribution of flocculated CHO cells with EM240CT at CHO cell density of 0.50 wt%: (a) 100, (b) 300 and (c) 500 rpm

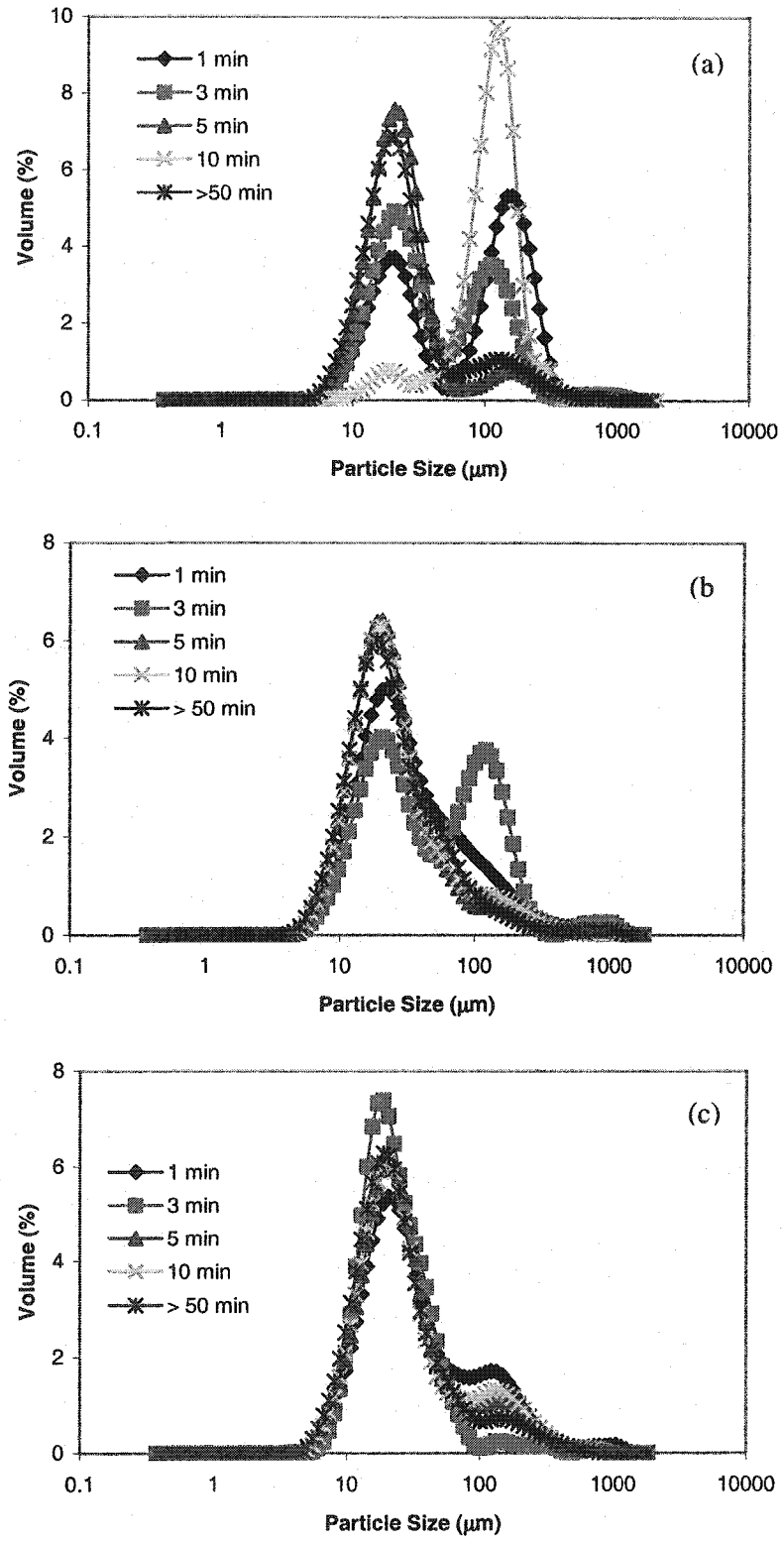

Figure J-3 Particle size distribution of flocculated CHO cells with EM240L at CHO cell density of 0.50 wt%: (a) 100, (b) 300 and (c) 500 rpm

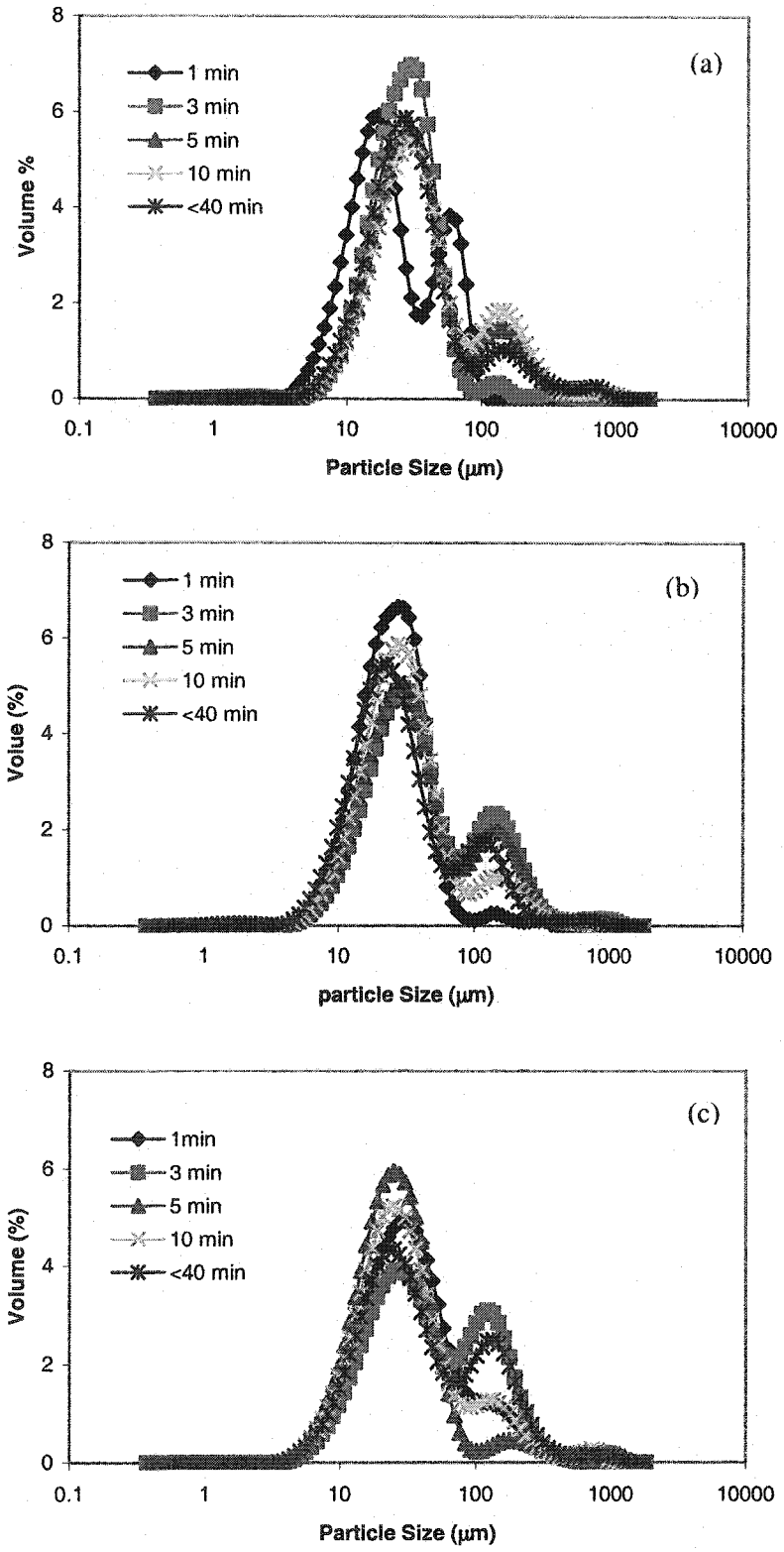

Figure J-4 Particle size distribution of flocculated CHO cells with EM240LH at CHO cell density of 0.50 wt%: (a) 100, (b) 300 and (c) 500 rpm

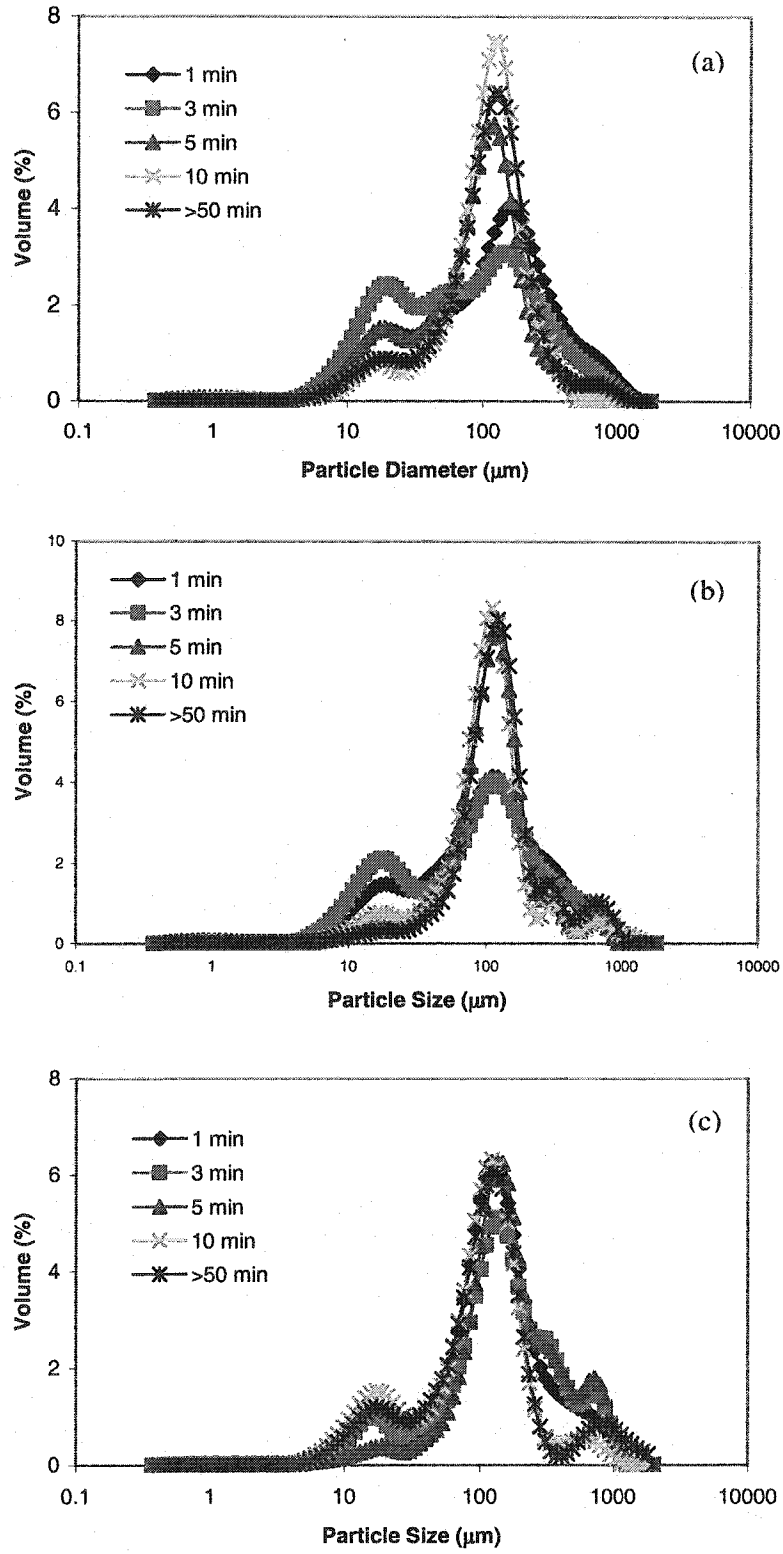

Figure J-5 Particle size distribution of flocculated CHO cells with EM441L at CHO cell density of 0.50 wt%: (a) 100, (b) 300 and (c) 500 rpm

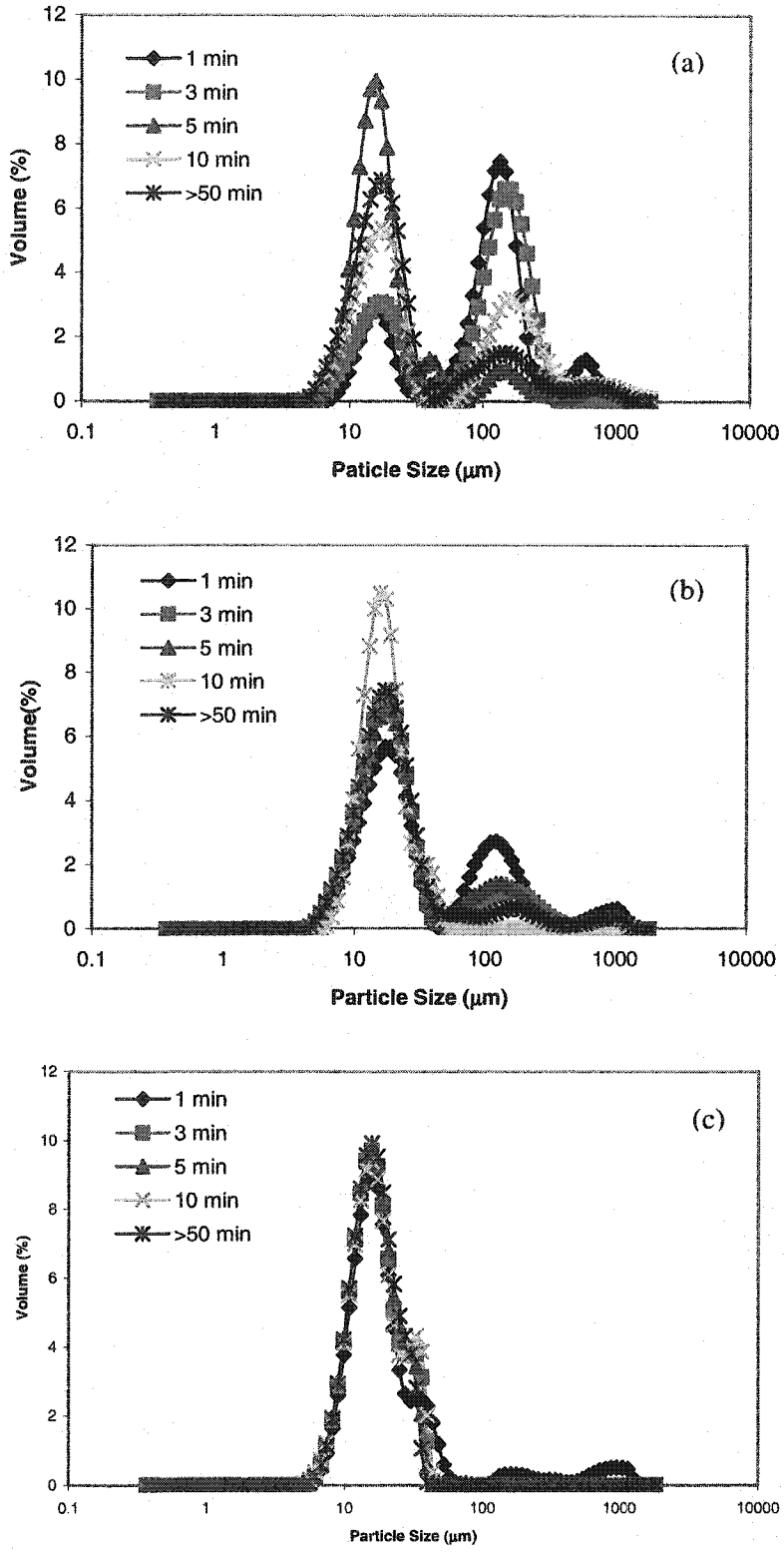

Figure J-6 Particle size distribution of flocculated CHO cells with EM441LH at CHO cell density of 0.50 wt%: (a) 100, (b) 300 and (c) 500 rpm

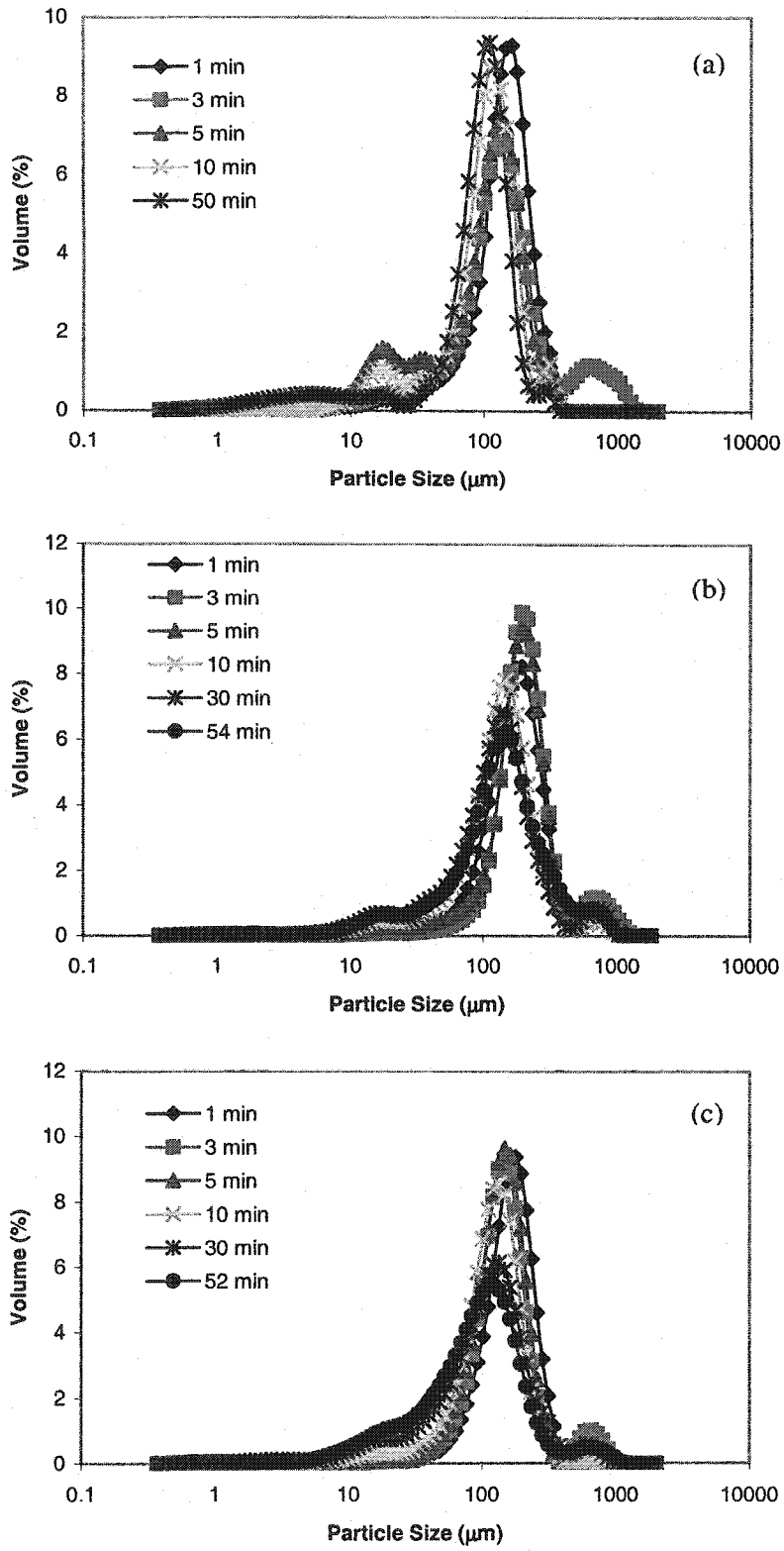

Figure J-7 Particle size distribution of flocculated CHO cells with EM440CT at CHO cell density of 1.0 wt%: (a) 100, (b) 300 and (c) 500 rpm

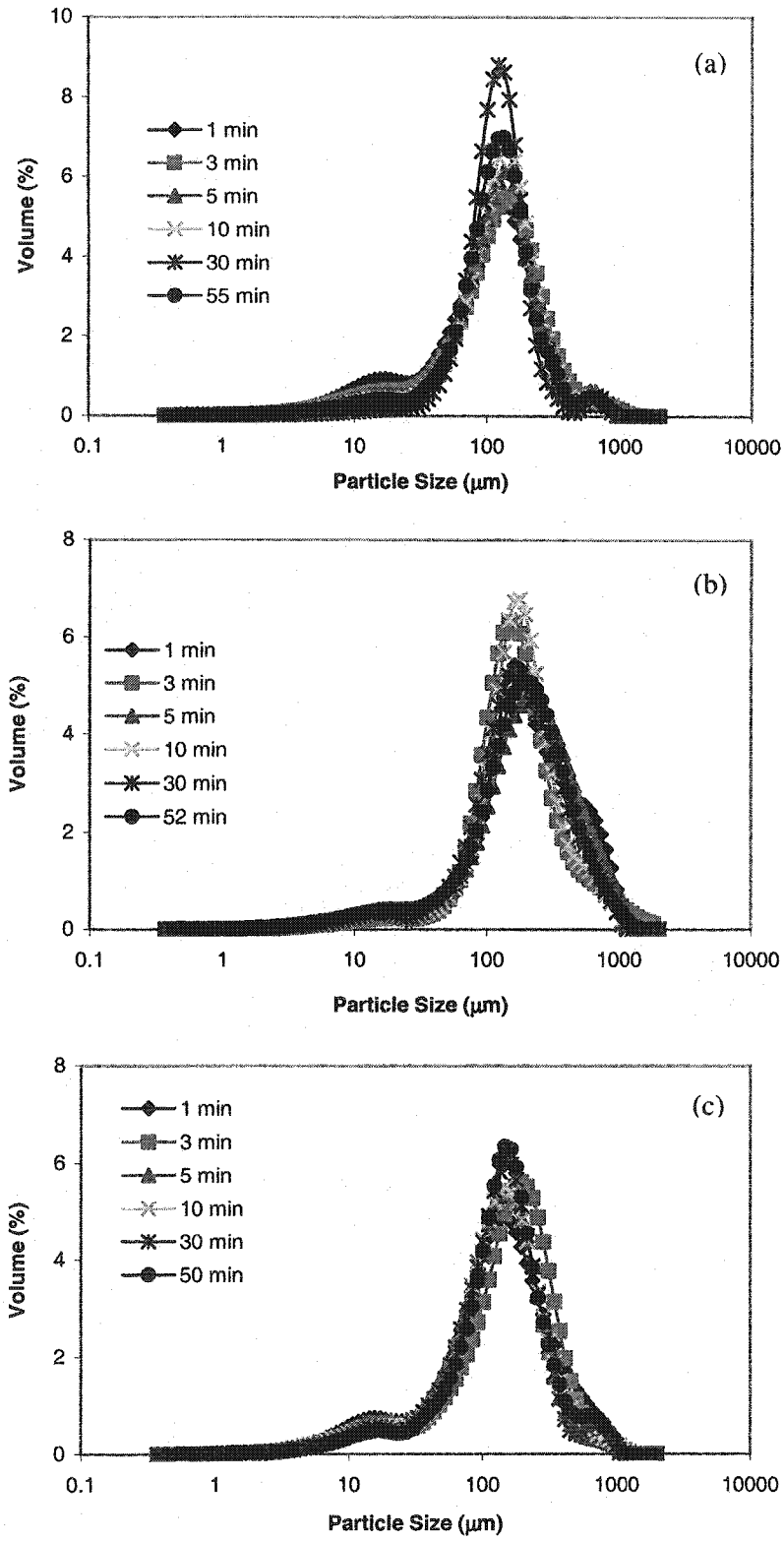

Figure J-8 Particle size distribution of flocculated CHO cells with EM441L at CHO cell density of 1.0 wt%: (a) 100, (b) 300 and (c) 500 rpm

APPENDIX K

OPTIMUM STIRRING SPEED AND TIME

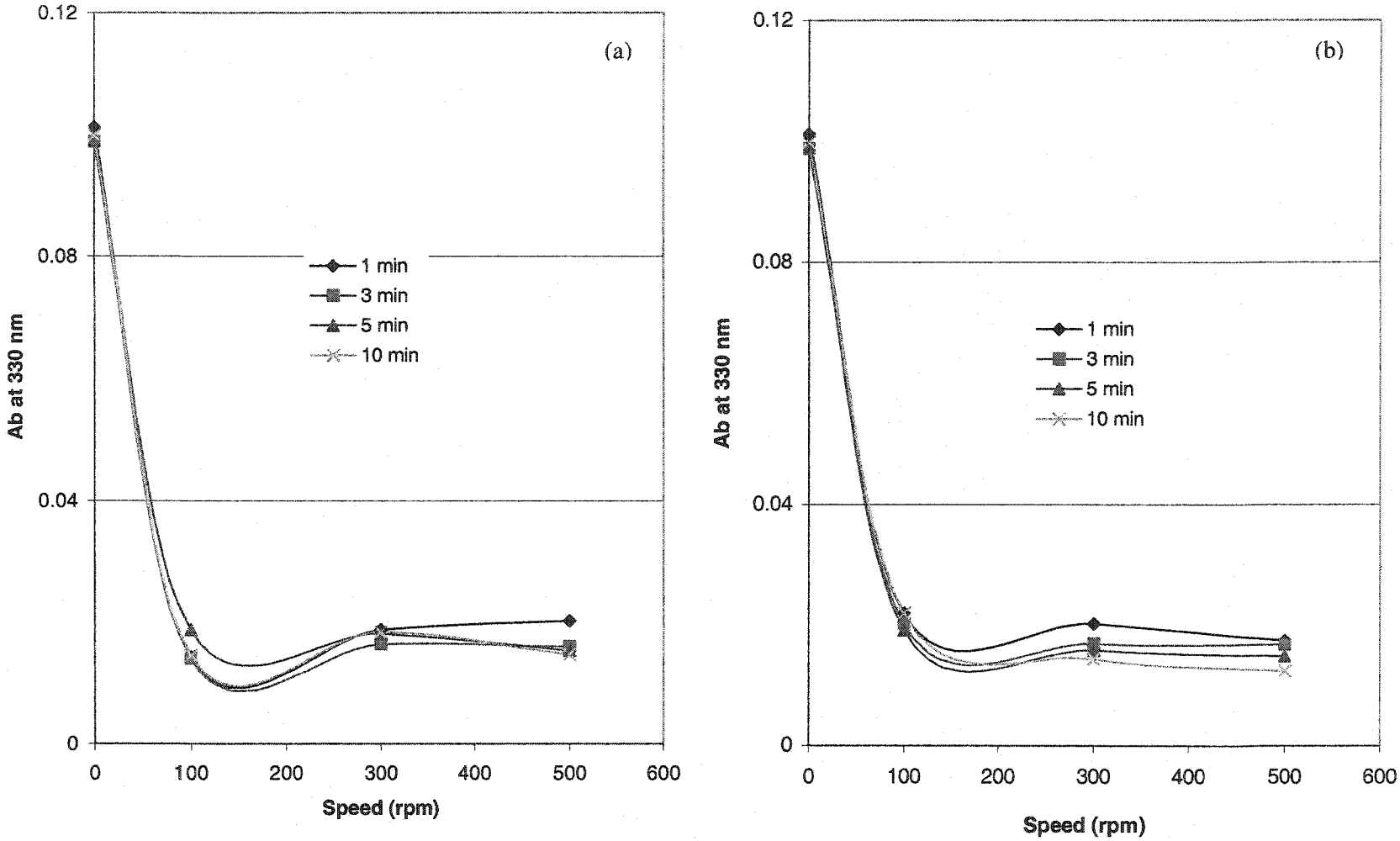

Figure K-1 Optimum Stirring speed and time for cationic polyacrylamide with 5 % charge density for 0.5 wt% CHO cell concentration: (a) EM1540CT and (b) EM1540L

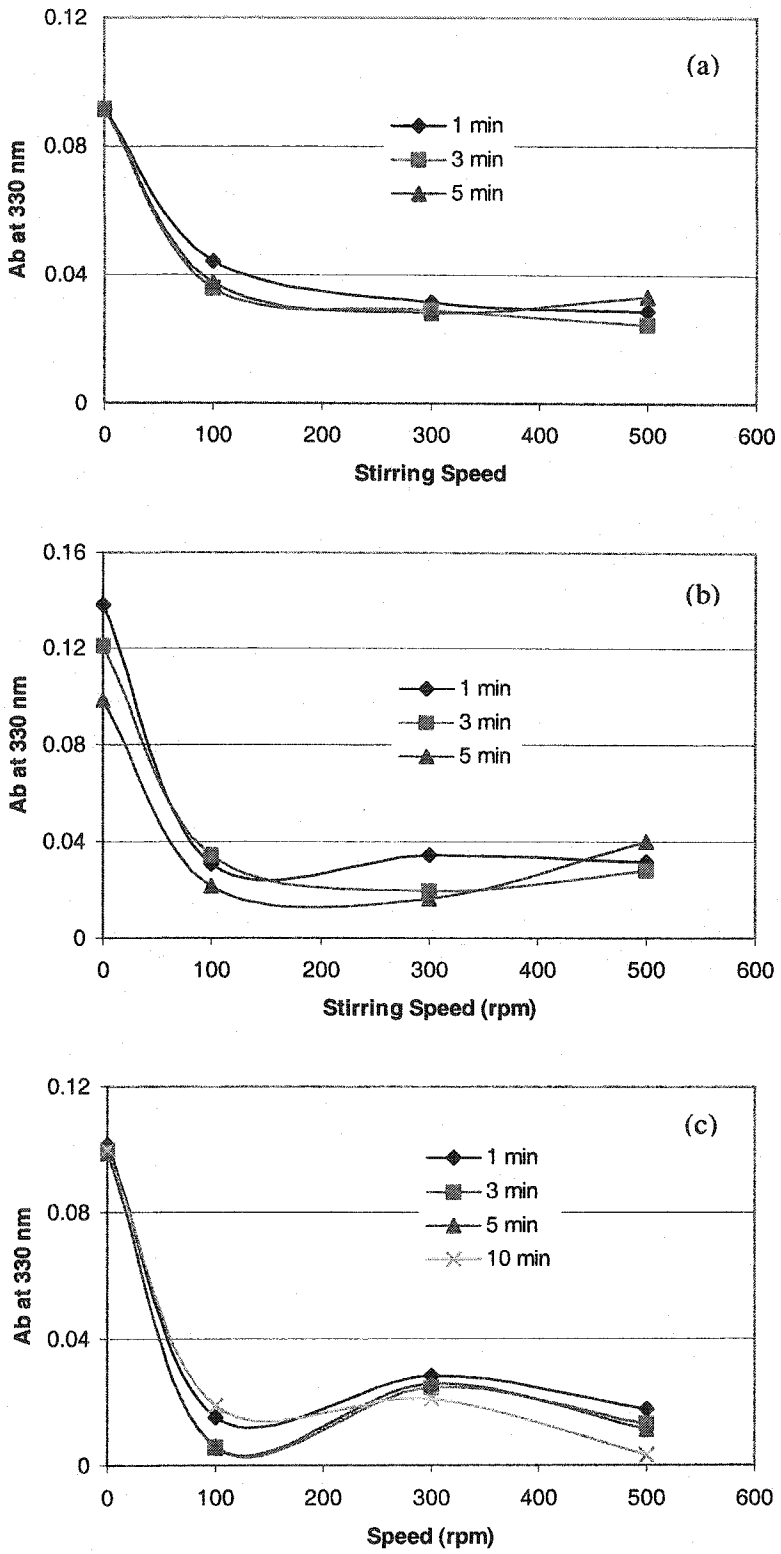

Figure K-2 Optimum Stirring speed and time for cationic polyacrylamide with 20 % charge density for 0.5 wt% CHO cell concentration: (a) EM240CT, (b) EM240L and (c) EM240L

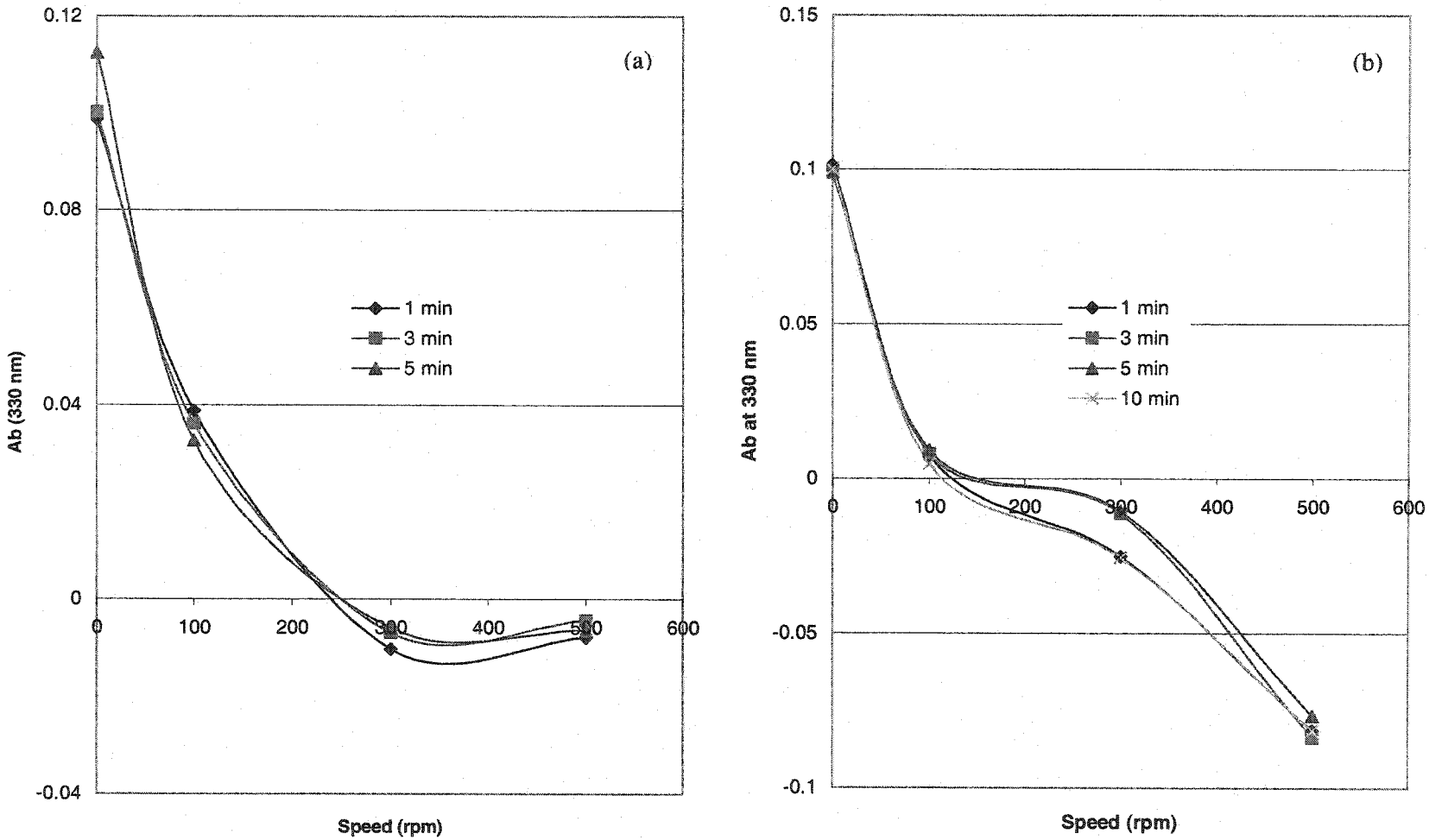

Figure K-3 Optimum Stirring speed and time for cationic polyacrylamide with 80 % charge density for 0.5 wt% CHO cell concentration: (a) EM840CT and (b) EM840L

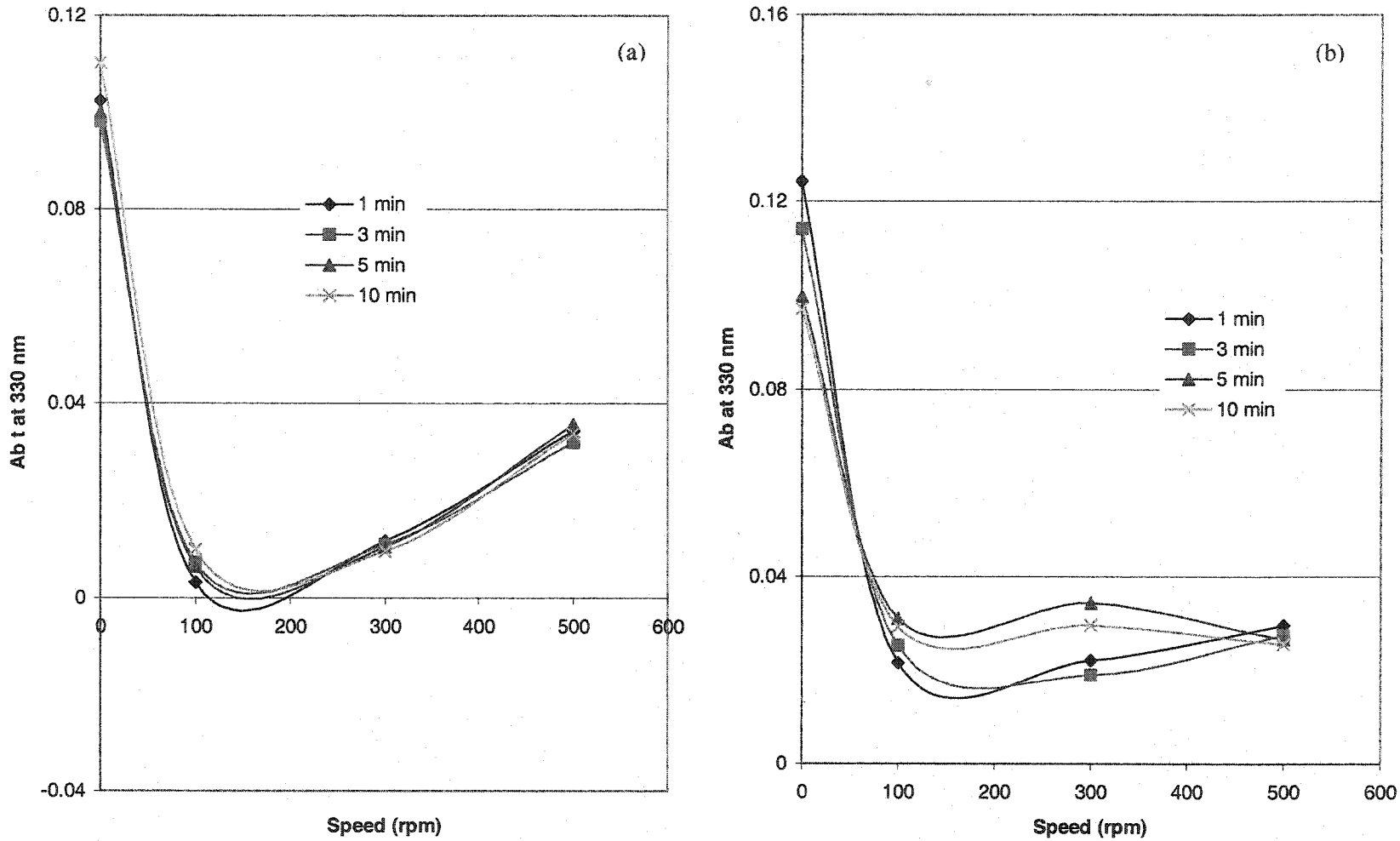

Figure K-4 Optimum Stirring speed and time for cationic polyacrylamide with 5 % charge density for 0.25 wt% CHO cell concentration: (a) EM1540CT and (b) EM1540L

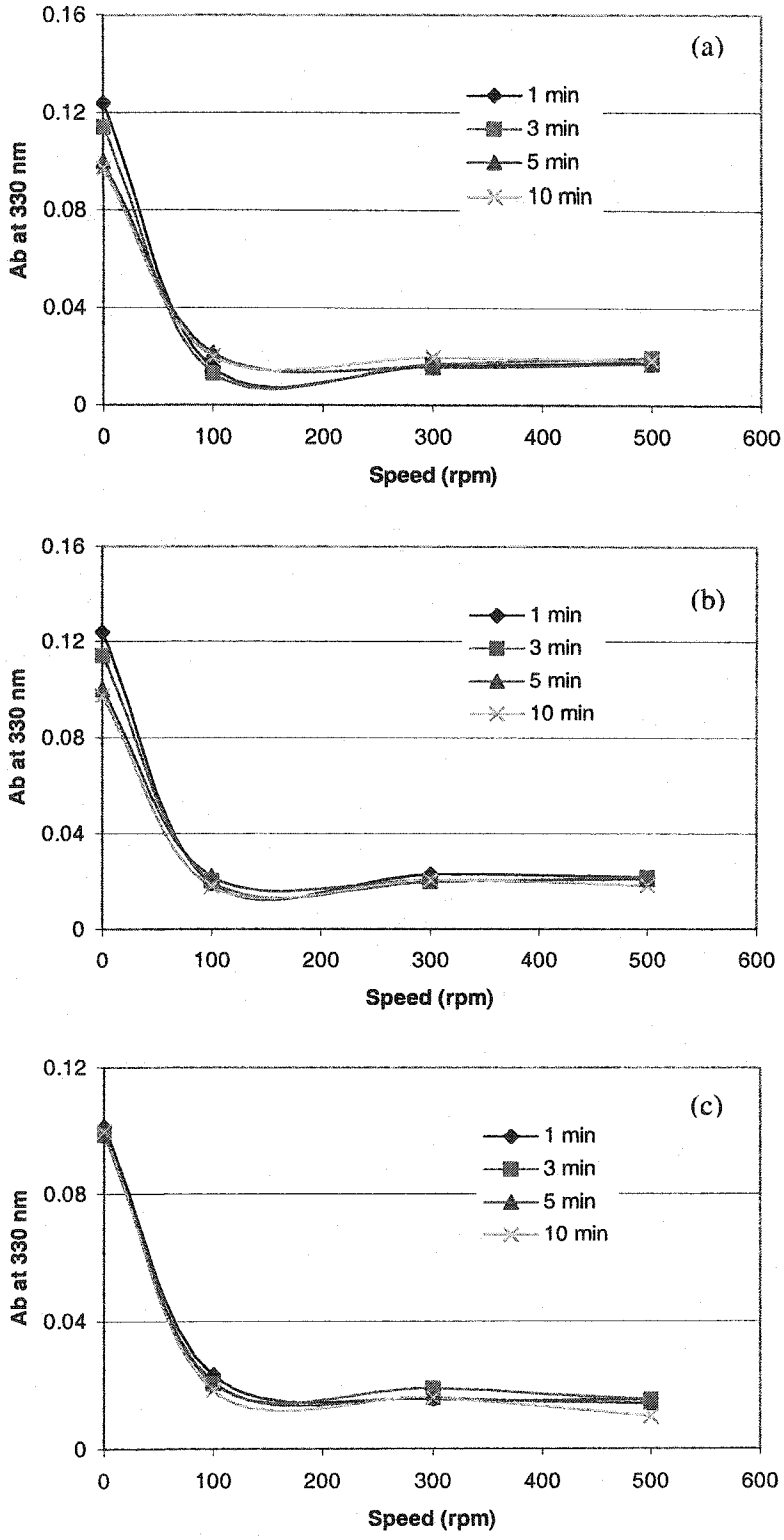

Figure K-5 Optimum Stirring speed and time for cationic polyacrylamide with 20 % charge density for 0.25 wt% CHO cell concentration: (a) EM240CT, (b) EM240L and (c) EM240LH

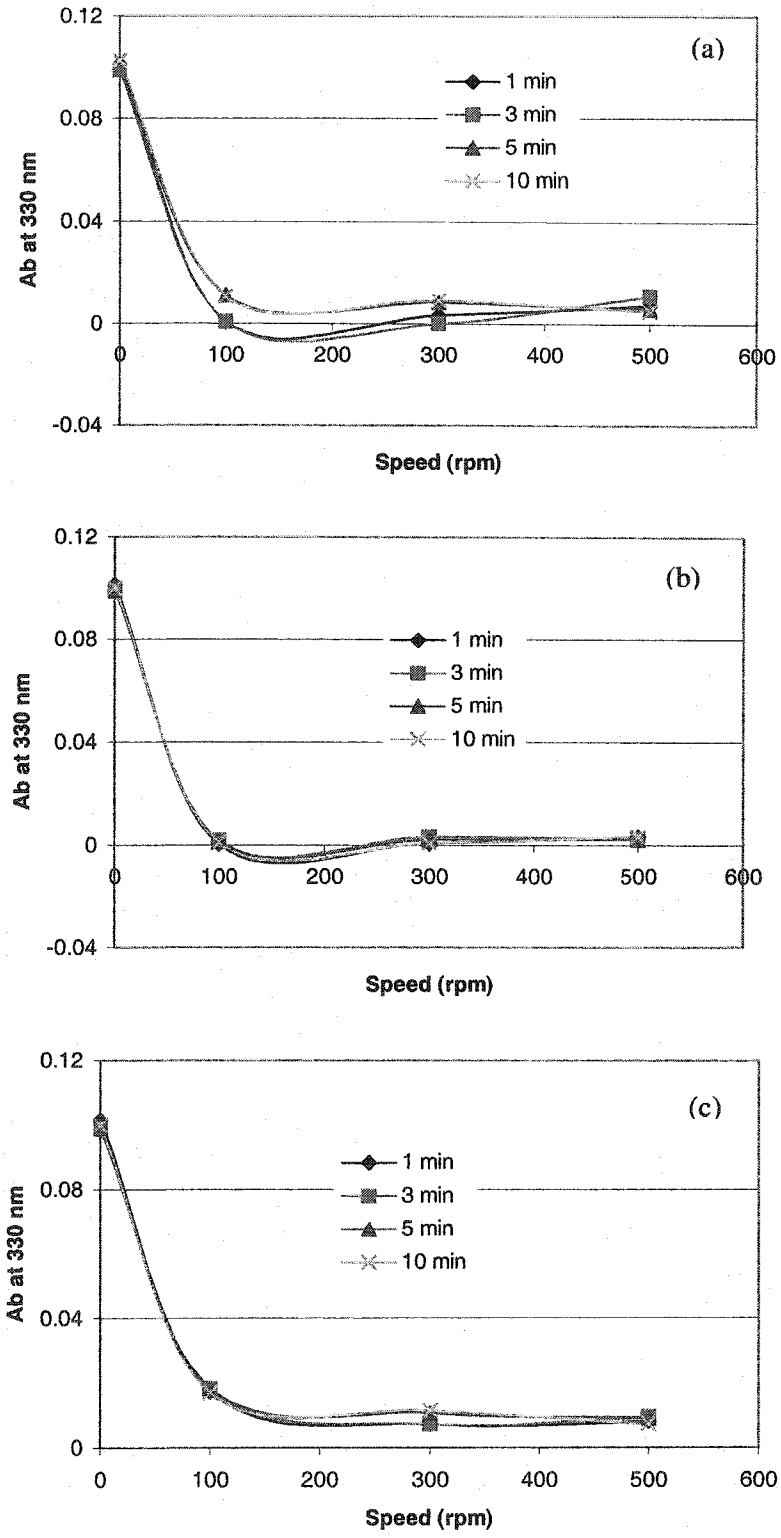

Figure K-6 Optimum Stirring speed and time for cationic polyacrylamide with 40 % charge density for 0.25 wt% CHO cell concentration: (a) EM440CT, (b) EM441L and (c) EM440LH

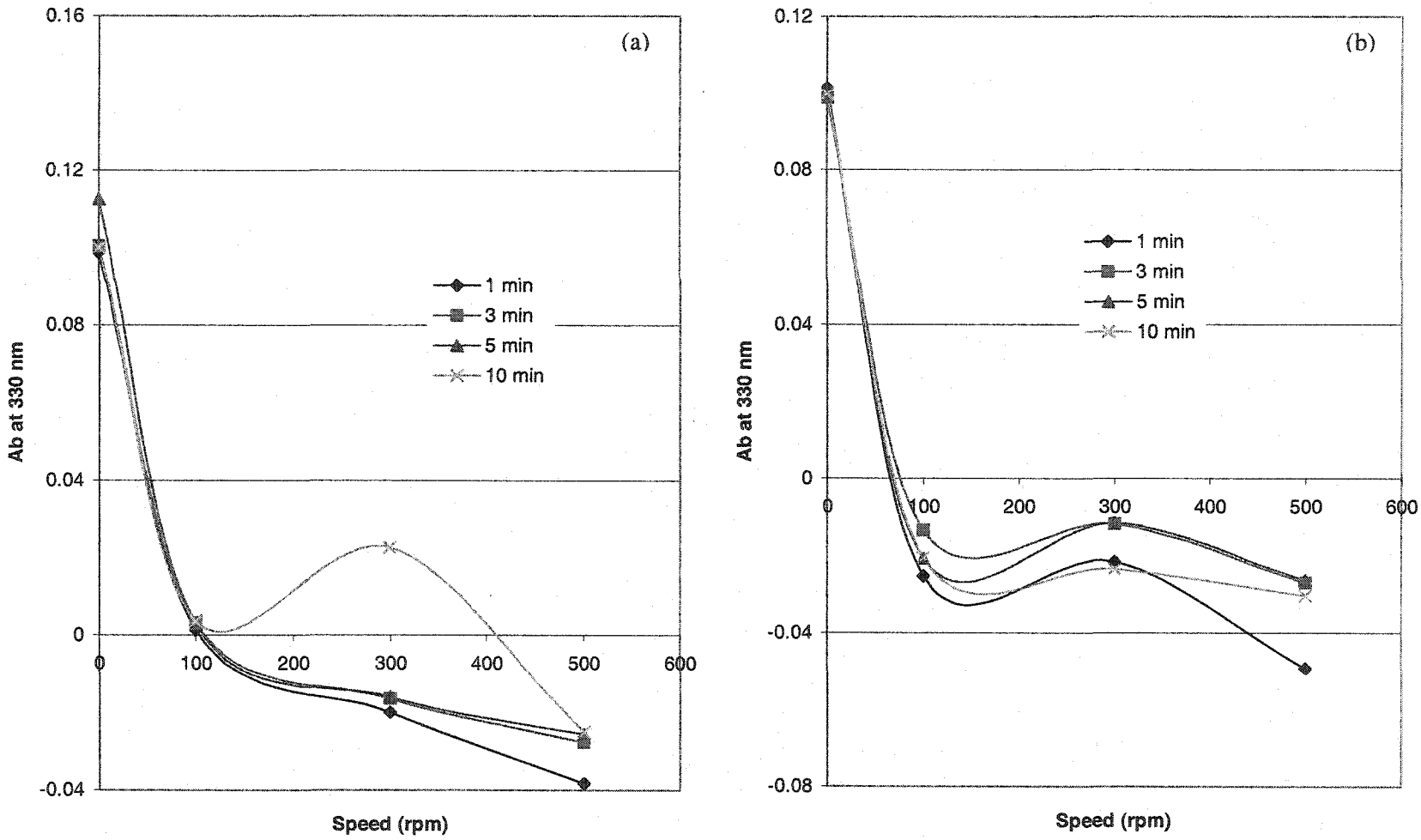

Figure K-7 Optimum Stirring speed and time for cationic polyacrylamide with 80 % charge density for 0.25 wt% CHO cell concentration: (a) EM840CT and (b) EM840L

APPENDIX L

LIST OF PUBLICATONS

Kim, J.S. Akeprathumchai, S. and Wickramasinghe, S.R. (2001) *Flocculation to Enhanced Microfiltration, J. Membrane Sci.,* 182(1-2): 161-172

Wickramsinghe, S.R., Han, B., Akeprathumchai, S. and Qian, X. (2003) *Modelling Flocculated Cell Suspensions using a Population Balance Approach: Application to Microfiltration, Mat. Res. Symp. Proc.*, 752: 309-314

Han, B., Akeprathumchai, S., Qian, X. and Wickramasinghe, S.R. (2003) *Flocculation of Biological Cells: Comparisons between Experiment and Theory, AICHE J.*, 49(7): 16871701

Wickramasinghe, S.R., Han, B., Akeprathumchai, S., Chen, V., Neal, P. and Qian, X. (2003) *Improved Permeate Flux by Flocculation of Biological Feeds: Comparison between Theory and Experiment, J. Membr. Sci.*, (acceptted)

Wickramasinghe, S. R., Han, B., Akeprathumchai, S., Jaganjac, A. and X. Qian (2003). *Modeling flocculation of biological cells, Powder Technology. (submitted)*